

NASA TECHNICAL
TRANSLATION



NASA TT F-613

NASA TT F-613



TECH LIBRARY KAFB, NM

TWO-PHASE FLOW IN TURBINES AND REACTION NOZZLES

by V. D. Venediktov

Mashinostroyeniye Press, Moscow, 1969

NATIONAL AERONAUTICS AND SPACE ADMINISTRATION • WASHINGTON, D. C. • JUNE 1970



TWO-PHASE FLOW IN TURBINES AND REACTION NOZZLES

By V. D. Venediktov

Translation of "Turbiny i Reaktivnyye Sopla na Dvukhfaznykh Potokakh"
Mashinostroyeniye Press, Moscow, 1969

NATIONAL AERONAUTICS AND SPACE ADMINISTRATION

For sale by the Clearinghouse for Federal Scientific and Technical Information
Springfield, Virginia 22151 - CFSTI price \$3.00

ANNOTATION

The characteristics of the operation of turbines and jet nozzles on double-phase working fluids are examined in this book.

By the method of successive approximations the flow of a double-phase flow, containing small particles, is examined with regard to the velocity and temperature lag of particles behind the gas; the results of computer calculations are presented, permitting a swift evaluation of the fundamental parameters of the exhaust of a double-phase flow from a nozzle. It is shown that the presence of a liquid undulating film on the wall of a nozzle leads to substantial losses in the boundary layer and causes a significant lowering of nozzle efficiency.

A method for evaluating turbines on double-phase flows with liquid particles is given in the book and the basic types of supplementary losses are examined: those due to impact of the liquid particles on the nozzle blade and as a result of friction on the undulating film covering the surface of the flow portion. In order to achieve a decrease in the losses due to particle impact on the blades, it is expedient to increase the axial clearance between the nozzle apparatus and the turbine wheel, at the same time lowering the erosional attrition of the rotor blades. In a birotative turbine the losses indicated above are essentially decreased and its effectiveness and reliability are maintained at a high level.

A great amount of attention was given to the operation of a turbine on moist vapor and coal dust fuel.

The book is intended for scientific and technical engineering workers in power machine construction and aviation industry. 12 Tables, 92 illustrations, bibliography, 72 citations.

Reviewer Candidate Technical Sciences
G.A. Filippov
Editor Eng. V.L. Samsonov

TABLE OF CONTENTS

ANNOTATION.....	iii
FOREWORD.....	vii
CONVENTIONAL SIGNS.....	ix
INTRODUCTION.....	xi
CHAPTER I. ELEMENTS OF THE HYDRODYNAMICS OF DOUBLE-PHASE FLOWS.....1	
§1. Basic Assumptions and Formulation of the Problem.....1	
§2. Basic Hydrodynamic Equations of Double-Phase Linear Flows.....5	
§3. Limiting Cases of the Flow of Double-Phase Mixtures.....15	
§4. Equation for the Reduction of Influences in the Study of Double-Phase Flows.....26	
CHAPTER 2. FLOW OF DOUBLE-PHASE MIXTURES IN JET NOZZLES.....31	
§1. The Method of Successive Approximations in Studying Double-Phase Flows.....32	
§2. Losses Due to Friction of the Gas on the Particles.....42	
§3. Losses Due to Incomplete Heat Exchange Between the Particles and the Gas.....53	
§4. Exhaust of a Double-Phase Mixture in the Nozzle in the Case Where $\bar{a} \approx 1 + b(\xi e^{1-\xi})^q$ and $10^{-4} < Re_{rel} < 100$55	
§5. Experimental Studies of Nozzles in Double-Phase Flows.....65	
§6. Similarity Criteria and Characteristics of Experimental Investigations of Double-Phase Flows.....76	
CHAPTER 3. THE OPERATION OF A TURBINE ON A DOUBLE-PHASE FLOW WITH A CONSTANT CONCENTRATION OF PHASES.....80	
§1. Basic Characteristics of the Operation of the Turbine Stage on a Double-Phase Flow with Liquid Particles.....80	
§2. Experimental Investigations of Turbine Stages on Double-Phase Flows.....96	
§3. Flow of a Double-Phase Mixture in a Turbine with Increased Axial Clearance. Particle Separation in the Axial Clearance.....101	
§4. Operation of a Birotative Turbine on a Double-Phase Flow.....116	
§5. Turbine Operation on a Double-Phase Flow with Solid Particles.....123	

CHAPTER 4. THE OPERATION OF AXISYMMETRICAL NOZZLES AND TURBINES ON MOIST VAPOR.....	134
§1. Several Thermodynamic Relationships With Moist Vapor.....	135
§2. The Exhaust of a Moist Vapor from a Supersonic Nozzle.....	139
§3. The Speed of Sound and Adiabatic Index for Moist Vapor.....	149
§4. Coefficient of Moist Vapor Consumption.....	156
§5. Equilibrium Exhaust of an Ideal Gas-Condensing Vapor Mixture from a Nozzle.....	163
§6. Characteristics of Moist Vapor Flow in the Flow Section of the Turbine.....	169
§7. Birotative Turbine Operation on Moist Vapor.....	175
§8. Erosion of Elements of a Turbine Operating on Moist Water Vapor.....	178
REFERENCES.....	182

FOREWORD

The actuality of investigating double-phase flows is determined by the contemporary vigorous development of thermo-energetics, the application of new fuels and working fluids in gas turbine apparatus and engines of flight apparatus. Practice sets a number of new problems before investigators, which problems basically come down to the following: determination of regular laws of the processes in the flow of double-phase liquids in turbines and jet engines, the creation of methods of evaluating such flows, ensuring high effectiveness and reliability in the operation of turbines and jet nozzles. In the present book a first attempt is made towards a complex consideration of these problems on the basis of published data, and also of results of investigations obtained by the author.

Expansion in the nozzle is the basic process of the flow of double-phase mixtures in the flow portion of an engine. Therefore, the chapters dedicated to the flow of a mixture in nozzles, precede the chapters dedicated to the flow in turbines. In view of the comparatively small volume of experimental data on the flow of double-phase mixtures and of the large number of physical parameters simultaneously influencing it, many aspects of this phenomenon are examined only in the first approximation. Therefore, the book does not pretend to make an exhaustive illumination of the problems mentioned, and the information presented in it, undoubtedly, will be supplemented and dealt with in greater depth in the future.

In setting the tasks of the investigation and the discussion of results obtained, the author received a great amount of help from Doctor of Technical Sciences V.V. Uvarov and Doctor of Technical Sciences V. Kh. Abiants. In reviewing and examining the manuscript a number of useful comments were made by Candidate of Technical Sciences G.A. Filippov and Candidate of Physical Mathematical Sciences R.I. Nigmatulin. The author expresses heartfelt thanks to all of them. The author is also indebted to I.I. Vlasov and Ye.K. Gavrilova, who participated in conducting the investigations.

CONVENTIONAL SIGNS

p	Pressure of gas or vapor phase	x	Coordinate calculated on the initial cross section of the conduit; axial coordinate of a particle in axial clearance; degree of dryness of the vapor
T	Temperature	$\xi = x/L$	Dimensionless coordinate
$t = T/T_0$	Dimensionless temperature	q	Acceleration of the force of gravity /4
v	Specific volume	L	Characteristic dimension of the flow
ρ	Density: degree of reaction	L_c	Nozzle length
i	Enthalpy	u	Circumferential rotation velocity of rotor blades
c	Velocity	D	Diameter of turbine or nozzle
G	Mass flow rate of phase	α	Coefficient of heat emission
F	Area of conduit cross section	τ	Time
$f = F/F_0$	Dimensionless area of conduit cross section	$\pi_T = p_0^*/p_T$	Degree of pressure drop in turbines
$g_r = \frac{G_r}{G_r + G_K}; g_K = \frac{G_K}{G_r + G_K}$	Consumption mass concentration of gas and particles	μ, ν	Coefficient of viscosity, kinematic viscosity of phase
R	Gas constant	λ	Coefficient of heat conductivity; reduced velocity
c_p, c_v	Specific heat with constant pressure and volume	σ	Coefficient of surface tension
k, n	Adiabatic index, polytropic index	$Sto = \frac{\rho_K c_0 d^2}{18 \mu_T L}$	Stokes number
k_c	Coefficient of particle separation	$Re_{rel} = \frac{c_{rel} \rho r d}{\mu_T}$	Reynolds number
$n_v = \frac{G_K}{m F c_K}$	Number of particles per unit volume	$\delta = \frac{n-1}{n} \frac{c_0^2}{q_T R T_0^2}$	Dimensionless parameter
A	Work	Subscripts	
H	Net energy		
Q	Volume of heat	ad	Adiabatic flow of a pure gas
P	Force: interaction force of particles and gas: specific impulse;	Γ	Gas phase
d	Particle diameter	l	Liquid phase
m	Particle mass	K	Particles, condensate
r	Radius: vapor formation heat		

II Vapor phase
e Equilibrium flow
d Second approximation,
real process
rel Relative motion

cr Critical section
s Exit section of nozzle;
separation
0 State at the beginning
of expansion
* Stagnant state
- Dimensionless volume
(relative to the initial
value of the same para-
meter)

INTRODUCTION

In recent years, in connection with the brisk development of engine construction and thermal energetics, the necessity for studying double-phase flows has appeared, i.e., flows of gas or vapor containing a large amount of suspended liquid or solid particles. Such a type of double-phase mixture may serve as the working fluid in turbines and jet engines, for example in turbines operating on moist vapors of various substances (water, freons, mercury, alkaline metals); in turbines and jet engines operating on combustion products with a large content of liquid or solid oxide particles; in stationary and transport gas turbine engines, operating on powered coal fuel; in auxiliary turbines and jet nozzles of solid propellant engines.

/5

Double-phase flows are found also in pneumo-transportation, hydro-transportation (pulp conductors), and in furnaces burning pulverized fuel.

The flow of double-phase mixtures and their mechanical aerodynamic and thermophysical characteristics has been insufficiently studied at the present time. However, available experimental and theoretical data from a number of authors indicate that the presence of a large amount of suspended liquid or solid particles in a gas can essentially change the characteristics of the working fluid (work capacity, heat transmission characteristics) in comparison with pure gas.

The hydromechanical and thermophysical characteristics have been more fully investigated only for liquid vapor mixtures with a great content of the liquid phase and with small velocities of flow (cf. for example the work of S.S. Kutaladze [32]).

A large number of studies was dedicated to the investigation of turbines operating on moist water vapor. In the majority of early publications [14], questions were examined that involved blade erosion of actual turbines which were in use, and several measures for decreasing erosion were proposed. These measures basically come down to a hardening of the intake edges of the rotor blades and also to collection and removal of moisture from the peripheral surface of the flow portion. A generalization of the published data (the majority of which are of an empirical nature) allows one to find a means for increasing reliability of turbine operation.

In several works [15, 28, 60] the flow of a moist vapor in the continuous flow portion of the turbine is considered with regard to the characteristics of the motion of the liquid and vapor phases as well as interaction between the phases. However, even here, in the majority of cases the authors are limited to obtaining empirical formulas for evaluating the decrease in efficiency and determining

/6

other parameters of the turbine.

Recently results of investigations were published in which physical processes accompanying the flow of a moist vapor in a turbine were studied: supercooling and abrupt changes in condensation on the exhaust of the vapor from the nozzle, precipitation of drops from the vapor flow and growth of drops with motion of the moist vapor through the turbine [18, 26, 49, 62]. Significant investigations in this region were conducted in the Moscow Electrical Technical Institute by a group of authors under the leadership of Director of Technical Sciences M. Ye. Deych, and also Directors of Technical Sciences I.I. Kirillov, R.M. Yablonik and others.

It is necessary to emphasize that the majority of published materials relates to the investigation of turbine operation on moist water vapor and does not contain a clear classification of supplementary losses in a turbine operating on a double-phase flow.

Even the influence of basic parameters of the suspended phase (viscosity of the liquid, size and density of the particles), and the geometry of the flow portion of the turbine, on the amount of supplementary losses has not been studied in sufficient detail.

In order to calculate these losses, the majority of authors propose empirical formulas, according to which it is recommended that the efficiency degree be lowered by 0.75 to 1.5% for each percent of vapor moisture. Meanwhile, with conversion to other working fluids (for example, moist hydrogen vapors and alkaline metals) the nature and volume of supplementary losses, caused by double-phasing, may be substantially changed.

Recently, papers have appeared in which the flow of double-phase mixtures in a jet nozzle were considered. In several of them [66] the law of the motion of a specific particle is determined according to the given law of the motion of the gas phase, generally by numerical methods. Moreover, the reverse influence of particles upon the gas flow has not been considered.

In a number of works [29, 30, 56, 69], the motion of powder-gas mixtures with regard to thermal and mechanical interaction of particles and gas has been studied. Thus in one article [69], it is shown that heat exchange between particles and gas with an expansion of the double-phase flow leads to a deviation of the indices of the expansion process from the adiabatic index of the gas phase k . In another article [56], results are given on the calculation of a double-phase flow in the ultrasonic conical section of a nozzle with the aid of the method of characteristics. In the assumption of a one-dimensional flow on a subsonic portion of the nozzle and of the constancy of particle lag in the throat, the influence of the cone angle, relation of areas, diameter of nozzle throat, etc., on thrust is investigated. /7

Reference [29] presents a system of equations describing the one-dimensional flow of a double-phase mono-dispersion mixture in a nozzle. In addition, it is accepted that the mixture is exhausted with a constant particle lag, and the flow of particles in the gas follows Stoke's equation. Results of the investigation indicate the possibility of increasing particle concentration in the zone of the nozzle axis behind its throat. This leads to a retardation of the gas on the axis and an increase in its temperature in comparison with the gas flowing along the wall of the nozzle. Moreover it was shown that an impulse, calculated according to one-dimensional theory, differs from an impulse calculated according to two-dimensional theory by no more than 0.2%.

In reference [5] a gas flow with solid particles in an axially symmetrical nozzle was considered. It was shown that with a particle size of $4\mu\text{m}$ a drop in the thrust in comparison with an equilibrium flow comprises approximately 5% with a concentration of particles $g_k = 0.4$.

In studying a double-phase flow in the flow portion of an engine, it is necessary to keep in mind the following basic characteristics differentiating it from the flow of a pure gas;

(1) The forces of the aerodynamic interaction of the phases are specified by the viscosity and also the whirling of the gas, and are analogous to the usual forces of friction. The processes of heat exchange, between the phases, flow in a majority of instances with a finite difference in temperatures. Therefore the flow process of double-phase mixtures is theoretically irreversible. (If the particles are very small or very large, then with a moderate concentration of them it is possible to ignore the irreversibility of this process).

(2) In a double-phase flow with high accelerations, a substantial difference in the velocities and temperatures of the flow components (phases) is possible.

(3) In a majority of instances, a double-phase flow is heterogeneous, where upon heterogeneity in the flow process can be substantially increased due to a redistribution of concentrations of the phases according to the cross section of the flow.

(4) If the suspended phase is in a liquid state, then portions of it precipitate on the walls and consequently change the micro-geometry of the surface of the conduit and the form of the flow portion.

The above-noted characteristics may prove to be a cause for substantial supplementary losses in the flow portion of the engine. It is necessary to attribute to such losses:

- (1) losses due to friction of the gas on particles;
- (2) losses due to incomplete heat exchange between the phases;
- (3) losses caused by interaction of the particles with elements of the flow portion of the engine, for example upon impact of the particles against the rotor blades of the turbine or losses of kinetic energy of the particles with their precipitation onto the walls;
- (4) losses due to a change in the microgeometry of the surface and forms of the conduits with a precipitation of liquid particles on the walls of the continuous flow portion or with erosional attrition of the elements of the flow portion by liquid or solid particles. /8

In the present book, results are presented on the study of specific characteristics of double-phase flows in the flow portions of a turbine and in a jet nozzle and also supplementary losses specified by the double-phase nature of the flow. Moreover, several means for increasing reliability and effectiveness of turbine operation are considered, i.e., separation of particles in axial clearance and the possibility of application of a birotative turbine.

The thermodynamic method of investigation is broadly applied in this work. An evaluation of the fundamental parameters of double-phase flows is conducted by the method of successive approximations. This allows one to substantially simplify the task of investigation, makes the obtained results more graphic, and ensures completely acceptable accuracy for a majority of practical cases.

In view of the complexity of double-phase flows, great significance, especially with the clarification of the physical essence of the phenomena, is acquired by experimental investigation. In some cases, for example, with the evaluation of losses due to friction of the gas on the liquid undulating film covering the nozzle blades of the turbines or walls of the jet nozzle, quantitative data may be obtained only from experiment.

The book contains results of investigations conducted by the author; calculated and experimental data which have been published are also used.

CHAPTER I

ELEMENTS OF THE HYDRODYNAMICS OF DOUBLE-PHASE FLOWS

§1. Basic Assumptions and Formulation of the Problem

The flow of a double-phase mixture in the flow portion of turbines and jet nozzles has a complex nature which is specified by a multiplicity of physical phenomena taking place simultaneously. Up to the present time the most important characteristics of such a flow have been insufficiently studied. This relates in particular to the process of heat exchange between phases, proceeding, generally speaking, under nonstationary conditions due to the instability of temperatures and velocities of the phases, to the phenomena of separation of particles on the walls, to the turbulent wave flow of liquid films, etc. Attempting to keep in mind the above-mentioned characteristics of the flow of double-phase mixtures demands an exceptionally complex analytical apparatus and will hardly prove to be successful. /9*

An even narrower task, i.e., the investigation of the hydrodynamic aspect of the phenomenon and calculation of the interaction and velocities of the phases, has still not been solved at the present time in general form. Equations for the flow of double-phase media, analogous to the general equations of hydrodynamics [31] are known. However, the use of a system of such equations for practical problems is not always possible, due to the large volume of calculation work, since the number of equations involved is approximately twice that of the system of equations for a single-phase flow. Moreover, precision of solutions to the problems is conditional, since in a model of the flow, assumptions are established which only very approximately correspond to actuality. These assumptions must be supplemented by the usual assumptions on the monodispersion of particles, on their equal density and spherical form and on the absence of mechanical interaction between the particles.

Therefore, in the investigation of double-phase flows, it is expedient to use the simplest methods, in particular, the thermodynamic method.¹ As is known [10], the thermodynamic method of investigation is based on two theoretical assumptions: on the stationarity and the unidimensionality of the flow processes (hydraulic model of flow).

¹ We will understand the term "thermodynamic method" to mean the method of classical, i.e., equilibrium, thermodynamics (author's note).

* Numbers in the margin indicate pagination in the foreign text.

These assumptions substantially simplify the task of investigation and in a number of practically important instances (where the influence of nonstationarity and non-unidimensionality of flow are small), allow the possibility of obtaining correct overall quantitative evaluations. The application of this method is especially expedient at the present stage of investigation of double-phase flows, when the physical picture of the flow is still insufficiently clear and many effects, caused by the double-phase nature of the flow, are evaluated in first approximation. /10

Certainly characteristics of double-phase flows such as the separation of particles in curvilinear conduits, and also in axisymmetrical nozzles with a large expansion, erosion loss of particles on a wall due to turbulent diffusion, etc., cannot be considered at the same time. Therefore the inclusion of other methods of analysis is necessary in order to study them.

It is necessary to note that the application of the thermodynamic method of investigation is especially effective for the study of double-phase flows with small particles. With a decrease in the diameter of the particles, the mass force (force of inertia), acting upon a particle, decreases proportional to d^3 , and the surface force (force of aerodynamic gas action) is proportional to d^2 or d , so that the relative influence of the surface force increases. Therefore, rather small particles are easily borne away by the gas and follow its lines of flow. The flow of such double-phase mixtures in each small stream can be considered to be unidimensional.

Since the total surface of all particles substantially increases with a decrease in their diameter, the speed of heat exchange processes between phases can greatly exceed the speed of change under heat exchange conditions. This allows one to disregard nonstationarity of heat exchange and, in particular, to use coefficients of heat emission obtained for stationary conditions for calculating heat emission from particles to the gas. An analogous conclusion can be made concerning selection of the resistance coefficient of a particle for defining the law of its motion.

In this chapter we shall consider the simplest cases of the flow of double-phase mixtures with small particles. We shall extract basic assumptions (including assumptions about phase stationarity and linearity of the flow), usually applied for consideration of double-phase flows and allowing a still greater simplification of the task:

- (1) the flow is stationary and linear;
- (2) the flow takes place without heat exchange with the surrounding medium;
- (3) the specific heats of the phases c_{pk} and c_{pr} and the coefficient of dynamic viscosity of the gas μ_r do not depend upon

temperature;

(4) mass consumptions of the phases are constant (phase transitions are absent, i.e., there is no condensation, burning or evaporation of particles);

(5) break-up or coagulation of particles does not take place /11 in the flow;

(6) the total volume of the particles is negligibly small in comparison with the volume of the gas phase;

(7) abrupt changes in consolidation in the flow are absent and the velocity of the particles relative to the gas does not exceed the speed of sound;

(8) all particles have a spherical shape and equal diameter;

(9) mechanical interaction of the particles can be disregarded, which allows one to assume the partial pressure of the particles to be equal to zero.

Moreover, for evaluating the influence of the double-phase nature of a flow on its basic hydromechanical parameters, it is possible to ignore the interaction between the working fluid and the walls of the conduit. Actually with the exception of losses due to the friction of the flow on the wall (which must be considered separately), this interaction will appear as a change in the law governing the motion of particles near the wall. However, as was shown in reference [54], at the same time the resistance coefficient of a particle changes proportional to the factor $1 + (bd/2x)$, where x is the distance of a particle from the wall and b is a coefficient depending upon the shape of the wall. For example, with particle motion along a flat wall $b = 0.55$, but along the axis of a cylinder we find that $b = 2.1$. Therefore the influence of the law of particle motion on the wall will appear only at a distance $x \ll 10d$ from the wall, or, since the value d is on the order of several microns, at a distance of $x \ll 1$ mm. This region relates to the zone of the boundary layer and does not have any significant influence on the nucleus of a double-phase flow in full-scale conduits and nozzles.

Let us consider the last two assumptions in somewhat greater detail. The assumption of a spherical shape is completely justified for small liquid drops and for solid particles formed by the solidification of such drops. Actually, the shape of a drop is determined by the ratio of hydrodynamic forces acting upon the drops on the part of the passing flow and the forces of surface tension. As is well known, the ratio of these forces is characterized by Weber's criterion $We = \rho r c_{rel}^2 d / \sigma$. With a decrease in the diameter of a particle even its lag in velocity c_{rel} decreases, therefore the numerator of this expression swiftly decreases. With values of

We < 8 the forces of surface tension have the predominating influence and the drops retain a nearly spherical shape. Most often it is these particles that are found in jet engine nozzles.

The interaction between particles in a moving double-phase mixture may be both hydrodynamic (interaction at a distance through the carrier medium), and mechanical (when they collide). As is well known, the hydrodynamic interaction of particles involves the following situation. With the motion of an individual particle the nature of a gas flow in the region adjacent to it changes somewhat. With the motion of a large number of particles these changes, equally distributed throughout the entire volume of the flow, are totalled, thus leading to a difference between the parameters of the flow of the gas phase in a double-phase flow and the flow of a pure gas. Therefore, even the conditions of the flow of each particle of the gas phase will differ from the conditions of its flow in a single-phase flow. For example, with the accelerated flow of a double-phase mixture in a conduit, the velocity of the gas phase in each of its cross sections will be due to the inhibiting influence of the particles which is somewhat less than the flow speed of a pure gas. This decrease in gas velocity can be considered to be the result of the superposition of a supplementary velocity on the basic gas velocity, which is induced in the entire volume of the gas by particles moving in the flow at a relative velocity $c_p - c_k$, and directed opposite to the gas velocity. /12

The study of the influence of particles on gas flow, interaction of phases and, consequently, even the mutual hydrodynamic influence of particles, comprises one of the chief aspects of the present book.

With the motion of double-phase mixtures, even a collision of particles with one another may take place. As is well known, collision of gas molecules taking place according to the laws of the collision of absolutely elastic bodies, leads to the appearance of internal pressure in the gas. However, the partial pressure of particles suspended in gas (with $d > 0.001 \mu\text{m}$) will be negligible, due to the small number of particles in comparison with the number of gas molecules, and the relative infrequency of their collisions, and also due to the fact that in the majority of cases, collisions of particles cannot be considered as absolutely elastic. Therefore, in the present study, pressure in the double-phase flow will be taken as being equal to the pressure of the gas phase.

Collisions will be most frequent if the particles are very small and easily attracted by turbulent pulsations of the gas and also with a great polydispersion of the particles (due to an essential difference in the velocity of the motion of different sized particles). Collisions of particles cannot lead to noticeable changes in any characteristics of the flow and must only be considered in the investigation of certain specific flow characteristics; for example, in the consideration of particle coagulation.

We shall formulate the task of investigation in the following way: to define the parameters of a double-phase flow (both the total parameters as well as those of the individual phases) in any cross section of the conduit according to the parameters set in the initial cross section of the conduit.

§2. Basic Hydrodynamic Equations of Double-Phase Linear Flows /13

In the double-phase flows under consideration (the gas-particle type) it is the gas which is the carrier medium and that which performs the work. However the basic parameters of the gas and, in particular, its efficiency, depend upon its mechanical and thermal interaction with the particles. Therefore, with the investigation of double-phase flows it is necessary to study the basic laws governing the mechanical and thermal interaction of the phases. In the first place, it is expedient to consider the motion of an individual particle in the gas flow. Given the above-mentioned assumption of an absence of mechanical interaction between the particles, dependences characterizing the motion of one particle can be extrapolated to the case involving the motion of several (many) particles. Furthermore, considering the effect of particles on the gas, it is possible to define the parameters of the flow of the gas phase and of the double-phase flow as a whole.

Let us now consider the basic laws governing the flow of double-phase mixtures.

1. Equations of Consumption

From the assumptions made about the stationarity of the flow and of the constancy of the mass consumptions of the phases, it follows that in each cross section of the channel the mass consumption of the phase concentrations will be constant. As is well known, in double-phase flows it is necessary to distinguish between local mass concentration of phases (concentration of phases in a given volume) and consumption mass concentration of phases (correlation between mass consumption of the phases through one and the same cross section of the conduit.) With the above-given assumptions the local mass concentration of phases will depend upon the correlation of phase velocities at a given point and may vary within very broad limits.

Actually if the mass consumptions and the velocities of the phases in the given cross section of the channel are respectively equal to G_{Γ} and G_K , c_{Γ} and c_K , then a unit volume near the section under consideration contains $\rho_{\Gamma v} = G_{\Gamma}/Fc_{\Gamma}$ kg of gas and $\rho_{Kv} = G_K/Fc_K$ kg of particles. The values of $\rho_{\Gamma v}$ or ρ_{Kv} can be considered as the density of the phase, averaged according to volume. Between the mean density of the phase and its true density the following correlations exist:

$$\rho_{r \ v} = \rho_r \left(1 - \frac{\rho_{k \ v}}{\rho_k}\right); \quad \rho_{k \ v} = \rho_k \left(1 - \frac{\rho_{r \ v}}{\rho_r}\right),$$

where the true densities of the phases ρ_r and ρ_k are determined from state equations of the phases. We will consider the gas phase to be a pure gas and the particles to be incompressible, then the state equations of the phases have the form:

$$\rho_r = \frac{p}{RT}; \quad (1)$$

$$\rho_k = \text{const.} \quad (2)$$

The correlations for the local mass and consumption mass concentration of the phases are: /14

$$g_{r \ v} = \frac{\rho_{r \ v}}{\rho_{r \ v} + \rho_{k \ v}} = \frac{1}{1 + \frac{G_k c_r}{G_r c_k}}, \quad g_{k \ v} = \frac{\rho_{k \ v}}{\rho_{r \ v} + \rho_{k \ v}} = \frac{1}{1 + \frac{G_r c_k}{G_k c_r}}; \quad (3)$$

$$g_r = \frac{G_r}{G_r + G_k}, \quad g_k = \frac{G_k}{G_r + G_k}. \quad (4)$$

From equation (3) it is seen that with constant mass consumptions of the phases and changes in the velocity of the particles of a given cross section from zero to c_r , the local concentration of particles decreases from unity to g_k , at the same time the local concentration of the gas is increased from zero to g_r . Where $c_k \equiv c_r$, the local and consumption concentration of the phases correspond.

For a linear flow the equations for phase consumption are:

$$G_r = F c_r \rho_{r \ v} = F c_r \rho_r \left(1 - \frac{G_k \rho_{r \ v} c_r}{G_r \rho_k c_k}\right),$$

$$G_k = F c_k \rho_{k \ v} = F c_k \rho_k \left(1 - \frac{\rho_{r \ v}}{\rho_r}\right).$$

These expressions are distinguished from the usual equations of consumption $G = F c \rho$ of a single-phase flow by the fact that they have a supplementary factor which allows for the blocking of the conduit cross-sections by the other phase. For example, for the gas phase the blocking of the cross section by particles comprises

$$\frac{G_K \rho_r c_r}{G_r \rho_K c_K} \approx \frac{G_K \rho_r c_r}{G_r \rho_K c_K}.$$

With a great consumption of particles ($G_K \gg G_r$) or where their velocity is small in comparison with the gas ($c_K \ll c_r$), the blocking of a cross section may be substantial. However, with $G_K \leq G_r$ and small particles (when the particles lag insignificantly behind the flow of the gas, i.e., $c_K \approx c_r$) the blocking of a cross section is a value on the order of ρ_r/ρ_K . Under the moderate pressures that are characteristic of the flow portion of engines, and even more at high temperatures, the density of a gas is 100-1000 times lower than the density of a majority of liquid and solid bodies; therefore, the relationship ρ_r/ρ_K in comparison with unity can be ignored and the equations of consumption of the gas phase can be accepted in the usual form:

$$G_r = F c_r \rho_r. \quad (5)$$

Equations of particle consumption can even be written in the following form:

$$G_K = F c_K n_v m. \quad (6)$$

2. The Equation of Particle Motion

/15

In the general case, with the motion of a particle in a gas flow, the following forces act upon it:

- (a) the force of aerodynamic resistance;
- (b) the force due to acceleration of particles relative to the gas;
- (c) the force due to the pressure gradient in the flow;
- (d) the force due to temperature gradient in the flow;
- (e) mass force (for example, the force of gravity or electromagnetic force with the motion of a charged particle in an electromagnetic field).

In the majority of practical cases, the force of aerodynamic resistance is the fundamental force acting upon a particle; the remaining forces are small in comparison with it.

Actually, for example, a supplementary force equal to $\rho_r V_K (dc_{rel}/d\tau)$, where V_K is the volume of the particle in an accelerating flow, acts upon a particle with the relative acceleration $dc_{rel}/d\tau$. Under the action of the longitudinal pressure gradient,

the mass of gas in a volume occupied by particles would move with an acceleration $dc_r/d\tau$; therefore, the force caused by the pressure gradient is equal to $\rho_r V_K (dc_r/d\tau)$. Both of these forces act according to the direction of the flow velocity so that their sum is

$$P_\Sigma = \rho_r V_K \left(\frac{dc_{rel}}{d\tau} + \frac{dc_r}{d\tau} \right).$$

With large particles $dc_{rel}/d\tau \rightarrow dc_r/d\tau$ and $P_\Sigma \sim 2\rho_r V_K (dc_r/d\tau)$. The order of magnitude of the ratio of this force to the force of the hydrodynamic activity of a flow P is equal to

$$\frac{P_\Sigma}{P} = \frac{\rho_r \pi d^3 2 dc_r}{6 d c_K \pi d^2 \rho_r c_{rel}^2} \sim 5 \frac{d}{L_c}.$$

Since usually $d \ll L_c$, it is then possible to ignore the value P_Σ , which is small in comparison with P .

With small particles $(dc_{rel}/d\tau) \rightarrow 0$ and $P_\Sigma \sim \rho_r V_K (dc_K/d\tau)$, i.e., the effect of this force is equivalent to the effect of an apparent increase in the particle mass on the mass of the displaced gas volume. Where $\rho_r \leq 0.01 \rho_K$, ignoring the effect of the increase in particle mass does not lead to noticeable error.

Certainly, with motion of light particles in the flow of a very intensely compressed gas or in the flow of their liquid it is impossible to ignore this effect. In particular this relates to the motion of gas bubbles in an incompressible liquid; in this case the effect of mass increase will, to a significant degree, determine the nature of their motion.

The force specified by the pressure gradient can only be significant with the passage of a particle through a compression wave. /16
If the diameter of the particle is significantly greater than the thickness of the compression wave, then the force acting upon the particle with the passage of the compression wave, can be evaluated according to formula

$$P_{ck} \sim \frac{\pi d^2}{4} \Delta p,$$

where Δp is the change in gas pressure in the compression wave.

Relating this force to the force of gravity acting upon the particle $mg = \frac{\pi d^3}{6} \rho_K g$, we obtain

$$\frac{P_{ck}}{mg} \sim \frac{3}{2} \frac{\Delta p}{\rho_K g d}. \quad (7)$$

where $\Delta p = 10^5 \text{ n/m}^2$, $\rho_K = 1000 \text{ kg/m}^3$; $g = 9.81 \text{ m/sec}^2$ and $d = 5 \cdot 10^{-6} \text{ m}$, the ratio of P_{ck}/mg $3 \cdot 10^6$.

It is necessary to bear in mind that the duration of the effect of this force, with passage of a particle through compression waves, is $\Delta\tau \approx d/c_K$. Using the equation for a change in the amount of motion in the form $P_{ck}\Delta\tau \sim m\Delta C_K$, it is possible to judge the amount of change in velocity of a particle in a compression wave:

$$\Delta C_K \sim \frac{P_{ck}\Delta\tau}{m} \sim \frac{3\Delta p}{2\rho_K c_K}. \quad (8)$$

with the same values of Δp and ρ_K , as above, $\Delta C_K \sim 150/c_K$.

From the correlation obtained, it is seen that due to the effect of the force caused by the pressure gradient, the velocity of a particle, in passing through a compression wave, changes little. Therefore, after the compression wave the particle velocity will substantially exceed the gas velocity. This leads to the appearance of an inhibiting force of hydrodynamic resistance, the value of which may also be very significant. Under the effect of the indicated forces, with the passage of a compression wave, deformation and even destruction of the liquid particles may take place.

Let us consider the force caused by the temperature gradient in a flow. As is well known, a particle placed in a medium with a large temperature gradient, begins to move under the influence of the gas molecules towards the region with a lower temperature. Such a phenomenon, which has been called thermophoresis, is considered in reference [54], in which the following formula for determining the force of thermophoresis, accurate for moderate temperature gradients, is presented:

$$P_\tau = -\alpha \frac{\mu_r^2 d \text{grad } T}{2\rho_r T}, \quad (9)$$

where $\alpha = \frac{9\pi\lambda_\Gamma}{2\lambda_\Gamma + \lambda_K}$.

We equate this force with the force of gravity upon the particle: /17

$$\frac{P_\tau}{mg} = \frac{\alpha}{g\rho_r\rho_K} \frac{\mu_r^2}{d^2} \frac{\text{grad } T}{T}. \quad (10)$$

Under usual flow conditions the temperature gradient is small, and this ratio may be less than unity. However, in the case of a highly heated double-phase flow over an intensively cooled surface, the temperature gradient in the thermal boundary layer may be very large ($\text{grad } T > 10^5 \text{ }^\circ\text{K/m}$). In this case relationship (10) may be

substantially higher than unity. Thus, where $\lambda_K = 5\lambda_T$, $\mu_T = 5 \cdot 10^{-5}$ n \times sec/m², $d = 5 \cdot 10^{-6}$ m, grad $T = 10^5$ °K/m, $T = 1000$ °K, $\rho_T = 1$ kg/m³, $\rho_K = 1000$ kg/m³, this ratio is approximately equal to 4. With $d = 10^{-6}$ m and the same other parameters, the force produced by the temperature gradient exceeds the force of gravity acting upon a particle by approximately 100 times. This force is relatively small, however, it may have substantial influence on the motion of particles near the surface and in particular may facilitate its precipitation upon this surface [42].

Let us now consider the aerodynamic resistance force of a particle. As is well known, the force of the aerodynamic effect of a gas upon a body moving in it is

$$P = C_x f \rho_T \frac{c_{rel}^2}{2}, \quad (11)$$

where $C_x = C_x(Re_{rel})$ is the coefficient of space resistance of a body;

$$Re_{rel} = \frac{c_{rel} \rho_T d}{\mu_T} \text{ is the Reynolds number in relative motion;}$$

f is the cross section area of the body.

For very small spherical solid particles moving at a low constant speed in an immobile gas with $Re_{rel} < 1$, the coefficient of resistance was theoretically determined by Stokes in the form

$$C_x = \frac{24}{Re_{rel}}. \quad (12)$$

For larger particles moving at a constant speed with elevated Reynolds numbers ($1 < Re_{rel} < 10^4$), the coefficient of resistance C_x , determined experimentally by a number of investigators, is presented in Figure 1.

The resistance coefficient of a particle depends upon its acceleration. However, data available in the literature on the influence of acceleration on C_x are contradictory; it is only possible to note that with accelerations of the flow, characteristic of jet nozzles, it is small. Therefore, with a precision sufficient for engineering calculations it is possible to accept the values of the resistance coefficient of liquids and solid particles, moving with an acceleration, based on the data obtained at a constant relative velocity of particle motion.² /18

² In reference [58] it is noted that with the passage of a shock wave, i.e., with very great accelerations, the resistance coefficient of a particle may differ by 2-3 times from the resistance coefficient obtained under stationary conditions (author's note).

Moreover the resistance coefficient of a liquid particle must depend upon the degree of its deformation by the leading flow and

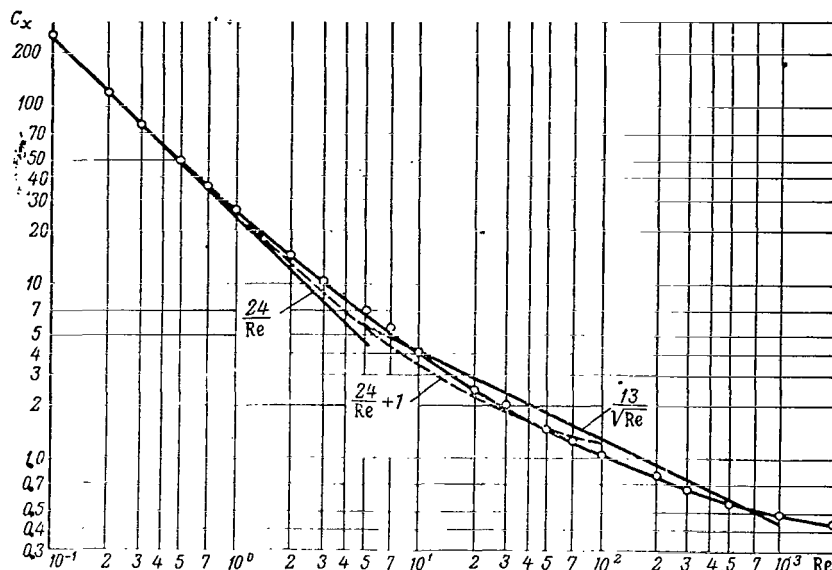


Fig. 1. Resistance Coefficient of a Sphere as a Function of the Reynolds Number.

upon the circulation in it directed toward the lateral surface according to the relative velocity and the decreasing resistance of the particle. However, as was already noted, it is possible to ignore the deformation of small particles. Experimental studies showed that, due to the influence of surface-active substances, the amount of circulation appearing in a liquid particle and its influence on the resistance coefficient are negligible. This is even more true of a rotating liquid particle.

With very low pressures, when the length of the free path of gas molecules significantly exceeds the diameter of the particles, the coefficient of its resistance will even depend upon the rarefaction of the gas [22]. However, if the pressure in the exit section of the nozzle $p_c > 0.05 \cdot 10^5 \text{ n/m}^2$, it is possible to ignore the /19 influence of gas rarefaction.

With an analytical investigation, particles of motion approximate the experimental curves (cf. Fig. 1) by various dependences [34]:

$$\left. \begin{array}{ll} \text{when } Re_{rel} = 10^{-4} - 1 & C_x = \frac{24}{Re_{rel}}; \\ \text{when } Re_{rel} = 10 - 10^3 & C_x = \frac{13}{\sqrt{Re_{rel}}}; \\ \text{when } Re_{rel} \geq 10^3 & C_x \approx 0.48. \end{array} \right\} \quad (13)$$

Moreover, if Re_{rel} does not exceed several hundreds, the resistance coefficient of the particle may be approximated by the dependence

$$C_x = \frac{a}{Re_{rel}} + b, \quad (14)$$

where a and b are certain constant values determined from the condition of maximum approximation to the experimental curve.

From equations (11) and (12) we obtain the following expression for the force acting upon a particle (Stokes' formula):

$$P = 3\pi\mu_r d c_{rel}. \quad (15)$$

The formula is correct in the range $10^{-4} < Re_{rel} < 1$. The ratio of this force to the force of gravity acting upon the particle is

$$\frac{P}{mg} = \frac{18\mu_r c_{rel}}{\rho_K g d^2}. \quad (16)$$

Where $\mu_r = 5 \cdot 10^{-5}$ n.sec/m², $\rho_K = 1000$ kg/m³, $d = 5 \cdot 10^{-6}$ m and $c_{rel} = 10$ m/sec, this ratio is equal to $3.6 \cdot 10^4$; where $d = 2 \cdot 10^{-6}$ m and the same other parameters remain, the force of the aerodynamic influence of a flow on a particle exceeds the force of gravity acting upon the particle by more than $20 \cdot 10^4$ times.

According to Figure 1, with a motion of larger particles, characterized by $Re_{rel} > 1$ numbers, the resistance coefficient C_x is decreased; however, at the same time the velocity of the particles relative to the gas substantially increases. Therefore, the hydrodynamic force of the influence of a flow on a particle will also be several orders of magnitude higher than the force of gravity acting upon it.

From the above-given evaluation it follows that with study of the fundamental characteristics of the flow of double-phase mixtures, under conditions characteristic of jet nozzles and turbines, it is possible to ignore all supplementary forces acting upon a particle as being small in comparison with the force of the aerodynamic influence of the flow. Thus, the equation for linear motion of a particle will have the following appearance:

/20

$$m \frac{dc_K}{dt} = P = C_x f \rho_r \frac{c_{rel}^2}{2}.$$

Insofar as $d\tau = dx/c_K$, then

$$\frac{dc_k}{dx} = 0.75C_x \frac{\rho_r}{\rho_k} \frac{c_{rel}^2}{c_{kd}}. \quad (17)$$

In the case of a nonlinear flow, when the directions of the velocity of the gas and the particle do not correspond, this equation can be written in vector form:

$$\frac{\vec{dc_k}}{dx} = 0.75C_x \frac{\rho_r}{\rho_k} \frac{c_{rel}}{c_{kd}} \vec{c_{rel}}$$

3. The Equation of Gas Motion

In a double phase flow, besides the forces of pressure on the part of the neighboring elements, the total force of resistance of all particles present in the considered volume act upon each element of the gas phase. With a positive acceleration this force is directed against the flow and leads to a certain retardation of it. In this case the equations of motion of an elementary gas volume Fdx will have the form

$$\rho_r F dx \frac{dc_r}{dx} = -F dp - P n_g F dx.$$

After transformations this equation, relative to 1 kg of gas, can be written as

$$\frac{dc_r}{dx} + \frac{g_k}{g_r} \frac{dc_k}{dx} + \frac{1}{c_r \rho_r} \frac{dp}{dx} = 0. \quad (18)$$

4. The Energy Equation

From the assumptions of flow stationarity and absence of heat exchange with the surrounding medium, it follows that the total energy of a double-phase flow in any cross section of the conduit must be equal, i.e.,

$$G_r \left(\frac{c_r^2}{2} + i_r \right) + G_k \left(\frac{c_k^2}{2} + i_k \right) = \text{const.}$$

This equation, relative to 1 kg of the gas phase, acquires the following appearance:

$$\frac{c_r^2 - c_{r0}^2}{2} + \frac{g_k}{g_r} \frac{c_k^2 - c_{k0}^2}{2} = c_{pr} (T_{r0} - T_r) + \frac{g_k}{g_r} c_{pk} (T_{k0} - T_k). \quad (19)$$

The left-hand side of (19) expresses the change of kinetic energy of the mixture and the right-hand side, the change in enthalpy

of its components. As opposed to a single-phase flow, where the gas temperature T_r and T_{r0} are connected by a simple adiabatic equation, in the obtained equation the value of T_r is a complex function of the thermal and mechanical interaction of the gas with the particles. The temperature of the particles T_k depends basically upon the intensity of their heat exchange with the gas.

5. *The Equation for the Heat Exchange Between Particles and Gas*

The heat exchange between particles and a gas is a nonstationary process since the temperature of the phases and the conditions of the particle flow are directly changed by the gas (density of the gas, relative velocity of the flow). However in double-phase flows with small particles these changes proceed at velocities substantially smaller than the velocity of the processes of heat exchange between phases. Therefore, in first approximation, the process of heat exchange can be considered to be stationary.

As is well known, the distribution of temperature in a sphere, which has a liquid flowing past it, to a significant degree is determined by the Biot number $Bi = \alpha d / 2\lambda_k$ (where α is the coefficient of heat emission), representing the ratio of the internal thermal resistance of heat conductivity to the external thermal resistance of heat emission. With small values of the Biot number ($Bi < 0.1$) it is possible to ignore the temperature gradient along the radius of the sphere since, in this case, the heat flow is limited basically by the external thermal resistance and, due to the relatively small internal thermal resistance, the temperature inside the sphere is leveled out.

For small particles moving in a gas at small relative velocities, (i.e., with small Re_{rel} numbers), the coefficient of heat emission α is basically determined by the coefficients of heat conductivity in the gas, so that $\alpha = 2\lambda_r / d$ and $Bi \approx (\lambda_r / \lambda_k)$. Since usually the coefficient of heat conductivity of gases λ_r is significantly less than the coefficient of heat conductivity of liquid and solid bodies λ_k , then $Bi \ll 1$. Thus it is possible to accept, with a sufficient degree of precision, that the temperature in the center and on the surface of small particles is equal.

Considering the preceding, the equation of heat exchange between particles and the gas can be written in the form

$$\frac{\pi d^3}{6} \rho_k c_{p_k} dT_k = \frac{\pi d^2 \alpha}{c_k} (T_r - T_k) dx$$

or

$$\frac{dT_k}{dx} = \frac{6\alpha}{c_{p_k} \rho_k d} \frac{T_r - T_k}{c_k}. \quad (20)$$

There are a number of theoretical and experimental studies on /22 the coefficient of heat emission of various bodies as a function of the conditions of heat exchange. In particular, for a sphere with small Re_{rel} numbers and $Pr \approx 1$, according to the experimental data of A.P. Sokol'skiy [23], it is possible to accept

$$Nu = 2(1 + 0.08 Re_{rel}^{0.66}), \quad (21)$$

where $Nu = \alpha d / \lambda_r$, i.e., the Nusselt number.

Thus, after several simplifications and transformations, we obtain the following system of equations describing the linear flow of a double-phase mixture in a conduit of the given form $F = F(x)$:

$$\left. \begin{aligned} \frac{dc_K}{dx} &= 0.75 C_x \frac{\rho_r}{\rho_K} \frac{c_{rel}^2}{c_K d}; \\ \frac{dc_r}{dx} + \frac{g_K}{g_r} \frac{dc_K}{dx} + \frac{R}{c_r \rho_r} \left(\rho_r \frac{dT_r}{dx} + T_r \frac{d\rho_r}{dx} \right) &= 0; \\ \frac{c_r^2 - c_{r0}^2}{2} + \frac{g_K}{g_r} \frac{c_K^2 - c_{K0}^2}{2} &= c_{pr} (T_{r0} - T_r) + \frac{g_K}{g_r} c_{pK} (T_{K0} - T_K); \\ \frac{dT_K}{dx} &= \frac{6\alpha}{c_{pK} \rho_K d} \frac{T_r - T_K}{c_K}; \\ F \rho_r c_r &= G_r, \end{aligned} \right\} \quad (22)$$

where $C_x = C_x(Re_{rel})$; $\alpha = \frac{\lambda_r}{d} Nu(Re_{rel})$; $Re_{rel} = \frac{c_{rel} \rho_r d}{\mu_r}$.

This system consists of five equations and contains five unknown quantities: c_r , c_K , ρ_r , T_r and T_K , depending upon x , consequently system (22) is closed. The values g_K and g_r (or consumptions of the phases G_K and G_r), ρ_r , d and the physical characteristics of the gas c_{pK} , c_{pr} , λ_r , μ_r , will be considered to be known.

§3. Limiting Cases of the Flow of Double-Phase Mixtures

1. Transformation of the System of Equations (22) in the Case of Very Large or Very Small Particles

With very large or very small particles the system of equations (22) is significantly simplified. Actually very large particles and especially particles possessing high density are weakly attracted by a gas flow due to their own inertia. Therefore, as a limiting case it is possible to accept that they pass through a conduit at a constant velocity equal to the initial velocity of their motion and it is possible to ignore the equation of particle motion.

Moreover, with large particles it is possible to ignore even the heat exchange between phases. In particular this relates to /23 the case when, in the initial cross section of the conduit the tem-

peratures of the particles and the gas are equal, since at the same time the heat exchange is to a significant degree still hindered by the fact that the temperature of the gas in the boundary layer on the surface of a particle is constant and equal to the initial temperature of the flow (i.e., the temperature of the particle).

Since $dc_K/dx = 0$, the second term of the left-hand side of the equation of gas phase motion vanishes and is then converted into the usual equation for gas motion

$$c_r dc_r + \frac{dp}{\rho_r} = 0. \quad (23)$$

The energy equation also takes on the form which is usual for the flow of a pure gas:

$$\frac{c_r^2 - c_{r0}^2}{2} = c_{pr}(T_{r0} - T_r). \quad (24)$$

Certainly, particles moving in a gas at a great relative velocity perturb the flow and may lead to a deviation in the gas flow process from a reversible adiabatic process. However, as will be shown in the following chapter, losses due to friction of the gas on large particles, when they are in constant moderate concentration, are small. This is explained by the fact that with an increase in the diameter of the particles their number in a double-phase flow swiftly diminishes.

Thus, in the case of very large particles in moderate concentration, the flow of a gas phase in almost no way differs from the flow of a pure gas.

We shall now consider the Stokes' equation of motion for very small particles:

$$\frac{dc_K}{dx} = \frac{18\mu_r}{\rho_K d^2} \frac{c_r - c_K}{c_K}. \quad (25)$$

Since where $d \rightarrow 0$ the coefficient $(18\mu_r/\rho_K d^2) \rightarrow \infty$ and the left-hand side of the equation is limited (with the exception of compression waves, which are not considered in this study), then the relative velocity $c_r - c_K \rightarrow 0$. Thus, with a decrease in the diameter of a particle, its velocity will approximate the velocity of the gas. Let us suppose that for very small particles $c_K \equiv c_r$.³

³ According to reference [54], where $d < 10^{-8}$ m, the resistance of a particle $P \sim d^2 c_{rel}$; therefore, the coefficient where $(c_r - c_K)/c_K$ will be proportional to $1/d$. Evidently at the same time results of the discussions are not changed (author's note).

Analogously, considering the equation for heat exchange between particles and gas and, keeping in mind that with very small particles having coefficients of heat emission $\alpha = (2\lambda_{\Gamma}/d) \rightarrow \infty$, in the limiting case we obtain $T_K \equiv T_{\Gamma}$. Then the equation for gas phase motion /24 and the energy equation acquire the following form:

$$\frac{cd c}{g_r} + \frac{dp}{p_r} = 0; \quad (26)$$

$$\frac{c^2 - c_0^2}{2g_r} = c_p (T_0 - T), \quad (27)$$

where $c \equiv c_K \equiv c_{\Gamma}$ and $T \equiv T_K \equiv T_{\Gamma}$ are the equilibrium velocity and temperature of the mixture (in the future, parameters without indices relate to an equilibrium flow of the mixture);

$$c_p = c_{p\Gamma} + \frac{g_K}{g_{\Gamma}} c_{pK} \text{ is the specific heat } 1 + \frac{g_K}{g_{\Gamma}} \text{ kg of a mixture.}$$

The obtained equations differ from the equations for a flow of a pure gas only by the supplementary factors. Thus the factor $1/g_{\Gamma}$ in the equations of motion and energy equations is due to the fact that the work of extending 1 kg of the gas phase in the case of an equilibrium flow leads to an increase in kinetic energy of $1/g_{\Gamma}$ kg of the mixture. The difference of the coefficient c_p from $c_{p\Gamma}$ in the right-hand side of the energy equation characterizes the increase in the efficiency of the gas due to the conduction of heat from the particles to it. Let us examine how the state of the gas phase changes with an equilibrium expansion of a double-phase flow. With a change in temperature of the particles by dT , the amount of heat

conducted from the particles to 1 kg of gas is equal to $\frac{g_K}{g_{\Gamma}} c_{pK} dT$.

According to the first law of thermodynamics this heat is expended on the change in gas enthalpy and on the work of forcing it in a field of variable pressures; i.e.,

$$-\frac{g_K}{g_r} c_{pK} dT = c_{p\Gamma} dT - \frac{dp}{p_r}. \quad (28)$$

Having substituted expression (1) here, we obtain

$$(c_{p\Gamma} + c_{pK} \frac{g_K}{g_r}) \frac{dT}{RT} = \frac{dp}{p}.$$

Integration of this equation gives

$$\frac{p}{\rho_r^n} = \frac{p_0}{\rho_{r0}^n} = \text{const} \quad \text{or} \quad \frac{T}{T_0} = \left(\frac{p}{p_0} \right)^{\frac{n-1}{n}}. \quad (29)$$

In these expressions

$$n = \frac{c_{p\Gamma} + \frac{g_K}{g_\Gamma} c_{pK}}{c_{v\Gamma} + \frac{g_K}{g_\Gamma} c_{pK}} = \frac{1 + \vartheta}{\frac{1}{k} + \vartheta}, \quad (30)$$

where

/25

$$k = \frac{c_{p\Gamma}}{c_{v\Gamma}}; \quad \vartheta = \frac{g_K}{g_\Gamma} \frac{c_{pK}}{c_{p\Gamma}}.$$

Thus with an equilibrium expansion of a double-phase mixture, the change in the state of the gas phase takes place according to polytropic law with the index n , defined according to formula (30).

The difference in the polytropic index n from the adiabatic index k is defined by the amount of heat contained in the suspended phase. With a decrease in the value $\vartheta = g_K c_{pK} / (g_\Gamma c_{p\Gamma})$ the index $n \rightarrow k$. In the limiting case ($\vartheta \rightarrow 0$) $n = k$, i.e., the process of expansion of the gas phase will usually be adiabatic. With an increase in ϑ the value n may substantially differ from the value k ; here in any case $n \leq k$.

We note that analogous conclusions may be obtained even for the case of an equilibrium compression of a double-phase mixture. Actually, the amount of heat conducted from the gas to the suspended phase with an increase in the temperature of the mixture in the process of compression by dT , is equal to $\frac{g_K}{g_\Gamma} c_{pK} dT$. At the same time, (28) (29) and (30) remain without change.

2. The Speed of Sound in Double-Phase Mixtures

As is well known, the speed of sound propagation in an elastic medium is

$$a = \sqrt{\left(\frac{\partial p}{\partial \rho} \right)_s}. \quad (31)$$

The partial derivative $\partial p / \partial \rho$ is taken with constant entropy, which in a single-phase medium is equivalent to the assumption of absence of heat exchange in a sound wave with the surrounding medium,

and dissipation of energy independent of the nature of change in the state of the medium as a whole. (For example, in a pure gas, even given polytropic processes with elevation or elimination of heat and a polytropic index $n \neq k$, the speed of sound is determined by the value of the adiabatic index k).

Since the values p and ρ are connected by the adiabatic equation, resulting from the condition $S = \text{const}$, the partial derivative $(\partial p / \partial \rho)_S$ in equation (31) may be replaced by the usual derivative $dp/d\rho$.

In double-phase mixtures with very small particles, even with the absence of heat exchange with the surrounding medium, a process of expansion i.e., contraction of the gas in a sound wave can be distinguished from the adiabatic, due to the heat and energy exchange of the gas with the particles. As was shown above, in the limiting case where $T_{\Gamma} \equiv T_K$, the process of expansion and contraction of the gas is polytropic, with the index $n < k$. Substituting the polytropic equation (29) into expression (31) and considering that where $c_{\Gamma} \equiv \frac{1}{26}$ c_K the density of the mixture is

$$\rho = \rho_{\Gamma} v + \rho_K v = \frac{1}{g_{\Gamma}} \rho_{\Gamma}, \quad (32)$$

we obtain the following expression for an equilibrium speed of sound in a double-phase mixture:

$$a_p = \sqrt{g_{\Gamma} n R T}. \quad (33)$$

The difference between this formula and the usual expression for the speed of sound in a pure gas $a = \sqrt{k R T}$ consists in the appearance of a supplementary factor g_{Γ} which allows for the increase in the oscillating mass and in the substitution of the adiabatic index k by the polytropic index n .

If the particles are very large, then they participate very slightly in the acoustic oscillations of the medium and the heat exchange between phases is also substantially worsened. In this case, the speed of sound in a double-phase mixture will approximate the speed of sound in a pure gas:

$$a = \sqrt{k R T}. \quad (34)$$

The oscillations of particles suspended in gas under the action of sound waves is considered in [54]. Let us assume that the resistance of the medium is inertialess and follows Stokes' law, and that the medium performs harmonic oscillations

$$u_r = u_{r0} \sin \omega \tau, \quad (35)$$

where u_{r0} is the amplitude of oscillation velocity of the medium; $\omega = 2\pi\nu$ is the angular frequency of oscillations; ν is the frequency of oscillations. Then the equation for the oscillating motion of the particle will have the form

$$m \frac{du_k}{d\tau} = 3\pi\mu_r d(u_r - u_k) \quad \text{or}$$

$$m \frac{du_k}{d\tau} + 3\pi\mu_r du_k = 3\pi\mu_r du_{r0} \sin \omega\tau. \quad (36)$$

Solution to this equation gives the following expression for the relation of amplitudes of oscillation velocities of a particle in the medium, and for a shift in oscillation phases:

$$\frac{u_{k0}}{u_{r0}} = \frac{1}{\sqrt{1 + z_u^2}} \quad (37)$$

$$\tan(\varphi_r - \varphi_k) = z_u, \quad (38)$$

where $z_u = \frac{\pi\nu\rho_K d^2}{9\mu_r}$ is a dimensionless parameter; and $\varphi_r - \varphi_k$ is the shift in oscillation phase of the medium and particle.

Oscillation of the temperature of a particle θ_K which is located in a medium with variable temperature can be considered to be completely analogous. Let us consider the case when the temperature of the medium also varies according to sinusoidal law $\theta_r = \theta_{r0} \sin \omega\tau$. In this case the equation of heat exchange (20) is rewritten in the form

$$\frac{d\theta_k}{d\tau} + \frac{12\lambda_r}{c_p \kappa \rho_K d^2} \theta_k = \frac{12\lambda_r}{c_p \kappa \rho_K d^2} \theta_{r0} \sin \omega\tau. \quad (39)$$

Evidently, the solution to this equation will have a form analogous to the solution to equation (36). In particular, the ratio between the amplitude of oscillation of the temperature of a particle and that of the gas is

$$\frac{\theta_{k0}}{\theta_{r0}} = \frac{1}{\sqrt{1 + z_\theta^2}}, \quad (40)$$

and the phase shift is

$$\tan(\varphi_r - \varphi_k) = z_\theta, \quad (41)$$

where $z_\theta = \frac{\pi\nu c_p \rho_K d^2}{6\lambda_K}$ is a dimensionless parameter.

As follows from formulas (37), (38), (40) and (41) where $z_u \leq 0.1$ and $z_\theta \leq 0.1$ the velocity of oscillations of particles and their temperature are changed with almost the same amplitude and in the same phase as that of the medium. Therefore, in such environments the speed of sound propagation can be determined according to the formula for the equilibrium speed of sound (33). For example, in a double-phase mixture with the parameters $\mu_r = 5 \cdot 10^{-5} \text{ n} \cdot \text{sec}/\text{m}^2$, $\lambda_r = 0.146 \text{ W}/\text{m} \cdot \text{°K}$, $c_{pK} = 2100 \text{ J}/\text{kg} \cdot \text{°K}$, $d = 2 \mu\text{m}$, $\rho_K = 2000 \text{ kg}/\text{m}^3$ and $\nu \leq 2000 \text{ Hz}$, the values z_u and z_θ do not exceed 0.1, so that the speed of sound can be considered to be equilibrium.

Where $z_u \geq 10$ and $z_\theta \geq 10$ amplitudes of velocity and temperature of a particle are made negligibly small in comparison with the amplitude of velocity and temperature of the gas, moreover, a great shift in phase occurs. Therefore, it is possible to consider that a particle does not participate in acoustic oscillations and that heat exchange between particles and the gas is not present in a sound wave. In such a double-phase mixture it will be equal to the speed of sound in a pure gas [cf. equation (34)].

It is possible to have a case when $z_u \leq 0.1$ and z_θ is rather high. For example, this is possible with a gas of very low heat conductivity. In this case, particles oscillate together with the gas, but heat exchanges between the phases in the sound waves are absent, and the speed of sound can be determined according to the formula:

$$a = \sqrt{g_r k R T}. \quad (42)$$

(In addition the flow of a double-phase mixture in a channel may, /28
generally speaking, be equilibrium even in temperature, i.e.,
polytropic with the index $n < k$).

It is apparent from the given formulas that the degree of increase of particles by the gas, and the intensity of heat exchange between the phases in sound waves where $0.1 < z_u$, $\theta < 10$ depends on the entire number of physical parameters of the phases, on the size of particle d and also on the frequency of sound waves. With an increase in the frequency of oscillations, the velocity and temperature lag of the particles behind the gas increases. Therefore the speed of sound propagation in double-phase mixtures will depend, as opposed to single-phase media, even on tone height. It is known that in gases an analogous dependence takes place only at a very high frequency of the sound waves. In double-phase media with a very low wave frequency, the speed of sound even depends upon the form of the leading front of the perturbation.

3. Use of Hydrodynamic Functions for Calculating Equilibrium Double-Phase Flows

As was already noted, equations of motion and energy of an

equilibrium flow of double-phase mixtures are very similar to the corresponding equations of single-phase flows. Having made use of this similarity, it is possible to obtain a number of correlations between the parameters of equilibrium double-phase flows analogous to the corresponding correlations for the flow of a pure gas. This allows one to use the well-developed methods for studying gas flows; in particular the method of hydrodynamic functions can be used even for studying double-phase flows.

Let us first introduce the concept of temperature damping of an equilibrium double-phase flow. Just as for a pure gas, we shall consider temperature damping of an equilibrium flow to be its temperature in a cross section where the velocity is equal to zero. From the energy equation (27) it follows that

$$T^* = T + \frac{1}{g_r c_p} \frac{c^2}{2}. \quad (43)$$

Hence the exhaust velocity of the mixture is

$$c = \sqrt{2g_r c_p (T^* - T)}. \quad (44)$$

By the critical section in a double-phase equilibrium flow of a pure gas, we mean that cross section of the conduit, in which the velocity of flow is equal to the local speed of sound. The temperature of a mixture in the critical cross section of an equilibrium double-phase flow can be determined, having used expression (33), from the correlation

$$c_{cr} = \sqrt{2g_r c_p (T^* - T_{cr})} = \sqrt{g_r n R T_{cr}} \quad \text{in the form} \quad (45)$$

$$T_{cr} = \frac{2}{n+1} T^*.$$

Substituting this expression into equation (33), we find the speed of sound in the critical section /29

$$a_{p, cr} = \sqrt{g_r \frac{2n}{n+1} R T^*}. \quad (46)$$

The reduced speed of a phase mixture is

$$\lambda = \frac{c}{a_{p, cr}} = \sqrt{\frac{n+1}{n-1} \left(1 - \frac{T}{T^*}\right)}. \quad (47)$$

From this correlation we determine the hydrodynamic function τ of an equilibrium double-phase flow:

$$\tau = \frac{T}{T^*} = 1 - \frac{n-1}{n+1} \lambda^2. \quad (48)$$

Having used the polytropic equation (29) we obtain the following expressions for two other hydrodynamic functions:

$$\pi = \frac{p}{p^*} = \left(1 - \frac{n-1}{n+1} \lambda^2\right)^{\frac{n}{n-1}}; \quad (49)$$

$$\varepsilon = \frac{\rho}{\rho^*} = \frac{\rho_r}{\rho_r^*} = \left(1 - \frac{n-1}{n+1} \lambda^2\right)^{\frac{1}{n-1}}. \quad (50)$$

For the critical section these hydrodynamic functions are written thus:

$$\left. \begin{aligned} \tau_{cr} &= \frac{T_{icr}}{T^*} = \frac{2}{n+1}; \\ \pi_{cr} &= \frac{p_{cr}}{p^*} = \left(\frac{2}{n+1}\right)^{\frac{n}{n-1}}; \\ \varepsilon_{cr} &= \frac{\rho_{icr}}{\rho^*} = \frac{\rho_{r,icr}}{\rho_r^*} = \left(\frac{2}{n+1}\right)^{\frac{1}{n-1}}. \end{aligned} \right\} \quad (51)$$

Figure 2 presents changes in the parameters τ_{cr} , π_{cr} , ε_{cr} , $m_{cr} = \sqrt{n \left(\frac{2}{n+1}\right)^{\frac{n+1}{n-1}}}$ and n depending upon the value $\vartheta = \frac{g_r}{g_r^*} \frac{c_{p,r}}{c_{p,r}^*}$, determining, according to equation (30), the dependence of n on k ; the value k for the gas phase is taken to be equal to 1.4. As is seen from this figure, the critical ratio of pressures $\pi_{cr} = p_{cr}/p^*$, and consequently, even the temperature $\tau_{cr} = T_{cr}/T^*$ for a mixture can prove to be greater for a pure gas. The values ε_{cr} and m_{cr} for a mixture are somewhat reduced in comparison with the pure gas.

Analogously we obtain expressions for the remaining hydrodynamic functions of an equilibrium double-phase flow: /30

$$q(\lambda) = \frac{\rho c}{\rho_{cr} a_{p,cr}} = \frac{F_{cr}}{F} = \left(\frac{n+1}{2}\right)^{\frac{1}{n-1}} \left(1 - \frac{n-1}{n+1} \lambda^2\right)^{\frac{1}{n-1}} \lambda; \quad (52)$$

$$y(\lambda) = \frac{q(\lambda)}{\pi(\lambda)} = \frac{\rho^* F_{cr}}{\rho F} = \left(\frac{n+1}{2}\right)^{\frac{1}{n-1}} \frac{1}{1 - \frac{n-1}{n+1} \lambda^2}; \quad (53)$$

$$z(\lambda) = \frac{(G_r + G_n) c + \rho F}{(G_r + G_n) a_{p,cr} + \rho_{n,p} F_{cr}} = \frac{1}{2} \left(\lambda + \frac{1}{\lambda}\right); \quad (54)$$

$$f(\lambda) = \frac{p + \rho c^2}{p^*} = (1 + \lambda^2) \left(1 - \frac{n-1}{n+1} \lambda^2\right)^{\frac{1}{n-1}}; \quad (55)$$

$$r(\lambda) = \frac{\rho F}{(G_r + G_k) c + \rho F} = \frac{1 - \frac{n-1}{n+1} \lambda^2}{1 + \lambda^2}. \quad (56)$$

These correlations correspond with the respective hydrodynamic functions of single-phase flows, the only difference being that the adiabatic index k is replaced by the polytropic index n . Therefore, all characteristics of the flow of the curves for λ and the nature of the dependence even upon n will be the same as for single-phase flows.

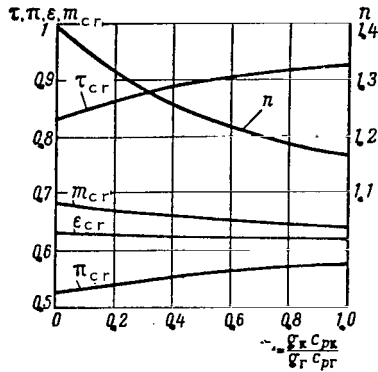


Fig. 2. Critical Values of Hydrodynamic Functions of a Mixture as a Function of the Parameter

$$\vartheta = \frac{g_k}{g_r} \frac{c_{pk}}{c_{pr}}.$$

corresponds with the throat of a conduit.

The expression for mass expenditure of an equilibrium double-phase mixture $G = F c \rho$ with the aid of hydrodynamic functions, can be reduced to the form:

$$G = m_{cr} \frac{F p^* q(\lambda)}{\sqrt{g_r R T^*}}. \quad (57)$$

Here

/31

$$m_{cr} = \sqrt{n \left(\frac{2}{n+1} \right)^{\frac{n+1}{n-1}}}. \quad (58)$$

This expression differs from the usual expression for gas consumption by the factor $\sqrt{g_r}$ in the denominator. From equation (57) written for the critical section,

$$G = \frac{m_{cr}}{\sqrt{g_r}} \frac{F_{cr} p^*}{\sqrt{R T^*}} = m_{cr} F_{cr} \sqrt{\frac{p^* \rho_r^*}{g_r}} = m_{cr} F_{cr} \sqrt{p^* \rho^*} \quad (59)$$

it is seen that with equal initial temperature and pressure, the consumption of a mixture in one and the same nozzle, despite a certain lowering of m_{cr} , will evidently be $1/\sqrt{g\Gamma}$ times greater than the consumption of a pure gas.

It is necessary once more to note that all that has been presented in this section relates only to the equilibrium flow of a double-phase mixture.

We shall evaluate the limiting values of dimensionless parameters, characterizing the velocity and temperature lag of the particles, where the flow still can be considered to be equilibrium. We will conditionally consider the flow of the double-phase mixture to be equilibrium if the relative lag in velocity and temperature of the particles does not exceed 1%, i.e.,

$$\left| \frac{c_r - c_k}{c_k} \right| \leq 0.01; \quad \left| \frac{T_k - T_r}{T_r} \right| \leq 0.01. \quad (60)$$

As the calculations indicate (cf. the next chapter), it is possible to ignore errors at the same time arising due to a difference in the actual process from an equilibrium process in the majority of the engineering problems.

The equation of small particle motion (25) can be rewritten in dimensionless form:

$$\frac{d\bar{c}_k}{d\xi} = \frac{1}{Sto} \frac{\bar{c}_r - \bar{c}_k}{\bar{c}_k}, \quad (61)$$

where $Sto = \frac{\rho_k c_0 d^2}{18\mu_r L}$, i.e., Stokes' similarity criterion.

In the case of motion of small particles with small lag which we are considering, the gradient of particle velocity according to the length of the channel is close to the gradient of gas density; therefore, from equation (61) it is possible to evaluate the limiting value of the Stokes criterion. For example with a flow in a nozzle

$$Sto_{lim} \leq \frac{0.01}{\frac{d\bar{c}}{d\xi}} \approx \frac{0.01}{\bar{c}_{max} - 1}, \quad (62)$$

where \bar{c}_{max} is the maximum dimensionless velocity of a mixture in the nozzle. /32

Considering that with small lag in speed $Re_{rel} \rightarrow 0$ and $\alpha \rightarrow (2\lambda_r/d)$, the equation of heat exchange between the particles and

the gas may be reduced to the following dimensionless form:

$$\frac{dt}{d\xi} = K \frac{t_r - t_k}{\bar{c}_k}, \quad (63)$$

where $K = \frac{12\lambda_{\Gamma}L}{c_{pK}\rho_K c_0 d^2}$ is a dimensionless parameter.

Analyzing this equation in a way analogous to the preceding one, we find that with the flow of a double-phase mixture in a nozzle, the limiting value under which the temperature lag does not exceed 1%, can be evaluated according to the formula

$$K_{lim} \geq 100 (1 + \bar{c}_{max}) \frac{1 - t_{min}}{1 + t_{min}}, \quad (64)$$

where t_{min} is the dimensionless temperature of gas at the end of the nozzle.

If the values St_0 and K substantially differ from the limiting values then the flow cannot be considered to be equilibrium. In this case, using the regular laws introduced in this section for the calculation of double-phase flows, is already forbidden. In particular, for mixtures with a noticeable lag of the particles in velocity and temperature it is impossible to introduce concepts such as damped temperature, pressure, etc. In order to study such flows it is necessary to consider the entire system of equations in (22) or to introduce other methods of physical analysis.

§4. Equation for the Reduction of Influences in the Study of Double-Phase Flows

With the flow of a double-phase mixture in a conduit of variable cross section, the gas phase performs an action of accelerating the particles, accompanied by losses due to friction of the gas on the particles; between the gas and the particles an intensive heat exchange may take place. Thus, the change in the parameters of the gas takes place as a result of the simultaneous influence of a whole number of factors: a change in the area of a cross section of the conduit, the effects of external work, friction and heat exchange. The influence of various types of effects upon the basic parameters of gas flow was most fully investigated by L.A. Vulis [10]. In particular, he cited equations for reducing the influences for flow rate, density, pressure and temperature of the gas, describing the influence of various actions on the change in these parameters with subsonic and supersonic gas flows.

In the present section we shall attempt to apply the basic equation for reduction of influences, i.e., the equation written

for the gas flow, rate, in order to investigate certain cases of the flow of a double-phase mixture. In the simplest cases, it is possible to integrate this equation and to obtain quantitative correlations between the parameters of the flow. In the more complex cases it may be used for qualitative analysis, which is very important for a correct understanding of the characteristics of double-phase flows. We shall give (without any conclusion) the equation for reduction of influences for the gas velocity obtained by L.A. Vulis: /33

$$\left(\frac{c_r^2}{kRT_r} - 1 \right) \frac{dc_r}{c_r} = \frac{dF}{F} - \frac{1}{kRT_r} [dA_r + dA_{fr} + (k-1)(dQ_{ex} + dQ_{fr})], \quad (65)$$

where dA_r is the elementary external work of the gas;
 dA_{fr} is the elementary work of the forces of friction;
 dQ_{ex} is the amount of heat conducted to the gas from an external source;
 dQ_{fr} is the amount of heat given off in the flow due to friction.

For a double-phase flow these elementary influences can be expressed in the following fashion. The elementary external work of a gas on the portion dx is equivalent to an increase in kinetic energy of the particles on the same portion, i.e., $dA_r = \frac{g_K}{g_\Gamma} c_K dc_K$.

The work of the forces of friction of the gas on the particles

$$dA_{fr} = \frac{g_K}{g_r} \frac{P}{m} (c_r - c_K) \frac{dx}{c_K} = \frac{g_K}{g_r} (c_r - c_K) dc_K.$$

Thus, the complete work of the gas equal to the sum of external work and work of friction is $dA_r + dA_{fr} = \frac{g_K}{g_\Gamma} c_\Gamma dc_K$.

The amount of heat conducted from the particles to the gas of a portion dx is equal to $dQ_{ex} = - \frac{g_K}{g_\Gamma} c_{pK} dT_K$; therefore, the total amount of heat conducted to the gas is

$$dQ_{ex} + dQ_{fr} = \frac{g_K}{g_r} [-c_{pK} dT_K + (c_r - c_K) dc_K].$$

With regard to the obtained expressions the equation for reduction of influences can be rewritten in the form

$$\begin{aligned} \left(\frac{c_r^2}{kRT_r} - 1 \right) \frac{dc_r}{c_r} = & \frac{dF}{F} - \frac{1}{kRT_r} \frac{g_K}{g_r} c_r dc_K - \\ & - \frac{k-1}{kRT_r} \frac{g_K}{g_r} [-c_{pK} dT_K + (c_r - c_K) dc_K]. \end{aligned} \quad (66)$$

In the case of very large particles their acceleration and heat exchange of the gas can be ignored and it may be considered that $dc_K = 0$ and $dT_K = 0$. Therefore, equation (66) has the form of the usual equation of an energetically isolated gas flow: /34

$$(M^2 - 1) \frac{dc_r}{c_r} = \frac{dF}{F}. \quad (67)$$

On the other hand, in a double-phase flow with very small particles it is possible to place $c_r \equiv c_K \equiv c$ and $T_r \equiv T_K \equiv T$; an increase in temperature dT_K is easily determined from the energy equation (27):

$$dT_K = dT = - \frac{cdc}{grc_p}.$$

Then equation (66) can be rewritten as:

$$\left(\frac{c^2}{kRT} - 1 \right) \frac{dc}{c} = \frac{dF}{F} - \frac{c^2}{kRT} \frac{g_K}{g_r} \frac{dc}{c} - \frac{c^2}{kRT} \frac{g_K}{g_r} \frac{(k-1)c_{p_K}}{grc_p} \frac{dc}{c}.$$

Transferring the last two terms into the left-hand side and deriving complex transformations we obtain

$$\left(\frac{c^2}{grkRT} - 1 \right) \frac{dc}{c} = \frac{dF}{F}.$$

With regard to expression (33) for the equilibrium speed of sound, this equation can be rewritten in the form

$$(M_p^2 - 1) \frac{dc}{c} = \frac{dF}{F}, \quad (68)$$

where $M_p = \frac{c}{a_p}$ is the Mach number for an equilibrium flow of a mixture.

Thus, despite the performance of external work by the gas on particle acceleration and intensive conduction of heat from the particles to the gas, the equation for reduction of influences, for an equilibrium double-phase flow corresponds with the equation of an energetically isolated flow of pure gas (cf. also the preceding section). This is explained by the fact that with an equilibrium double-phase flow, the performance of external work by a gas and the conduction of heat to the gas is compensated for by a corresponding decrease in the equilibrium speed of sound in the mixture in comparison with the speed of sound in a pure gas.

As is seen from equation (66) in the usual case of the flow of a double-phase mixture with a lag of the particles in speed and temperature, a critical section, i.e., a section in which $c_r^2/kRT_r =$

1, no longer corresponds with the throat of the conduit. The velocity of the gas phase in this section is equal to the speed of sound in a pure gas: $c_T = \sqrt{kRT_T}$.

Weak perturbations propagating in a double-phase mixture can have both a periodic nature (sound waves) and a unilaterally directed nature (for example perturbations elicited by a change in the area of the cross section of the conduit or by an insignificant change in pressure in a given section). As was shown in the preceding section, the speed of sound in a double-phase mixture, depending upon the dispersion and concentration of particles, may acquire significance within the bounds of $a = \sqrt{ng_T RT} - \sqrt{kRT_T}$. Its value does not exceed the speed of sound in a pure gas, i.e., $a \leq \sqrt{kRT_T}$. /35

The propagation speed of unilaterally directed weak perturbations in the gas phase of a double-phase mixture also cannot exceed the speed of sound in a pure gas. With a decrease in the intensity of such perturbations, even the interaction of the phases decreases; therefore, the speed of their propagation approximates the speed of sound in a pure gas.

Thus, the maximally possible speed of propagation of weak perturbations in a double-phase medium is equal to the speed of sound in a pure gas. Just such a speed of the gas phase is established in the critical section of the conduit. Therefore, weak perturbations (both of the periodic type of sound waves and of unilaterally directed ones), propagating through the gas phase cannot penetrate from a region lying below this section along the flow into a region lying above the section. In other words, the critical section separates the region of flow of double-phase mixtures, in which weak perturbations are propagated upward along the flow, from the region of friction in which weak perturbations are borne by the flow.

Thus with a nonequilibrium flow of a double-phase mixture under the concept of speed of propagation of weak perturbations, it is necessary to understand their maximally possible speed, equal to the speed of sound in a pure gas. Only in the limiting case of equilibrium flow, i.e., with $c_K \equiv c_T$ and $T_K \equiv T_T$, does the speed of propagation of weak perturbations correspond with the equilibrium speed of sound in a mixture.

Since the second and third components in the right-hand sides of equations (66) have a negative value, from the condition that in the critical section the left-hand and right-hand sides of this equation vanish, it follows that $(dF/F) > 0$, i.e., the critical section with a nonequilibrium flow of a double-phase mixture is displaced into the expanding portion of the conduit. In the throat of the conduit (where $dF = 0$) the velocity of the gas phase is determined to be less than the critical velocity, whereupon the velocity value depends upon the intensity of interaction between

the gas phase and the particles.

Figure 3 gives the dependencies of $f = F/F_0$ on the number $M = c_{\Gamma}/\sqrt{kRT_{\Gamma}}$, calculated according to equation (66) for nonequilibrium double-phase flow, assuming that the velocity and temperature lag of the particles from the gas is small. Calculations were conducted for various values of $M_0 = c_{\Gamma 0}/\sqrt{kRT_{\Gamma 0}}$, $k/g_{\Gamma}n$, where $n = 1.2$.

As was seen from Figure 3, the critical section and the throat of the conduit correspond only with a parameter value $k/g_{\Gamma}n = 1$. Since this equation is only possible where $k = n$ and $g_{\Gamma} = 1$, this case corresponds to the flow of a pure gas. Where $(k/g_{\Gamma}n) > 1$, the critical section is displaced into the expanding portion of the conduit and the minimal dimensionless area of the conduit increases

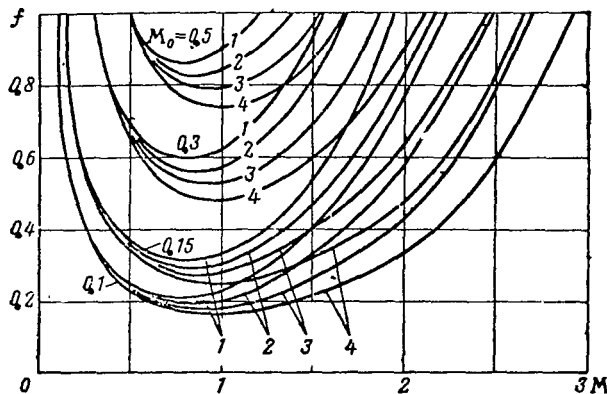


Fig. 3. Relative Area of the Conduit $f = F/F_0$ as a Function of the Number M with a Nonequilibrium Flow of a Double-Phase Mixture:

- (1) $k/g_{\Gamma}n = 1.6$; (2) $k/g_{\Gamma}n = 1.4$;
(3) $k/g_{\Gamma}n = 1.2$; (4) $k/g_{\Gamma}n = 1$

with one and the same value of the number M_0 . Consequently, with the nonequilibrium exhaust of a double-phase flow from a contracting nozzle, with a critical or supercritical drop in pressures, the velocity of the gas phase in the exit section of the nozzle remains lower than in the critical section, and the pressure higher than in the critical section. Only with a further expansion of a double-phase mixture behind the cross section of the nozzle, in the same cross section of the stream where the condition

$$\frac{dF}{F} = \frac{1}{kRT_{\Gamma}} \frac{g_{\kappa}}{g_{\Gamma}} c_{\Gamma} dc_{\kappa} + \frac{k-1}{kRT_{\Gamma}} \frac{g_{\kappa}}{g_{\Gamma}} [-c_{\rho \kappa} dT_{\kappa} + (c_{\Gamma} - c_{\kappa}) dc_{\kappa}],$$

is fulfilled, are the speed of the gas phase and the pressure in the stream made equal to their critical values.

CHAPTER 2

FLOW OF DOUBLE-PHASE MIXTURES IN JET NOZZLES

Using a high-speed computer, the given system of equations (22), permits a swift determination of the flow parameters in a conduit of given shape (the initial values of all parameters under consideration must be known).

/37

However, a parametric study of various double-phase flows, i.e., obtaining dependences of unknown values on the basic dimensionless parameters and defining the flow with the aid of the obtained system of equations, is very difficult. This is explained by the fact that the number of such parameters simultaneously influencing a flow is great. Actually, even in the simplest case of the flow of a mixture with small particles, when the interaction of the gas and the particles is determined by Stokes' law ($Re_{rel} < 1$), the system consists of the following dimensionless equations:

$$\left. \begin{aligned} \frac{dc_k}{d\xi} &= \frac{Sto}{c_k} \frac{\bar{c}_r - \bar{c}_k}{\bar{c}_k}; \\ \frac{d\bar{c}_r}{d\xi} + \frac{g_k}{g_r} \frac{d\bar{c}_k}{d\xi} + K_1 f(\xi) \left(\bar{p}_r \frac{dt_r}{d\xi} + t_r \frac{d\bar{p}_r}{d\xi} \right); \\ \frac{\bar{c}_r^2 - 1}{\bar{c}_r} + \frac{g_k}{g_r} \frac{\bar{c}_k^2 - 1}{2} &= K_2 (1 - t_r) + \frac{g_k}{g_r} K_3 (1 - t_k); \\ \frac{dt_k}{d\xi} &= \frac{K_4}{Sto} \frac{t_r - t_k}{\bar{c}_k}; \\ \bar{p}_r \bar{c}_r &= 1, \end{aligned} \right\} \quad (69)$$

where $K_1 = \frac{RT_0}{c_0^2}$, $K_2 = \frac{c_{pr} T_0}{c_0^2}$; $K_3 = \frac{c_{pk} T_0}{c_0^2}$; $K_4 = \frac{2\lambda_r}{3\mu_r c_{pk}}$ — are dimensionless parameters.

In order to simplify the equations in this system it was assumed that in the initial cross section of the conduit the velocities and temperatures of the phases were equal, i.e., $c_{r0} = c_{k0} = c_0$ and $T_{r0} = T_{k0} = T_0$. This assumption is valid in considering the exhaust of double-phase flows from jet nozzles. Actually, in the majority of cases, the velocities of a mixture flow in front of a nozzle are not great; therefore there is sufficient time to equalize the temperatures and velocities of the phases. This assumption

/38

From the last system of equations it is apparent that, under the given initial values of dimensionless unknown quantities \bar{c}_r , \bar{c}_k , \bar{p}_r , t_r and t_k , the solution depends upon the following six dimensionless parameters: Sto , K_1 , K_2 , K_3 , K_4 and g_k/g_r . For the flow of double-phase mixtures with small Re_{rel} numbers these parameters can be considered as similarity criteria. Actually, for all

geometrically similar conduits [$f(\xi)$ i.e., for all conduits equally] with invarious initial values of the unknown quantities and equal values of the indicated similarity criteria, the solution to this system of equations will be the same.

In a parametric study of the flow of a double-phase mixture, even in a conduit of only one given form, it is necessary to vary all six dimensionless similarity parameters which, besides the sharp increase in the number of calculation variants, as a result of a significant increase in the volume of work leads to an essential deterioration of the clarity and visibility of the obtained results. Where $Re_{rel} > 1$ the task is complicated even more.

Therefore, it is necessary to find a method of investigation which would allow, without solving the entire system of equations, obtaining with sufficient precision and rapidity the most important characteristics of double-phase flows, depending upon the basic determining criteria. One of these methods, based upon successive approximations and broadly used in the study of double-phase flows in this book, is set forth in the following section.

§1. The Method of Successive Approximations in Studying Double-Phase Flows

As was already mentioned the parameters of a double-phase flow are determined sufficiently simply only for very large particles, when it is possible to ignore the interaction of phases, or with very small particles when the flow can be considered to be equilibrium in speed and temperature of the phases.

The flow of double-phase mixtures with small particles which possess a relatively small lag behind the gas in speed and temperature is of the greatest interest. This case is basically considered in the present chapter. With particle lag behind the gas and incomplete heat exchange between phases, supplementary losses appear in the flow, leading to a deviation in the actual parameters of mixture exhaust from the equilibrium parameters. With moderate concentration of particles these deviations are relatively small; therefore, it is convenient to perform the investigation with the aid of successive approximations.

In addition, in first approximation the flow is taken as being /39 equilibrium in velocity and temperature of the phases, since all parameters of the mixture are easily defined according to the formulas for an equilibrium flow.

Furthermore, according to the values of the velocity and temperature of the gas phase found with the aid of the equations for particle motion (17) and heat exchange (20) the velocity of a particle and its temperature as well as losses due to friction of the gas on particles and losses due to incomplete heat exchange between the particles and the gas are determined.

In second approximation, using the energy equation, we evaluate the influence of these losses on the basic parameters of the exhaust. In addition it is assumed that the velocity and temperature lag of the particles behind the gas in second approximation remain the same as in first approximation, i.e.,

$$c_{rel} = c_r - c_k = idem \quad \text{and} \quad \Delta T = T_k - T_r = idem. \quad (70)$$

This is explained by the fact that a decrease in the work of the gas during acceleration of the particles to a significant degree is compensated for by the losses mentioned above, as a result of which the increase in velocity of the gas is small. Analogously, the decrease in gas temperature due to incomplete heat exchange is compensated for by the heat emitted with the friction of the gas on particles. Therefore, the differences in the laws of speed and temperature change of the gas phase along the nozzle in both approximation may prove to be negligibly small.

If necessary, it is possible to perform a third approximation, etc.; however, with a moderate concentration of particles ($g_k < 0.4$) and sufficiently small particle dimensions, the second approximation ensures completely acceptable accuracy in calculation.

The given method of investigating double-phase flows has the following values:

- simplicity and comparatively small difficulty, since it is not necessary to investigate the entire system of equations describing the flow;
- possibility of obtaining a solution to arbitrary expansion of the particle dimensions;
- clarity of analysis, since specific aspects of the phenomena are directly considered simultaneously, i.e., friction of the gas on the particles and heat exchange between phases;
- it provides more visible results since they depend upon a smaller number of dimensionless criteria than in the case of solving the system as a whole;
- it is sufficiently accurate since small deviations of the flow parameters from the ideal parameters are calculated.

The formulas necessary for calculation are presented below, relative to 1 kg of the gas phase.

1. Determination of the Parameters of a Double-Phase Flow in First Approximation

/40

The thermodynamic parameters of the gas phase in first approxi-

mation are expressed in equations (27), (29) and (5) in the form of functions of the velocity in the following way:

$$t = \frac{T}{T_0} = 1 - \delta (\bar{c}^2 - 1); \quad (71)$$

$$\bar{\rho}_r = \frac{\rho_r}{\rho_{r0}} = t^{\frac{1}{n-1}}; \quad (72)$$

$$\frac{p}{p_0} = t^{\frac{n}{n-1}}; \quad (73)$$

$$f = \frac{1}{\bar{c} t^{\frac{1}{n-1}}}, \quad (74)$$

where $\delta = \frac{n-1}{ng_r RT_0} \frac{c_0^2}{2}$ and $\frac{nR}{n-1} = c_p$.

For determining the losses due to friction of the gas on the particles we shall consider the motion of an individual particle under the action of the aerodynamic force P at a certain moment in time. Here, the gas velocity c_r and the particle velocity c_K may have arbitrary values. Let $c_r > c_K$; then under the action of the force P the particle is moved at a certain positive acceleration. The work expendable for acceleration of a particle per unit of time is $dA_K/d\tau = Pc_K$.

According to Newton's third law the same force P acts from a particle on the gas mass surrounding it. Since the gas is moved at acceleration c_r , the work expendable by the gas per unit of time is $dA_K/d\tau = Pc_K$.

The difference in the work expendable by the gas and obtainable by the particle consists in the loss of kinetic energy of the gas, becoming heat:

$$\frac{dA_{rpl}}{d\tau} = \frac{dA_r}{d\tau} - \frac{dA_K}{d\tau} = Pc_{rel},$$

The elementary work of the forces of friction with the movement of one particle by a distance dx is

$$dA_l = P \frac{c_{rel}}{c_K} dx. \quad (75)$$

Let us consider polydispersional mixtures with an arbitrary distribution of particles according to sizes. Let the mass allotment of the particles, having diameter d , be characterized by the

distribution function $\phi(\tilde{d})$, so that

$$\int_{d_{\min}}^{d_{\max}} \phi(\tilde{d}) d\tilde{d} = 1, \quad (76) \quad \underline{/41}$$

where d_{\min} and d_{\max} are the minimum and maximum diameters of particles in the mixture, and \tilde{d} is the diameter of the particles (variable integration).

The elementary work of the forces of friction of the gas on all particles with their movement by a distance $d\mathbf{x}$ relative to 1 kg of the gas phase, is

$$dA_{fr} = d\mathbf{x} \int_{d_{\min}}^{d_{\max}} \frac{g_K}{g_r m} \phi(\tilde{d}) P \frac{c_{rel}}{c_K} d\tilde{d},$$

where g_K/g_r is the mass of the particles per 1 kg of gas;

$\frac{g_K}{g_r} \frac{\phi(\tilde{d}) d\tilde{d}}{m}$ is the number of particles having diameters within the limits $\tilde{d} - \tilde{d} + d\tilde{d}$.

The energy losses irreversibly turning into heat are

$$Q_{fr} = T \int_0^x \frac{dA_{fr}}{T} = \frac{g_K}{g_r} T \int_0^x \frac{1}{T} \left[\int_{d_{\min}}^{d_{\max}} \frac{\phi(\tilde{d})}{m} P \frac{c_{rel}}{c_K} d\tilde{d} \right] dx.$$

Changing the order of integration and considering that the gas temperature is not a function of particle diameter and that the distribution function $\phi(\tilde{d})$ does not depend upon the coordinate x , we obtain

$$Q_{fr} = \frac{g_K}{g_r} \int_{d_{\min}}^{d_{\max}} \phi(\tilde{d}) \left[T \int_0^x \frac{P}{Tm} \frac{c_{rel}}{c_K} dx \right] d\tilde{d}.$$

The coefficient of losses due to the friction of gas on particles is

$$\Delta\eta_{fr} = \frac{Q_{fr}}{H_{disp}},$$

where $H_{disp} = \frac{c_0^2}{2g_r} + H$ — is the disposable energy of a double-phase

flow relative to 1 kg of the gas phase;

$H = \frac{n}{n-1} RT_0 \left[1 - \left(\frac{p}{p_0} \right)^{\frac{n-1}{n}} \right]$ — is the maximum work of a polytropic expansion of 1 kg of the gas phase.

Between the disposable energy and the velocity of the flow, /42
in first approximation the correlation $H_{\text{disp}} = c^2/2g_T$ is valid.

Using this correlation as well as equation (17), the expression for the coefficient of losses due to friction can be written in the form

$$\Delta \eta_{fr} = g_K \int_{d_{\min}}^{d_{\max}} \Delta \bar{\eta}_{fr} \varphi(\bar{d}) d\bar{d}, \quad (77)$$

where

$$\Delta \bar{\eta}_{fr} = 2 \frac{T}{c^2} \frac{0.75}{\rho_K d} \int C_{x\rho_T} \frac{c_{rel}^3}{c_K T} dx. \quad (78)$$

In the case of a monodispersion mixture ($d = \text{const}$) the value $\Delta \eta_{fr}$ depends only on the coordinate x . Therefore, from equations (77) and (76) we obtain

$$\Delta \eta_{fr} = g_K \Delta \bar{\eta}_{fr}. \quad (79)$$

The lag in particle temperature behind the gas temperature leads to a deviation in the expansion process of the gas phase from an equilibrium polytropic process and to a certain decrease in the work of gas expansion. For determining the decrease in efficiency of the gas due to incomplete heat exchange we shall consider how the state of the gas phase changes in the process of a nonequilibrium expansion of a double-phase flow.

With movement of the particles by a distance dx let their temperature be decreased to the values dT_K . With movement g_K/g_T of the particles per 1 kg of the gas phase, a heat is conducted to the gas

$$dQ_r = - \int_{d_{\min}}^{d_{\max}} \frac{g_K}{g_T} \varphi(\bar{d}) c_{p_K} dT_K d\bar{d}. \quad (80)$$

Let us consider the case when, in the process of mixture expansion, the temperature of the particles T_K is represented by a linear function of the gas temperature, i.e.,

$$T_k = T_0 - \varepsilon(T_0 - T_r) \text{ or } dT_k = \varepsilon dT_r, \quad (81)$$

where $\varepsilon = \varepsilon(\tilde{d})$ is the proportionality coefficient;
 dT_r is the change in gas temperature by a distance dx .

As will be shown below, the same case is most characteristic of double-phase flows with small particles.

From equations (80) and (81) we obtain

$$dQ_r = -\frac{g_k}{g_r} c_{pk} \left[\int_{d_{\min}}^{d_{\max}} \varepsilon(\tilde{d}) \varphi(\tilde{d}) d\tilde{d} \right] dT_r.$$

For the given law of particle expansion according to sizes, /43
the expression in the brackets represents a certain constant value.
Having designated it as

$$\varepsilon^* = \int_{d_{\min}}^{d_{\max}} \varepsilon(\tilde{d}) \varphi(\tilde{d}) d\tilde{d}, \quad (82)$$

we obtain

$$dQ_r = -\frac{g_k}{g_r} c_{pk} \varepsilon^* dT_r. \quad (83)$$

The equation for the first principle of thermodynamics

$$dQ_r = c_{pr} dT_r - \frac{dp}{\rho_r}$$

with regard to expression (83) can be rewritten in the form

$$\left(c_{pr} + \frac{g_k}{g_r} c_{pk} \varepsilon^* \right) \frac{dT_r}{RT_r} = \frac{dp}{p}. \quad (84)$$

Integration of this equation gives

$$\frac{T_r}{T_0} = \left(\frac{p}{p_0} \right)^{\frac{n^*-1}{n^*}}, \quad (85)$$

where

$$n^* = \frac{c_{pr} + \frac{g_k}{g_r} c_{pk} \varepsilon^*}{c_{vr} + \frac{g_k}{g_r} c_{pv} \varepsilon^*} \cdot \frac{1 + \varepsilon^*}{\frac{1}{k} + \varepsilon^*}. \quad (86)$$

Thus, in the case of incomplete heat exchange between particles and gas and with condition (81) the process of expansion of the gas phase of a mixture follows the polytropic law with n^* .

With complete temperature equilibrium between the particles and gas ($T_K \equiv T_F$) $\epsilon = \epsilon^* = 1$. In this case expression (86) for n^* is converted into expression (30) for the polytropic index of an equilibrium expansion of the gas phase.

In the case when all particles have equal diameter, from correlation (83) it follows that

$$\epsilon^* = \epsilon. \quad (87)$$

Efficiency losses of the gas phases due to incomplete heat exchange between the phases will, in the case under consideration, be equal to the differences in the polytropic work of the equilibrium and nonequilibrium processes of expansion with the same pressure change:

$$\Delta A_Q = \frac{n}{n-1} RT_0 \left(1 - \pi^{\frac{n-1}{n}} \right) - \frac{n^*}{n^*-1} RT_0 \left(1 - \pi^{\frac{n^*-1}{n^*}} \right).$$

Having divided this equation by the disposable energy of a double-phase mixture, after transformations we obtain the following formula for the coefficient of losses due to incomplete heat exchange between the phases under condition (81):

/44

$$\Delta \eta_Q = \frac{\Delta A_Q}{H_{disp}} = 1 - \frac{1}{\bar{c}^2} - \frac{1}{\delta \bar{c}^2 \bar{n}} \{ 1 - [1 - \delta (\bar{c}^2 - 1)]^{\bar{n}} \}, \quad (88)$$

where

$$\bar{n} = \frac{n}{n-1} \frac{n^*-1}{n^*} = \frac{1+\delta}{1+\delta \epsilon^*}. \quad (89)$$

Where $\epsilon^* = 1$ (the case where $T_K \equiv T_F$), $\bar{n} = 1$ and $\Delta \eta_Q = 0$, i.e., losses from incomplete heat exchange are absent.

Where $\epsilon^* = 0$ (heat exchange between phases is absent so that $\epsilon = 0$ and $T_K = T_0 = \text{const}$) $\bar{n} = 1 + \delta$ and losses attain maximum value, equal to the differences in work of the polytropic equilibrium and adiabatic processes of expansion of the gas phase with the same pressure change.

The dependency of the value $\Delta \eta_Q$ upon equilibrium velocity of the gas (mixture) with various values of \bar{n} and δ is presented in Figure 4.

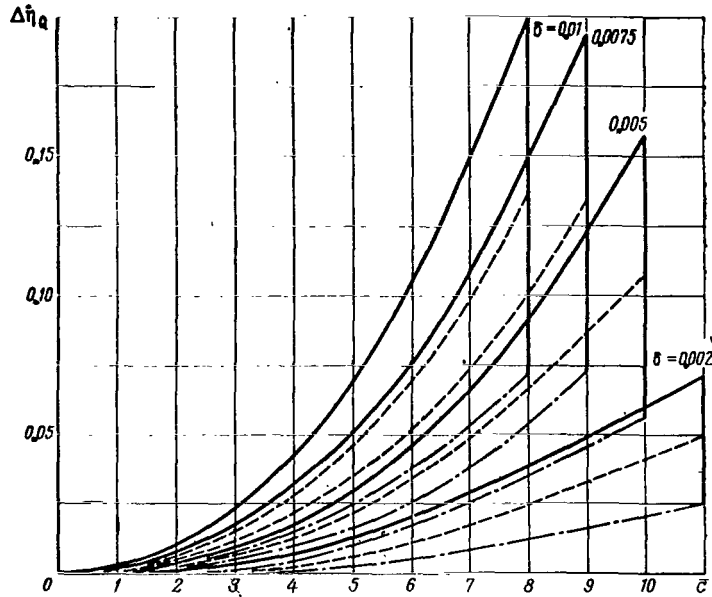


Fig. 4. Dependency of $\Delta\eta_Q$ Upon the Dimensionless Velocity of the Mixture in the Case of Polytropic Expansion of the Gas Phase:

$$\text{---} \quad \bar{n} = \frac{1+\theta}{1+\theta_0} = 1.6; \quad \text{---} \quad \bar{n} = 1.4; \\ \text{---} \quad \bar{n} = 1.2$$

2. Determination of the Parameters of a Double-Phase Flow in Second Approximation

/45

Let us consider the basic dependences between the parameters of the exhaust of a mixture in second approximation. Since in both the first and second approximation the drop capable of operating in a nozzle is assumed to be invariable it is possible to assume that the distribution of pressures and consequently even the disposable energy along the nozzle remain the same as in first approximation. Certainly, at the same time a certain correction of the flow passage cross sectional areas of the nozzle is necessary in comparison with the values which may be determined by formula (74).

The energy equation (27) with regard to losses due to friction of gas on particles and due to incomplete heat exchange between the phases can be written thus:

$$H_{\text{disp}}(1 - \Delta\eta_{\text{fr}} - \Delta\eta_Q) = \frac{c_r^2}{2} + \frac{g_K}{g_r} \int_{d_{\min}}^{d_{\max}} \frac{c_K^2}{2} \varphi(\tilde{d}) d\tilde{d}. \quad (90)$$

Having substituted the expression $c_K = c_r - c_{\text{rel}}$, after transformation, we obtain

$$c_r^2 - 2g_k c_0 J_1 c_r + g_k c_0^2 J_2 - 2g_r H_{\text{disp}} (1 - \Delta\eta_{fr} - \Delta\eta_Q) = 0. \quad (91)$$

Solving this quadratic equation relative to c_r , it is possible to determine the velocity of the gas phase and of the particles. We shall express them in dimensionless form:

$$\left. \begin{aligned} \bar{c}_r &= \bar{c} \sqrt{1 - \Delta\eta_{fr} - \Delta\eta_Q - \frac{g_k}{c^2} (J_2 - g_k J_1^2) + g_k J_1} \\ \bar{c}_k &= \bar{c}_r - \bar{c}_{\text{rel}} \end{aligned} \right\} \quad (92)$$

where $\bar{c} = \frac{1}{c_0} \sqrt{2g_r H_{\text{disp}}}$ is the dimensionless velocity of the gas (mixture), found in first approximation:

$$J_1 = \int_{d_{\min}}^{d_{\max}} \bar{c}_{\text{rel}} \varphi(\tilde{d}) d\tilde{d}; \quad J_2 = \int_{d_{\min}}^{d_{\max}} \bar{c}_{\text{rel}}^2 \varphi(\tilde{d}) d\tilde{d}; \quad (93)$$

$\bar{c}_{\text{rel}} = \bar{c}_r - \bar{c}_k = \bar{c} - \bar{c}_k$ is known from calculating the first approximation.

The specific impulse of the double-phase flow, per 1 kg of the gas phase, is

$$P_d = c_r + \frac{g_k}{g_r} \int_{d_{\min}}^{d_{\max}} c_k \varphi(\tilde{d}) d\tilde{d}.$$

Substituting expressions for velocities of the phases, after /46 transformation we obtain

$$P_d = P_p \sqrt{1 - \Delta\eta_{fr} - \Delta\eta_Q - \frac{g_k}{c^2} (J_2 - g_k J_1^2)}, \quad (94)$$

where $P_p = \sqrt{\frac{2H_{\text{disp}}}{g_r}} = \frac{c}{g_r}$ is the specific impulse of 1/ g_r kg of a mixture with an equilibrium exhaust.

In this expression the value $\frac{g_k}{c^2} (J_2 - g_k J_1^2)$ considers the decrease in specific impulse due to inequality of the velocities of the particles and the gas on a section of the nozzle.⁴

⁴ As is known with an invariable kinetic energy of a system the amount of its motion will be maximum given equality of the velocities of all its components (author's note).

If all particles of a mixture have an equal diameter then the expressions for J_1 and J_2 , the velocities of the phases and the specific impulse, will be written thus:

$$\left. \begin{aligned} J_1 &= \bar{c}_{rel}; & J_2 &= \bar{c}_{rel}^2; \\ \bar{c}_r &= \bar{c} \sqrt{1 - \Delta\eta_{fr} - \Delta\eta_Q - g_k g_r \left(\frac{\bar{c}_{rel}}{\bar{c}}\right)^2} + g_k \bar{c}_{rel}; \\ \bar{c}_k &= \bar{c}_r - \bar{c}_{rel}; \\ P_d &= P_p \sqrt{1 - \Delta\eta_{fr} - \Delta\eta_Q - g_k g_r \left(\frac{\bar{c}_{rel}}{\bar{c}}\right)^2}. \end{aligned} \right\} \quad (95)$$

The temperature of the gas phase in second approximation will be calculated according to the formula

$$t_r = \left(\frac{p}{p_0}\right)^{\frac{\lambda^* - 1}{n^*}} + \frac{Q_{fr}}{c_{pr} T_0},$$

where Q_{fr}/c_{pr} is the heating of the gas phase due to friction on the particles.

This expression can be reduced to the following form:

$$t_r = t^n + \frac{\Delta\eta_{fr} H_{disp}}{c_{pr} T_0}. \quad (96)$$

Considering that the distribution of pressure along the nozzle remains invariable, from the state equation (1) it is possible to obtain an expression for the relation of gas densities determined in second and in first approximations:

$$\frac{\rho_{rd}}{\rho_r} = \frac{t}{t_r}. \quad (97)$$

Finally, from the consumption equation (74) we obtain the following expression for the relationship between cross sectional areas of nozzle determined in the second and in the first approximations: /47

$$\frac{f_d}{f} = \frac{t_r c}{t c_r}. \quad (98)$$

In conclusion we note the following. As the preliminary analysis of the given equation showed, the particle lag $c_{rel} = c_r - c_k$, the coefficient of losses due to friction of the gas on the particles $\Delta\eta_{fr}$ and the coefficient of losses due to incomplete heat exchange between the phases $\Delta\eta_Q$ directly depend upon the law of velocity change of the gas along the nozzle. In other words, with a small deviation in the law of velocity change of the gas along the nozzle

from the original values, c_{rel} , Δn_{fr} and Δn_Q also change insignificantly.

This circumstance permits one to be limited to the consideration of several more typical laws of velocity change of the gas along the nozzle (or of laws of the mixture exhaust in the first approximation). At the same time the obtained values c_{rel} , Δn_{fr} and Δn_Q may be used for determining the parameters of any real exhaust process in the second approximation, if only the actual exhaust loss does not differ essentially from one of the considered laws.

§2. Losses Due to Friction of the Gas on the Particles

We shall evaluate losses due to friction of gas on the particles with exhaust of a double-phase mixture from a nozzle. We shall consider the most typical laws of increase in the velocity of the gas along the nozzle, namely when the velocity of the gas changes in the first approximation:

(1) according to parabolic law when:

$$c = \sqrt{c_0^2 + 2\beta_1 x} \text{ or } \bar{c} = \sqrt{1 + \xi_1}; \quad (99)$$

(2) according to linear law when

$$c = c_0 + \beta_2 x \text{ or } \bar{c} = 1 + \xi_2; \quad (100)$$

(3) according to quadratic law when

$$c = (\sqrt{c_0} + \beta_3 x)^2 \text{ or } \bar{c} = (1 + \xi_3)^2. \quad (101)$$

Here $\xi_1 = \frac{2\beta_1 x}{c_0^2}$; $\xi_2 = \frac{\beta_2 x}{c_0}$; $\xi_3 = \frac{\beta_3 x}{\sqrt{c_0}}$ are dimensionless coordinates along the nozzle;

$$\beta_1 = \frac{c_0^2}{2L_c} (\bar{c}_{\max}^2 - 1), \beta_2 = \frac{c_0}{L_c} (\bar{c}_{\max} - 1), \quad /48$$

$\beta_3 = \frac{\sqrt{c_0}}{L_c} (\sqrt{\bar{c}_{\max}} - 1)$ are coefficients characterizing acceleration of the gas along the nozzle;

\bar{c}_{\max} - maximum dimensionless velocity of the gas at the end of the nozzle.

In this section it is assumed that the mixture is monodispersed.

With the aid of the corresponding formulas introduced in the preceding section, correlations which will be obtained below may be generalized, even for the case of a polydispersed mixture.

1. Exhaust of a Double-Phase Mixture Where $Re_{rel} < 1$

In the case of a double-phase mixture with small particles, the motion of which is characterized by numbers $Re_{rel} < 1$, the equation for particle motion and the expression in (79) for the coefficient of losses due to friction acquire the following form:

$$\frac{dc_k}{dx} = k_1 \frac{c - c_k}{c_k}; \quad (102)$$

$$\Delta\eta_{fr} = 2g_* \frac{T}{c^2} k_1 \int \frac{c_{rel}^2}{c_k T} dx, \quad (103)$$

where $k_1 = \frac{18\mu_T}{\rho_K d^2}$.

Substituting (99) - (101) into (71) we obtain the following dependencies of dimensionless temperature of the gas t upon dimensionless coordinate ξ_i for the laws of velocity change of the gas along the nozzle, considered in first approximation:

$$\left. \begin{aligned} t &= 1 - \delta\xi_1; \\ t &= 1 - \delta[(1 + \xi_2)^2 - 1]; \\ t &= 1 - \delta[(1 + \xi_3)^4 - 1]. \end{aligned} \right\} \quad (104)$$

In the case of parabolic law of velocity change of the gas along the nozzle ($\beta = \sqrt{1 + \xi_1}$) the equation for the particle motion (102) can be presented in the form

$$\frac{d^2x}{d\tau^2} = k_1 \sqrt{c_0^2 + 2\beta_1 x} - k_1 \frac{dx}{d\tau}. \quad (105)$$

This equation may be solved numerically. However, for an approximate study of the losses with the flow of a double-phase mixture in a nozzle such a solution is not necessary. We must indicate that the nature of particle motion in the nozzle is the following: in a certain initial time interval (for small particle which is small in comparison with the time particles remain in the nozzle) particles lag behind the gas and are moved with an acceleration, increasing from zero to the maximum value, equal to the acceleration of the gas β_1 . Actually, having taken the derivative from the right-hand side of (105) and equating it to zero, we obtain $(\frac{d^2x}{d\tau^2})_{\max}$ /49

$= \beta_1 \frac{c_K}{c} \approx \beta_1$, since for small particles $c_K \approx c$. Substituting this expression in the motion equation (105), we obtain the maximum particle lag $c_{rel \max} = \beta_1/k_1$.

Ignoring the value of the initial portion, it is possible to consider that a particle passes through the nozzle with a constant acceleration β_1 and a constant lag $c_{rel} = \beta_1/k_1$, whereby its velocity is

$$c_K = c_0 \sqrt{1 + \xi_1} - \frac{\beta_1}{k_1}.$$

Since in this case $c_{rel} \ll c = c_0 \sqrt{1 + \xi_1}$, then the coefficient of losses due to friction (103) can be expressed thus:

$$\Delta \eta_{fr} = g_K \frac{1 - \delta \xi_1}{1 + \xi_1} \frac{1}{a_1} \int_0^{\xi_1} \frac{d\xi_1}{\sqrt{1 + \xi_1} (1 - \delta \xi_1)}.$$

After integration and transformation we obtain

$$\Delta \eta_{fr} = g_K \frac{1 - \delta \xi_1}{a_1 (1 + \xi_1) \sqrt{\delta} (1 + \delta)} \ln \frac{(1 - \sqrt{\delta})(1 + \sqrt{\delta}(1 + \xi_1))}{(1 + \sqrt{\delta})(1 - \sqrt{\delta}(1 + \xi_1))}, \quad (106)$$

where $a_1 = \frac{k_1 c_0}{\beta_1} = \frac{18 \mu_\Gamma c_0}{\rho_K \beta_1 d^2}$ is a dimensionless parameter; $\bar{\delta} = \frac{\delta}{1 + \delta}$.

Figure 5 shows the dependence of the value $\Delta \eta_{fr} a_1 / g_K = \Delta_{1fr}$ upon the dimensionless length of the nozzle ξ_1 with different values of the parameter δ . As is seen from the graphs, Δ_{1fr} , and consequently even $\Delta \eta_{fr}$ are maximum with a certain value of ξ_1 . With greater values of ξ_1 the coefficient $\Delta \eta_{fr}$ is decreased. Since with $d \rightarrow 0$ the value $a_1 \rightarrow \infty$, then the coefficient of losses due to friction is $\Delta \eta_{fr} = \frac{g_K}{a_1} \Delta_{1fr} \rightarrow 0$.

In the case of a linear law of velocity change of the gas ($\bar{c} = 1 + \xi_2$), the equation for particle motion can be reduced to the form

$$\frac{dc_K}{d\xi_2} = a_2 \left(\frac{1 + \xi_2}{c_K} - 1 \right), \quad (107)$$

where $a = \frac{k_1}{\beta_2} = \frac{18 \mu_\Gamma}{\rho_K \beta_2 d^2}$ is a dimensionless parameter. The substitution $y = \frac{c}{c_K} = \frac{1 + \xi_2}{\bar{c}_K}$ reduces to an equation with separating variables

$$\frac{d\xi_2}{1 + \xi_2} = \frac{dy}{y(1 + a_2 y - a_2 y^2)},$$

the solution of which is written thus:

/50

$$1 + \xi_2 = -\frac{y}{\sqrt{1 + a_2 y - a_2 y^2}} \times$$

$$\times \left[\frac{\left(\sqrt{1 + \frac{4}{a_2}} + 1 \right) \left(\sqrt{1 + \frac{4}{a_2}} - 2y + 1 \right)}{\left(\sqrt{1 + \frac{4}{a_2}} - 1 \right) \left(\sqrt{1 + \frac{4}{a_2}} + 2y - 1 \right)} \right]^{\frac{1}{2\sqrt{1 + \frac{4}{a_2}}}} \quad (108)$$

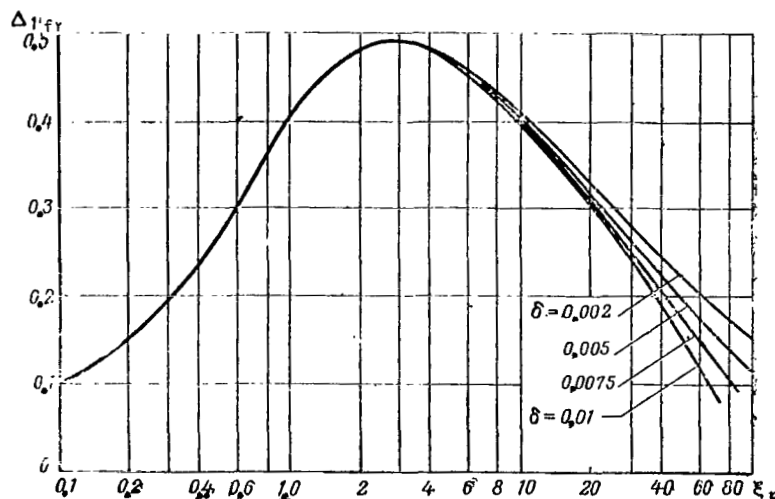


Fig. 5. Dependence of the Value of $\Delta_{1fr} = \frac{a_1}{g_K}$ Upon the Dimensionless Length of the Nozzle ξ_1 in the Case of $\bar{c} = \sqrt{1 + \xi_1}$ and $Re_{rel} < 1$.

Analyzing the obtained equation it is possible to note that the limiting value of the quantity y is

$$y_{lim} = \frac{1}{2} \left(1 + \sqrt{1 + \frac{4}{a_2}} \right) \quad (109)$$

(y_{lim} is the root of the equation $1 + a_2 y - a_2 y^2 = 0$). Where $y \rightarrow y_{lim}$ the value $\sqrt{1 + a_2 y - a_2 y^2}$ standing in the denominator (108) approaches zero more quickly than the value

$$\left(\sqrt{1 + \frac{4}{a_2}} - 2y + 1 \right)^{\frac{1}{2\sqrt{1 + \frac{4}{a_2}}}},$$

entering the numerator. Therefore, the right-hand side of equation /51 (108) and consequently even ξ_2 approach infinity; i.e., with the

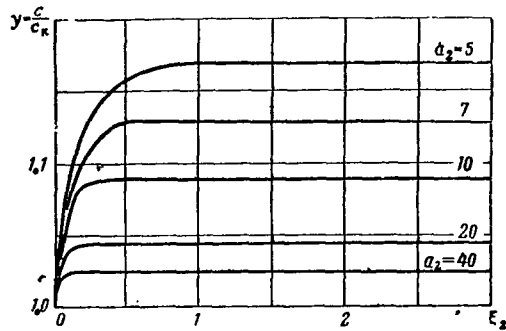


Fig. 6. Dependence of the Ratio $y = c/c_K$ Upon the Dimensionless Length of Nozzle ξ_2 in the Case Where $\bar{c} = 1 + \xi_2$ and $Re_{rel} < 1$.

exception of the initial portion of the motion the ratio between velocities of gas and particle y does not depend upon the particle coordinate ξ_2 , and is determined only by the value of the dimensionless parameter a_2 according to formula (109).

Figure 6 shows $y = c/c_K$ as a function of the dimensionless coordinate ξ_2 for various values of parameter a_2 . As is shown on the graph, the limiting values of the quantity y are attained on a relatively short initial section of the nozzle.

Ignoring this section it is possible to consider that particles pass through the nozzle with a velocity

$$c_K = \frac{c}{y_{lim}} = \frac{2c}{1 + \sqrt{1 + \frac{4}{a_2}}}.$$

With regard to this, the expression for the coefficient of losses (103) may be reduced to the form

$$\Delta\eta_{fr} = g_K A \frac{1 + \delta - \delta(1 + \xi_2)^2}{\delta(1 + \xi_2)^2} \ln \frac{1}{1 + \frac{\delta}{1 + \xi_2} - \frac{\delta^2}{1 + \xi_2^2}}, \quad (110)$$

where $A = \frac{a_2(y_{lim} - 1)^2}{y_{lim}} = \frac{a_2 \left(\sqrt{1 + \frac{4}{a_2}} - 1 \right)^2}{2 \left(\sqrt{1 + \frac{4}{a_2}} + 1 \right)}$ is a dimensionless coefficient.

Figure 7 shows the dependence

$$\Delta_{2fr} = \frac{\Delta\eta_{fr}}{g_K A} = \frac{1 + \delta - \delta(1 + \xi_2)^2}{\delta(1 + \xi_2)^2} \ln \frac{1}{1 + \frac{\delta}{1 + \xi_2} - \frac{\delta^2}{1 + \xi_2^2}}$$

upon the dimensionless coordinate of the nozzle ξ_2 for various values of the parameter δ . The dependence of coefficient A upon the dimensionless parameter a_2 is given in Figure 8.

The dependences (106) and (110) and the graphs presented in Figures 5 and 7 allow us to evaluate the losses due to friction of

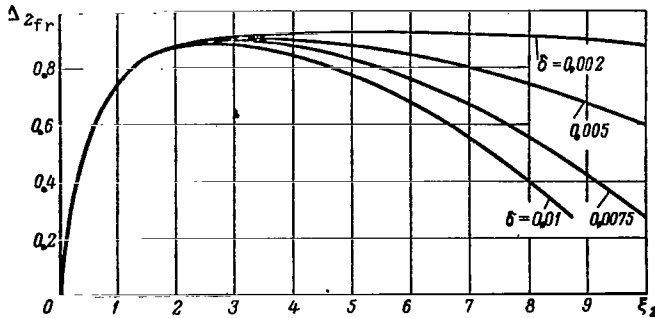


Fig. 7. The Dependence of the Value $\Delta_{2fr} = \frac{1}{g_K A} \Delta \eta_{fr}$ Upon the Dimensionless Length of the Nozzle ξ_2 in the Case of $\bar{c} = 1 + \xi_2$ and $Re_{rel} < 1$.

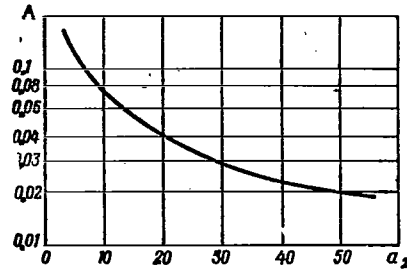


Fig. 8. Dependence of Coefficient A Upon Parameter a_2 ($Re_{rel} < 1$).

the gas on a particle with the exhaust of double-phase flows in the case of $Re_{rel} < 1$ and with a velocity change in the gas in the first approximation, approximately corresponding to equations (99) and (100).

For example, with the exhaust from a nozzle 1 m in length of a double-phase mixture having parameters: $c = 1500$ m/sec; $c_0 = 150$ m/sec; $g_K = 0.25$; $\mu_r = 8 \times 10^{-5}$ n·sec/m²; $d = 2 \mu\text{m}$; $\rho_K = 2000$ kg/m³; $T_0 = 3000^\circ\text{K}$; $n = 1.2$; $R = 300$ J/kg·°K; $\delta = 0.0028$, the coefficient of losses due to friction $\Delta \eta_{fr}$ in both of the considered cases of exhaust (99) and (100) is approximately equal to 0.15%. With the same parameters in a particle size of $5 \mu\text{m}$, the coefficient of losses $\Delta \eta_{fr} = 1\%$ for $\bar{c} = \sqrt{1 + \xi_1}$ and $\Delta \eta_{fr} = 0.8\%$ for $\bar{c} = 1 + \xi_2$.

From this example it is apparent that in the case of small particles ($Re_{rel} < 1$) the coefficient of losses due to the friction of gas on particles weakly depends on the law of velocity change in the gas along the nozzle. Therefore in the first approximation, losses in double-phase flows with small particles may be evaluated according to data obtained for the linear law of velocity change of the gas.

/53

2. Exhaust of a Double-Phase Mixture Where $10 < Re_{rel} < 1000$

For particles of average size, the motion of which is characterized by the number $Re_{rel} = 10 \sim 1000$, it is possible to obtain $C_x = 13/\sqrt{Re_{rel}}$, so that the equation of motion and the expression for $\Delta \eta_{fr}$ are written thus:

$$\frac{dc_K}{dx} = k_2 \frac{(c - c_K)^{1/2}}{c_K}; \quad (111)$$

$$\Delta \eta_{fr} = 2g_K \frac{T}{c^2} \int k_2 \frac{(c - c_K)^{1/2}}{c_K T} dx, \quad (112)$$

where $k_2 = 9.75 \frac{\sqrt{\mu_r \rho_r}}{\rho_K d^{3/2}}$.

For the laws of the flow of the gas phase (99) - (101) under consideration, the equation for particle motion may be reduced, respectively, to the following dimensionless forms:

$$\left. \begin{aligned} \frac{d\bar{c}_K}{d\xi_1} &= b_1 (1 - \delta \xi_1)^{\frac{1}{2(n-1)}} \frac{(1 + \xi_1 - \bar{c}_K)^{1/2}}{\bar{c}_K}; \\ \frac{d\bar{c}_K}{d\xi_2} &= b_2 [1 - \delta (2\xi_2 + \xi_2^2)]^{\frac{1}{2(n-1)}} \frac{(1 + \xi_2 - \bar{c}_K)^{1/2}}{\bar{c}_K}; \\ \frac{d\bar{c}_K}{d\xi_3} &= b_3 [1 - \delta (4\xi_3 + 6\xi_3^2 + 4\xi_3^3 + \xi_3^4)]^{\frac{1}{2(n-1)}} \frac{[(1 + \xi_3)^2 - \bar{c}_K]^{1/2}}{\bar{c}_K}, \end{aligned} \right\} \quad (113)$$

where

$$\begin{aligned} b_1 &= \frac{k_{20}}{2\beta_1} c_0^{1/2} = 9.75 \frac{\sqrt{\mu_r \rho_{r0}}}{\rho_K d^{3/2}} \frac{c_0^{1/2}}{2\beta_1}; \\ b_2 &= \frac{k_{20}}{\beta_2} c_0^{1/2} = 9.75 \frac{\sqrt{\mu_r \rho_{r0}}}{\rho_K d^{3/2}} \frac{c_0^{1/2}}{\beta_2}; \\ b_3 &= \frac{k_{20}}{\beta_3} = 9.75 \frac{\sqrt{\mu_r \rho_{r0}}}{\rho_K d^{3/2}} \frac{1}{\beta_3}. \end{aligned}$$

The numerical solution to the equations in (113), where $n = 1.33$ and various values of the dimensionless parameters b_1, b_2, b_3 and δ are presented in the form of graphs in Figures 9, 10 and 11. The values of the dimensionless velocity of a gas determined according to formulas (99) - (101) are also plotted on the graphs. It is necessary to note that the change in the parameter n within the limits of $n = 1.25 - 1.4$ weakly influences the value of dimensionless velocity \bar{c}_K .

In the calculations it is accepted that at the beginning of the nozzle the velocity of the particles is equal to the velocity of the gas. As a consequence of this, on the initial section of the nozzle the value of $Re_{rel} < 1$ and the expression for a coefficient of resistance ought to be accepted in the form $C_x = \frac{24}{Re_{rel}}$.

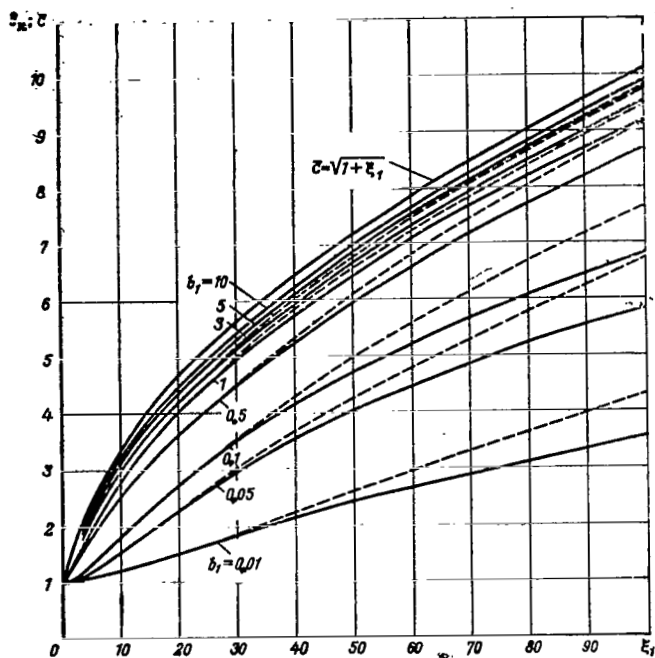


Fig. 9. Dependence of \bar{c}_K Upon the Dimensionless Length of Nozzle ξ_1 in the Case Where $c = \sqrt{1 + \xi_1}$ and $10 < Re_{rel} < 1000$; — $\delta = 0.005$; ---- $\delta = 0$.

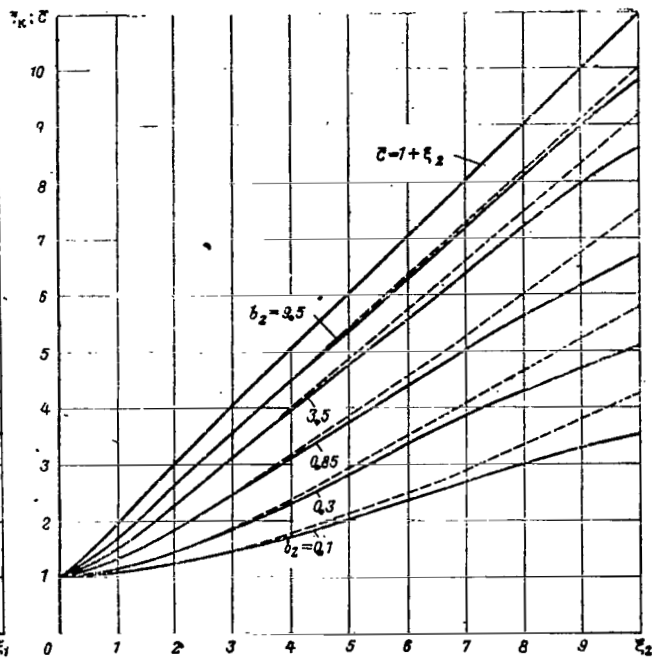


Fig. 10. Dependence of \bar{c}_K Upon the Dimensionless Length of Nozzle ξ_2 in the Case Where $c = 1 + \xi_2$ and $10 < Re_{rel} < 1000$; — $\delta = 0.005$; ---- $\delta = 0$.

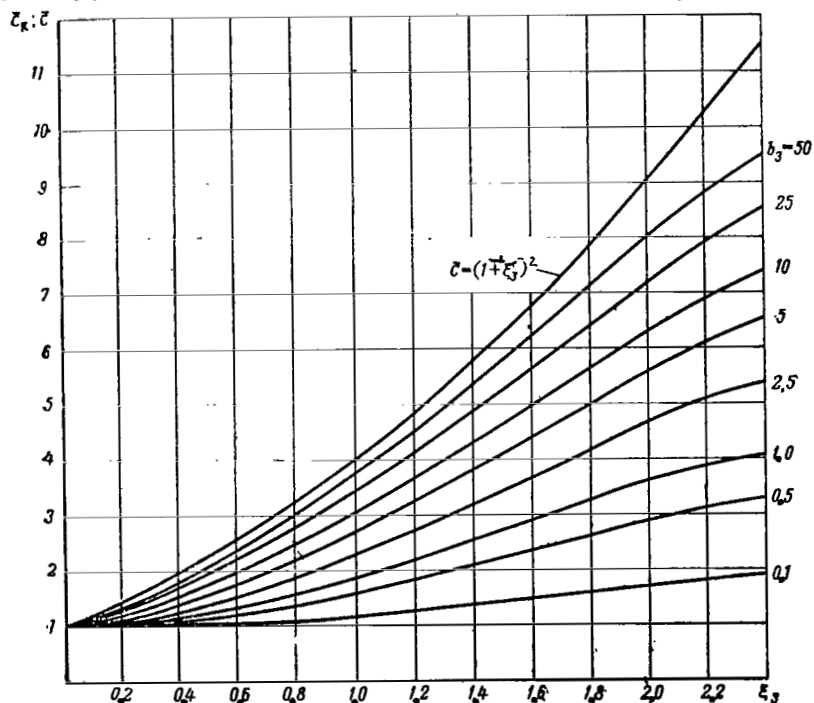


Fig. 11. The Dependence of \bar{c}_K Upon the Dimensionless Length of the Nozzle ξ_3 in the Case Where $c = (1 + \xi_3)^2$, $10 < Re_{rel} < 1000$ and $\delta = 0.005$.

/54

/55

However, the length of this portion is relatively small; therefore the difference on an initial section between the accepted law of

resistance ($C_x = \frac{13}{\sqrt{\text{Re}_{\text{rel}}}}$) and Stokes' law does not lead to significant errors in the final results of calculation.

Using the obtained dependence of \bar{c} upon ξ_1 , it is possible to calculate the significance of the coefficient of losses due to friction of gas on the particles. Expression (112) for the cases of /56 exhaust (99) - (101), respectively, assumes the forms

$$\left. \begin{aligned} \Delta\eta_{fr} &= 2g_K \frac{1-\delta\xi_1}{1+\xi_1} b_1 \int \frac{(1-\delta\xi_1)^{\frac{3-2n}{2(n-1)}} (\sqrt{1+\xi_1-\bar{c}_K})^{1/2}}{\bar{c}_K} d\xi_1; \\ \Delta\eta_{fr} &= 2g_K \frac{tb_2}{(1+\xi_2)^2} \int \frac{t^{\frac{3-2n}{2(n-1)}} (1+\xi_2-\bar{c}_K)^{1/2}}{\bar{c}_K} d\xi_2, \\ \text{where } t &= 1-\delta[(1+\xi_2)^2-1]; \\ \Delta\eta_{fr} &= 2g_K \frac{tb_3}{(1+\xi_3)^4} \int \frac{t^{\frac{3-2n}{2(n-1)}} [(1+\xi_3)^2-\bar{c}_K]^{1/2}}{\bar{c}_K} d\xi_3, \\ \text{where } t &= 1-\delta[(1+\xi_3)^4-1]. \end{aligned} \right\} \quad (114)$$

Graphs of the values $\Delta\bar{\eta}_{fr} = \Delta\eta_{fr}/g_K$ where $n = 1.33$ calculated according to these formulas are presented in Figures 12, 13 and 14. As follows from these figures, with a decrease in the parameters b_1 , b_2 and b_3 (for example, with an increase in particle diameter) the value $\Delta\bar{\eta}_{fr}$ increases initially, attains a maximum and then decreases. The value $\Delta\bar{\eta}_{fr}$ has a maximum even with a change in the dimensionless length of the nozzle; i.e., with a change in the degree of expansion of the gas phase.

In Figure 15 the dependences of $\Delta\eta_{fr}$ upon the parameters b_1 , b_2 and b_3 are shown with values of the dimensionless length of the nozzle $\xi_1 = 30$ and 100, $\xi_2 = 5$ and 10, $\xi_3 = 0.8$ and 2.2, corresponding to the dimensionless velocity of the gas phase $\bar{c} = 5.5$ and 10. Where $\bar{c} = 5.5$ the maxima of the values of $\Delta\eta_{fr}$, respectively, equal 0.24, 0.2 and 0.18.

Analogous calculations conducted for double-phase flows with particles whose motion is characterized by $\text{Re}_{\text{rel}} > 1000$ ($C_x \approx 0.48$) indicate that with an increase in the particle lag behind the gas the coefficient of losses due to friction of gas on the particles continues to decrease. To illustrate, in Graphs 16 and 17 the

values $\Delta\bar{\eta}_{fr} = \frac{\Delta\eta_{fr} g_\Gamma}{g_K}$ are presented as a function of the dimensionless lengths of the nozzle ξ_1 and ξ_2 for four cases of the gas flow $\bar{c} = \sqrt{1+\xi_1}$ and $\bar{c} = 1+\xi_2$, where $n = 1.33$ and various values of dimensionless parameters:

$$b_4 = 0,36 \frac{\rho_{ro}}{\rho_K d} \frac{c_0^2}{2\beta_1} \left(\text{where } \bar{c} = \sqrt{1 + \xi_1} \right),$$

/57

$$b_5 = 0,36 \frac{\rho_{ro}}{\rho_K d} \frac{c_0}{\beta_2} \left(\text{where } \bar{c} = 1 + \xi_2 \right)$$

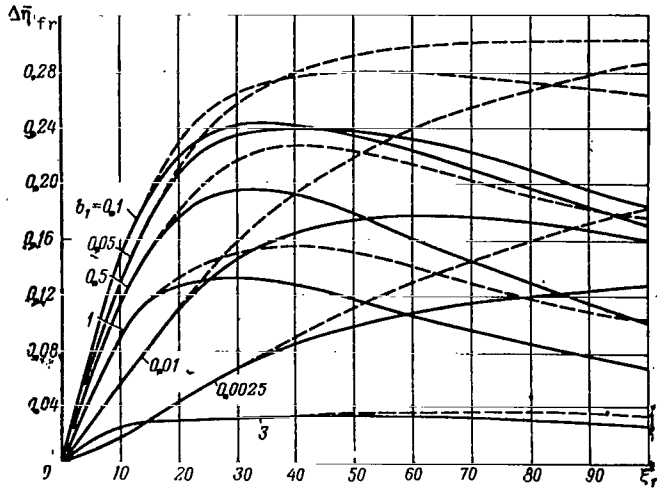


Fig. 12. Dependence of the Value of $\Delta \bar{n}_{fr} = \frac{1}{g_K} \Delta n_{fr}$ Upon ξ_1 in the Case Where $\bar{c} = \sqrt{1 + \xi_1}$ and $10 < Re_{rel} < 1000$: — $\delta = 0.005$; - - - $\delta = 0$.

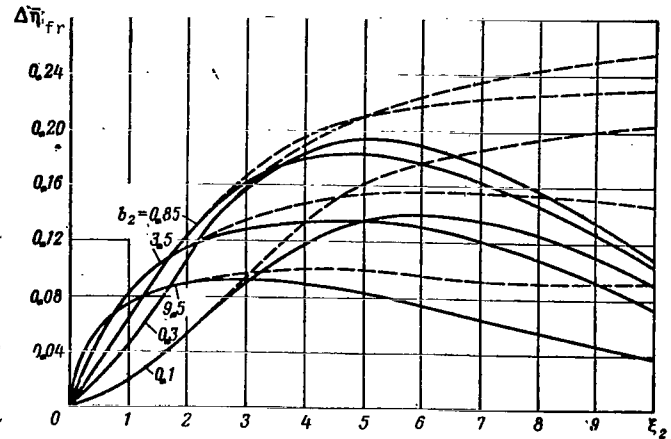


Fig. 13. Dependence of the Value of $\Delta \bar{n}_{fr} = \frac{1}{g_K} \Delta n_{fr}$ upon ξ_2 in the Case Where $\bar{c} = 1 + \xi_2$ and $10 < Re_{rel} < 1000$: — $\delta = 0.005$; - - - $\delta = 0$.

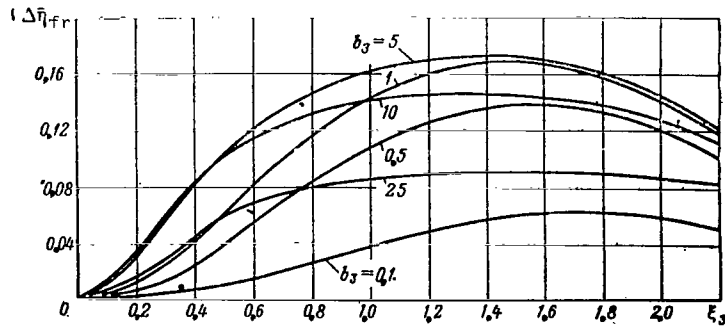


Fig. 14. Dependence of the Value of $\Delta \bar{n}_{fr} = \frac{1}{g_K} \Delta n_{fr}$ Upon ξ_3 in the Case Where $\bar{c} = (1 + \xi_3)^2$, $10 < Re_{rel} < 1000$ and $\delta = 0.005$.

/58

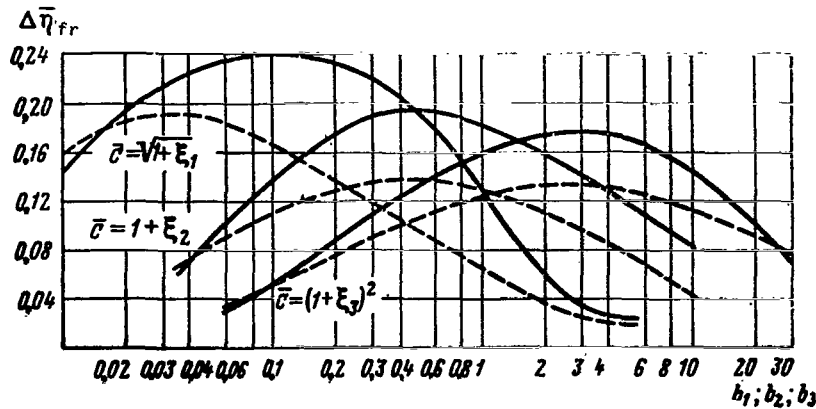


Fig. 15. Dependence of the Value of $\Delta\bar{\eta}_{fr} = \frac{1}{g_K} \Delta\eta_{fr}$ Upon the Parameters b_1, b_2, b_3 where $\delta = 0.005$ and $10 < Re_{rel} < 1000$: — $\bar{c} = 5.5$; ---- $\bar{c} = 10$.

Calculations were carried out according to formulas (17) and (79) /59 in which C_x was assumed to equal 0.48.

As may be seen from the graphs, with a decrease in the parameters b_4 and b_5 (i.e., with the remaining invariable conditions

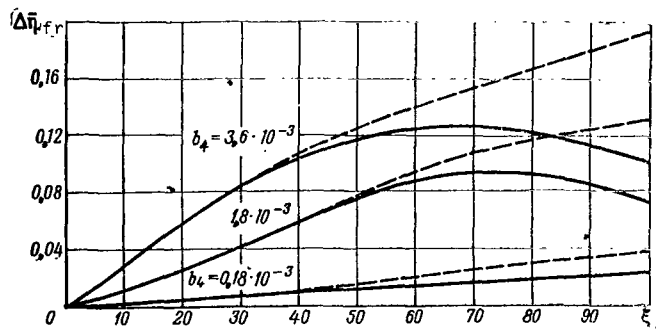


Fig. 16. Dependence of the Value of $\Delta\bar{\eta}_{fr} = \frac{g_{\Gamma}}{g_K} \Delta\eta_{fr}$ Upon the Dimensionless Length of the Nozzle ξ_1 in the Case Where $\bar{c} = \sqrt{1 + \xi_1}$ and $Re_{rel} > 1000$: — $\delta = 0.005$; --- $\delta = 0$.

with an increase in particle diameter) the value $\Delta\bar{\eta}_{fr}$ continues to decrease.

Thus, with the rest of the parameters of the mixture invariable and a constant concentration of phases, with an increase in particle diameter losses due to friction of the gas on the particles $\Delta\eta_{fr} = (g_K/g_{\Gamma})\Delta\eta_{fr}$ at first increase, reach a maximum and then decrease. With very small and very large particles, losses due to friction of the gas on the particles approach zero.

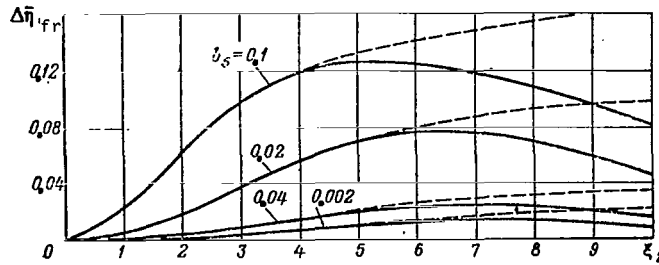


Fig. 17. Dependence of the Value of $\Delta\bar{n}_{fr} = \frac{g_{\Gamma}}{g_K} \Delta n_{fr}$ Upon the Dimensionless Length of the Nozzle ξ_2 in the Case Where $\bar{c} = 1 + \xi_2$ and $Re_{rel} > 1000$: — $\delta = 0.005$; --- $\delta = 0$.

§3. Losses Due to Incomplete Heat Exchange Between the Particles and the Gas

/60

Evaluating the gas temperature T_{Γ} from a calculation of the flow in the first approximation and the velocity of a particle and Re_{rel} according to the formulas and graphs of the preceding section from equation (20), it is possible to determine the particle temperature T_K , and consequently, even the losses due to incomplete heat exchange between the particles and the gas.

The particle temperature can be more simply determined only in the case of exhaust of a double-phase mixture with small particles, the relative motion of which is characterized by a number $Re_{rel} < 1$. In this case it is possible to ignore the second term of equation (21) and to consider $Nu = 2$ or $\alpha = 2\lambda_{\Gamma}/d$. As is known [23], such a value of the coefficient of heat emission corresponds to the heat exchange between a sphere and an immobile gas taking place only due to the heat conductivity of the gas.

Small particles move with a velocity near the velocity of the gas; therefore, by considering the process of heat exchange it is possible to assume $c_K \approx c_{\Gamma} = c$ with a sufficient degree of accuracy. Then (20) may be rewritten in the form

$$\frac{dT_K}{dx} = \frac{12\lambda_{\Gamma}}{c_p \kappa \rho_K d^2} \frac{T - T_K}{c}. \quad (115)$$

Let us examine this equation for the same cases of the flow of a double-phase mixture as in the preceding section: With regard to expression (71), equation (115) for the laws of flow (99)-(101) may be rewritten in the following way:

$$\left. \begin{aligned} \text{for the case where } \bar{c} = \sqrt{1 + \xi_1}, \quad & \frac{dt_K}{d\xi_1} + \frac{B_1}{\sqrt{1 + \xi_1}} t_K = B_1 \frac{1 + \delta - \delta(1 + \xi_1)}{\sqrt{1 + \xi_1}}; \\ \text{for the case where } \bar{c} = 1 + \xi_2, \quad & \frac{dt_K}{d\xi_2} + \frac{B_2}{1 + \xi_2} t_K = B_2 \frac{1 + \delta - \delta(1 + \xi_2)^2}{1 + \xi_2}; \\ \text{for the case where } \bar{c} = (1 + \xi_3)^2, \quad & \frac{dt_K}{d\xi_3} + \frac{B_3}{(1 + \xi_3)^2} t_K = B_3 \frac{1 + \delta - \delta(1 + \xi_3)^4}{(1 + \xi_3)^2}, \end{aligned} \right\} \quad (116)$$

$$\text{where } B_1 = \frac{12\lambda_r}{c_p \kappa \rho_K d^2} \frac{c_0}{2\beta_1}; B_2 = \frac{12\lambda_r}{c_p \kappa \rho_K d^2} \frac{1}{\beta_2}; B_3 = \frac{12\lambda_r}{c_p \kappa \rho_K d^2} \frac{1}{\beta_3 \sqrt{c_0}}$$

dimensionless criteria characterizing heat exchange between particles and gas.

With the initial conditions $t_K = 1$ and $\xi = 0$ (at the initial moment of motion, the temperatures of the phases are equal), the solutions to the equation will be, respectively: /61

$$\left. \begin{aligned} t_K &= 1 - \delta \left[\frac{1}{2B_1^2} + \xi_1 - \left(\frac{1}{2B_1^2} - \frac{1}{B_1} \right) e^{-2B_1(\sqrt{1+\xi_1}-1)} - \frac{\sqrt{1+\xi_1}}{B_1} \right]; \\ t_K &= 1 - \delta \left[\frac{B_2}{B_2+2} (1+\xi_2)^2 + \left(1 - \frac{B_2}{B_2+2} \right) \frac{1}{(1+\xi_2)^{B_2}} - 1 \right]; \\ t_K &= 1 - \delta \left[B_3 e^{\frac{B_3}{1+\xi_3} \xi} \int_0^\xi (1+\xi_3)^2 e^{-\frac{B_3}{1+\xi_3} d\xi_3} + e^{-\frac{B_3 \xi_3}{1+\xi_3}} - 1 \right]. \end{aligned} \right\} \quad (117)$$

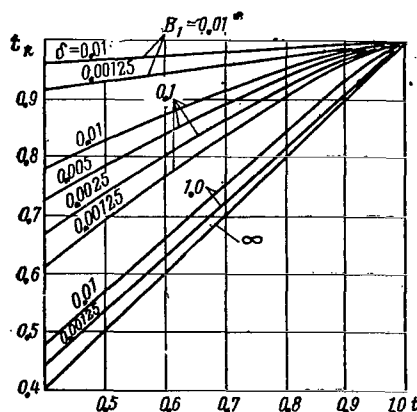


Fig. 18. Dependence of Temperature t_K Upon t in the Case Where $\bar{c} = \sqrt{1 + \xi_1}$ and $Re_{rel} < 1$.

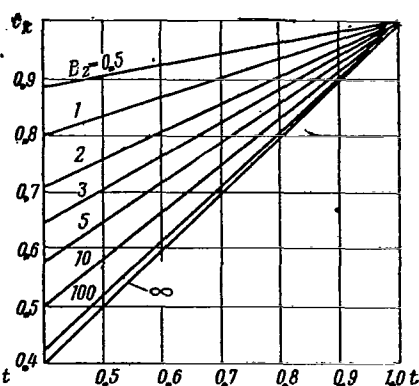


Fig. 19. Dependence of Temperature t_K Upon t in the Case Where $\bar{c} = 1 + \xi_2$ and $Re_{rel} < 1$.

Figures 18, 19 and 20 give the dimensionless temperatures t_K as a function of t determined by formulas (117) and (104). The dependence of particles upon the gas temperature in all the cases of exhaust considered proved to be close to linear. According to these graphs it is possible to find the value of the coefficient

$$\epsilon = \frac{T_0 - T_K}{T_0 - T_r} = \frac{1 - t_K}{1 - t}, \quad (118)$$

entering the expression for the polytropic index (86) and for the coefficient of losses due to incomplete heat exchange between the phases (88). The dependency of δ upon dimensionless criteria B_1 , B_2 and B_3 for a number of values and various cases of exhaust is presented in Figure 21. It is necessary to note that with a linear

law of change in velocity of a gas the temperature of a particle and the value of ϵ do not depend upon δ but are determined only by the value of criterion B_2 .

In the case of double-phase mixtures with even larger particles ($Re_{rel} \gg 1$) the equation for heat exchange (20) cannot be con-

sidered separate from the equation of particle motion. Moreover, the coefficient of heat emission is no longer a constant value, but depends upon the number Re_{rel} , according to equation (21). This significantly hinders calculation of heat exchange between the phases.

§4. Exhaust of a Double-Phase Mixture in the Nozzle in the Case Where $\bar{c} = 1 + b(\xi e^{1-\xi})^q$ and $10^{-4} < Re_{rel} < 100$.

In a majority of supersonic nozzles the curve of the increase in the speed of a mixture along the conduit has a point of inflection: on the subsonic portion it is convex downward, on the supersonic portion it has an approximately parabolic shape and is turned to be convex upward.

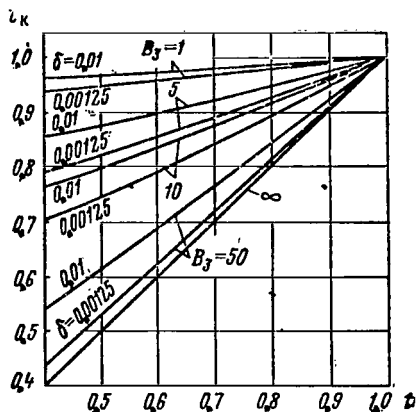


Fig. 20. Dependence of Temperature t_K Upon t in the Case Where $\bar{c} = (1 + \xi_3)^2$ and $Re_{rel} < 1$.

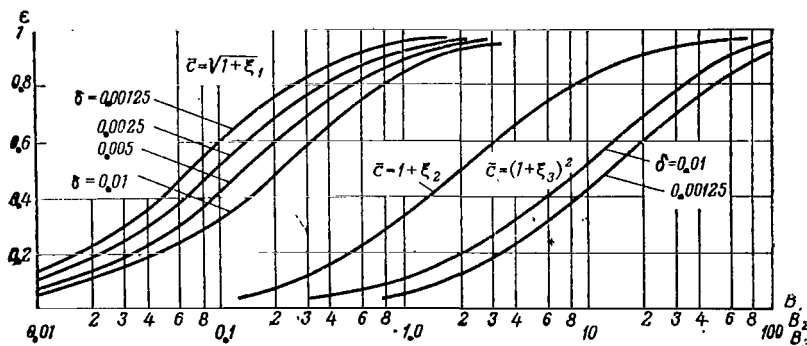


Fig. 21. Dependence of Coefficient ϵ Upon the Dimensionless Criteria B_1 , B_2 , B_3 .

The sinusoid shifted relative to the beginning of the coordinate has an analogous nature. However, a sinusoid is a symmetrical curve, while in real nozzles the subsonic part is usually shorter than the supersonic so that the point of inflection is displaced to the left. More appropriate for a description of the indicated characteristic of the flow of a mixture in supersonic nozzles is the curve defined by

/63

$$\bar{c} = 1 + b(\xi e^{1-\xi})^q, \quad (119)$$

where $\xi = \frac{x}{L}$ is dimensionless coordinate along the axis of the nozzle;

L is the characteristic length;

b and q are parameters defining the amplitude and shape of the curve.

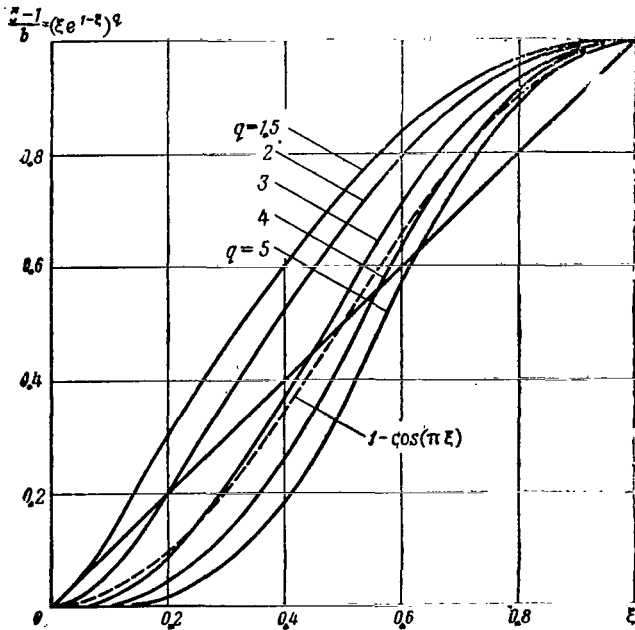


Fig. 22. Nature of the Increase in Gas Velocity Along a Nozzle Depending Upon Shape Parameter q .

$10^{-4} < Re_{rel} < 100$. It is possible to replace the experimental dependence of the coefficient of resistance C_x for a sphere in the indicated range of change in the Re_{rel} number by an analytical dependence (cf. Fig. 1):

$$C_x = \frac{24}{Re_{rel}} + 1.1. \quad (120)$$

Moreover, we shall accept the following dependences of coefficients of viscosity and heat conductivity of the gas upon temperature:

$$\frac{\mu_r}{\mu_{r0}} = \left(\frac{T_r}{T_{r0}} \right)^{0.75} = t^{0.75}; \quad (121)$$

Figure 22 shows the change in the value $(\bar{c} - 1)/b = (\xi e^{1-\xi})^q$ as a function of ξ for various values of parameter q . It is apparent from the figure that selecting the value of amplitude b in a corresponding way, the value of shape parameter q and also the characteristic length L with the aid of equation (119), it is possible to encompass a wide range of supersonic nozzles found in practice. If $L > L_c$, then the dimensionless coordinate ξ_c , corresponding to the exit section of the nozzle becomes less than unity.

In the present section ^{/64} we shall consider the exhaust of double-phase mixtures with particles in the range of

$$\bar{\lambda}_r = \frac{\lambda_r}{\lambda_{r0}} = t^{0.85}. \quad (122)$$

Equations for particle motion (17) and heat exchange (20) in the given case can be reduced to the following dimensionless form:

$$\frac{d\bar{c}_K}{d\xi} = \frac{1}{Sto} \bar{\mu}_r \frac{\bar{c} - \bar{c}_K}{\bar{c}_K} + \frac{Re_0}{21.8 Sto} \bar{p}_r \frac{(\bar{c} - \bar{c}_K)^2}{\bar{c}_K}; \quad (123)$$

$$\frac{dt_K}{d\xi} = \frac{K_4}{Sto} (1 + 0.08 Re_{rel}^{0.66}) \bar{\lambda}_r \frac{t - t_K}{\bar{c}_K}, \quad (124)$$

where $Sto = \frac{\rho_K c_0 d^2}{18 \mu_{r0} L}$; $K_4 = \frac{2 \lambda_{r0}}{3 \mu_{r0} c_{pK}}$;

$Re_0 = \frac{c_0 \rho_{r0} d}{\mu_{r0}}$ is a criterion based upon the initial values of the parameters of the flow and having the structure of a Reynolds number.

Expression (78) for the relative coefficient of losses due to friction of gas on particles in this case is written thus:

$$\Delta \bar{\eta}_{fr} = 2 \frac{t}{c^2} \frac{1}{Sto} \left(\int \bar{\mu}_r \frac{\bar{c}_{rel}^2}{\bar{c}_K t} d\xi + \frac{Re_0}{21.8} \int \bar{p}_r \frac{\bar{c}_{rel}^3}{\bar{c}_K t} d\xi \right); \quad (125)$$

Here t and \bar{p}_r are determined, respectively, according to formulas (71) and (72) depending upon the velocity of the gas phase determined in the first approximation from equation (119).

Equations (123) and (124), after substituting in them the expressions for \bar{c} , t , $\bar{\mu}_r$, \bar{p}_r , $Re_{rel} = Re_0 [(\bar{c} - \bar{c}_K) \bar{p}_r] / \bar{\mu}_r$ etc., contain only two unknown values: \bar{c}_K and t_K and may be solved independent of the remaining equations. However, it is convenient to calculate the integrals entering (125) parallel to the calculation of \bar{c}_K and t_K ; therefore, when using a computer, all three equations from (123)-(125) must be solved simultaneously.

After solving such an expanded system of equation it is possible to define the parameters of a double-phase flow in the second approximation according to the correlation in (92)-(98). /65

The dimensionless coefficients Sto , Re_0 , δ , n and K_4 entering equations (123)-(125) must be considered as similarity criteria in the indicated conditions of mixture exhaust. The first three coefficients depend on both the physical characteristics of the working fluid and upon its initial state; the criterion K_4 depends only upon the physical characteristics of the working fluid; the polytropic index of expansion of the gas phase n still depends upon the

concentrations of the phases.

We shall consider the obtained system of equations to be applicable to the exhaust of a high-temperature double-phase mixture with particles of the aluminum oxide type. The polytropic index of such a mixture with a concentration of particles up to 30-40% may change within the limits of 1.12-1.2. However calculations will be conducted with a certain mean value $n = 1.16 = \text{const}$. This does not lead to noticeable error in the second approximation with the determination of the exhaust parameters of a double-phase mixture from a nozzle if, certainly, calculation of the first approximation was conducted using the true value of the polytropic index n .

The value of the parameter K_4 for such a mixture may be taken to be approximately equal to 2.15. The change in this parameter within the limits $K_4 = 2 - 2.5$ weakly influences the results of the calculation.

The system of equations in (123)-(125) was solved with values of the parameter $K_4 = 2.15$, $n = 1.16$ and various values of St_0 , Re_0 , b and δ on an M-20 computer. The results of the solution are presented in Figures 23-26. In Figure 23 the change in velocity of the particles in gas along the nozzle obtained in first approximation is presented. The Re_{rel} number, even with the greatest particle lag, does not exceed 90. At the beginning of the nozzle $Re_{rel} = 0$; then it increases and, approximately in the middle of the nozzle, attains a maximum; in the final section of the nozzle Re_{rel} decreases significantly due to the rapid decrease in the density of the gas prevailing above the reversed influence of monotonal increase in the particle lag.

In Figure 24 the dependences of Δn_{fp} upon the length of the nozzle are presented. In Figure 25 graphs of the dependence of the dimensionless temperature t_K upon t where $q = 3$ and $b = 30$ are shown. This dependence proves to be nearly linear. An analogous dependence was obtained even with other values of b . Only in the terminal section of the nozzle, where the velocity of the gas approximates a constant value, does this dependence diverge from a linear one and the temperature of the particles approximate the temperature of the gas.

In a majority of cases, especially if the exit section of the nozzle under consideration corresponds to the coordinate $\xi_c < 1$, it is possible to ignore the influence of the terminal section of the nozzle on the parameters of the mixture exhaust and consider that all along the nozzle the particle temperature is a linear function of the gas temperature. It is possible to show that heat conduction from the particles to the gas on the terminal section of the nozzle very weakly influences the parameters of mixture exhaust.

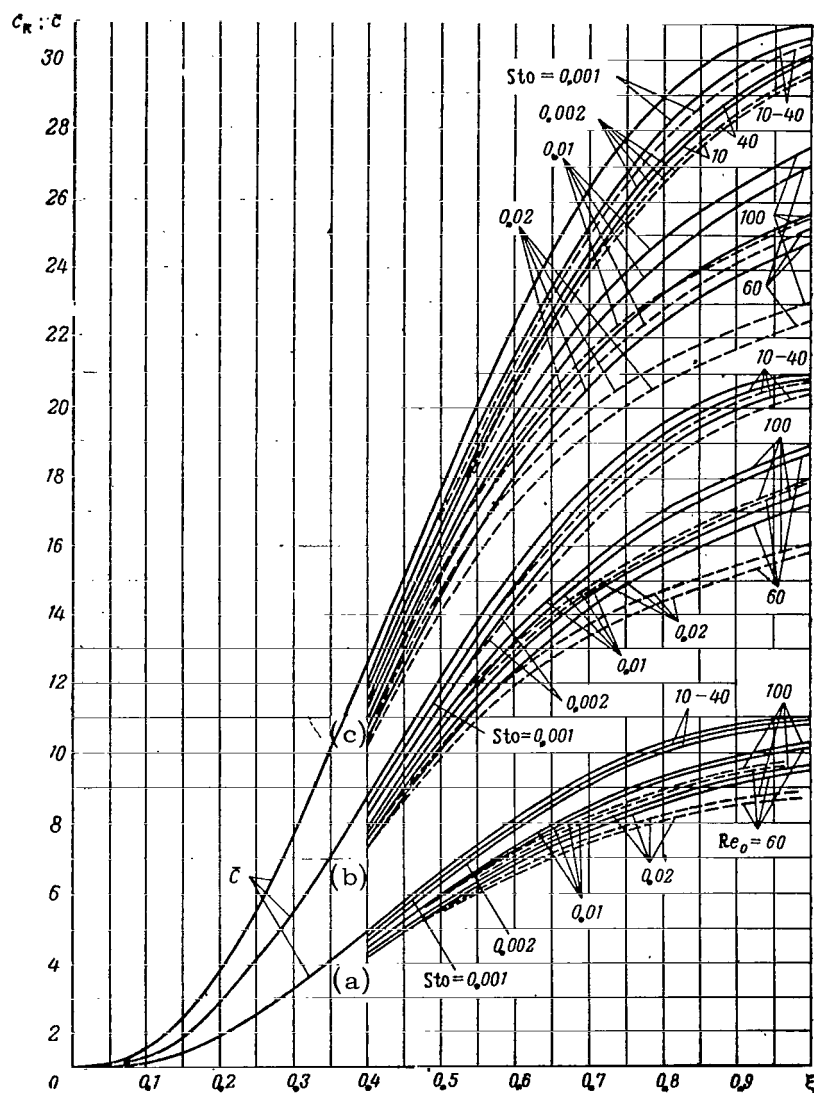


Fig. 23. Change in the Velocity of Phases Along the Nozzle:
 a--- $b = 10$: — $\delta = 5 \cdot 10^{-3}$; - - - $\delta = 6.5 \cdot 10^{-3}$
 b--- $b = 20$: — $\delta = 1.25 \cdot 10^{-3}$; - - - $\delta = 1.65 \cdot 10^{-3}$
 c--- $b = 30$: — $\delta = 5.5 \cdot 10^{-4}$; - - - $\delta = 7.25 \cdot 10^{-4}$

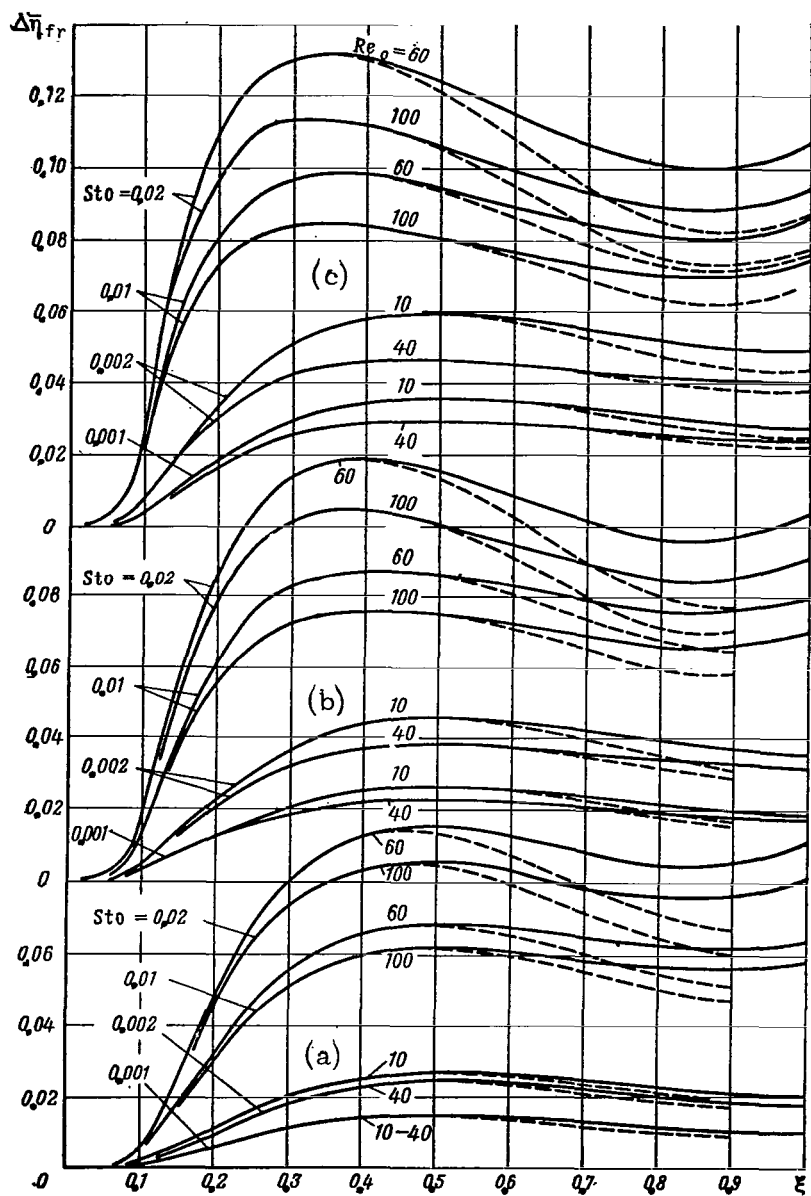


Fig. 24. Dependence of the Value $\Delta\eta_{fr}$ Upon the Dimensionless Length of the Nozzle $\xi = x/L$:

a--- b = 10: ————— $\delta = 5.0 \cdot 10^{-3}$: - - - - - $\delta = 6.5 \cdot 10^{-3}$
 b--- b = 20: ————— $\delta = 1.25 \cdot 10^{-3}$: - . - . - $\delta = 1.65 \cdot 10^{-3}$
 c--- b = 30: ————— $\delta = 5.5 \cdot 10^{-4}$: - - - - - $\delta = 7.25 \cdot 10^{-4}$

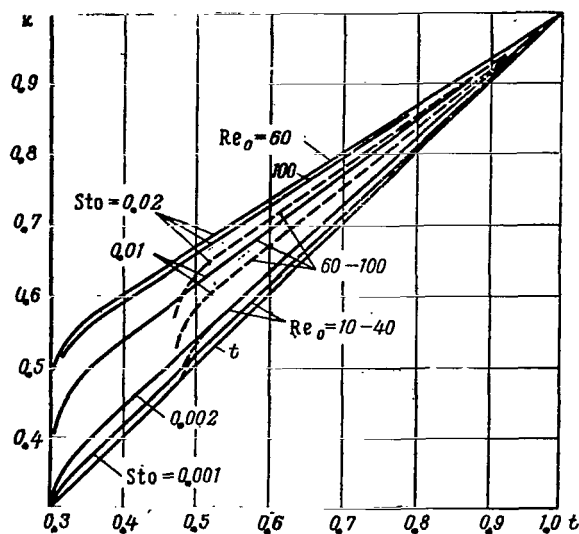


Fig. 25. Correlation Between Dimensionless Temperatures t_K and t Where $q = 3$ and $b = 30$:
 — $\delta = 7.25 \cdot 10^{-4}$;
 - - - $\delta = 5.5 \cdot 10^{-4}$

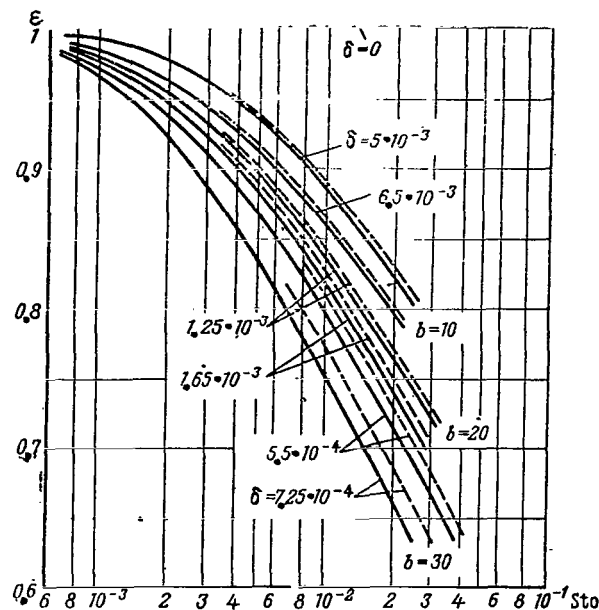


Fig. 26. Dependence of Coefficient ϵ Upon St_0 Where $q = 3$:
 — $Re_0 = 10$; - - - $Re_0 = 100$.

Figure 26 shows the dependence of the value $\epsilon = (T_0 - T_K)/(T_0 - T_\Gamma)$ upon St_0 for all variants of exhaust which were checked. From the figure it is apparent that the basic parameter determining the intensity of heat exchange is the Stokes number. Where $St_0 < 10^{-3}$ the influence of incomplete heat exchange upon parameters of the exhaust of the double-phase mixtures can be ignored.

/69

Interpolating (or extrapolating) the obtained results of the calculation to the case of exhaust of a real mixture it is possible to calculate rather rapidly the parameters of the exhaust and the shape of the nozzle.

A Calculation Example

To calculate the shape of the nozzle and parameters of the exhaust of a double-phase mixture having the following parameters: $T_0 = 3250^\circ K$; $p_0 = 5 \cdot 10^6 \text{ n/m}^2$, $p_c = 0.1 \cdot 10^6 \text{ n/m}^2$; $k = 1.2$; the polytropic index of an equilibrium expansion; $n = 1.15$; the constant of the gas phase $R = 0.360 \text{ kJ/kg} \cdot ^\circ K$; $c_{p\Gamma} = 2.16 \text{ kJ/kg} \cdot ^\circ K$; $c_{pK} = 1.36 \text{ kJ/kg} \cdot ^\circ K$; $c_0 = 115 \text{ m/sec}$; $\rho_{\Gamma 0} = 4.88 \text{ kg/m}^3$; $\zeta_K = 3900 \text{ kg/m}^3$; $\mu_{\Gamma 0} = 8 \cdot 10^{-5} \text{ n} \cdot \text{sec/m}^2$; $\lambda_{\Gamma 0} = 0.35 \text{ W/m} \cdot ^\circ K$; expenditure of the mixture $G_{\text{mix}} = 17.1 \text{ kg/sec}$; $g_K = 0.3$; diameter of the particles $d = 0-7 \mu\text{m}$, and the function of particle distribution according to sizes

$$\varphi(d) = \frac{1 - \cos\left(\frac{2\pi}{7} d \cdot 10^6\right)}{7 \cdot 10^{-6}}. \quad (126)$$

In order to simplify the study we shall ignore losses due to friction of the flow on the walls of the nozzle; these losses can be considered supplementally.

For the mixture under consideration dimensionless parameters are $B_4 = 2.15$ and $\delta = 1.05 \cdot 10^{-3}$.

(1) In first approximation we shall select a nozzle shape near the optimal. Its concourse is represented in Figure 27a; the length of the nozzle in this case is $L_c = 0.25$ m.

For the selected nozzle shape all parameters of exhaust in first approximation are calculated according to the formulas of exhaust equilibrium (71) - (74) or according to the tables of hydrodynamic functions for the given polytropic index of an equilibrium expansion $n = 1.15$.

For the given value $\pi = p_c/p_0 = 0.02$ the equilibrium velocity of a mixture on a section of the nozzle $c_c = 2240$ m/sec; therefore $\bar{c}_c = c_c/c_0 = 19.5$. Change in the value of \bar{c} along the nozzle is shown in Figure 27b. From this figure it is apparent that the law of velocity change of the gas in first approximation corresponds sufficiently accurately with the law studied in detail above, described by equation (119) in the case where $q = 3$ and $b = 20$ (dotted curve). However, in the last case where $\bar{c} = 19.5$, $\xi = 0.8$. Therefore, in the exit section of the nozzle under consideration we accept $\xi_c = 0.8$. Hence, we shall define the characteristic line $L = x_c/\xi_c = 0.32$ m, greater than $L_c = 0.25$ m.

(2) The value \bar{c}_{rel} , $\Delta\bar{n}_{fr}$ and $\Delta\bar{n}_Q$ necessary for determining parameters of exhaust in second approximation and for correction of the flow passage cross sectional areas of the nozzle are determined by extrapolation or interpolation of the results of the calculation obtained for the law in (119).

For this according to the data from Figure 23 and 24 with the 70 selected dimensionless length of the nozzle $\xi_c = 0.8$ it is convenient to construct supplementary graphs of the dependences \bar{c}_{rel} and $\Delta\bar{n}_{fr}$ upon δ (Fig. 28). The curves in Figure 28 are constructed according to two points; their extrapolation onto the region of the small values of δ (dotted lines) is constructed with regard to the nature of their flow in this region. Furthermore, with the aid of Figure 28 curves \bar{c}_{rel} and $\Delta\bar{n}_{fr}$ are constructed depending upon the Sto already for given values of the parameter $\delta = 1.05 \cdot 10^{-3}$; an analogous dependence of the values of ϵ upon the Sto with the same value of the parameter δ is a direct extrapolation of the curves in Figure 26. It is necessary to bear in mind that where $\delta \rightarrow 0$, $\epsilon \rightarrow 1$. The curves mentioned are presented in Figure 29.

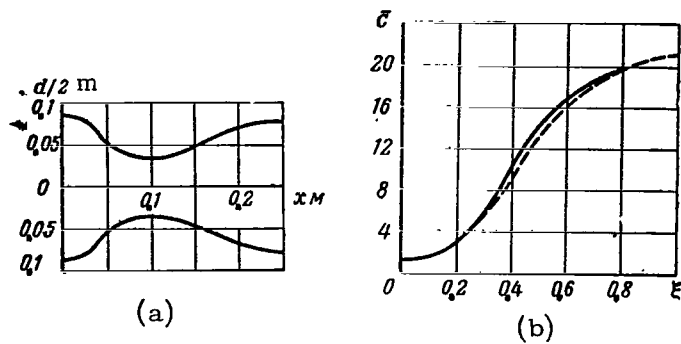


Fig. 27. Calculation of the Exhaust of a Double-Phase Mixture: (a) Shape of the Nozzle; (b) Increase in the Velocity of the Gas Along the Nozzle: ----- Law (119) Where $q = 3$; $b = 20$.

(3) The parameters Sto and Re_0 for particles of different diameters contained in the mixtures and corresponding values of \bar{c}_{rel} , $\Delta\bar{\eta}_{fr}$ and ϵ , determined from the graphs in Figure 29, and also the values of the function particle distribution according to sizes (126) are presented in Table 1.

TABLE 1

Particle Diameter in μm	0	1	2	3	4	5	6	7
$Stk \cdot 10^3$	0	0.1	0.39	0.88	1.57	2.45	3.5	4.8
Re_0	0	7	14	21	28	35	42	49
\bar{c}_{rel}	0	0.4	1.1	2	2.8	3.4	4.2	5
$\Delta\bar{\eta}_{fr}$	0	0.028	0.055	0.08	0.095	0.12	0.135	0.148
ϵ	1	0.985	0.915	0.86	0.82	0.775	0.74	0.71
$7\varphi(d) \cdot 10^{-6}$	0	0.377	1.225	1.9	1.9	1.225	0.377	0

(4) Using the data from Table 1 according to formulas (82), (86), (89) and (93), we shall determine the values of $\Delta\eta_{fr} = 0.026$, $\epsilon^* = 0.846$, $J_1 = 2.33$, $J_2 = 6.41$, $\vartheta = 0.27$, $n^* = 1.156$, $\bar{n} = 1.035$ by numerical integration.

(5) According to formulas (88) or from Figure 4 we shall determine the value $\Delta\eta_Q = 0.0074$.

(6) According to formulas (92), (94) and (96) we shall determine the values $c_T/c = 1.018$, $P_d/P_p = 0.982$ and $t_T/t = 0.998$.

Thus the velocity and temperature of the gas phase on a section of the nozzle differs only insignificantly from its velocity and temperature with an equilibrium exhaust. This confirms the correctness of the assumptions made above on the weak difference in the laws of distribution of velocity and temperature along the nozzle in both approximations; i.e., on the possibility of taking c_{rel} and

ΔT to be equal in both approximations.

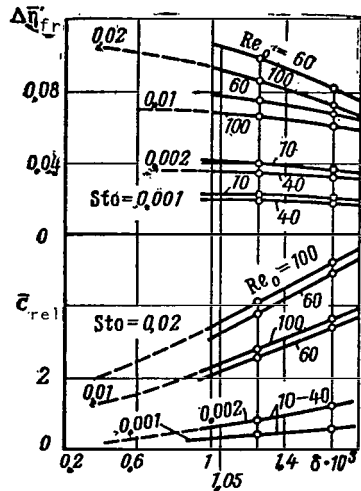


Fig. 28. Dependence of $\Delta\bar{\eta}_{fr}$ and c_{rel} upon δ Where $\xi_c = 0.8$.

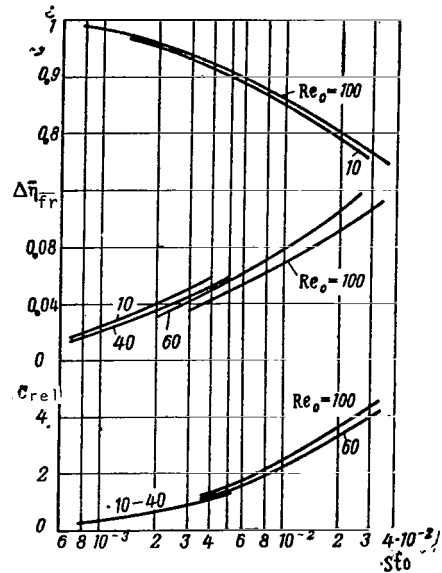


Fig. 29. Dependence of ϵ , $\Delta\bar{\eta}_{fr}$ and c_{rel} upon St_0 Where $\xi_c = 0.8$ and $\delta = 1.05 \cdot 10^{-3}$.

Finally, from (98) we obtain that $\frac{f_d}{f} = 0.98$; i.e., the exit section of a nozzle must decrease by 2% in comparison with the nozzle calculated for an equilibrium exhaust.

(7) For correction of the shape of the nozzle (i.e., for changing all of its other sections including the critical) it is still necessary to conduct analogous calculations for two or three intermediate sections. Correction of any flow section of the nozzle may be performed by interpolation of results of calculation.

(8) Thus with the exhaust of the mixture there are: losses in impulse due to particle lag behind the gas and due to incomplete heat exchange between the phases is approximately 1.8%; decrease in efficiency of the nozzle due to friction of the gas on the particle $\Delta\eta_{fr} = 0.026$; decrease in efficiency of the nozzle due to incomplete heat exchange $\Delta\eta_q = 0.0074$. In particular, this confirms the well-known hypothesis that particle lag behind the gas influences the specific impulse of the mixture significantly more strongly than incomplete heat exchange between the phases.

(9) In the case of a monodispersed mixture with particles from 1-7 μm in diameter and with the same other parameters according to the data of Table 1 and formulas (78), (79), (88) and (95) the parameters of exhaust are determined immediately in the second approximation. Results of calculating the exhaust of such mono-

dispersed mixtures with different particle diameters are presented in Table 2.

TABLE 2

/72

Particle Diameter μm	0	1	2	3	4	5	6	7
\bar{c}_{rel}	0	0.4	1.1	2	2.8	3.4	4.2	4.8
$\Delta\eta_{fr} = g_k \Delta\eta_{fr}$	0	0.0084	0.0165	0.024	0.0285	0.036	0.0405	0.0445
ϵ	1	0.985	0.915	0.86	0.82	0.775	0.74	0.71
\bar{n}	1	1.01	1.02	1.03	1.04	1.05	1.057	1.065
$\Delta\eta_Q$	0	0.003	0.006	0.0084	0.010	0.0114	0.0126	0.0134
c_r/c	1	1.004	1.008	1.014	1.019	1.025	1.032	1.038
P_d/P_p	1	0.994	0.988	0.983	0.977	0.973	0.968	0.964
t_r/t	1	1	0.9995	0.999	0.998	0.997	0.996	0.994
f_d/\bar{h}	1	0.996	0.992	0.985	0.98	0.973	0.965	0.958

§5. Experimental Studies of Nozzles in Double-Phase Flows

In recent years, attempts at experimental determination of particle lag according to temperature and velocity behind the gas have been made. Also, the other parameters characterizing exhaust of a double-phase mixture from a nozzle were studied.

Thus, in article [20] results are presented of the experimental determination of the temperature of particles with an expansion of a double-phase mixture in a nozzle. It was shown that the temperature lag of particles of MgO with a diameter of $1.85\mu\text{m}$ is $150-180^\circ\text{C}$ with a gas temperature on the order of $1400-1800^\circ\text{K}$. These data are sufficiently close to the calculated values of temperature lag obtained for the same conditions of flow.

In study [21], the lag of MgO particles with a diameter of $\sim 3\mu\text{m}$ on a section of nozzle with a thrust of 4500 n was determined. The amount of particle lag was judged according to the light absorption of a double-phase mixture, depending upon the local concentration of particles, i.e., upon the correlation of velocities of the phases. A satisfactory correlation between experimental and calculated velocity was obtained from the experiment.

In [55], the velocities of aluminum particles suspended in helium for a section of a subsonic nozzle were determined photographically. The particle lag obtained was somewhat less than the calculated lag, which may be explained by the irregular shape of the particles and also by the rapid equilization of the velocities of the phases for the nozzle section.

In article [35] losses of thrust in tonic and profiled supersonic nozzles are compared. It proved to be the case that experi-

mental values of the losses of thrust in full-sized nozzles correspond to their calculated values with sufficient accuracy. /73

In study [11], the expenditure of the double-phase mixture through a nozzle is measured. In order to evaluate the influence of particle lag on the expenditure, the subsonic part of the nozzle was made of different configuration; the diameter of the nozzle throat was equal to 6.35 mm. The double-phase mixture consisted of glass spheres suspended in nitrogen or helium. An increase in the concentration of particles in the nozzle axis zone in its supersonic part with a sphere diameter of $14.4\mu\text{m}$ was noted in the experiments; a certain separation was noted even with the diameter of the spheres equal to $2.7\mu\text{m}$.

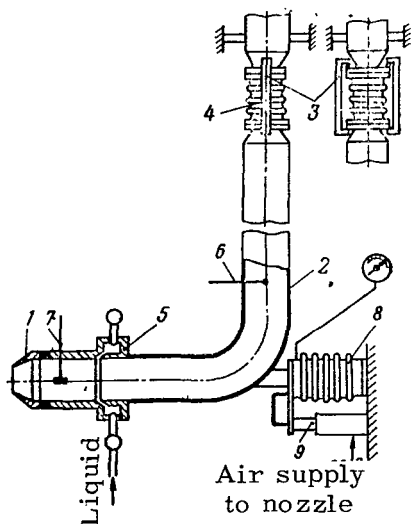


Fig. 30. Schematic Drawing of an Apparatus for Studying Nozzles: (1) Nozzle; (2) Corpus; (3) Knife Suspension; (4) Sylphon (5) Collector; (6) Thermocouple; (7) Full Pressure Cap; (8) Dynamometer Sylphon; (9) Valve Apparatus.

a pendulum on legs and connected with the basic aerial magistral by a sylphon (Fig. 30). In the process of the experiments such parameters of flow as expenditure of air ($G \approx 1\text{ kg/sec}$) total nozzle thrust ($R_{\Sigma} \approx 350\text{ n}$), temperature, static and full gas pressure in front of the nozzle, expenditure of suspended phase, etc., were measured.

Careful experiments with subsonic nozzles on a mixture of air and powder particles with $d = 10\mu\text{m}$ or iron spheres with $d = 20, 80, 350\mu\text{m}$ [30] indicated a satisfactory agreement between experimental and calculated values of impulse in the range $g_K = 0.2 - 0.8$.

Despite a certain disconnected and fragmentary nature of the published experimental results, they will allow us to establish that all the theoretical dependences based on their assumptions analogous to those made in this book (relative, for example, to the selection of coefficients of resistance and heat emission of a particle, linearity of flow, etc.) are satisfactorily confirmed by the experiment.

Results are presented below of the experimental study of the operation of subsonic conic nozzles on double-phase flows conducted by the author of this work together with D.L. Podvid. Investigations were conducted on an apparatus in the form of an elbow-shaped pipe suspended like

Moreover, the experimental apparatus insured the possibility of studying the operation of nozzles with walls covered by a liquid /74

film. For this purpose, on the corpus in front of the nozzle a ring collector distributor was fixed which provided a thin layer of liquid on the internal surface of the nozzle. The liquid was supplied at an angle to the axis of the nozzle not exceeding 15° . This decreased the possibility of tearing the film from the walls of the nozzle under a high velocity of feeding the liquid.

1. Study of the Exhaust of Double-Phase Flows

In the process of the experiments conic subsonic nozzles with a length of $L_c = 36$ and 76 mm, intake diameter $D_0 = 85$ mm and exit diameter $D_c = 55$ mm were studied. The nozzles worked on air and on double-phase flows consisting of a mixture of cold air ($t = 20^\circ\text{C}$) with one of the following components: (a) particles of water scattered by a centrifugal nozzle; (b) particles of powder; (c) particles of coal ash removed from TEC electrofilters; (d) aluminum powders.

The basic parameters of particles are presented in Table 3.

TABLE 3

Suspended Phase	Density ρ_K kg/m ³	Average Particle Diameter μm	Specific Thermal Capacity c_{pK} J/kg. $^\circ\text{K}$	Coefficient of Heat Conductivity λ_K J/m.sec. $^\circ\text{K}$
Water	1000	100	4190	0.545
Talc	2700	10	872	-
Ash	2300	12.5	755	1.26
Aluminum powder	2600	< 5	890	201

In the process of the experiments the degree of pressure lowering in nozzles corresponded to the reduced velocity of the gas phase $\lambda_F = 0.9 - 0.95$.

We shall compare the specific impulses of single-phase and double-phase working fluid flows having equal parameters upon entrance into the nozzle and discharging into the medium with the same pressure. The specific impulse of a double-phase flow can be calculated according to formula (95). The specific impulse with exhaust of a pure gas without regard to losses due to friction on the nozzle wall is

$$P_0 = c_{pd} = \sqrt{2H_{\text{diso ad}}} \quad (127)$$

where $H_{\text{disp.ad}} = H_{\text{ad}} + \frac{a_0^2}{2}$ is the disposable energy for expansion of a pure gas;

$H_{ad} = \frac{k}{k-1} RT_0 \left[1 - \left(\frac{p}{p_0} \right)^{\frac{k-1}{k}} \right]$ adiabatic work of the expansion of 1 kg of gas. /75

The relative increase in specific impulse of a double-phase flow is

$$\Delta \bar{P}_c = \frac{P_d - P_0}{P_0} = \sqrt{\frac{H_{disp}}{H_{disp.ad}}} \sqrt{\frac{1 - \Delta \eta_{fr} - \Delta \eta_Q - g_k g_r \left(\frac{c_{rel}}{c} \right)^2}{g_r}} - 1. \quad (128)$$

Analogously, it is possible to obtain a formula for determining the relative decrease of expenditure of the gas phase through the nozzle in comparison with the exhaust of a pure gas:

$$\Delta \bar{G}_r = \frac{G_0 - G_r}{G_0} = 1 - \sqrt{\frac{g_r H_{disp}}{H_{disp.ad}}} \times \left(\sqrt{1 - \Delta \eta_{fr} - \Delta \eta_Q - g_k g_r \left(\frac{c_{rel}}{c} \right)^2} + g_k \frac{c_{rel}}{c} \right) \frac{T_{ad}}{T_r}, \quad (129)$$

where $G_0 = F_c c_{ad} \rho_{ad}$ is the expenditure of pure gas with exhaust without losses;

$G_r = F_c c_{r\theta} \rho_r$ is the expenditure of the gas phase with exhaust of the mixture.

Due to the great tendency for aluminum particles to scale (they have the form of scales with a maximum diameter of around 5 μm) it is possible to ignore their lag behind the gas flow and consequently even losses due to friction of the gas on the particles and due to incomplete heat exchange, i.e., the flow of the double-phase mixture with aluminum particles can be considered to be equilibrium in speed and temperature. In this case $\Delta \bar{P}_c$ and $\Delta \bar{G}_r$ will attain maximum values

$$\left. \begin{aligned} (\Delta \bar{P}_c)_{max} &= \sqrt{\frac{1}{g_r} \frac{H_{disp}}{H_{disp.ad}}} - 1, \\ (\Delta \bar{G}_r)_{max} &= 1 - \sqrt{\frac{g_r H_{disp}}{H_{disp.ad}} \left(\frac{p_c}{p_0} \right)^{\frac{k-1}{k}} - \frac{n-1}{n}} \end{aligned} \right\} \quad (130)$$

These values of $\Delta \bar{P}_c$ and $\Delta \bar{G}_r$ calculated according to formulas (128) - (130) are shown in Figures 31 and 32 by solid lines. As is seen from these figures, a satisfactory agreement between experimental data and calculated data was obtained.

The dotted line in the figures indicates the maximum value of $\Delta \bar{P}_c$ and $\Delta \bar{G}_r$, calculated given the condition that the particle lag and consequently losses due to friction may be ignored and that heat exchange between the phases is absent; i.e., the flow is equilibrium

in speed phases and completely nonequilibrium in temperatures of the phases.

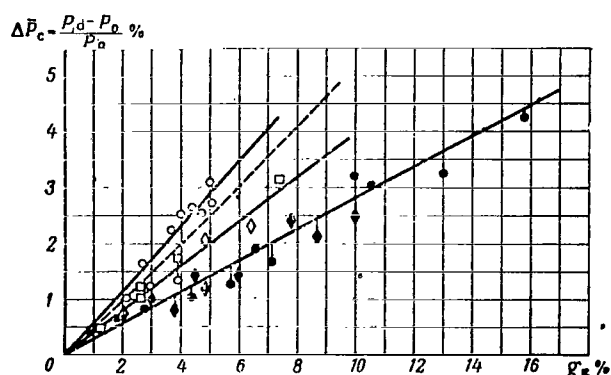


Fig. 31. Dependence of $\Delta \bar{P}_c$ Upon the Concentration of Particles ($L_c = 76$ mm): ● = Water; ◊ = Talc; □ = Ash; ○ = Aluminum Powder; ◆ = Water ($L_c = 36$ mm).

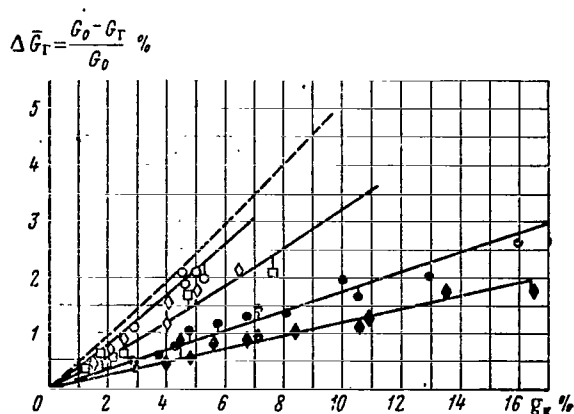


Fig. 32. Dependence of $\Delta \bar{G}_r$ Upon the Concentration of Particles ($L_c = 76$ mm): ● = Water; ◊ = Talc; □ = Ash; ○ = Aluminum Powder; ◆ = Water ($L_c = 36$ mm).

/76

2. Study of the Influence of a Liquid Film Covering the Walls of the Nozzle on Losses in the Boundary Layer

/77

With a nozzle using a double-phase working fluid with liquid particles, its walls are covered with the film formed by particles precipitated from the flow. The presence of a liquid film on the walls of the nozzle moving with velocity substantially less than the velocity of the gas can lead to a change in the losses in the boundary layer and consequently to a change in the velocity and expenditure of gas. In order to study the influence of a film on the effectiveness and thrust of a nozzle, a comparative investigation of the same conical nozzle working on air with clean walls and with walls covered with a film of water or diesel fuel DS was conducted. The study was conducted in the range of the reduced velocity $\lambda_{ad} = 0.4 - 1$ and with relative liquid expenditure in the film $g_{liq} = 0 - 0.6$.

Two equations were used for processing experimental data: the equation for gas expenditure and the equation defining the change in specific impulse per 1 kg of the gas phase.

The equation for gas expenditure through the nozzle with clean walls can be written in the following form:

$$\frac{G_0 \sqrt{T_0}}{p_0^* F_c} = 0.059 m_{cr} q (\varphi \lambda_{ad}) \frac{\pi (\lambda_{ad})}{\pi (\varphi \lambda_{ad})}, \quad (131)$$

where

$$m_{cr} = \sqrt{k \left(\frac{2}{k+1} \right)^{\frac{k+1}{k-1}}};$$

$$q(\varphi \lambda_{ad}) = \left(\frac{k+1}{2} \right)^{\frac{1}{k-1}} \left(1 - \frac{k-1}{k+1} \varphi^2 \lambda_{ad}^2 \right)^{\frac{1}{k-1}} \varphi \lambda_{ad};$$

$$\pi(\lambda_{ad}) = \frac{p_c}{p_0^*}; \quad \pi(\varphi \lambda_{ad}) = \frac{p_c}{p_c^*},$$

λ_{ad} is the reduced velocity of the adiabatic isentropic exhaust corresponding to the degree of pressure lowering p_c/p_0^* ;

ϕ is the coefficient of gas velocity.

The equation for gas expenditure through the same nozzle but with walls covered with a liquid film will have an analogous appearance:

$$\frac{G_r \sqrt{T_0^*}}{p_0^* (F_c - \Delta F_c)} = 0.059 m_{cr} q [(\varphi - \Delta \varphi) \lambda_{ad}] \frac{\pi(\lambda_{ad})}{\pi[(\varphi - \Delta \varphi) \lambda_{ad}]}, \quad (132)$$

where $\Delta F_c = \pi D_c \delta_{film}$ change in the area of the exit section of the nozzle due to the presence of a liquid film on its wall;

δ_{film} is the mean thickness of the film on a nozzle section; /78

$\Delta \phi = \phi - \phi_{film}$ is the decrease in the coefficient of the gas velocity due to change in losses due to friction and the vortex formation in the boundary layer;

ϕ_{film} is the coefficient of gas velocity in the nozzle with walls covered with a liquid film.

Let us examine the specific impulse per kg of gas discharging from the nozzle. With exhaust from a usual nozzle

$$P_0 = \frac{R_\Sigma}{G_0} = \varphi \lambda_{ad} a_{cr}^*, \quad (133)$$

where R_Σ is the total thrust of the nozzle;

$$a_{cr}^* = \sqrt{\frac{2k}{k+1} RT_0^*} \text{ is the critical velocity of gas flow.}$$

With exhaust of the gas from a nozzle with walls covered with a liquid film the specific impulse per 1 kg of gas is equal to the sum of the impulse of 1 kg of gas and the impulse g_{liq}/g_T kg of

film, i.e.,:

$$P_{\Sigma} = \frac{R_{\Sigma}}{G_r} = (\varphi - \Delta\varphi) \lambda_{ad} a_{cr}^* + \frac{g_{liq}}{g_r} c_{film},$$

where c_{film} is the mean velocity of the film on a section of the nozzle; $g_{liq} = \frac{G_{liq}}{G_{liq} + G_r}$ and $g_r = \frac{G_r}{G_{liq} + G_r}$ are the relative mass concentrations of liquid and gas.

The mean film thickness δ_{film} and its mean velocity on a section of the nozzle c_{film} are related by the expenditure equation for a liquid

$$G_{liq} = \frac{g_{liq}}{g_r} G_r = \pi D_c \delta_{film} \rho_{liq} c_{film},$$

whence

$$c_{film} = \frac{g_{liq}}{g_r} \pi D_c \frac{G_r}{\delta_{film} \rho_{liq}}.$$

With regard to this correlation, the expression for P_{Σ} can be reduced to the form

$$P_{\Sigma} = (\phi - \Delta\phi) \lambda_{ad} a_{cr}^* + \left(\frac{g_{liq}}{g_r} \right)^2 \frac{G_r}{\pi D_c \delta_{film} \rho_{liq}}. \quad (134)$$

The relative change in specific impulse in a nozzle with walls covered with a liquid film is:

$$\Delta \bar{P}_c = \frac{P_{\Sigma} - P_0}{P_0} = -\frac{\Delta\phi}{\phi} + \left(\frac{g_{liq}}{g_r} \right)^2 \frac{G_r}{\pi D_c \delta_{film} \rho_{liq} \phi \lambda_{ad} a_{cr}^*}. \quad (135)$$

As was already noted, in the process of conducting the experiment the values T_0^* , p_0^* , p_c , G_r , G_{liq} and R_{Σ} were measured. The velocity coefficient ϕ of the nozzle with clean walls is easily determined by selection according to the expenditure equation (131). Therefore the two equations (132) and (135) contain only the two unknown values $\Delta\phi$ and δ_{film} and represents a closed system. For the case of exhaust of cold air from a nozzle ($k = 1.4$)

$$\frac{G_r \sqrt{T_0^*}}{p_0^* F_c \left(1 - \frac{4 \delta_{film}}{D_c} \right)} = 0.0404 q [(\phi - \Delta\phi) \lambda_{ad}] \frac{\pi (\lambda_{ad})}{\pi [(\phi - \Delta\phi) \lambda_{ad}]};$$

$$\Delta \bar{P}_c = -\frac{\Delta\phi}{\phi} + \left(\frac{g_{liq}}{g_r} \right)^2 \frac{G_r}{\pi D_c \delta_{film} \rho_{liq} \phi \lambda_{ad} a_{cr}^*}. \quad (136)$$

The values of $\Delta\phi$ and δ_{film} are also determined from these equations by the selection method.

In Figures 33 and 34, dependences of the relative lowering of air expenditure through a nozzle with walls covered with a film

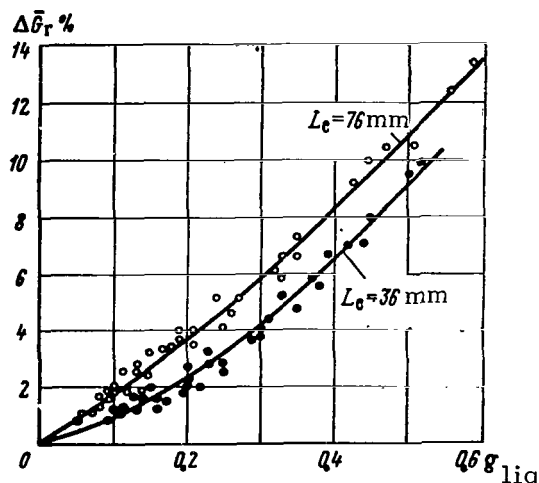


Fig. 33. Dependence of $\Delta\bar{G}_\Gamma$ Upon the Concentration of Liquid (Water, DS) With $\lambda_{\text{ad}} = 0.4 - 1$.

from the concentration of the liquid phase. Curves were drawn according to the mean values obtained from the experiment.

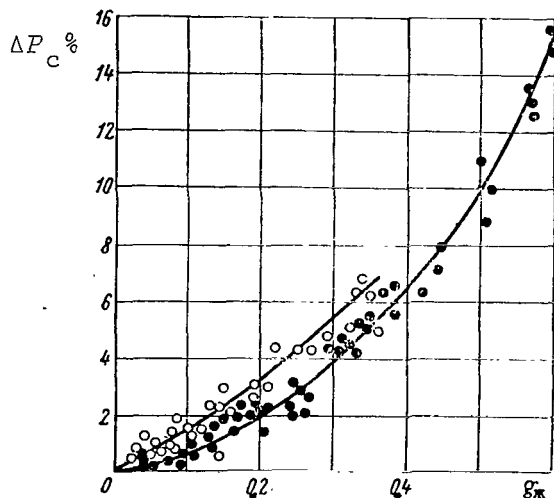


Fig. 34. Dependence of $\Delta\bar{P}_C$ Upon the Concentration of Liquid ($L_c = 36$ and 76 mm); $\lambda_{\text{ad}} = 0.4 - 1$:
= Water; = DS.

$\Delta\bar{G}_\Gamma = (G_0 - G_\Gamma)/G_0$ and values $\Delta\bar{P}_C$ upon the concentration of the liquid phase are given. It proved to be the case that the relative increase in the specific impulse of a nozzle with walls covered with the film does not depend upon the length of the nozzle; the increase in specific impulse in a nozzle with a film of diesel fuel DS is somewhat greater than in a nozzle with a water film.

Figure 35 shows the dependency of the impulse g_{liq}/g_Γ (kg) of a film per 1 kg of gas directed to the impulse of a gas,

$$\bar{P}_{\text{film}} = \frac{P_{\text{film}}}{P_0} = \frac{g_{\text{liq}} c_{\text{film}}}{g_\Gamma \phi \lambda_{\text{ad}} a_{\text{cr}}^*} = \left(\frac{g_{\text{liq}}}{g_\Gamma} \right) \frac{1}{\pi D_c \delta_{\text{film}} \rho_{\text{liq}} \phi \lambda_{\text{ad}} a_{\text{cr}}^*}$$

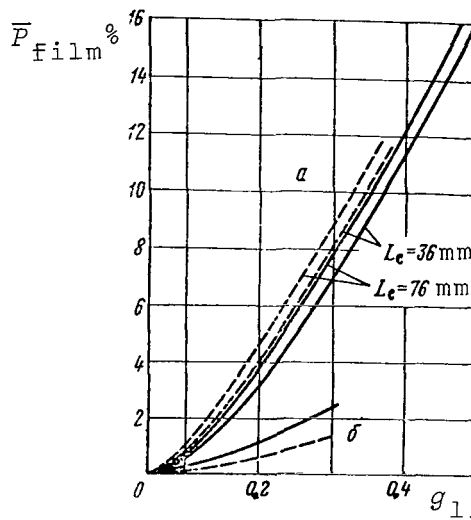


Fig. 35. Dependence of the Relative Impulse of a Film P_{film} upon the Concentration of Liquid: (a) Experimental Curves; (b) Calculated Curves: — Water; --- DS.

It proved to be the case that the relative impulse P_{film} of the DS film somewhat exceeds the impulse of a water film. Consequently, despite the substantially higher viscosity (viscosity of DS is 3-4 times higher than the viscosity of water), a DS film has a velocity on the section of the nozzle equal to or greater than the velocity of water. This indicates that the flow of a film in a nozzle is not laminar but of a clearly defined wave nature. As is well known, with intense wave flow of a film the basic transfer of the liquid mass takes place in the waves themselves, whereupon the velocity of the waves may substantially exceed the velocity of the flow of the lower layers of the liquid. Moreover, with a wave flow the crests of the wave may be broken off and carried away by the gas flow (superficial dispersion), which also increases the relative impulse of the film.

In connection with this it is necessary to note that the mean /81 thickness of the film δ_{film} , determined from the system of equations in (131) and (135), is a conditional value corresponding to the mean velocity of the liquid flow.

A change in the value \bar{P}_{film} obtained by calculation is also shown on Figure 35. Calculations of the flow of a liquid film in nozzles was conducted with the aid of Carmen's integral correlation with the usual assumption for the calculation of a boundary layer. In addition the surface of the film is assumed to be smooth and the flow to be steady.

As is seen from a comparison of the curves the calculated and experimental values of the relative impulse of the film correspond only with a low concentration of the liquid phase (or with small thicknesses of the film or small Re_{film} numbers). With values of g_{liq} greater than 0.08, the experimental curves have a break and the value of the relative impulse of the film begins to increase swiftly in comparison with the calculated impulse. The divergence of experimental and calculated curves can be explained by the fact that where g_{liq} is greater than 0.08, the nature of the film flow changes. While before the critical value of g_{liq} the film flow is of laminar nature and its surfaces smooth, with greater expenditure of liquid the flow becomes unstable and wave-like. Energy transmitted by the gas to the undulating film is much greater than the energy transmitted by the gas to a smooth film. Therefore the velocity of flow and the impulse of the film begin to increase swiftly in comparison with their calculated values.

The decrease in the velocity coefficient $\Delta\phi$ of nozzles with walls covered by a liquid film, depending upon the concentration of the liquid, is presented in Figure 36. The decrease in the velocity coefficients in a nozzle with films of water and DS prove to be approximately equal. As is seen from this figure, with small concentrations of the liquid $\Delta\phi < 0$; consequently, in this region the velocity coefficient of the nozzle with walls covered with a film is higher than that of a clean nozzle. This also indicates that

with small expenditures of liquid, a film has a smooth surface; in addition, the thickness of the film exceeds the height of projection of the original roughness of the nozzle walls by 2-4 times, which allows one to consider the walls to be aerodynamically smooth.

An increase in the liquid consumption in the region corresponding to the minimal value of $\Delta\phi$ leads to the appearance of capillary waves on the surface of the film. Evidently, in the region where the curve intersects the axis of abscissas the roughness determined by capillary waves is equivalent to the original roughness of the nozzle walls. With a further increase in the liquid expenditure the film flow becomes wave-like and forces in the boundary layer sharply increase.

With large values of g_{liq} the decrease in the velocity coefficient in a long nozzle takes place more intensely than in a short nozzle due to the increase in total friction surface of the first. /82

In Figures 37 and 38 the value $\Delta\phi = \phi - \phi_{film}$ of a short nozzle is shown depending on the Re_{film} number = $\frac{\delta_{film} \sigma_{film} \rho_{liq}}{\mu_{liq}} = \frac{G_{liq}}{\pi D c \mu_{liq}}$ and upon the reduced gas velocity λ_{ad} . In these figures points are

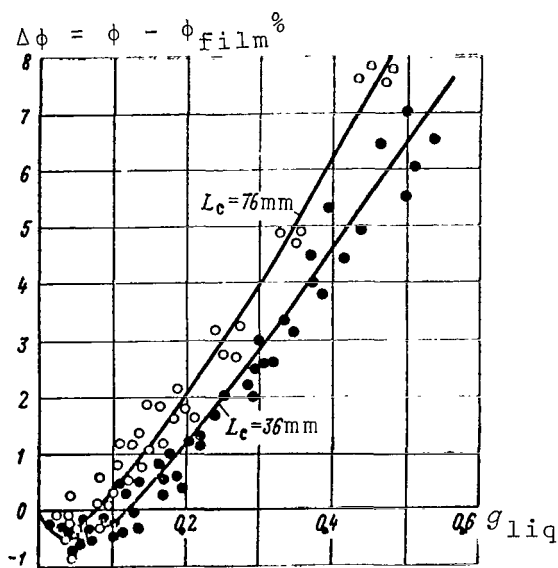


Fig. 36. Decrease in the Velocity Coefficient of the Gas in a Nozzle With Walls Covered by a Film of Water and DS.

plotted corresponding to experimental values of λ_{ad} and solid curves corresponding to a certain mean value of λ_{ad} . As is seen from a comparison of the curves, the critical value of the Re_{film} number, with which the film flow acquires an intensive wave nature (the region of the intersection of the curves with the abscissa), for a water film is higher than a DS film: $Re_{H_2O,cr} = 300 - 500$, and $Re_{DS,cr} = 60 - 90$. It is necessary, evidently, to explain the influences of the forces of surface tension. The coefficient of surface tension of water is approximately 2 times greater than DS diesel fuel ($\sigma_{H_2O} = 7 \cdot 10^{-2}$ n/m; $\sigma_{DS} = 3 \cdot 10^{-2}$ n/m). The surface tension inhibits the formation of waves; therefore, with an increase in the coefficient of surface tension the value of the critical Re_{film} number is displaced towards the region of greatest values.

For a water film the obtained values of the critical Re_{film} numbers are rather close to the values of this same parameter /83

obtained in [65] where the flow of water films in a cylindrical tube under the action of a gas flow was investigated.

It is necessary to note that due to the great turbulence of the flow and the influence of particles precipitating on the surface of the film, in full scale jet nozzles and in turbine grids the critical Re_{film} number, with which the wave flow of the film begins, evidently is much lower than in conical nozzles studied in the present section.

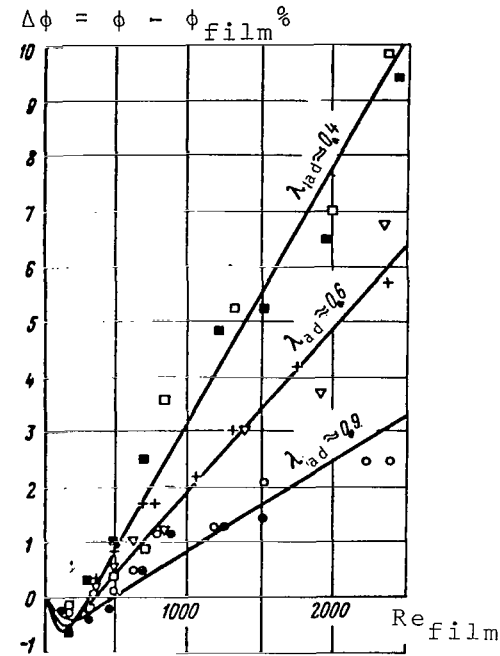


Fig. 37. Decrease in the Velocity Coefficient of the Gas in a Nozzle With $L_c = 36$ mm Depending Upon the Re_{H_2O} Number and Reduced Velocity of Gas λ_{ad} .

Conventional						
Signs	■	□	+	▽	●	○
λ_{ad}	0.35	0.45	0.55	0.65	0.85	0.95

tion of the nozzle was accomplished with the aid of a micrometer screw.

The calculated thickness of a smooth film of liquid $\delta_{film r}$ is shown in the figure (by dotted line) as well as the actual mean thickness of the film δ_{film} obtained with elaboration of experimental data from the system of equations in (136). As is seen from Figure 39, the heights of wave crests H exceeds the mean thickness of the

Finally, in Figure 39 results are presented of experimental determination of the height of the wave crests H and the thickness of a double-phase boundary layer δ_{db} in the exit section of a nozzle. The measurement was performed by a special probe 0.3 mm in thickness analogous to a Pitot tube. Moving the probe across the flow on a sec-

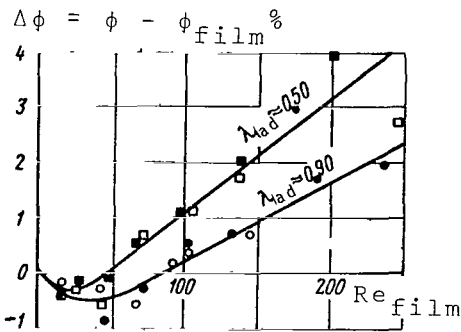


Fig. 38. Decrease in the Velocity Coefficient of the Gas in a Nozzle With $L_c = 36$ mm Depending Upon the Re_{DS} Number and Reduced Velocity of the Gas λ_{ad} .

Conventional				
Signs	■	□	●	○
λ_{ad}	0.4	0.6	0.8	1.0

film δ_{film} by 3-5 times. The thickness of a double-phase boundary layer δ_{db} formed due to the removal of a certain portion of the liquid by the gas flow proved to be approximately 10 times greater than the maximum height of the wave crest.

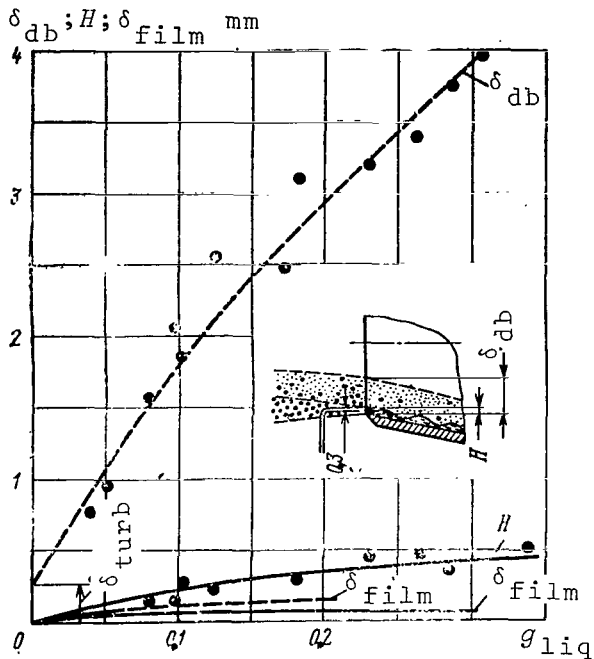


Fig. 39. Dependence of the Thickness of the Double-Phase Boundary Layer δ_{db} , the Height of the Wave Crest H and the Mean Thickness of the Water Film δ_{film} Upon the Concentration of the Liquid Phase ($\lambda_{\text{ad}} = 0.8 - 1.0$).

In conclusion, we note that since experiments were conducted on cold air, i.e., with an absence of intense heat exchange, evaporation of the liquid, precipitation of particles, etc., the results of the investigation which have been presented are basically only of a qualitative nature.

§6. Similarity Criteria and Characteristics of Experimental Investigations of Double-Phase Flows

The similarity criteria of a physical phenomena can be obtained from the system of equations describing this phenomena reduced to dimensionless form. Complexes composed of physical constants and initial values of parameters entering the equations as coefficients serve as similarity criteria. If we do not succeed in composing sys-

tems of equations, i.e., the connection between the parameters of the phenomena not explained in the similarity criteria can be obtained on the basis of a π -theorem by means of an analysis of the regularity in the physical parameters influencing this phenomena. /85

In the simplest case of a linear flow of a double-phase mixture with small particles in geometrically similar nozzles, the following values entering the system of equations in (69) serve as similarity criteria:

$$\text{Sto} = \frac{c_0 \rho_{\kappa} d^2}{18 \mu_r L}; \quad K_1 = \frac{R_r T_0}{c_0^2}; \quad K_2 = \frac{c_p r T_0}{c_0^2}; \quad K_3 = \frac{[c_p \kappa T_0^*]}{c_{0,\kappa}^2};$$

$$K_4 = \frac{2 \lambda_r}{3 \mu_r c_p \kappa}; \quad \frac{g_{\kappa}}{g_t}.$$

If, at the same time, the flow of a liquid film along the walls of a nozzle formed by precipitating particles is considered, then it is necessary to add the criterion characterizing the film flow:

$$Re_{\text{film}} = \frac{c_{\text{film}} \delta_{\text{film}}}{\nu_K}; \quad (137)$$

The criterion characterizing the interaction between the gas phase and the film is:

$$K_5 = \frac{\rho_r c_r}{\rho_K c_{\text{film}}}; \quad (138)$$

The criterion characterizing the relationship of the forces of viscosity and the forces of surface tension:

$$K_6 = \frac{\mu_K c_{\text{film}}}{\sigma} \quad (139)$$

and others. In view of the large number of criteria it is practically impossible to have a complete similarity with experimental studies. Therefore the most important processes are simulated and investigated separately.

For complex phenomena for which it is impossible to present a system of equations, dependences between dimensionless criteria obtained on the basis of dimension theory are determined with the aid of experiment. For the most simple phenomena having a satisfactory physical and mathematical model, an experiment is necessary in order to confirm the accuracy of assumptions in formulating the problem; this is especially pertinent to problems with a great number of equations and dimensionless parameters determining the phenomena. Furthermore, it is possible to determine dependences between the most important parameters of a phenomena with the aid of a computer.

We shall rely on certain characteristics of the experimental study of double-phase flows. In measuring the total pressure of the gas phase of the usual Pitot tube, the particles penetrating the intake adjust the gas and distort the instrument readings. Adjusting the change in the amount of particle motion penetrating the cylindrical intake part of a Pitot tube, the pressure differences on a braking portion, we obtain that the magnitude of error in the measurement is

$$\Delta p' = k_c \frac{g_{\kappa}}{g_r} \rho_r c_0 \Delta c_{\kappa}. \quad (140)$$

The relative magnitude of error is

$$\frac{\Delta p}{p} = k_c \frac{g_{\kappa}}{g_r} \frac{c_0 \Delta c_{\kappa}}{RT}, \quad (141)$$

where k_c is the coefficient characterizing the deflection of particle motion from the rectilinear with a flow around the intake portion of the nozzle;

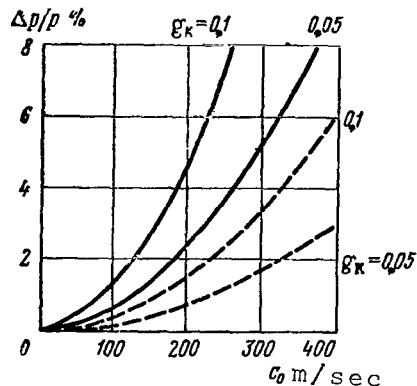


Fig. 40. The Maximum Relative Error in Measuring the Total Pressure of the Gas Phase by a Pitot Tube: $R_T = 288 \text{ J/kg} \cdot ^\circ\text{K}$:
 — $T = 300^\circ\text{K}$ ---- $T = 1000^\circ\text{K}$

c_0 is the velocity of the mixture at the point of measurement;

Δc_K is the change in the particle velocity in the nozzle.

In first approximation it is possible to judge the value k_c for a Pitot tube according to the formula

$$k_0 = \frac{\text{Sto}^2}{(0.125 + \text{Sto})^2} \quad (142)$$

where the diameter of the tube enters as a linear measure into the expression for Sto . Where $\text{Sto} < 0.05$ it is possible to accept $k_c = 0$.

With a total deceleration of particles the error attains a maximum value

$$\frac{\Delta p}{p} = k_c \frac{g_\kappa}{g_r} \frac{c_0^2}{RT} \quad (143)$$

The maximum error for air, depending on the velocity of the flow, is presented on Figure 40 ($k_c = 1$).

According to reference [54], the distance at which the velocity of a particle in an immobile gas lowers to zero is

$$l_{\max} = \frac{c_0 \rho_\kappa d^2}{18 \mu_r} \quad (144)$$

For example, in it where $c_0 = 100 \text{ m/sec}$ $l_{\max} = 2 \text{ mm}$ where $d = 1 \text{ } \mu\text{m}$ and $l_{\max} = 50 \text{ mm}$ where $d = 5 \text{ } \mu\text{m}$. Since the length of the intake portion of a Pitot tube does not usually exceed several mm, then where $d > 6 \text{ } \mu\text{m}$ it is possible to ignore deceleration of the particles in the nozzle, and consequently even an error in the measurements. However, with large particles it is possible that the liquid phase striking the intake portion of the nozzle and the conduit leading to the measuring instrument may influence the results of the measurements. Therefore axial or cylindrical nozzles are usually provided with a drainage opening (Fig. 41) and also provide for blowing air through them. /87

Still greater difficulties arise in measuring the temperature of the gas phase, since a thermocouple in a double-phase flow with

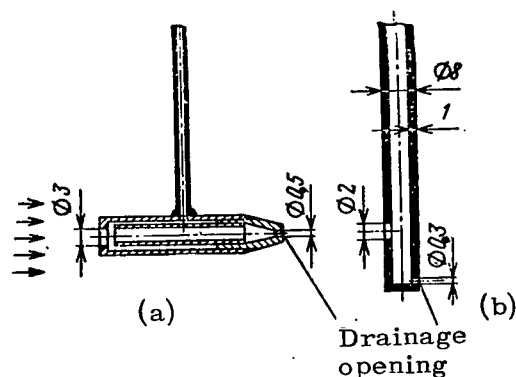


Fig. 41. Schematic Drawing of Nozzles for Measuring the Total Pressure of the Gas Phase in a Flow With Liquid Particles.

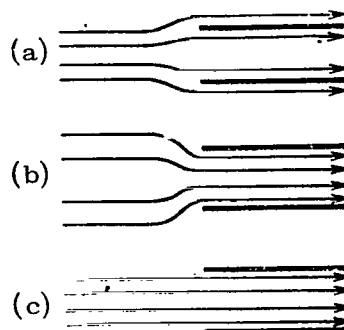


Fig. 42. Schematic Drawing of the Test Intake: (a) Velocity in the Intake Less Than the Flow Velocity; (b) Velocity in the Intake Greater Than the Flow Velocity; (c) Isokinetic Test Intake.

liquid particles is covered by a film isolating it from the external flow. Insofar as particle temperature may greatly differ from the gas temperature, thermocouple readings will not be reliable. In the majority of cases the temperature of the gas phase is determined by calculation (for example, according to the heat balance equation) or by a translation of the temperature measured in the zones protected from the action of the liquid phase.

Selection of tests of a double-phase flow must be conducted in such a way that the velocity in the intake portion of the intake valve remains equal to the velocity of the basic flow (isokinetic test selection). In this case error due to deviation of the trajectories of the particles in front of the intake valve will be minimal (Fig. 42). Such an equality of velocities can be obtained by maintaining static pressure inside the intake valve equal to the static pressure in the external flow.

CHAPTER 3

THE OPERATION OF A TURBINE ON A DOUBLE-PHASE FLOW WITH A CONSTANT CONCENTRATION OF PHASES

§1. Basic Characteristics of the Operation of the Turbine Stage on a Double-Phase Flow with Liquid Particles

As experimental studies show, the flow of a double-phase mixture with liquid particles in the flow portion of a turbine is of a very complex nature and possesses the following characteristics: /88

(1) The flow is characterized by sharp reversals and great acceleration. Therefore, the particles, due to their own inertia, noticeably lag behind the gas; as a result of the losses due to friction of the gas on the particles arising here, the flow process is irreversible.

(2) The flow is accompanied by a redistribution in the concentration of phases along a section of the flow portion due to the inertial lag of the particles behind the gas flow. This redistribution is especially intensive in the blade apparatus where the velocity of the gas sharply changes in volume and direction, and also in the axial clearance between the nozzle and working blades under the influence of the great vortex of the flow.

(3) All the elements of the flow portion of the turbine (in particular, its nozzle apparatus) are covered with a film formed by particles precipitating from the flow. Large particles ($d > 10 \mu\text{m}$) precipitate out under the action of inertial forces; precipitation of small particles ($d < 1 \mu\text{m}$) is of a turbulent diffuse nature. Moreover, thermophoretic precipitation of particles may take place in cooled blade rims.

(4) The film surface, under the action of turbulent flow pulsations and the impact of particles striking it, acquires a wave-like form, whereby the height of the crest, the waveforms and velocity of their motion depends in the first place upon the viscosity, surface tension and thickness of the layer of liquids, velocity and density of the flow, nature of the boundary layer and upon the curvature of the wall along which the film flows. It has still not been possible to establish the precise dependence of height and form of the waves upon the basic parameters determining the flow. However, it is known from experiments that the height of the crest increases with an increase in the mean thickness of the layer, viscosity of the liquid and whirling of the boundary layer and decreases with an increase in the density and velocity of the gas flow.

In conduits with cooled walls with a temperature near the freezing point of the liquid phase, the liquid phase "freezes" on the walls, which leads to a further deterioration of the flow condition.

/89

(5) Tearing away from the exit edges of the nozzle blades and also from the internal and peripheral surfaces of the flow portion, a film under the action of gas forces is fragmented into secondary drops, the diameter of which may reach several tenths of a millimeter.

Such drops substantially lag behind the gas flow and strike the working blades under large negative angles of attack, causing a decrease in the effectiveness of the turbine, and with prolonged exploitation, even erosional wear of the working blades.

(6) In the expansion process of a double-phase flow, heat exchange between the phases takes place in which heat is conducted from the particles to the gas. Therefore, the effectiveness of the gas phase is somewhat increased. With a moderate degree of expansion ($\pi_T < 2$) and a particle concentration $g_K < 0.1$ the increase in the effectiveness may be from 1 to 2.5%.

However, due to intensive precipitation of particles on the walls of the flow portion, the surface of the division (heat exchange) is sharply curtailed. And although due to the low velocity of the film flow equal to $(0.05 - 0.15)c_T$, the time the liquid phase remains in the flow portion is significantly increased, and the coefficient of heat emission from the liquid to the gas increases due to the increase in the relative velocity of the liquid and the gas, and the total amount of transmittable heat may decrease by several times. As a result of this, in the majority of cases, especially with a moderate concentration of the liquid phase and a particle diameter $d > 10 \mu m$, the increase in efficiency of a gas phase due to heat exchange with particles may be ignored in first approximation.

In turbines operating on double-phase flows with liquid particles, supplementary losses appear. These losses may be classified in the following way.

(1) Losses in the nozzle apparatus accumulating from: (a) losses due to friction of the gas on the particles; (b) losses with the separation of particles onto the nozzle blades (the kinetic energy of the particles is almost completely lost when they precipitate onto an immobile surface); (c) losses due to friction of the gas on the liquid undulating film covering the nozzle blades, as well as the internal and peripheral surface, bounding the flow portions of the nozzle apparatus.

(2) Losses in the axial clearance between the nozzle and working blades, consisting of: (a) losses due to friction of gas on the particles; (b) losses with precipitation of the particle onto the peripheral wall; (c) losses due to friction of the gas on the liquid

undulating film, covering the internal and external surface in the axial clearance.

(3) Losses in the working wheel, the majority being losses /90 due to impact of the liquid particles on the input edge of the working blades, and due to scattering of the liquid phase toward the periphery. It is possible to ignore the increase in profile losses on the working blades, since the film is directly scattered by centripetal forces to the periphery, and therefore its thickness on the working blades does not exceed several hundredths of a millimeter, even when the fluid is very viscous. However, in blades having erosional wear profile losses can be significant.

(4) Losses in the radial clearance. The viscous liquid phase, separated out onto the peripheral surface in nozzles and in the axial clearance in front of the working wheel, flows out under the action of gas forces in the radial clearance above the working wheel. With a small concentration of the liquid phase, this leads to a decrease in radial clearance and, consequently, to a certain increase in the effectiveness of the turbine. However, with great expenditures of the liquid phase the end of the working blades may touch the wave crests. This leads to a decrease in turbine effectiveness, and also may cause an increase in vibrational strains in the working blades. Therefore the radial clearance must be chosen in such a way that the ends of the blades do not touch the wave crests of the liquid film in all operational regimens.

Therefore it is necessary to consider the possible deterioration of the parameters of turbine operation due to a decrease in the nozzle flow sections and a change in the reactivity of its stages.

With a very viscous liquid the flow sections of the turbine may be decreased by 5-10%, which will lead to a decrease in gas expenditure through the turbine in comparison with a turbine operating on a pure gas. In the case of such a turbine working in a gas turbine system or in a stationary gas turbine installation system, this may lead to a decrease in the margin of stable operation and even to compressor stalling. Therefore, in calculating the effectiveness of turbines on double-phase mixtures it is necessary to consider the clogging of flow sections by a viscous liquid film. In the case of a liquid phase of low viscosity such as water or kerosene in a moderate concentration ($g_K \leq 5\%$), it is possible to ignore clogging of the flow section stages.

A change in the reactivity of the stage depends upon flow section clogging in the nozzle apparatus by a film which decreases the reactivity of the stage and upon the interaction between the gas and the particles in the exhaust process, which increases its reactivity. Actually, with the same pressure drop, the exhaust velocity of a mixture is less than the exhaust velocity of a pure gas. Therefore, with an invariable circumferential velocity, the flow angle β_1 and, consequently, even the geometric configuration of the film in the

working wheel $\sin \beta_1 / \sin \beta_2$ increase. It is well known that this leads to an increase in the resistance of the working grid; i.e., to an increase in the reactivity of the stage. /91

With large ($d > 15 \mu\text{m}$) and very viscous particles, clogging of the flow sections by film is the predominating factor and the reactivity of the stage decreases. With small particles ($d < 5 \mu\text{m}$) and particles of low viscosity, the second factor predominates and the reactivity of the stage increases. With high expenditures of the liquid phase a change in turbine reactivity may be significant.

1. *The Flow of a Double-Phase Mixture in the Nozzle Apparatus of a Turbine*

The flow of a double-phase mixture in plane and ring-nozzle turbine grids was studied by a number of investigators [28,37,61], and also by the author of the present book. Let us consider the basic characteristics of such a flow.

Particles Separation on Nozzle Blades

Due to the sharp change in the value and direction of the gas phase velocity in nozzle apparatus, the suspended phase lags behind the gas phase. Large particles may be deflected from their original rectilinear motion and precipitate on the intake edge and concave surface of nozzle blades (inertial separation). Small particles precipitate onto elements of the flow portion due to great flow turbulence.

In reference [54] the following empirical formula for determining the coefficient of particle separation on the surface of a cylinder with a double-phase flow flowing past it is presented:

$$k_c = \frac{(Sto)^3}{(Sto)^3 + 0.77 (Sto)^2 + 0.22}, \quad (145)$$

where $Sto = \frac{c_0 \rho_K d^2}{18 \mu_T D}$;

c_0 = velocity of a mixture far from the cylinder;
 D = diameter of the cylinder.

It is apparent from the formula that where $Sto > 7$ the value of k_c is near unity; where $Sto < 0.2$ it is possible to accept $k_c = 0$.

The value of k_c characterizes the degree of deviation from the rectilinear in the direction of particle motion. Where $k_c \ll 1$ the particle trajectory corresponds to the line of gas flow; where $k_c = 1$ the particle motion is rectilinear.

With flow past the nozzle blades of a turbine it is possible to accept $l \cdot \cos \gamma$ as a characteristic measurement, where l is the

length of a profile chord; and γ is the angle of the profile arrangement (cf. Fig. 71). Assuming the mixture velocity and the nozzle entrance to be $c_0 = 200$ m/sec; $l \cdot \cos \gamma = 3 \cdot 10^{-2}$ m and the relative /92
pitch of the grid to be $t/l = 0.6-0.8$, from the condition $Sto > 7$ we obtain the following limiting values for particle diameter, with which their total separation takes place on the nozzle blades:

- $d > 8 \text{ } \mu\text{m}$ for particles of mercury in mercury vapor;
- $d > 15 \text{ } \mu\text{m}$ for particles of ash in hot air;
- $d > 16 \text{ } \mu\text{m}$ for particles of water in water vapor.

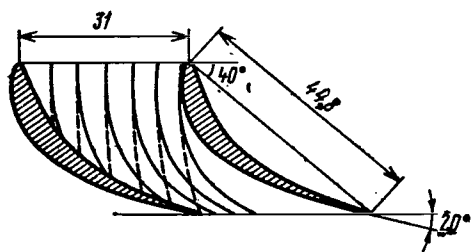


Fig. 43. Particle Trajectories in the Conduit of a Nozzle Apparatus:

—— $d = 10 \text{ } \mu\text{m}$;
 ----- $d = 70 \text{ } \mu\text{m}$.

We shall determine the particle diameters for the same grid from the condition $Sto < 0.2$, with which it is possible to ignore inertial separation:

$d < 1.5 \text{ } \mu\text{m}$ for particles of mercury in mercury vapor;

$d < 3.5 \text{ } \mu\text{m}$ for particles of ash in hot air and particles of water in water vapor.

For particles with motion characterized by a number $0.2 < Sto < 7$, the value k_c may be evaluated according to formula (145).

Of course, this volume formula is applicable only in rough evaluations. In order to determine the actual particle trajectories in interblade conduits and the degree of settling on the convex surface of the blades, it is necessary to consider the equation for particle motion with regard to the velocity gradient and gas density transversely and along the interblade conduits.

Such a problem is solved by the method of finite differences in [37] for the case of particle motion with a density of $\rho_k = 785 \text{ kg/m}^3$ where $T^* = 1200^\circ \text{ K}$ and $p = 0.5 \cdot 10^6 \text{ n/m}^2$. The particle velocity in front of the grid was assumed to be equal to the gas velocity. It was assumed that in a narrow section of the conduit the flow velocity is equal to the speed of sound.

The basic parameters of the grid where $t/l = 0.7$ together with the results of calculating the trajectory of particles with diameters $d = 70 \text{ } \mu\text{m}$ and $d = 10 \text{ } \mu\text{m}$ are presented in Figure 43. Particles with diameter $d > 70 \text{ } \mu\text{m}$ all settle on the convex surface of the blades; particles with diameter $d = 10 \text{ } \mu\text{m}$ are only partially separated. More than 40% of such particles pass through the grid without impact on the convex surface, whereupon the velocity increases to approximately 0.8 of the gas velocity behind the grid.

With a decrease in gas pressure the inertial separation of the particles is increased. Thus, with pressure $p = 0.15 \cdot 10^6 \text{ n/m}^2$ and the same conditions, total particle separation takes place even where

$d = 40 \text{ } \mu\text{m}$. This is explained by the corresponding decrease in gas density which causes particles to move with less curved trajectories. The results of the solution also depend upon the viscosity of the gas. With a decrease in the viscosity of the gas, particles lag behind the flow more strongly; therefore their separation increases. /93

Analogous calculations [40] for ash particles with a density of $\rho_K = 3000\text{--}4000 \text{ kg/m}^3$ showed that in a typical grid of gas turbine nozzle blades almost total particle separation takes place where $d > 12 \text{ } \mu\text{m}$.

The values of the coefficient of separation k_c , determined from calculating actual particle trajectories in interblade conduits, proved to be somewhat greater than those calculated according to (145). This is explained by the approximate nature of formula (145) obtained under conditions of a flow passing around a cylinder at low velocity. A sharper gas velocity gradient based on quantity and direction in the interblade conduits in comparison with the case of flow around a cylinder and a significant decrease in gas density and viscosity along the conduit lead to more intensive particle separation on the nozzle blades.

The coefficient of particle separation is a function of the angle of flow revolution and of grid thickness; with an increase in the latter this coefficient also increases. With a decrease in particle diameter inertial separation becomes weaker. Particles with a diameter $d \leq 1 \text{ } \mu\text{m}$ may precipitate on the surface of the blades only under the action of turbulent pulsations in the flow and diffusion. Considering the high level of turbulence in the flow portions of the turbine, it is possible to assume that the separation of small particles is also very intensive.

The precipitation of particles from the flow is facilitated if the nozzle (or working) blades are highly cooled. In this case, a supplementary force produced by the temperature gradient and directed toward the cooled surface affects the particle moving in the boundary layer⁵; as was mentioned, such a force is called thermophoresis. Experimental studies presented in [42] confirmed the influence of this factor upon particle precipitation and, in particular, showed that particles settle on a cooled plate more intensively than on a non-cooled one; when the particle temperature was substantially greater than the flow temperature, particle settling generally did not take place.

⁵ For air it is possible to assume that the thicknesses of hydrodynamic and thermal boundary layers are approximately equal. (Author's note).

Flow of Liquid Film Along Nozzle Blades

The interaction between liquid particles precipitating out of a flow and the wall to a great degree depends upon particle size and upon whether the liquid was "wetting" in relation to the surface. With the impact of large particles, possessing a high degree of kinetic energy on a wall, it is possible that an intensive scattering of the particles themselves may take place, as has already taken place on the surface of the film. The secondary drops which are now formed are carried by the gas flow. Atomizing small particles hardly ever takes place. /94

Atomization outflow of particles is significantly increased if the liquid does not wet the surface. In addition, particles bouncing off the surface maintain a high velocity and the formation of a solid film on the surface is improbable. Such a flow pattern is observed, for example, in gas turbines with external liquid cooling, when the particles or water or another cooling agent are sprayed directly into the gas flow in front of the nozzle apparatus.

However, in the majority of cases the liquid phase wets the surface of the flow section of the turbine. Therefore, the particles cling to the surface, their velocity sharply decreases and they flow together to form a solid liquid film covering all elements of the nozzle apparatus of the turbine. If the particles are large, then the thickest film forms on the concave surface of the nozzle blades due to inertial particle separation. On the convex surface of the blades a film forms due to inertial particle separation on the intake edge as well as turbulent diffuse separation of small particles on its surface.

The flow of a film along the surfaces of the flow section of a turbine, independent of the liquid consumption, is always wave-like. This is explained by the high level of turbulence in the flow moving past the film, and also by the intensive nonstationary processes taking place on the surface of the film (precipitation of particles, atomization and carrying away of some of the liquid).

The wave nature of the film flow was noted in particular in [61], which studied the flow of moist water vapor in nozzle apparatus with an initial degree of moisture of up to 10%. The same article noted elevated pulsation of the film in the region of a vapor vortex.

With an increase in the viscosity of the liquid, the height of wave crests noticeably increases. Figure 44a shows a photograph of a nozzle blade of a turbine after its operation on a double-phase flow with viscous particles. The wave nature of film flow and also the increase in wave intensity in the zone of a vapor vortex is readily apparent. Evidently a liquid film covering elements of the flow portion of a turbine has already acquired an undulant surface with a consumption corresponding to a relative concentration of

liquid $g_K = 1 - 1.5\%$.

Centrifugal forces arising here strongly influence the shape of a film surface flowing along a curvilinear wall. Calculations show that centripetal acceleration acting on the film flowing along nozzle blades may exceed 100-200 g . Therefore on the concave surface of ^{/95} the nozzle blades the roughness of the film (height of wave crests), despite its greater mean thickness, is usually significantly less than on a convex surface, where centrifugal forces strive to tear the film from the surface and thereby increase the roughness of the film.



Fig. 44. A Nozzle Blade After Turbine Operation on a Double-Phase Flow With a Viscous Liquid Phase.

Also, the existence of a binary boundary layer which is sometimes observed on the convex surface of the blades must be explained by the effect of centrifugal forces. Actually, drops of liquid formed by carrying away of some of the film by a turbulent gas flow are affected, on the one hand by forces related to turbulent pulsations of gas and forces striving to decentralize the drops along an entire section of the conduit, and on the other hand, by centrifugal forces scattering drops toward the convex surface of the blades. Equilibrium of these forces leads to the formation of a stable double-phase boundary layer on the convex sur-

face. In contrast, on the concave surface of the blades the forces mentioned in one direction strive to remove particles from the wall; therefore, the existence of a binary boundary layer on the convex surface of the blades is improbable.

Experimental investigations show that with a significant change in liquid consumption in a film the mean thickness of the film and the height of wave crests change significantly. This is explained by the fact that an increase in consumption is primarily due to the upper layers of the film having maximum velocity.

Losses in Nozzle Apparatus Due to the Double-Phase Nature of a Flow

As calculational and experimental investigations have shown, the mean flow velocity even of a film of low viscosity (such as water or kerosene) does not exceed 10% of the velocity of the gas flow attracting the film. Therefore it is possible to eliminate, with a sufficient degree of accuracy, the case of a gas flow around an immobile and very rough surface.

It is well known that the surface roughness of nozzle blades substantially influences their effectiveness, since losses due to friction and vortex formation in the boundary layer increase with an increase in roughness. The coefficient of profile losses in a nozzle grid with rough walls with the exhaust of a pure gas can be calculated according to the semi-empirical formula of G.Yu. Stepanov [51]:

$$\zeta_{\text{rough}} = (0.05 - 0.08)\epsilon^{0.25} \frac{l}{a}, \quad (146)$$

where $\epsilon = H/l$ is the relative surface roughness;

H is the height of the elements of roughness;

l is the length of a profile chord;

a is the width of the narrow section of the interblade conduit. As follows from formula (146), with increased surface roughness the coefficient of losses ζ_{rough} may attain large values.

Analogous losses are observed even in a nozzle grid operating on a double-phase flow with liquid particles. With an increase in the viscosity of the liquid, the roughness of the film increases and losses due to friction of the gas on the wall also increase substantially.

From the graph in Figure 45, obtained by the author of this book experimentally, it is possible to see the influence of viscosity of the liquid on the decrease in efficiency of a turbine system when the flow portion is covered by an undulating film, in comparison with the same stage without a film. In the experiments particle concentration in the flow $g_K = 3-8\%$; particle size $d = 5-30 \mu\text{m}$; particle density $\rho_K = 1000-1260 \text{ kg/m}^3$; degree of reaction of the stage $\rho \approx 0.3$ and $u/c_{ad} = 0.5$. On the graph it is apparent that the decrease in turbine efficiency due to an increase in losses due to friction of a rough film in nozzle apparatus $\Delta\eta_{\text{rough}}$ is directly proportional to the logarithm of viscosity of the liquid phase. With an increase in the degree of reaction of the stage, the value of $\Delta\eta_{\text{rough}}$ decreases somewhat due to a decrease in drop in heat operating in a nozzle apparatus. The value of $\Delta\eta_{\text{rough}}$ weakly depends even upon u/c_{ad} , since with a decrease in the number of turns the reaction of the stage usually also changes.

For a liquid of low viscosity (for example, water) $\Delta\eta_{\text{rough}}$ does not exceed 1.5%. On the other hand, in the case of a highly viscous liquid (liquid slag) the losses comprise the fundamental portion of all supplementary losses caused by the double-phase nature of the flow.

We note that the remaining losses of the second kind in nozzle apparatus, i.e., those due to friction of the gas on the particles and with particle separation on the nozzle blades with moderate particle concentration in the mixture ($g_K < 5\%$) do not exceed 0.5%. If necessary, these losses can be determined more accurately from a

detailed calculation of particle motion in nozzle apparatus.

Several authors relate energy expenditures of the gas during break-up of the liquid film to losses in the nozzle apparatus. However, for the typical turbine stage the coefficient of these losses $\Delta\eta_{br} = 2F_{\Sigma}\sigma/c_{ad}^2$ is negligibly small. (In the given expression F_{Σ} is the total surface of all secondary drops formed upon the destruction of the liquid film). For example, in the case of a water film with $g_K = 0.1$ and $d = 1 \mu m$ the value of $\Delta\eta_{br} < 0.1\%$.

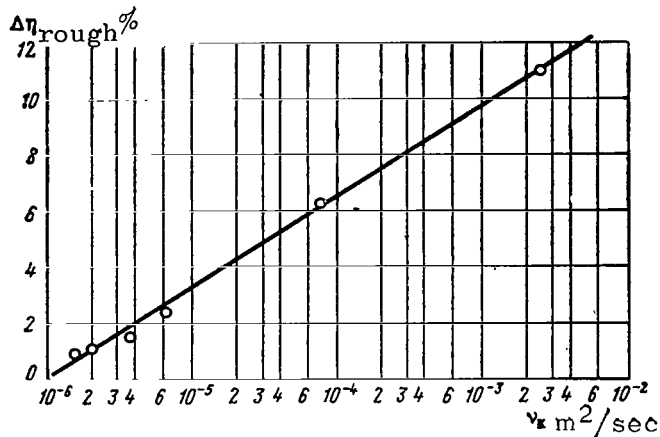


Fig. 45. Coefficient of Losses Due to Friction on the Film in the Turbine Stage $\Delta\eta_{rough}$ As a Function of Viscosity of the Liquid Phase:
 $u/c_{ad} = 0.5$; $g_K = 3-8\%$.

A double-phase flow is heterogeneous upon exit from the nozzle apparatus. In the case of large particles and their intensive separation on the blades the basic part of the liquid is concentrated in the edge traces where the liquid film flowing from the blades is destroyed. In the nucleus of the flow there are only small particles which do not precipitate on the walls; the velocity of these particles is near the velocity of the gas.

2. The Flow of a Double-Phase Mixture in Axial Clearance Between Nozzle and Working Blades

Let us consider the motion in the axial clearance of the particles formed upon destruction of the film flowing from the nozzle blades. For the sake of simplicity, we shall consider the clearance to be so small that radial particle displacement may be ignored. In this case, it is possible to assume that particles are attracted by a gas flow having a constant velocity. In the case of short blades ($D_m/h_b > 8$) it is possible to consider that the velocity of the flow, flowing past all particles, is equal to the velocity of the gas on the mean diameter. In the case of long blades ($D_m/h_b < 4$) the velocity of the flow flowing past a particle depends upon the radius, on which the particle is formed, and it is necessary to determine it with regard to a change in the degree of reaction according to blade height.

*Particle Motion in a Flow at Constant Velocity
of the Gas Phase*

We shall write the basic ratios characterizing particle motions in a double-phase flow at constant velocity of the gas phase. Determining the value of the coefficient of particle resistance from the dependences in (13), it is possible to express the force acting on a particle from the gas and also the equation for particle motion in the following way:

$$\left. \begin{aligned} P &= k_1 m c_{rel} \text{ for } Re_{rel} < 1; \\ P &= k_2 m c_{rel}^{1.5} \text{ for } 10 < Re_{rel} < 1000; \\ P &= k_3 m c_{rel}^2 \text{ for } Re_{rel} > 1000; \end{aligned} \right\} \quad (147)$$

and

$$\left. \begin{aligned} -\frac{dc_{rel}}{d\tau} &= k_1 c_{rel}; \\ -\frac{dc_{rel}}{d\tau} &= k_2 c_{rel}^{1.5}; \\ -\frac{dc_{rel}}{d\tau} &= k_3 c_{rel}^2, \end{aligned} \right\} \quad (148) \quad \frac{/99}{}$$

where $\frac{dc_{rel}}{d\tau} = -\frac{d(c_r - c_k)}{d\tau} = \frac{dc_r}{d\tau} = \frac{d^2 S}{d\tau^2}$ is particle acceleration; S is the path which particles may take;

$$k_1 = \frac{18\mu_r}{\rho_k d^2}; \quad k_2 = 9.75 \frac{\sqrt{\mu_r \rho_r}}{\rho_k d^{1.5}}; \quad k_3 = 0.36 \frac{\rho_r}{\rho_k d}.$$

Doubly integrating the motion equation and substituting the initial conditions: where $\tau = 0$, $c_{rel} = c_{rel0}$ and $S = 0$, we obtain the following expression for relative velocity c_{rel} and paths which particles may take, S :

$$\left. \begin{aligned} c_{rel} &= c_{rel0} e^{-k_1 \tau}; \\ c_{rel} &= c_{rel0} \left(1 + \frac{\sqrt{c_{rel0}}}{2} k_2 \tau\right)^{-2}; \\ c_{rel} &= c_{rel0} (1 + c_{rel0} k_3 \tau)^{-1}; \end{aligned} \right\} \quad (149)$$

and

$$\left. \begin{aligned} S &= c_r \tau - \frac{c_{rel0}}{k_1} (1 - e^{-k_1 \tau}); \\ S &= c_r \tau - \frac{2\sqrt{c_{rel0}}}{k_2} \left(1 - \frac{2}{2 + k_2 \sqrt{c_{rel0}} \tau}\right); \\ S &= c_r \tau - \frac{1}{k_3} \ln(1 + k_3 c_{rel0} \tau). \end{aligned} \right\} \quad (150)$$

We shall determine losses due to friction of the gas on particles. The elementary energy loss with a particle motion $g_K/g_{\Gamma m}$, per 1 kg of the gas phase, $dA_{fr} = \frac{g_K}{g_{\Gamma m}} P c_{rel} d\tau$. Having substituted here the values of P from (147) and the value $d\tau$ from (148), we obtain that for any range of variation in the Re_{rel} number the elementary energy loss is $dA_{fr} = \frac{g_K}{g_r} c_{rel} dc_{rel}$, and the complete energy loss due to friction is

$$A_{fr} = \frac{g_K}{g_r} \frac{c_{rel0}^2 - c_{rel}^2}{2}. \quad (151)$$

As is apparent in (149), for sufficiently large time intervals the value $c_{rel} \rightarrow 0$, and losses approach the maximum value

$$A_{fr, max} = \frac{g_K}{g_r} \frac{c_{rel0}^2}{2}. \quad (152)$$

From the equations in (151) and (149) it is possible to obtain the following dependences of losses on time for all three ranges of variation in the Re_{rel} number:

$$\left. \begin{aligned} A_{fr} &= \frac{g_K}{g_r} \frac{c_{rel0}^2}{2} (1 - e^{-2k_1\tau}); \\ A_{fr} &= \frac{g_K}{g_r} \frac{c_{rel0}^2}{2} \left[1 - \frac{16}{(2 + k_2 \sqrt{c_{rel0}\tau})^4} \right]; \\ A_{fr} &= \frac{g_K}{g_r} \frac{c_{rel0}^2}{2} \left[1 - \frac{1}{(1 + k_3 c_{rel0}\tau)^2} \right]. \end{aligned} \right\} \quad (153)$$

Particle Motion in the Axial Clearance of the Turbine

Usually for particles formed with destruction of the film in axial clearance, $Re_{rel} \gg 1$. Moreover, it is possible to ignore the velocity of the film flow from the exit edges in comparison with the gas velocity and to consider $c_{rel0} = c_1$, where c_1 is the gas velocity in axial clearance. In this case expressions for velocity and the path traversable by a particle in axial clearance as well as for losses due to friction may be transformed to ($Re_{rel} = 10-1000$):

$$\left. \begin{aligned} \frac{c_K}{c_1} &= 1 - \left(\frac{2}{2 + \tau} \right)^2; \\ \bar{x} &= \frac{k_2 x}{\sqrt{c_1} \sin \alpha_1} = \frac{\tau^2}{2 + \tau} \end{aligned} \right\} \quad (154)$$

$$\text{and} \quad A_{fr} = \frac{g_K}{g_r} \frac{c_1^2}{2} \left[1 - \left(\frac{2}{2 + \tau} \right)^2 \right]. \quad (155)$$

where α_1 is the angle of flow exit from the nozzle apparatus;

$\bar{\tau} = k_2 \sqrt{c_1} \tau$ is the dimensionless time of particle motion.

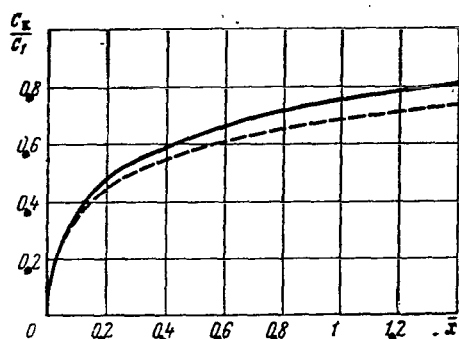


Fig. 46. c_K/c_1 as a Function of \bar{x} :

—— $10 < \text{Re}_{\text{rel}} < 1000$;

----- $\text{Re}_{\text{rel}} > 1000$.

Figure 46 represents the parametric dependence of c_K/c_1 upon \bar{x} , calculated according to (134). As the graph shows, particle velocity increases most sharply in the initial phase of motion. With the same axial clearance x and a decrease in particle diameter (k_2 increases) the dimensionless coordinate \bar{x} and, consequently, even the ratio c_K/c_1 increase.

With the aid of this graph it is possible to determine that the increase in

velocity of particles with a given size in axial clearance is small. For example, if $\mu_f = 8 \cdot 10^{-5} \text{ n} \cdot \text{sec}/\text{m}^2$, $\rho_f = 2 \text{ kg}/\text{m}^3$, $\rho_K = 1000 \text{ kg}/\text{m}^3$, $\alpha_1 = 20^\circ$, $x = 20 \text{ mm}$ and $c_1 = 400 \text{ m}/\text{sec}$, then the dimensionless value of axial clearance $\bar{x} = 0.36, 0.9, 0.033$, and the ratio of velocities $c_K/c_1 = 0.55, 0.33, 0.15$, respectively, for particles with diameters $d = 100, 250, 500 \text{ } \mu\text{m}$.

It is necessary to bear in mind that particle acceleration in the axial space is accompanied by deformation and fracturing; therefore, the above-given evaluation is correct only in first approximation. However, it allows us to trace the influence of very important parameters such as viscosity, density and velocity for great particle density due to particle acceleration in axial space. For example, in the final stages of turbines operating on moist water vapor $\mu_{\text{II}} = 2 \cdot 10^{-5} \text{ n} \cdot \text{sec}/\text{m}^2$ and $\rho_{\text{II}} < 0.2 \text{ kg}/\text{m}^3$, therefore with the same /101 vapor velocity and amount of axial clearance as in the preceding example, the ratio $c_K/c_1 = 0.25, 0.1, 0.05$ for particles with diameters $d = 100, 250$ and $500 \text{ } \mu\text{m}$, respectively. The weak particle acceleration of the condensate in the axial spaces during the final stages of condensation vapor turbines is indirectly confirmed by the fact that only in these stages does erosional wear of the working blades often occur. With a vapor pressure $p > 0.3 \cdot 10^6 \text{ n}/\text{m}^2$ and increased axial clearance, blade erosion almost ceases.

With an increase in particle density or the angle α_1 and a decrease in axial clearance, the ratio c_K/c_1 also decreases rapidly.

The dependence of c_K/c_1 upon the value $\bar{x} = k_3 x / \sin \alpha_1$ in the case of $\text{Re}_{\text{rel}} > 1000$ is shown in Figure 46 by a dotted line. This dependence is calculated according to the following expressions

obtained from the equations in (149) and (150) analogous to equation (154):

$$\frac{c_k}{c_1} = \frac{\bar{\tau}}{1 + \bar{\tau}}; \quad \bar{x} = \frac{k_3 x}{\sin \alpha_1} = \bar{\tau} - \ln(1 + \bar{\tau}), \quad (156)$$

where $\bar{\tau} = k_3 c_1 \tau$ is dimensionless time.

3. Flow of a Double-Phase Mixture in a Working Wheel

Let us consider first the flow of a mixture in the working blades with a small axial clearance x_c between the nozzle and working blades, when it is possible to ignore the change in flow parameters of the mixture in the space. In this case, a liquid film flowing at a low velocity from the nozzle apparatus strikes the working blades at a large negative angle of attack (Fig. 47a). This leads to the appearance of losses due to impact and with prolonged operation may cause erosional wear of the working blades. In turn, erosional wear of the intake edge will cause a further decrease in the effectiveness of the working wheel; moreover, progressive erosion may lead to the destruction of the eroded blades.

With an intensive separation of particles of low viscosity on nozzle blades and a small amount of axial clearance, losses due to impact of the liquid phase upon the working blades will predominate over all other causes of losses.

To evaluate losses due to impact, let us suppose that the concentration of the liquid phase in front of the turbine is equal over the entire section and that the velocity of the film flowing from the nozzle blades may be ignored as small in comparison with the circumferential velocity of the working blades. In such a case, the relative velocity of the secondary drops with their impact upon the working blades will be equal to the circumferential velocity and directed opposite the direction of rotation. Moreover, let us consider that these drops adhere to the surface of the blades; i.e., that impact is completely plastic.

The force of resistance applied to the elementary length of the working blades dr due to liquid particle impact is /102

$$dP_1 = 2\pi r \frac{G_k}{F_a} u dr,$$

where F_a is the cross sectional area of the flow section of the turbine;

r is the radius of the section under consideration;

u is the circumferential velocity.

Let us consider that a liquid which has precipitated on the working blades flows in a radial direction under the action of cen-

trifugal forces. In this case, a supplementary resistance force appears, which is applied to the blades and directed opposite rotation. The value of this force acting on the radius r and arising

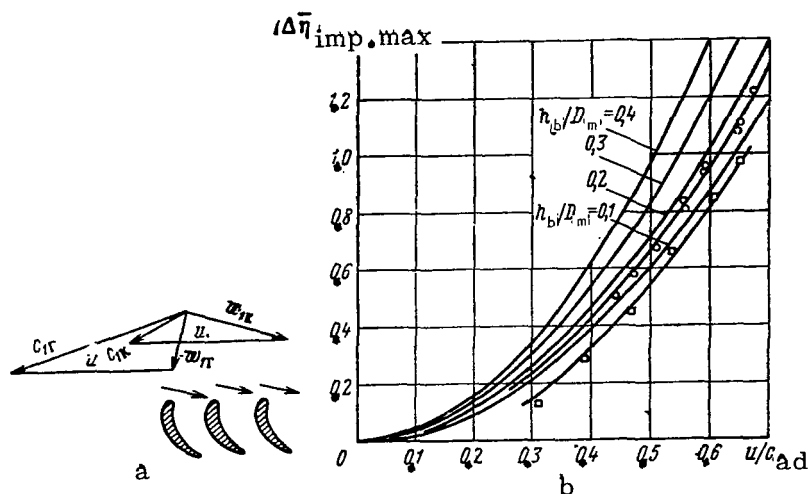


Fig. 47. Determination of Losses With Particle Impact on Working Blades: (a) Triangles of Velocities on the Entrance to the Working Grid; (b) The Value $\Delta\bar{\eta}_{imp.max}$ As a Function of u/c_{imp} :

- Calculated Dependences:
- o-o- Based on the Author's Experimental Data ($h_b/D_m = 0.164$, $x_c = 8$ mm, $\alpha_1 = 19^\circ 40'$);
- Based on Experimental Data from Reference [19].

with a motion of the mass dm in a radial direction is

$$dP_2 = dm 2\omega c_{r, film}$$

where $dm = F_{film} \rho_K dr$;

F_{film} is the total area of a section of film flowing along all blades on radius r ;

$c_{r, film}$ is the mean velocity of film flow along the base on radius r ;

ω is the angular velocity of rotor rotation.

With a complete precipitation of the liquid phase on the nozzle blades and small axial clearance, liquid consumption through the ring section along the working blades on radius r will be

$$F_{film} c_{r, film} \rho_K = \pi \frac{G_K}{F_a} (r^2 - r_{hub}^2),$$

where r_{hub} is the radius of the hub.

$$\text{Then } dP_2 = 2\omega\pi \frac{G_K}{F_a} (r^2 - r_{\text{hub}}^2) dr.$$

The total elementary force of resistance acting on the length of the working blades dr and the losses in power from this force are:

$$dP = dP_1 + dP_2 \text{ and } N_{\text{imp}} = \int_{h_{\text{fil m}}} u dP = 2\pi \frac{G_K}{F_a} \omega^2 \int_{h_{\text{fil m}}} (2r^2 - r_{\text{hub}}^2) r dr.$$

Having derived the integration and provided the obtained power by the adiabatic work of the gas phase, after transformations we obtain the expression for the coefficient of losses due to impact and scattering of the liquid phase by the working blades:

$$\Delta\eta_{\text{imp, max}} = 2k_c \frac{G_K}{g_r} \left(\frac{u}{c_{\text{ad}}}\right)^2 \left(1 + \frac{h_{\text{fil m}}^2}{D_m^2}\right), \quad (157)$$

where u is the circumferential velocity on the mean diameter;
 k_c is the coefficient of particles separation on nozzle blades;
 c_{ad} is the adiabatic velocity of the gas;
 h_b is the height of the working blades.

From the formula it is apparent that losses due to impact, calculated for the case of axial clearance, to a significant degree depend upon the ratio u/c_{ad} of the stage and also upon the relative length of the working blades h_b/D_m . The value

$$\bar{\Delta\eta}_{\text{imp, max}} = \frac{g_r}{G_K} \Delta\eta_{\text{imp, max}} = 2 \left(\frac{u}{c_{\text{ad}}}\right)^2 \left(1 + \frac{h_{\text{fil m}}^2}{D_m^2}\right),$$

characterizes the maximum losses due to impact with complete particle separation on the nozzle blades (i.e., in the case where $k_c = 1$). This value as a function of u/c_{ad} is presented in Figure 47b.

Let us note that formula (157) is accurate even in the case when the liquid particles are concentrated on the periphery of the flow portion in front of the entrance to the nozzle apparatus, as this often exists in the intermediate stage of a multistage turbine. Actually, due to a change in the circumferential component velocity of the liquid from zero to a velocity u_{ext} on the peripheral diameter a force $P = k_c G_K u_{\text{ext}}$ acts on the ends of the blade, directed against the rotation. Having divided the power of inhibition Pu_{ext} by the available gas energy in the stage $G_T(c_{\text{ad}}^2/2)$, again we obtain formula (157). /104

With an increase in actual clearance the velocity of secondary drops increases and the relative velocity of their impact on the working blades decreases. Therefore, with an invariable degree of

separation on the nozzle blades, losses due to impact will decrease.

§2. Experimental Investigations of Turbine Stages on Double-Phase Flows

As was noted above, the majority of experimental investigations (including experimental investigations conducted recently at the Moscow Electrotechnical Institute, the I.I. Polzanov Central Scientific Research Planning and Design Boiler and Turbine Institute and other organizations) are related to turbine operation on moist water vapor or on a water-air mixture. To clarify the flow characteristics of a double-phase mixture in a turbine in the most common form as well as to determine the dependence of supplementary losses upon the characteristics of the suspended phase, experimental investigations on other double-phase working fluids are necessary.

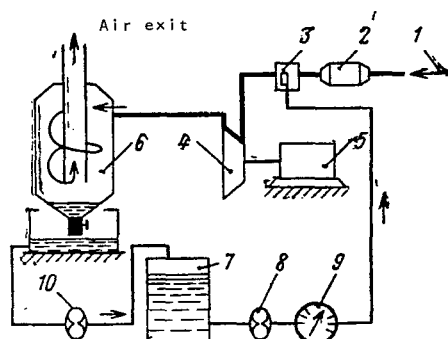


Fig. 48. Schematic Drawing of an Experimental Apparatus; (1) Air Magistral; (2) Preheater; (3) Sprayer; (4) Turbine; (5) Hydraulic Brake; (6) Separator; (7) Reservoir; (8) Basic Pump; (9) Volume Consumption Meter; (10) Transferring Pump.

ferring pump (10) from where, by the basic pump (8) through a volume consumption meter (9), it is forced to a sprayer (3). Due to the closed system supplying the liquid phase, the apparatus can work for an extended period of time with a minimum amount of liquid.

In the experimental process the operation of a turbine stage on /105 a mixture of cold air and particles of a liquid with a low viscosity (diesel fuel DS, DZ or water), sprayed by centrifugal or pneumatic jets, and a mixture of air preheated to 120-175° C and particles of a very viscous liquid (coal tar pitch: melting point of $t_{\text{melt}} = 70^\circ \text{C}$, mean particle diameter $d = 17 \mu\text{m}$).

The viscosity of these liquids as a function of temperature is

shown in Figure 49. Particles of coal pitch, solid at room temperature, were fed into the flow in front of the turbine by means of a feeding apparatus, schematically depicted in Figure 50.

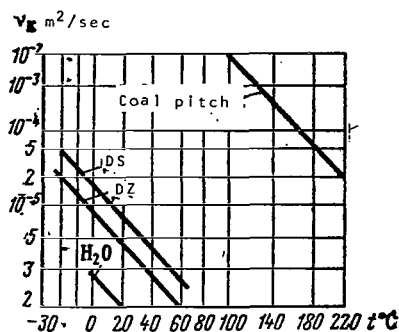


Fig. 49.

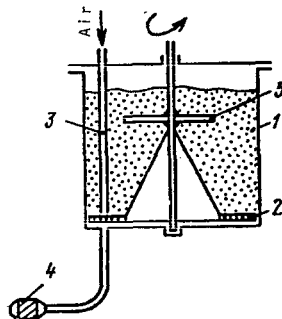


Fig. 50.

Fig. 49. Viscosity of the Liquid Phase as a Function of Temperature: $\rho_{\text{coal pitch}} = 1260 \text{ kg/m}^3$; $\rho_{\text{DS}} = 900 \text{ kg/m}^3$; $\rho_{\text{DZ}} = 850 \text{ kg/m}^3$; $\rho_{\text{H}_2\text{O}} = 1000 \text{ kg/m}^3$.

Fig. 50. Schematic Drawing of an Apparatus for Feeding Dust into the Gas-Air Tract in Front of the Turbine: (1) Bunker; (2) Feeder Grid; (3) Blow Pipes; (4) Screw Nozzles; (5) Axle Blades.

The dust-like substance charged in a bunker (1) where it is moved by blades (5) located on an axle which is rotated by an electric motor through a reducer. By means of feeder grid (2) the dust is directly supplied to the blast pipes (3) and is moved by compressed air. The dust-air mixture formed through the screw nozzles (4) is fed into the flow portion in front of the turbine.

Particles of coal pitch entering the hot compressed air flow are melted and converted into droplets of viscous liquid. A rather large distance between the nozzle and the turbine was chosen, around 3 m; therefore the particles melted completely.

Typical experimental characteristics of the turbine stage (cf. Table 4) are presented in Figure 51, working on a double-phase flow /106 with a liquid phase of low viscosity, i.e., DS diesel fuel with viscosity $\nu_k = 6 \cdot 10^{-6} \text{ m}^2/\text{sec}$, particles $d = 100 \mu\text{m}$ and various particle concentrations. The increase in the concentration of the liquid phase leads to a substantial decrease in turbine efficiency. The change in turbine efficiency as a function of the concentration of the liquid phase where $u/c_{\text{ad}} = 0.5$ and $\pi_T = 1.7 - 2.2$ is shown in Figure 52.

TABLE 4. BASIC PARAMETERS OF EXPERIMENTAL TURBINES

Item	Volume	Item	Volume
Diameter D in m:		Angle β_2 :	
in Base Section	0.245	in Base Section	34°
in Midsection	0.293	in Midsection	$32^\circ 50'$
in Peripheral Section	0.342	in Peripheral Section	$31^\circ 10'$
Height of Blade h_b in mm	48	Initial Temperature	290-450
Ratio D_m/h_b	6.1	T_0^* in $^\circ K$	
Axial Clearance x_c in mm	10	Degree of Reaction ρ :	
Angle α_1 :		in Root Section	0.015
in Base Section	$16^\circ 40'$	in Midsection	0.29
in Midsection	$19^\circ 40'$	in Peripheral Section	0.45
in Peripheral Section	$21^\circ 43'$	Degree of Pressure	2.2-1.7
Angle β_1 :		$\pi_T = p_0^*/p_T$	
in Base Section	31°	Air Consumption G_T in	7.5-5.4
in Midsection	42°	kg/sec	
in Peripheral Section	58°	Power N_T in kW	350-170

* Turbine profiled according to the law $c_u r = \text{const.}$

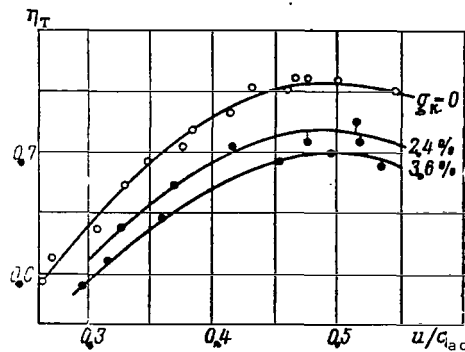


Fig. 51.

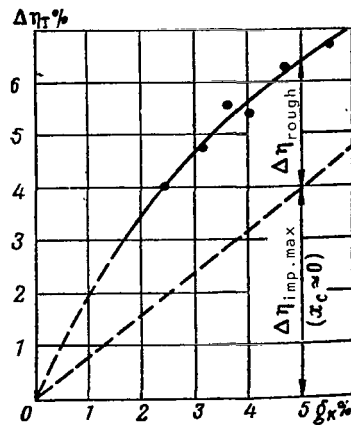


Fig. 52.

Fig. 51. Power Efficiency of the Turbine as a Function of u/c_{ad} with Operation on Pure Air and on a Double-Phase Flow with DS Particles $\pi_T = 2.2$.

Fig. 52. Decrease in Turbine Efficiency as a Function of the Concentration of the Liquid Phase DS Where $\pi_T = 1.7 - 2.2$ and $u/c_{ad} = 0.5$.

An experimental study of the concentration of the liquid phase by means of special probes analogous to Pitot tubes showed, as might be expected, that complete particle separation takes place on the nozzle blade. As calculations according to formula (154) showed, /107 the velocity of secondary particles ($d \geq 200 \mu\text{m}$) increased in axial clearance to 15-20% of the gas velocity. Therefore, losses due to impact on the working blades of a liquid film flowing from the nozzle blades may be evaluated according to (157), assuming $k_c = 1$.

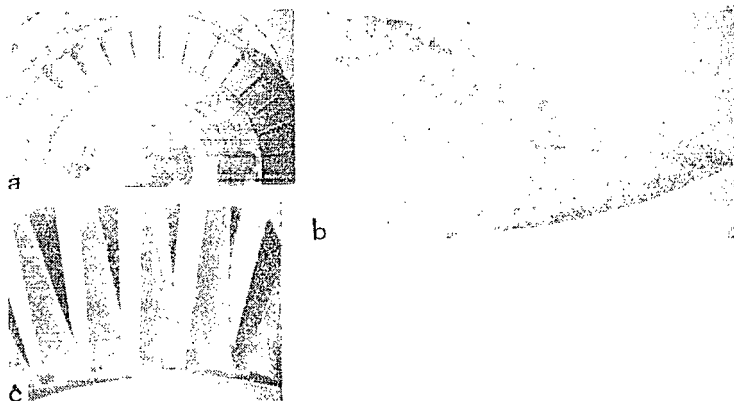


Fig. 53. Flow Section Elements of a Turbine after Operation on a Double-Phase Flow With a Viscous Liquid Phase: (a) Nozzle Apparatus; (b) Exit Cock; (c) Working Blades.

The dependence of the maximum value of these losses upon the concentration of the liquid phase is shown in Figure 52 by the dotted line. Experimental values for the decrease in turbine efficiency exceed the calculated values, considering only losses due to impact. This supplementary decrease in efficiency is completely determined by the increase in losses due to friction of the gas on the rough film covering the nozzle blades. Due to the large particle diameter it is possible to ignore losses from friction of the gas on the particles and on particle separation in the nozzle apparatus.

The general pattern of congealed precipitates of coal pitch is shown in Figure 53 ($v_K = 2.5 \cdot 10^{-3} \text{ m}^2/\text{sec}$) after turbine operation under the regime $\pi_T = 2.2$; $u/c_{ad} = 0.48$; $g_K = 5\%$. The wave nature of the film flow is readily apparent on photographs. It is necessary to note that due to polydispersion of coal pitch particles, their precipitation on the flow section walls has both an inertial and a turbulent diffuse nature.

The condition of the blade of the nozzle apparatus is shown in /108 Figure 53a. The convex part of the blade proved to be covered with an undulating film, the wave frequency and the height of the crests were usually great around the ends of the blades in the boundaries

of the vapor vortex zones. The height of the crests on the concave portion of the blades was substantially lower. Such a nature of the flow may be explained by the above-mentioned action of centrifugal forces striving to increase the undulating nature of the film on the concave part and to decrease it on the convex part.

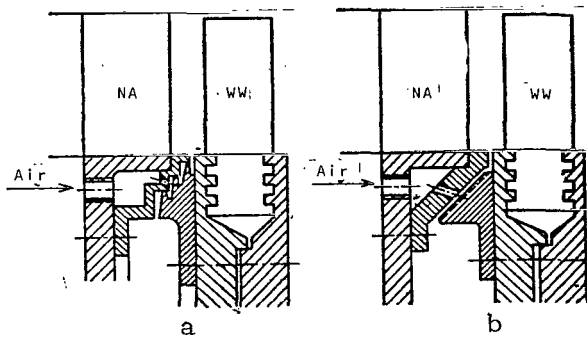


Fig. 54. Schematic Drawing of Consolidation of the Axial Clearance: (a) With diagonal Labyrinth; (b) With Screw Groove.

The working blades remained practically clean. The film thickness was insignificant on them, even with a very viscous liquid (such as melted ash), due to the great centrifugal forces casting the film onto the periphery. On the surface of the blades, traces of radial motion of the liquid phase are seen (cf. Fig. 53c).

stops and cools the rotor may be blocked by the frozen liquid phase, entering the actual space between the stator and the working disks of the turbine; such a blockage is observed in experiments. Blockage may occur even when the remnants of the liquid phase congeal in the radial space above the working blades.

If the melting point of the liquid phase is significantly higher than atmospheric temperature, then when the turbine

In order to prevent blockage it is necessary to carefully contract the axial space between the stator and the rotor. Figure 54 shows two types of consolidation: with a diagonal labyrinth and with screw grooves; these contractions were tested on a model turbine. Both contractions proved to be sufficiently effective: the liquid phase completely ceased to enter the axial space and the expenditure of air blown through the contraction was negligible.

Figure 55 shows the experimental characteristics of a turbine /109 with a clean flow section and with a flow section covered with congealed coal pitch film with an initial viscosity of $\nu_K = 0.8 \cdot 10^{-4}$ and $2.5 \cdot 10^{-3} \text{ m}^2/\text{sec}$ operating on pure air. An experimental point is plotted there characterizing turbine operation on a double-phase flow with $\pi_T = 2.2$; $g_K = 5\%$; $\nu_K = 2.5 \cdot 10^{-3} \text{ m}^2/\text{sec}$.

Here the total height of the crests of congealed coal pitch film from both sides of the nozzle blades in the region of the exit edge were equal to 0.5 mm with an initial film viscosity of $\nu_K = 0.8 \cdot 10^{-4} \text{ m}^2/\text{sec}$ and 0.9 mm where $\nu_K = 2.5 \cdot 10^{-3} \text{ m}^2/\text{sec}$. The total height of the crest was determined as an average value, measured

along all the blades in three sections. It is necessary to bear in mind that the height and shape of the waves of congealed film differ somewhat from the height and shape of the waves of liquid film under working conditions.

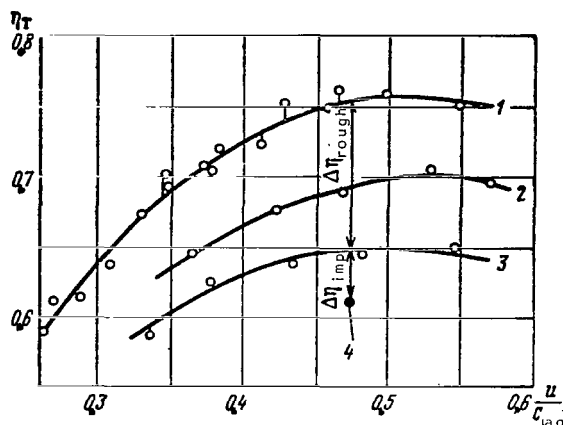


Fig. 55. Characteristics of a Turbine Operating on Air with $\pi_T = 2.2$: (1) Clean Flow Portion; (2) Flow Portion Covered with Congealed Film with an Initial Viscosity of $\nu_K = 0.8 \cdot 10^{-4} \text{ m}^2/\text{sec}$; (3) Initial Film Viscosity $\nu_K = 2.5 \cdot 10^{-3} \text{ m}^2/\text{sec}$; (4) Working Point of the Turbine on a Double-Phase Flow with Viscous Particles Where $\nu_K = 2.5 \cdot 10^{-3} \text{ m}^2/\text{sec}$ and $g_K = 5\%$.

The activity of the stage investigated as a function of u/c_{ad} is shown in Figure 56. The activity of the stage operating on air and on a double-phase flow with DS particles ($g_K = 3-6\%$) proved to be equal. This is explained by large particle diameter ($\bar{d} = 100 \text{ } \mu\text{m}$) and low viscosity of DS, due to which the total influence on the reactivity of the condition of phase interaction and clogging of the nozzle apparatus by film was insignificant.

On the other hand, in the case of very viscous liquid phase ($\nu_K = 0.8 \cdot 10^{-4} - 2.5 \cdot 10^{-3} \text{ m}^2/\text{sec}$) the degree of reactivity due to clogging the flow sections of the nozzle apparatus by film decreases noticeably. With a decrease in u/c_{ad} the reactivity of the stage is changed much more slowly than in a turbine operating on pure gas. This may be explained by the more intensive increase in losses in /110 the working grid due to large positive angles of attack arising with decreased reactivity.

§3. Flow of a Double-Phase Mixture in a Turbine with Increased Axial Clearance. Particle Separation in the Axial Clearance.

In a number of cases it is necessary to decrease the erosional wear of the working blades of a turbine by the suspended particles. With a small corrosive liquid phase and low working fluid parameters which may be observed, for example, in the final stages of condensed-vapor turbines, hardening of the intake edges of the working blades by melting hard alloys on them allows one to substantially decrease their erosional wear [14].

However, with high temperature and corrosivity of the working fluid, in particular of the liquid phase, erosional wear may be decreased only by other technological or construction methods. In particular, one of the most radical means for decreasing erosion of

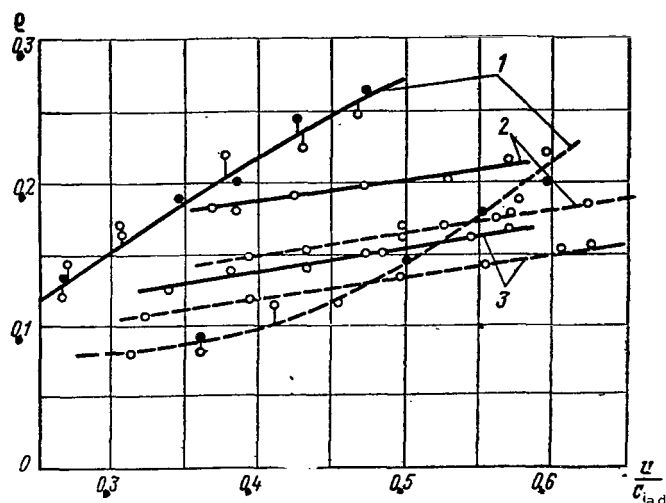


Fig. 56. Reactivity of a Stage on the Central Radius as a Function of u/c_{ad} :

—— $\pi_T = 2.2$; ---- $\pi_T = 1.7$:
 ○ = Operation on Pure Gas; ● = Operation on a Double-Phase Flow with DS Particles ($g_K = 3-6\%$);
 (1) Clean Flow Section; (2) Flow Section Covered With Congealed Film, Initial Viscosity $\nu_K = 0.8 \cdot 10^{-4}$ m²/sec; (3) Initial Film Viscosity $\nu_K = 2.5 \cdot 10^{-3}$ m²/sec.

the working blades is to increase the axial clearance between the nozzle and working blades. Actually, with an increase in the axial clearance the diameter of secondary drops decreases, since destruction of the film flowing from the nozzle blades is successfully accomplished; the relative velocity of particle impact on the working blades due to particle acceleration by the gas decreases substantially; partial separation of secondary drops on the peripheral wall takes place since the number of drops impacting against the working blades is decreased. /111

In this section we shall consider the questions concerning the motion and separation of liquid particles in a gas turbine with an increased axial clearance. In the case of complete particle separation, the base of the working wheel will be washed by a single-phase flow. This allows avoiding erosion of the working blades, an especially important factor in high-temperature turbines designed for prolonged operation. The expediency of particle separation in front of the working wheel is also noted in references [27] and [38].

1. Particle Motion in the Axial Clearance and Determination of the Size of the Separation Zone

The size of secondary drops formed by film destruction depends upon the velocity and density of the gas flow and also upon the viscosity and coefficient of surface tension of the liquid.

The break-up of the drops of liquid in an air flow was studied by a number of investigators; in particular, by Prandtl. In order to determine the maximum size of drops he proposed the following formula derived from an equilibrium condition of hydrodynamic forces and surface tension forces acting upon the drop

$$d_{\max} = \frac{7.7\sigma}{\rho r \frac{c_{\text{rel}}^2}{2}},$$

where c_{rel} is the average velocity of drop motion relative to the gas in a scattering process.

Ignoring the velocity of the drop small in comparison with the gas velocity, and considering that the film flowing from the nozzle blades is destroyed instantaneously, it is possible to assume $c_{\text{rel}} = c_1$. In this case, the maximum diameter of secondary drops can be calculated approximately by using the formula

$$d_{\max} = \frac{15.4 \sigma}{\rho r c_1^2}. \quad (158)$$

The viscosity of the liquid increases the time necessary for the break-up of large drops into smaller drops, the dimensions of which are determined by this formula. Therefore, with the destruction of the film flowing from the nozzle blades, equilibrium between

the hydrodynamic forces and the surface tension forces acting on the particle may not occur, especially in cases of liquids with elevated viscosity; under such conditions particle dimensions may substantially exceed the sizes calculated according to formula (158).

Large particles having a certain initial velocity move in the axial clearance due to their inertia along weakly curved trajectories. In reference [21] the maximum

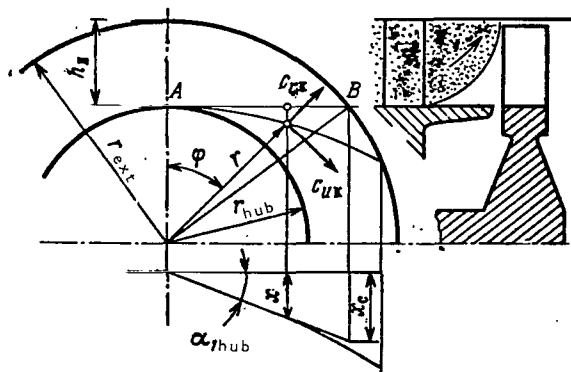


Fig. 57. Calculation of Particle Motion in the Axial Clearance.

size of axial clearance necessary for the separation of such particles was determined by assuming their trajectories to be straight, corresponding in direction with the velocity of the flow upon exit from the nozzle apparatus. The minimum length of the separating zone x_c is determined from the condition that particles formed at the hub precipitate on the peripheral surface in front of the working wheel⁶.

As follows from the geometric relationships in Figure 57

$$x_c = AB \tan \alpha_{1\text{hub}} = r_{\text{hub}} \sqrt{\bar{r}_{\text{ext}}^2 - 1} \tan \alpha_{1\text{hub}} \quad (159)$$

where x_c is the axial clearance;

$\alpha_{1\text{hub}}$ is the angle of low exit from the nozzle apparatus on the internal radius;

$\bar{r}_{\text{ext}} = \frac{r_{\text{ext}}}{r_{\text{hub}}}$ is the relative external radius of the flow section. /113

This expression may also be presented in the form

$$x_c = h_b \sqrt{\frac{D_m}{h_b} \tan \alpha_{1\text{hub}}}$$

where $D_m/h_b = 5-7$ and $\alpha_{1\text{hub}} < 20^\circ$, the value of $x_c < 0.8 h_b$.

The dependence of the dimensionless coordinate of a particle $\xi = x/r_{\text{hub}}$ (where x is the coordinate along the axis of the turbine) upon the ratio $\bar{r} = r/r_{\text{hub}}$, calculated according to formula (159) for various values of the angle $\alpha_{1\text{hub}}$, indicated by the dotted line in Figure 58.

The actual size of the separating clearance will be somewhat greater since the particle trajectories deviate from straight lines. Let us consider the motion of secondary drops in the axial clearance, assuming that they are spheres of equal diameter, and that their

⁶ As graduate student, B.A. Ponomarov showed that with long blades ($D_m/h_b < 6$) twisted according to the law $c_y r = \text{const}$, and rectilinear particle direction, the necessary size of the separating clearance will be determined by particles which are not formed at the hub but on a radius $r = r_{\text{ext}}/\sqrt{2}$. This relationship may be obtained from the condition of maximum function (159) described for a particle formed on radius r in the following form:

$$x_c = \sqrt{r_{\text{ext}}^2 - r^2} \tan \alpha_1 = \frac{r}{r_{\text{hub}}} \sqrt{r_{\text{ext}}^2 - r^2} \tan \alpha_{1\text{hub}}.$$

initial velocity is equal to zero. We shall assume the field of gas velocities to be equal along the circumference since, according to the data of a number of authors, the relative decrease in the gas velocity in the tracks behind the edges does not exceed 5% with a clearance size on the order of $0.1 h_b$, and with an increase in the clearance, the velocity rapidly decreases.

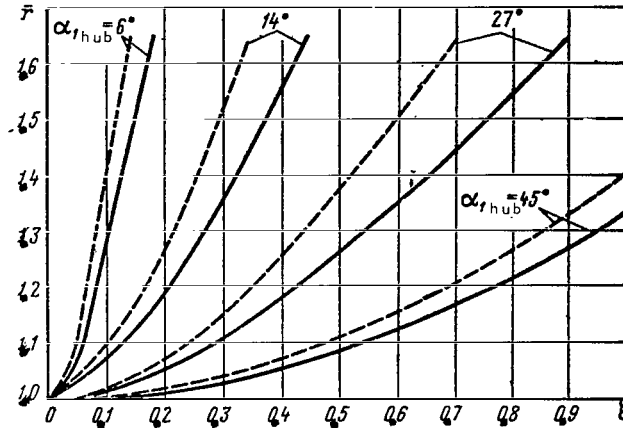


Fig. 58. Dependence of Dimensionless Axial $\xi = x/r_{\text{hub}}$ on the Radial $\bar{r} = r/r_{\text{hub}}$ Coordinates of Particles Moving From the Hub in the Axial Clearance of the Turbine:
 ----- Rectilinear Trajectories;
 ——— Actual Trajectories.

As was noted, with the motion of secondary drops in the separating zone the Re_{rel} number changes from several hundreds to several tens. In this range a change in the Re_{rel} number for the force of aerodynamic influence of gas on a particle is determined according to (147): $P = k_2 m \alpha_{\text{rel}}^{1.5}$. This force is directed according to particle velocity relative to the gas. The motion equation under the action of such a force is

$$\frac{d^2 S}{d\tau^2} = k_2 \alpha_{\text{rel}}^{1.5},$$

where $d^2 S/d\tau^2$ is the acceleration of a particle.

A motion equation for projections onto the cylindrical axis of coordinates is

$$\left. \begin{aligned} \frac{d^2 x}{d\tau^2} &= k_2 \left(c_{ar} - \frac{dx}{d\tau} \right) \alpha_{\text{rel}}^{0.5}; \\ \frac{d^2 r}{d\tau^2} &= r \left(\frac{d\varphi}{d\tau} \right)^2 - k_2 \frac{dr}{d\tau} \alpha_{\text{rel}}^{0.5}; \\ \frac{d^2 \varphi}{d\tau^2} &= \frac{k_2}{r} \left(c_{ar} - r \frac{d\varphi}{d\tau} \right) \alpha_{\text{rel}}^{0.5} - \frac{2}{r} \frac{dr}{d\tau} \frac{d\varphi}{d\tau}, \end{aligned} \right\} \quad (160)$$

where r, x, ϕ are cylindrical coordinates of a particle;
 $c_{a\Gamma}$ and $c_{u\Gamma}$ are axial and circumferential components of gas velocity.

For the case of a flow whirling in the axial clearance according to the law of constant circulation ($c_{u\Gamma}r = \Gamma = \text{const}$) the components are $c_{a\Gamma} = \text{const}$ and $c_{u\Gamma} = \Gamma/r$. Introducing the dimensionless coordinates $\xi = x/r_{\text{hub}}$, $\bar{r} = r/r_{\text{hub}}$ and the dimensionless time $\tau = (v_{\Gamma\text{ave}}/d^2)$ (where $v_{\Gamma\text{ave}}$ is the coefficient of kinematic viscosity of the gas on an average diameter), the equations in (160) may be reduced to the following dimensionless form:

$$\left. \begin{aligned} \frac{d^2\xi}{d\tau^2} &= A_c \left(a_c - \frac{d\xi}{d\tau} \right) M; \\ \frac{d^2\bar{r}}{d\tau^2} &= \bar{r} \left(\frac{d\phi}{d\tau} \right)^2 - A_c \frac{d\bar{r}}{d\tau} M; \\ \frac{d^2\phi}{d\tau^2} &= A_c \left(\frac{b_c}{\bar{r}^3} - \frac{d\phi}{d\tau} \right) M - \frac{2}{\bar{r}} \frac{d\bar{r}}{d\tau} \frac{d\phi}{d\tau}, \end{aligned} \right\} \quad (160a)$$

where $M = \sqrt{\left(a_c - \frac{d\xi}{d\tau} \right)^2 + \left(\frac{d\bar{r}}{d\tau} \right)^2 + \left(\frac{b_c}{\bar{r}} - \bar{r} \frac{d\phi}{d\tau} \right)^2}$,

$$A_c = 9.75 \frac{\rho_{\Gamma\text{ave}}}{\rho_K} \sqrt{\frac{r_{\text{hub}}}{d}}, \quad a_c = \frac{c_{a\Gamma} d^3}{r_{\text{hub}} v_{\Gamma\text{ave}}}$$

and $b_c = \frac{\Gamma d^2}{r_{\text{hub}}^2 v_{\Gamma\text{ave}}}$ are dimensionless parameters;

$\rho_{\Gamma\text{ave}}$ is the gas density on an average diameter.

Results of a numerical solution to system (160a) on the "Ural" /115
 computer for particles moving from the hub and possessing zero initial velocity with values of the parameters $A_c = 1; 0.5; 0.3$, $a_c = 10; 5; 1$, $b_c = 20, 10; 2$ are given in Figures 58-63. The calculations show that the relationship between the axial ξ and radial \bar{r} dimensionless coordinates of a particle weakly depend upon the parameters A_c , a_c and b_c and are defined by the basic ratio $a_c/b_c = c_{1a}/c_{1uhub} = \tan \alpha_{1hub}$.

As may be seen from Figure 58, the real coordinate of a particle ξ proved to be approximately 20-25% larger than the coordinate calculated according to the approximate formula (159).

The angular coordinate of the particle ϕ as a function of \bar{r} (solid curve) is given on Figure 59. It proved to be the case that a change $\phi(\bar{r})$ does not depend upon the primaries A_c , a_c and b_c ; i.e., the projection of the particle trajectory onto a plane perpendicular to the turbine axis is not a function of particle size and the parameters of the gas flow.

For comparison, in the same figure the dependence for the case when particle trajectories are straight lines tangent to the hub is plotted with a dotted line.

Thus, with the above-mentioned assumptions, the particle trajectory and the axial clearance is determined only by the geometric parameters of the flow section of the turbine. With accuracy for engineering calculations it is possible to consider that in the range of change $\alpha_{1\text{hub}} = 15\text{-}25\%$

$$\xi = \frac{x}{r_{\text{hub}}} = 1.25 \sqrt{r^2 - 1} \tan \alpha_{1\text{hub}} \quad (161)$$

or

$$\bar{r} = \frac{x}{1.25 r_{\text{hub}} \tan \alpha_{1\text{hub}}} = \sqrt{r^2 - 1}. \quad (162)$$

The dependence between the radial \bar{r} and given axial $\bar{\xi}$ particle coordinates determined by this formula is presented in Figure 60.

The change in relative components of the particle velocity along the coordinates axes depending upon its reduced coordinate $\bar{\xi}$ is shown in Figures 61-63. As follows from the graph, the values c_{aK}/c_a , c_{uK}/c_u and c_{rK}/c_u depend upon the parameters A_c and b_c . With an increase in A_c and a decrease in b_c (for example, with a decrease in particle diameter and other conditions unchanged), the particle velocity rapidly approaches the gas velocity.

The strongest increase in axial and circumferential components of particle velocity takes place with variation in $\bar{\xi}$ within the limits from 0 to 0.2, i.e., at the beginning of the axial clearance. In particular, this explains the phenomenon sometimes observed in steam turbine operation, when, even with an insignificant increase in the axial clearance erosional wear of working blades decreases substantially.

/116

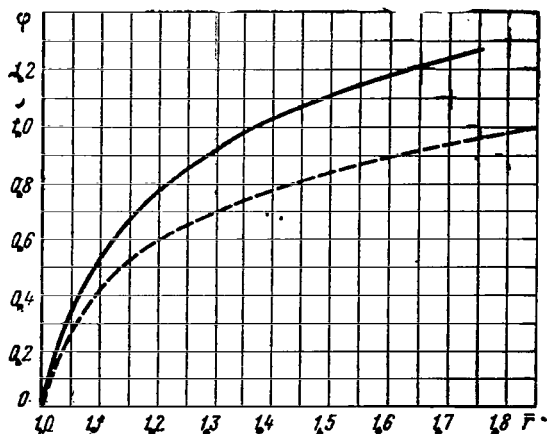


Fig. 59. Dependence Between the Angular and Radial Coordinates of a Particle Moving From the Hub:

-----Rectilinear Trajectories;
 ———Actual Trajectories.

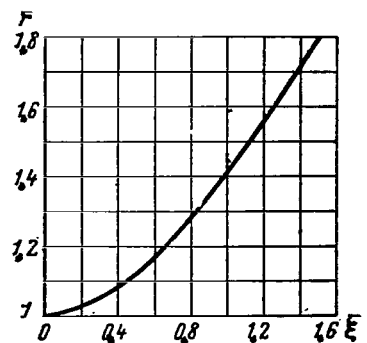


Fig. 60. Dependence Between the Radial \bar{r} and Reduced Axial $\bar{\xi}$ Coordinates of a Particle.

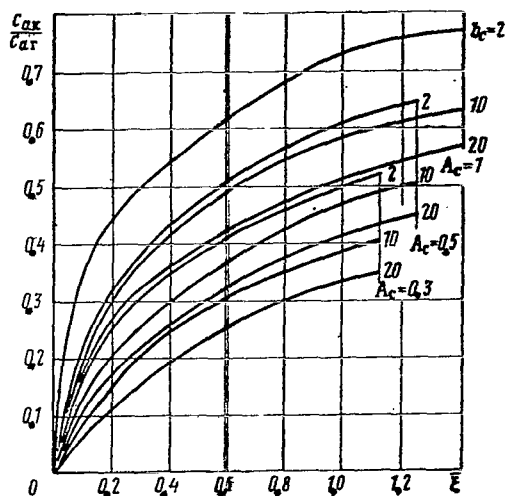


Fig. 61. Axial Relative Velocity of a Particle c_{ax}/c_{ur} as a Function of ξ .

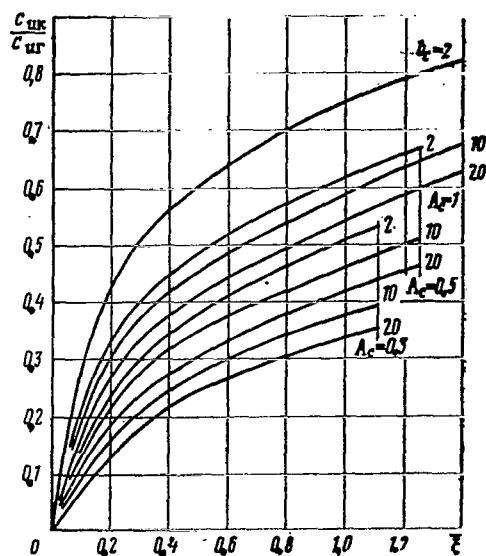


Fig. 62. Circumferential Relative Velocity of a Particle c_{ax}/c_{ur} as a Function of ξ .

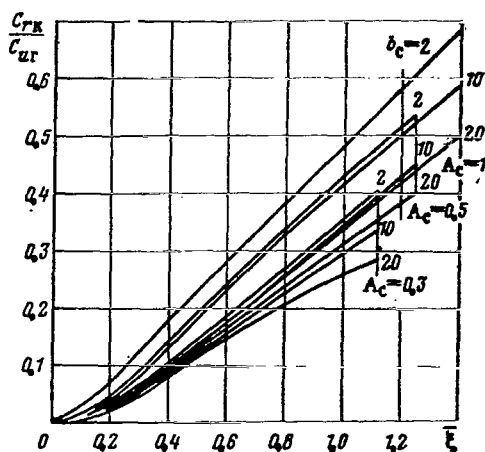


Fig. 63. Radial Relative Velocity of a Particle c_{ax}/c_{ur} as a Function of ξ .

Where $\bar{\xi} \geq 0.4$, the increase in particle velocity is somewhat delayed. In the investigated range of variation in the parameters A_c and b_c and in the value of $\bar{\xi}$, maximum particle velocity may reach the gas velocity. /118

It is necessary to emphasize that the obtained relationships characterizing particle motion in the axial clearance on the initial section of the trajectory are sufficiently close to dependence obtained for linear particle motion in §1 of this chapter.

2. Determination of Losses Due to Impact on the Working Blades with Regard to Particle Acceleration in the Axial Clearance

With a moderate size of axial clearance and long blades it is possible to ignore particle displacement in the clearance along the radius. Then, analogous to that which is set forth in §1 of this chapter, the force of resistance from particle impact acting upon the elementary link of the working blades dr ,

$$dP_1 = 2\pi r \frac{G_k}{F_a} (u - c_{uk}) dr,$$

where c_{uk} is the circumferential component of the particle velocity; the force of resistance dP_2 , arising with radial liquid flow, does not change here.

The power loss from the action of these forces is

$$N_{imp} = \int_{h_b} u d(P_1 + P_2) = 2\pi \frac{G_k}{F_a} \left[\omega^2 \int_{h_b} (2r^2 - r_{hub}^2) r dr - \omega \int_{h_b} c_{uk} r^2 dr \right].$$

Since $c_{ur} \cdot r = (c_{ur} \cdot r)_{ave} = \text{const}$ and c_u / c_{ur} changes insignificantly according to blade height, the integrand expression in the second term of the right-hand part may be thus transformed:

$$c_{uk} r^2 = \frac{c_{uk}}{c_{ur}} c_{ur} r r \approx \left(\frac{c_{uv}}{c_{ur,ave}} \right) (c_{ur})_{ave} \cdot r.$$

Then it is possible to integrate the expressions for N_{imp} . Having divided the power losses by the available gas work, after transformation we obtain

$$\Delta \eta_{imp} = \Delta \eta_{imp, max} \left[1 - \left(\frac{c_{uk}}{c_{ur}} \right)_{ave} \left(\frac{c_{ad}}{u} \right) \left(\frac{r_{ave}}{r_{ext}} \right)^2 \cos \alpha_{ave} \sqrt{1 - \rho} \right], \quad (163)$$

where ρ is the degree of reactivity on the average radius, and $\Delta \eta_{imp, max}$ represents losses determined according to formula (157).

The value $(c_{uK}/c_{u\Gamma})_{ave}$ may be evaluated according to Figure 62. However, in determining the values of dimensionless parameters A_c , b_c and $\bar{\xi}$ instead of r_{hub} it is necessary to substitute the average radius of the flow section of the turbine r_{ave} ; i.e.,

$$A_{c,ave} = 9,75 \frac{\rho r_{ave}}{\rho_K} \sqrt{\frac{r_{ave}}{d}}; \quad b_{c,ave} = \frac{I d^2}{r_{ave}^2 v r_{ave}};$$

$$\bar{\xi}_{ave} = \frac{x_{ave}}{1,25 r_{lim} \tan \alpha_{1,ave}},$$

where x is the average value of the axial clearance.

Since $c_{uK}/c_{u\Gamma} \approx c_K/c_1$, the ratio $(c_{uK}/c_{u\Gamma})_{ave}$ with a small size of axial clearance may also be determined from formula (154) or from Figure 46.

With a significant size of axial clearance, the losses due to impact will rapidly diminish; this is also due to separation of some of the liquid phase onto the peripheral wall. We shall determine the amount of separating liquid with a given value of axial clearance x_c ; to simplify we shall consider x_c to be constant relative to blade height. As Figure 64 shows, the amount of separating liquid will be determined by the limiting trajectory AB of secondary drop forming on a certain radius r_{lim} . According to expression (162) for this limiting trajectory the axial clearance is

$$x_c = 1,25 r_{lim} \sqrt{\left(\frac{r_{ext}}{r_{lim}}\right)^2 - 1} \tan \alpha_{1,lim} \quad (164)$$

where $\alpha_{1,lim}$ is the angle of flow exit from the nozzle apparatus on radius r_{lim} .

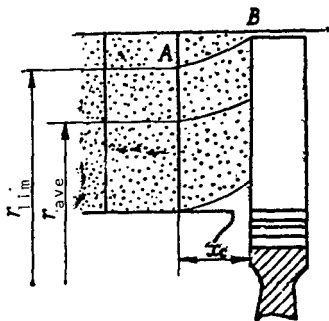


Fig. 64. Schematic Drawing of Double-Phase Flow in the Axial Clearance of a Turbine.

Since for a flow whirling in the axial clearance based on the law $c_u \cdot r = \text{const}$, the value $\tan \alpha_{1,lim} = (r_{lim}/r_{ave}) \tan \alpha_{1,ave}$, and from the latter expression we obtain

$$r_{lim}^2 = \frac{r_{ext}^2}{2} \left[1 + \sqrt{1 - \left(\frac{1,6 x_c r_{ave}}{\tan \alpha_{1,ave} r_{ext}^2} \right)^2} \right]. \quad (165)$$

According to formulas (164) and (165), it is convenient to determine the value of axial clearance necessary

for separation of the liquid in front of the working film if it is known that the fundamental mass of the liquid phase is concentrated in the peripheral zone of the flow section, as this is observed in the intermediate stages of multi-stage turbines.

In the case of uniform particle distribution in front of the nozzle apparatus, into formula (163) it is possible to introduce the supplementary coefficient /120

$$k_{c,s} = \frac{r_{im}^2 - r_{hub}^2}{r_{ext}^2 - r_{hub}^2}, \quad (166)$$

considering the partial separation of liquid phase in the clearance.

3. Determination of Losses Related to Separation

Particle separation in the axial clearance is accompanied by losses of gas energy including: losses due to friction with the motion of the gas relative to the particles; losses with precipitation of particles on the external row; losses due to friction of the gas on the rough undulating film, covering the external and internal walls in the axial clearance.

Let us evaluate the extent of these losses, assuming that all of the liquid phase precipitates on the nozzle blades; i.e., $k_c = 1$.

The work of the forces of friction of the gas on a particle with its motion in the axial clearance can be expressed from the relationship (75): $A_{fri} = \int P c_{rel} d\tau$. Total losses due to friction with motion of all $n = g_K/g_{fm}$ particles per 1 kg of the gas phase are

$$A_{fr} = \sum_{i=1}^n A_{fri}.$$

With precipitation of the particles on the wall, total kinetic energy

$$E_{kin} = \sum_{i=1}^n \frac{m c_{xi}^2}{2}$$

is almost completely lost, turning into heat. Thus, total losses during particle separation in the axial space are:

$$A_{sep} = A_{fr} + E_{kin} = \sum_{i=1}^n \left(A_{fri} + m \frac{c_{xi}^2}{2} \right).$$

In the turbine stage with blade height $h_b = (\frac{1}{4} - \frac{1}{7})D_m$ with sufficient accuracy for evaluations being conducted it is possible to assume $A_{sep} = (0.65-0.75)A_{sep \max}$, where $A_{sep \max}$ are the calculated losses from separation, assuming that all particles begin to move from the hub.

Using the relationship $P = k m c_{rel}^{1.5}$, we obtain

$$A_{sep} = (0.65 - 0.75) \frac{g_k}{g_r} \left(\int k_2 c_{rel}^{2.5} d\tau + \frac{c_k^2}{2} \right). \quad (167)$$

Here the values c_{rel} and c_k relate to the particles moving from the /121 hub. Therefore, in calculations it is possible to use the dependences obtained in preceding sections.

Having solved particle velocity in the axial clearance according to the direction of the gas velocity vector $c_{tK} = \sqrt{c_{uK}^2 + c_{aK}^2}$ and according to the radius c_{rK} and having substituted approximately $c_{rel} \approx \sqrt{(c_1 - c_{tK})^2 + c_{rK}^2}$ (where c_1 is the gas velocity on a mean diameter) by relating losses due to separation to the available gas energy, we obtain the coefficient of losses due to particle separation in the axial clearance:

$$\Delta \eta_{sep} = \frac{2A_{sep}}{c_{ad}^2} = (0.65 - 0.75) 2 \frac{g_k}{g_r} \left(\frac{c_1}{c_{ad}} \right)^2 (\Phi + E)$$

or finally

$$\Delta \eta_{sep} = (1.3 - 1.5) \frac{g_k}{g_r} (1 - \rho) (\Phi + E). \quad (168)$$

Here

$$\Phi = A_c \sqrt{\frac{b_c}{\cos \alpha_1}} \int \frac{\left[\left(1 - \frac{c_{tK}}{c_1} \right)^2 + \left(\frac{c_{rK}}{c_{ur}} \cos \alpha_1 \right)^2 \right]^{1/4}}{\bar{r}^{0.5}} d\bar{r}; \quad (169)$$

$$E = \frac{1}{2} \left[\left(\frac{c_{tK}}{c_1} \right)^2 + \left(\frac{c_{rK}}{c_{ur}} \right)^2 \right]; \quad (170)$$

α_1 is the angle of flow exit from the nozzle apparatus on a mean diameter.

Figures 65 and 66 show the value Φ characterizing losses due to friction of gas on the particles and the sums $\Phi + E$ characterizing the total losses from separation of particles forming at the hub as functions of the dimensionless reduced coordinate

$$\bar{\xi} = \frac{x}{1,25r_{\text{hub}} \tan \alpha_1}.$$

In calculating these dependences $\alpha_1 = 20^\circ$ was assumed. Variation in the angle α_1 within the limits of $15-25^\circ$ has a weak influence on the course of the curves.

In the case of a liquid phase of low viscosity (such as water or diesel fuel) and in a moderate concentration it is possible to ignore the increase in losses due to friction of the gas on the film covering the external and internal surfaces of the flow section in the axial clearance. These losses are somewhat compensated for by the decrease in losses in the radial clearance when it is partially filled by a liquid film.

With complete particle separation in the axial clearance, losses due to impact of the liquid phase on the working blades will be equal to zero.

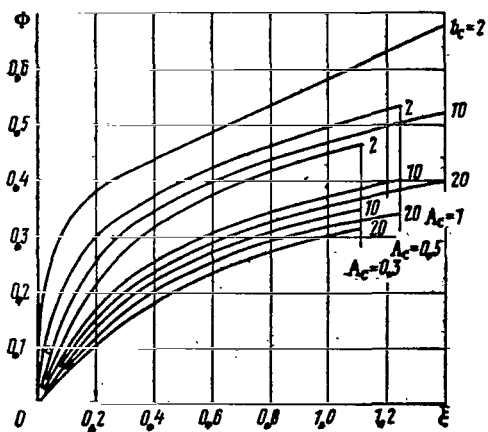


Fig. 65. The Value of Φ as a Function of ξ .

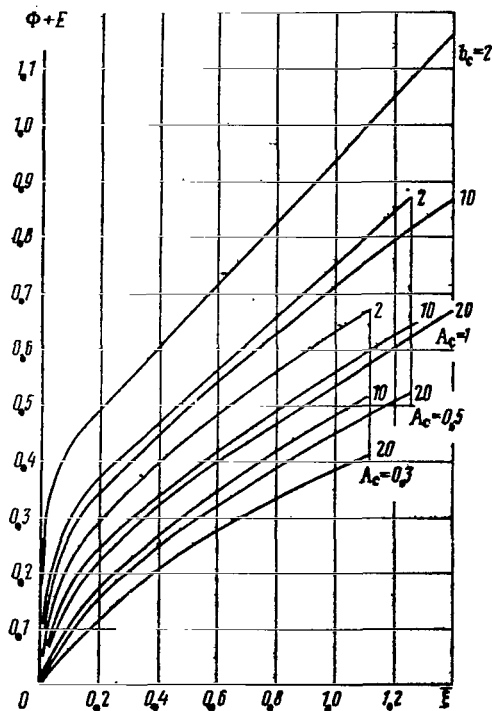


Fig. 66. The Value of $\Phi + E$ as a Function of ξ .

/122

The ratio of losses due to separation to maximum losses due to impact is

/123

$$\frac{\Delta \eta_{sep}}{\Delta \eta_{impmax}} \approx \frac{0,7 (1 - \rho) (\Phi + E)}{\left(\frac{u}{c_{ad}}\right)^3 \left(1 + \frac{h_b}{D_{fr}}\right)^3} \quad (171)$$

With variation in u/c_{ad} within the limits of 0.6-0.3 the numerator of this expression varies by not more than 20%, and the denominator by four times. Therefore, even the ratio of losses due to separation to those due to impact, depending upon u/c_{ad} , may vary within a very broad range. With small values of u/c_{ad} , losses due to separation may significantly exceed losses due to impact; with large values of u/c_{ad} , losses due to impact may prove to be greater than losses due to separation. Therefore, with $u/c_{ad} \geq 0.6$ particle separation in the axial clearance may be accompanied by an increase in turbine efficiency.

Tentative calculations, made for various turbines with a degree of reactivity $\rho = 0.25-0.35$, blade height $h_b = \left(\frac{1}{4} - \frac{1}{7}\right)D_m$ and flows with liquid phases of low viscosity, indicate that where $u/c_{ad} = 0.5-0.55$ this ratio is near unity. Therefore, in such turbines the decrease in efficiency due to the double-phase nature of the flows does not essentially depend on the amount of axial clearance, which is confirmed by experimental studies.

4. *Experimental Study of Separation in the Axial Clearance of a Turbine*

An experimental study of particle separation in the axial clearance was conducted on a turbine, the basic data from which are presented in Table 4. In the experimental process the axial clearance was varied within the limits from 8 to 58 mm. The suspended phase was DZ diesel fuel or water scattered by pneumatic nozzles. The mean diameter of the particles was 30-35 μm .

The experimental characteristics of the investigated turbine where $x_c = 8$ mm and 38 mm are presented in Figure 67. From the graphs it is apparent that with a small amount of axial clearance, when losses due to impact of the liquid phase on the working blades reach a maximum, the decrease in turbine efficiency due to the double-phase nature of the flow substantially depends on u/c_{ad} : with an increase in u/c_{ad} , losses sharply increase. It is necessary to note that curves agree satisfactorily with formula (157). The calculated and experimental values of $\Delta \eta_{imp max} = (g_I/g_K) \Delta \eta_{imp max}$ for the turbines studied are plotted in Figure 47.

On the other hand, with a large axial clearance, when almost complete particle separation takes place, the decrease in turbine efficiency, determined primarily from losses due to separation, is

almost independent of u/c_{ad} with variation in this parameter in a broad range. /124

Experimental points are plotted in Figure 68 which characterize the decrease in turbine efficiency on a double-phase flow with $u/c_{ad} = 0.52$ in comparison with a turbine operating on a pure gas. All experimental points independent of the amount of axial clearance lie satisfactorily on one curve. This confirms the assumption of the

weak influence of axial clearance, with the indicated value of u/c_{ad} , on total losses from the double-phase nature of the flow in a turbine. The change in maximum losses due to impact $\Delta\eta_{max}$ calculated according to formula (157) is plotted on the graph with a dotted line, as well as the distribution of losses with an axial clearance, ensuring particle separation of the liquid phase.

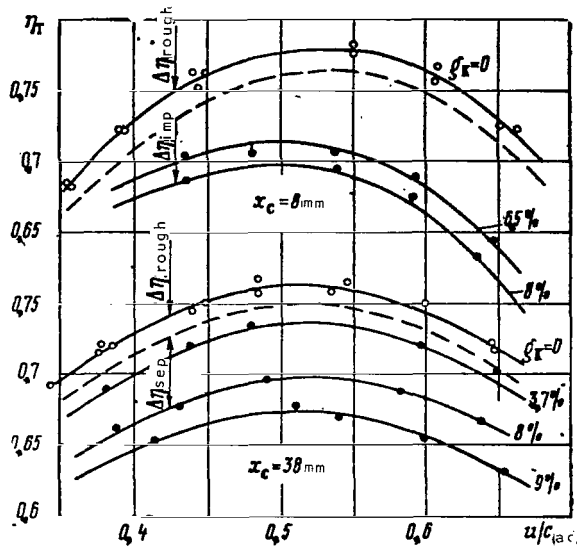


Fig. 67. Characteristics of a Turbine Operating on a Pure Gas and on a Double-Phase Flow with DZ where $x_c = 8$ and 38 mm; $\pi_T = 1.7$.

concentration of the liquid phase remains practically unchanged (however, due to an increase in losses with an equalization of the flow behind the exit edges of the nozzle blades, the value of η_T somewhat decreases).

On the corpus of the turbine in the region of the axial clearance and behind the working wheel there were a number of drainage openings. The liquid phase, having precipitated onto the peripheral/125 wall of the flow section, fell into these openings and was conducted further through rubber tubes into special collectors. According to the amount of liquid flowing into the drainage openings, it was possible to judge the liquid consumption in the film on the peripheral wall and, consequently, even the degree of particle separation. Moreover, with the aid of special probes analogous to a Pitot tube, change in the concentration of the liquid phase in a cross section of the flow section was studied.

As might be expected, the studies showed that complete particle separation takes place on the nozzle blades. Complete separation of secondary particles was accomplished where $x_c = 40-45$ mm. This agrees

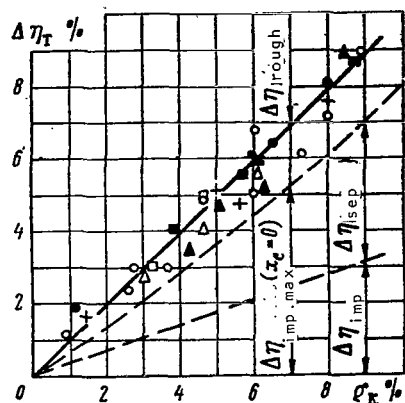


Fig. 68. Decrease in Turbine Efficiency as a Function of Concentration of the Liquid Phase Where $u/c_{ad} = 0.52$ and $\pi_T = 1.7-2.2$.

Conventional						
Signs	●	□	△	▲	○	+
x_c in mm	13	18	28	38	48	58

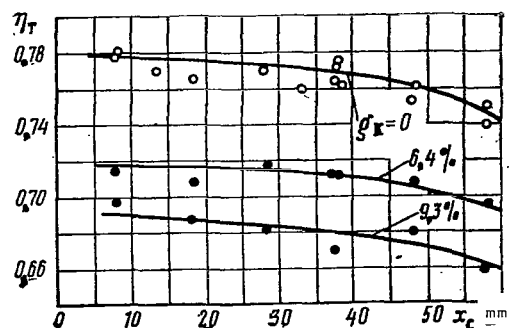


Fig. 69. Efficiency of a Turbine Operating on a Pure Gas and on a Double-Phase Flow as a Function of the Size of Axial Clearance Where $\pi_T = 1.7-2.2$ and $u/c_{ad} = 0.52$.

well with the calculated value of separating clearance $x_c = 44$ mm.

Thus with angles $\alpha_1 \leq 20^\circ$ the size of the separating clearance does not exceed the height of the working blade. For small size turbines with a blade height $h_b \leq 25$ mm, achieving such an axial clearance does not cause difficulties in construction and can be recommended for complete separation of the liquid phase in front of the working wheel. In large turbines with a blade height greater than 200 mm, it is possible to substantially decrease erosion by means of increasing the axial clearance to $0.2-0.3 h_b$. As indicated, with such a size of axial clearance, particle velocity increases significantly, which leads to a substantial decrease in the force of their impact on the working blades. /126

Results of investigations of the same turbine on a double-phase flow with water as the liquid phase agree satisfactorily with experimental results given for a double-phase flow with DZ diesel fuel.

§4. Operation of a Birotative Turbine on a Double-Phase Flow

As indicated above, the working blades of a turbine, even with a very viscous liquid phase, remain almost clean. The liquid precipitating on the working blade is scattered to the periphery by

centrifugal forces, the value of which is several orders greater than the tangential gas forces attracting the film in an axial direction. Therefore, in a birotative turbine operating on a double-phase flow both blade apparatuses (i.e., the rotating nozzle and working wheel) remain clean, and the increase in losses due to roughness of the film in the grids will be minimal. In a birotative turbine even the losses due to impact of the liquid phase on the working wheels characteristic of the usual turbine are absent, and, consequently, erosional wear of working blades is also absent.

With operation on double-phase flows with a constant concentration of phases a rotating nozzle apparatus may be used as a separator cleaning the flow in front of all subsequent stages (Fig. 70).

Let us consider the conditions of complete particle separation on the rotating grid. Here it is possible to assume that particles larger than 20 μm in diameter move with rectilinear trajectories in the blade apparatus. We shall consider that a double-phase flow on entrance to the grid has an axial direction; thus particle velocity is equal to the gas velocity.

From the velocity triangle (Fig. 71) $\tan\beta_1 = \frac{c_0}{u}$, where c_0 is the flow velocity in front of the grid.

So that particles moving with a relative velocity w_0 near the convex part of blade I fall on the concave part of blade II, the following relationship between the geometrical parameters of the grid must be maintained:

$$\tan\beta_1 \leq \frac{b}{l \sin\gamma - t},$$

where b and t are the width and spacing of the grid; l is the profile chord; γ is the angle of profile arrangement. /127

Comparing the right-hand sides of the two latter expressions, we obtain the condition for total separation of particles with diameters $d > 20 \mu\text{m}$ on the rotating turbine grid:

$$\frac{u}{c_0} \leq \frac{\sin\gamma - t/l}{\cos\gamma}. \quad (172)$$

Analysis of this formula indicates that for complete particle separation the stage must be slow moving. This lowers the level of stresses in the blades operating under elevated temperatures. Here, even with circumferential rotation velocities $u = 20 - 50 \text{ m/sec}$ and diameter of the flow section of the turbine $D \sim 1 \text{ m}$, the value of centrifugal forces acting on the film [$F_{cf} = 2\rho_K (u^2/D)$] will exceed the force of gravity of the liquid by 100-500 times and will exceed the tangential forces of gas friction, attracting the film in a tangential direction, by approximately the same factor.

Under the action of such great centrifugal forces the film will be intensively scattered to the periphery; its thickness on the blades and consequently even the value of Δn_{rough} will be minimal.

In order to arrange conduction of the liquid from the flow section of the turbine it is possible to apply a band seal on the blades (cf. Fig. 70). The low level of circumferential velocities allows one to use a band even with a very high gas temperature. Under the action of centrifugal forces, the liquid phase flows along the conical surface of the band and is spattered into the slit collector; analogous construction is used for collecting condensate in vapor turbines. Moreover, the band seal arrangement decreases leakage in the radial clearance, which may be significant in a rotating nozzle apparatus.

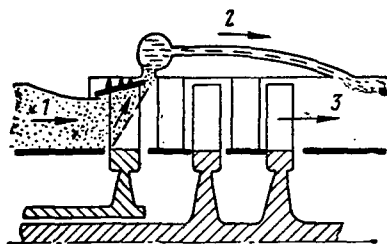


Fig. 70. Schematic Drawing of a Turbine with a Preincluded Slow-Speed Separating Stage: (1) Double-Phase Flow; (2) Liquid Phase; (3) Pure Gas.

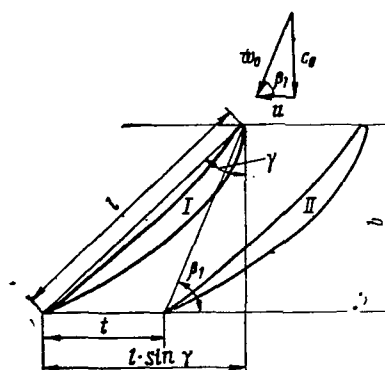


Fig. 71. Determination of the Conditions of Complete Particle Separation on the First Wheel of a Birotative Turbine.

In a slow-speed turbine stage losses due to separation of the liquid phase are also negligibly small. These losses, equal to /128 the losses due to impact of the liquid phase on the blades of the rotating first wheel, can be calculated according to formula (157). For slow speeds of rotation the value of u/c_{ad} does not exceed 0.15. Therefore, even with significant concentration of particles ($g > 15\%$) the value of Δn_{imp} will be negligibly small.

The slow speed of rotation of the separating stage is explained by the low power of this stage. This power may be used for driving an auxiliary system or transmitted to the basic axle of the engine.

Such a construction is promising for high temperature gas turbines operating on the combustion products of powdered coal fuel containing particles of liquid slag. Due to the great viscosity of the slag and, consequently, even an increase in profile losses, the

efficiency of the normal turbine may drop 8-15%. Moreover, intensive blade erosion due to the elevated erosional characteristics of the slag will take place in it. The efficiency and reliability of operation of the construction under consideration are evidently maintained at a high level.

Particles precipitate on the blades of the first low-speed wheel with small relative velocities and, usually, uniformly along the entire blade surface. Therefore, it is possible to expect that blade erosion will not take place here.

Experimental Study of a Birotative Turbine on a Double-Phase Flow

A birotative two-stage turbine without immobile controlling apparatus was studied using a mixture of cold air and water particles scattered by pneumatic nozzles. The mean particle diameter was 30-35 μm . The basic parameters of the turbine are shown in Table 5.

The power of both wheels was consumed by hydraulic brakes; the number of wheel revolutions could be related to one another. In conducting the experiments, special attention was given comparing the efficiency of the turbine in cases of a fixed (usual scheme) and rotating first wheel. Typical characteristics of a turbine with a fixed and rotating first wheel operating on clean air and on a double-phase flow with various concentrations of phases are shown on Figure 52. Along the abscissa is plotted the value

$$\left(\frac{u}{c_{ad}}\right)_{\Sigma} = \frac{\sqrt{u_1^2 + u_2^2}}{c_{ad}},$$

where u_1 and u_2 are circumferential velocities on the mean diameter of the first and second wheel, respectively. Plotted along the ordinate is the value of the power efficiency of the turbine (with regard to losses in the bearings) /129

$$\eta_r = \frac{2(N_1 + N_2)}{Grc_{ad}^2},$$

where N_1 and N_2 are measured powers of the first and second wheel, respectively. The turbine was studied on revolutions of $n_1 = 0$, 2500 and 3500 rpm with $\pi_T = 1.6$ and on revolutions of $n_1 = 0$, 3500 and 4500 rpm where $\pi_T = 2.2$.

In Figure 73 points are plotted characterizing the decrease in turbine efficiency as a function of concentration of the liquid phase with various revolutions of the first wheel and with $(u/c_{ad})_{\Sigma} = 0.5$. The upper curve relates to a turbine with a fixed first wheel.

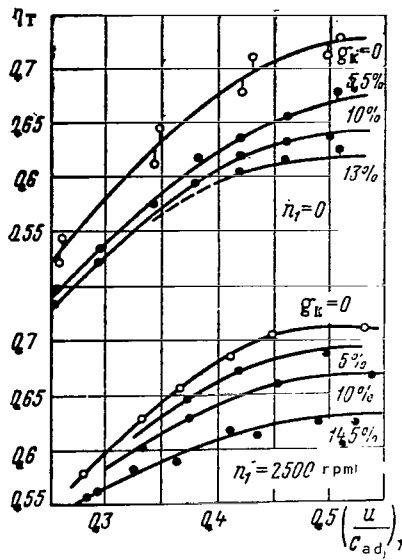


Fig. 72. Characteristics of a Birotative Turbine with a Brake and a Rotating First Wheel Operating on Air and on a Double-Phase Mixture with Water Particles: $\pi_T = 1.6$.

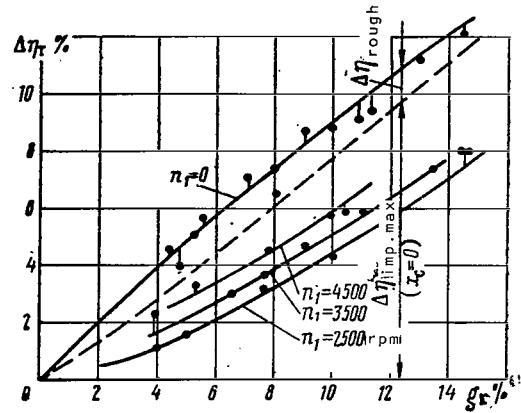


Fig. 73. Decrease in the Power Efficiency of a Birotative Turbine with an Inhibited and a Rotating First Wheel as a Function of Concentration of the Liquid Phase. $\pi_T = 1.6-2.2$; $(u/c_{ad})_\Sigma = 0.5$.

As is apparent from the graph, in this case the decrease in turbine efficiency as a function of the concentration of the liquid phase is almost rectilinear. In addition, a 1% increase in the relative concentration of particles decreases turbine efficiency approximately 0.9%. This agrees well with published data concerning a decrease in the efficiency of turbines operating on moist water vapor. /130

Change in $\Delta\eta_{imp, max}$ and losses from the roughness of the film $\Delta\eta_{rough}$ are shown in the same figure. It is apparent from the graph that $\Delta\eta_{rough}$ weakly depends upon the relative concentration of the liquid phase and for a liquid of such low viscosity as water is involved to a small degree in all supplementary losses.

The lower curves refer to the case of operation with a rotating first wheel. With the same concentrations of liquid, the decrease in turbine efficiency proved to be less than with a braked wheel. Where $n_1 = 2500$ rpm in the regions of low concentrations of the liquid phase ($g_K < 4\%$) the decrease in efficiency of a birotative turbine does not exceed 1%.

In the turbines studied with minimal revolutions of the first

TABLE 5. BASIC PARAMETERS OF AN EXPERIMENTAL BIROTATIVE TURBINE*

Item	Amount	Item	Amount
Mean Diameter of the Wheel D_m in m	0.225	Angle of Flow Revolution θ :	
Height of Blades h_b in mm	45	1st Wheel	22°10'
Ratio D_m/h_b	5	2nd Wheel	130°10'
Angle β_1 :		Number of Blades z :	
1st Wheel	135°50'	1st Wheel	27
2nd Wheel	48°50'	2nd Wheel	55
Angle β_2 :		Initial Temperature T_0^* in °K	290
1st Wheel	22°	Degree of Pressure Lowering $\pi_T = P_0^*/P$	2.2-1.6
2nd Wheel	28°	Axial Clearance x_c in mm	15
		Air Consumption G_T in kg/sec	6-4

* Law of Turbine Shaping $c_u r = \text{const}$

wheel, the value of u_1/c_{ad} varied within the limits of 0.10-0.15; therefore, even with the concentration $g_K = 14-15\%$, the maximum decrease in efficiency of the first wheel did not exceed 2%. The dependence of the power efficiency of the first wheel η_{T1} upon the ratio u_1/c_{ad} with $\pi_T = 1.6-2.2$ is given in Figure 74. The value

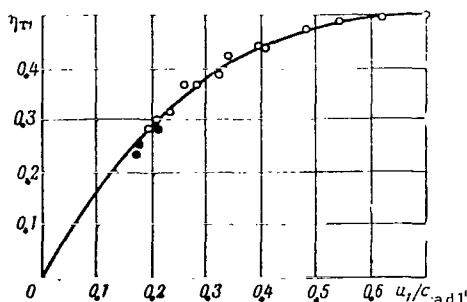


Fig. 74. Dependence of Power Efficiency of the First Stage Upon u_1/c_{ad1} with $\pi_T = 1.6-2.2$: O = Pure Air; ● = Double-Phase Flow (Water) with $g_K = 5-14\%$.

of η_{T1} is calculated according to the formula $\eta_{T1} = \frac{N1}{H_{ad1}}$ where H_{ad1} is the adiabatic thermal gradient in the first wheel. /131

Experimental points characterizing the operation of the stage on a double-phase flow are sufficiently close to the curve for pure air. This confirms the highly efficient consumption of the first (low-speed) wheel of a birotative turbine operating on a double-phase flow.

With an increase in the number of revolutions of the first wheel, losses due to separation of the liquid will increase. Moreover, on this wheel not all of the

liquid phase separates since the condition in (172) has not yet been fulfilled. Actually, in the turbines studied the angle of glade arrangement in the first stage was $\gamma = 60^\circ$ and the relative pitch $t/l = 0.6$. Therefore, according to (172) for complete separation on the first wheel it is necessary that

$$\frac{u_1}{c_0} \leq \frac{\sin \gamma - t/l}{\cos \gamma} \approx 0.5.$$

The axial velocity upon entrance to the turbine c_0 is approximately equal to 70 m/sec where $\pi_T = 2.2$ and 66 m/sec for $\pi_T = 1.6$. In the case where $n_1 = 2500$ rpm, the ratio $u_1/c_0 = 0.44$; where $n_1 = 3500$ rpm the ratio $u_1/c_0 = 0.58$ and where $n_1 = 4500$ rpm $u_1/c_0 = 0.75$. Thus, where $n_1 > 3000$ rpm part of the liquid phase passes through the blades of the first wheel and precipitates on the blades of the second wheel. Since the number of revolutions of the second wheel is significantly greater than that of the first ($n_2 = 12,000$ – $17,000$ rpm), losses due to impact are higher in it than in the first wheel. With additional increase in the number of revolutions of the first wheel a still greater portion of the liquid phase will precipitate on the blades of the second wheel, and the total losses in the turbine will increase.

Where $n_1 = 2500$ – 3500 rpm, the major portion of the liquid phase is separated on the first wheel, since the flow through the second wheel has a low concentration of the liquid phase.

The characteristics of the second wheel operating on pure air and on the double-phase flow ($n_1 = 2500$ rpm) are presented in Figure 75. As is apparent from the graph, with the concentration of particles at 5%, the efficiency of the second stage is almost identical to the efficiency of the stage operating on pure air. With greater concentrations of the liquid phase, losses in the wheel begin to increase rapidly. Thus, with the concentration $g_K = 14.5\%$ losses total 11.5% (the lower curve). Such an increase in losses

can be explained by the fact that with elevated consumptions of the liquid phase ($g_K > 8\%$) the radial clearance above the second wheel is filled with a viscous liquid, inhibiting wheel rotation.

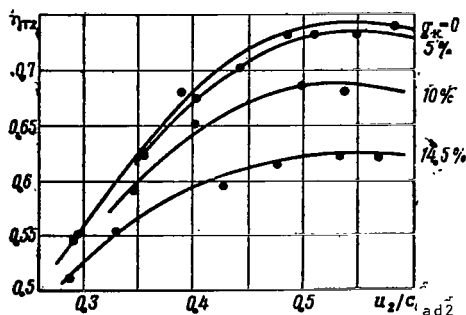


Fig. 75.(left) Dependence of Efficiency of the Second Stage upon u_2/c_{ad2} with Operation on Air and on a Double-Phase Flow; $n_1 = 2500$ rpm, $\pi_T = 1.6$.

§5. Turbine Operation on a Double-Phase Flow with Solid Particles

In practice there are cases of turbines operating on double-phase flows with solid particles. For example, a gas turbine included in the gudri technological oil refinery system operates on hot gases ($t_r = 550-600^\circ\text{C}$) with a significant content of porcelain particles used as a catalyzer. Solid particles are contained in the combustion products of liquid or solid fuel with the addition of aluminum, magnesium, etc. Finally, a large number of solid particles may be contained in the products of petroleum combustion containing ash and of coal fuel. The melting point of several chemical compounds found in the combustion products of various fuels is given in Table 6.

TABLE 6.

Substance	$t_{\text{melt}}^\circ\text{C}$	Substance	$t_{\text{melt}}^\circ\text{C}$	Substance	$t_{\text{melt}}^\circ\text{C}$
MgO	2500	Fe ₂ O ₃	1565	N ₂ O·V ₂ O ₅	630
CaO	2572	SiO ₂	1480	B ₂ O ₃	580
Al ₂ O ₃	2050	Na ₂ SO ₄	880	Na ₂ S ₂ O ₇	400
V ₂ O ₃	1970	V ₂ O ₅	680		

1. Turbine Operation on a Double-Phase with "Sticky" Particles

As is apparent from Table 6, several substances may be found in the flow parts of the turbine in a "sticky" state near the softening temperature. Such a state is most unfavorable for turbine operation, since particles precipitating on the walls of the flow section are not carried away by the flow, as are liquid particles, but form solid deposits. Even with an initial concentration of such particles in the flow of less than 0.1%, deposits on the blades quickly increase, leading to an abrupt deterioration of turbine efficiency. /133

Thus, according to reference [43], a gas turbine on the Wengau Power Plant in Switzerland, operating on the combustion products of heavy masut where $t_r = 650^\circ\text{C}$, must be washed with water for 20 hours after every 300-400 hours of operation in order to remove the ash deposits. In the turbine of the Parsons firm using an analogous fuel, efficiency dropped to almost zero 10 hours after operation began.

A growth of deposits of small "sticky" ash particles ($d < 10 \mu\text{m}$)

having a minimum kinetic energy is especially intensive. Large particles ($d > 20 \mu\text{m}$) having an elevated kinetic energy, precipitating on a surface, knock the previously formed deposits of ash off, and in a sufficiently large concentration in the flow, deposits may be substantially decreased. With dimensions of "sticky" particles of $d > 30 \mu\text{m}$ or with an elevated concentration of them, erosional wear of the surfaces undergoing impacts may take place.

In order to ensure prolonged efficiency of such turbines, the nozzle apparatus is protected by water vapor; also periodic washing of the flow part by water sprayed into the flow is used, which leads to a destruction of deposits and their being carried away by the gas flow; the addition of Si, Al, Mg etc. to the fuel, elevating the temperature of the softening point of the ash, may also be used. It is also expedient to use additives to lower the melting temperature of the ash, which will be carried away from the flow part in a liquid state, since deposits will not increase.

2. Turbine Operation on a Double-Phase Flow with Particles not Forming Deposits

From the experience in operating turbines on double-phase flows with solid particles not forming deposits, it is known that the basic difficulty is the struggle with erosional wear of the flow portion elements by the suspended particles. Basically the nozzle blades erode in the region of the intake edge and on the concave side; the working blades are also subject to wear, but to a significantly smaller degree (Fig. 76).

The distribution of particle concentrations in front of the turbine greatly depends upon the shape and dimensions of the conducting conduit, the presence of bends in it, stagnant zones, etc. In particular, along the conduit wall, especially in its lower portion, fly-ash may move slowly with a very high particle concentration. Therefore, nozzle blade wear will be very nonuniform along the circumference: in addition to intensively eroded blades (in the zone with increased concentration of particles), in the same ring there may be blades completely untouched by erosion. Due to the rotation of the working blades there is usually uniform wear along the circumference. /134

In nozzle apparatus an intensive separation of particles more than $15 \mu\text{m}$ in size takes place on the convex blade surface. Usually, at the entrance to the nozzle apparatus the flow velocity equals 150-200 m/sec. In nozzle apparatus the flow and particle velocities increase; therefore, with particle impact on the concave surface their velocity may reach 200-300 m/sec. In contrast to liquid drops, after impact on the surface solid particles bounce approximately according to the laws of elastic body collisions. At the moment of impact a particle may be destroyed.

A particle which has bounced from the surface of the blade

after impact maintains a high initial velocity of motion; moreover, it may acquire a whirling of up to $n = 10^4 - 10^6$ rpm.⁷

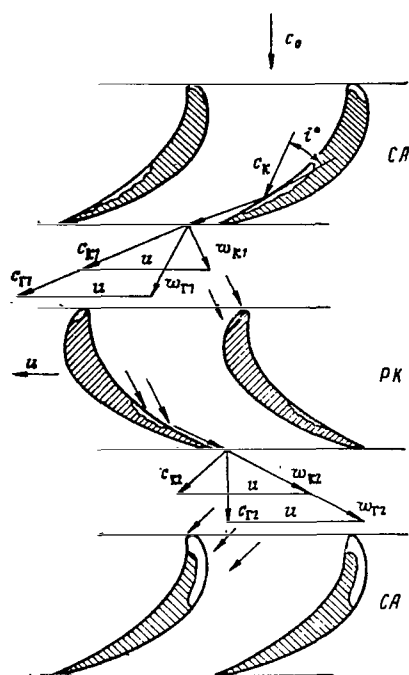


Fig. 76. Flow of a Double-Phase Mixture with Solid Particles in the Flow Section of a Multi-Stage Turbine (Zones of Erosional Wear of Blades are Noted).

Following stage with a negative angle of attack, which leads to characteristic erosional wear of their intake edges.

From a comparison of the velocity triangles shown in Figure 76, it is apparent that losses due to particle impact on the working blades are small. If the circumferential components of particle velocity in the working wheel decrease, then the particles will perform useful work.

Thus, if the particles are solid and do not form deposits, there is no source of great supplementary losses in the turbine; therefore,

⁷The rotation of a particle being blown about by a gas may lead to the appearance of a supplementary lateral force acting on the particle in the direction from the concave to the convex surface of the interblade conduit. This force may distort the trajectory of particle motion (author's note).

In a cross sectional area and in the axial clearance the particle velocity continues to increase, so that on entrance to the working blades it is usually near the gas velocity, especially where $d < 10 \mu\text{m}$. /135 Therefore, in the working conduits particles impact under small negative angles of attack which leads to insignificant wear of the intake edges and the concave surface of the working blades (cf. Fig. 76). With an increase in particle size their lag behind the gas and, consequently, even the angle of attack, increase; wear of the intake edge at the same time begins to predominate over the wear of the concave blade surface. With a particle diameter $d < 5 \mu\text{m}$ almost no blade erosion is observed.

In the majority of cases, particles maintained a high circumferential velocity component even upon exit from the working blade. Therefore, they impact upon the nozzle blades of the

its efficiency is maintained at a high level until a substantial change in the shape of the conduits and the clean state of the nozzle surface in working blades takes place due to erosion. With a concentration of particles $g_K < 5\%$, it is possible to ignore all other losses from the double-phase nature of the flow; i.e., those due to particle acceleration and their impact on immobile surfaces, those due to gas friction on the particles, etc.

3. Erosional Wear of the Flow Section Elements of a Turbine by Solid Particles

Erosion of the flow section elements depends upon the concentration and abrasive characteristics of the particles. Solid particles with a crystalline structure (such as Al_2O_3 or SiO_2) cause especially intensive wear. Moreover, erosion to a significant degree is a function of distribution of particle concentration in the cross sectional area. For example, in multi-stage turbines operating on a double-phase flow with a small content of solid particles ($g_K < 1\%$), often intensive erosional wear of the nozzle apparatus at intermediate stages is observed on the external diameter. The first stages and, in a number of cases, even the final stages are not eroded. This is explained by the fact that due to the intensive particle separation in the first stages their local concentration in the peripheral sections of the intermediate stages increases. In the final stages, erosion may be significantly decreased due to particle break-up in the preceding stages.

In one of the turbines studied by the author, the flow portion /136
of which is depicted on Figure 77, an intensive erosion of the exit

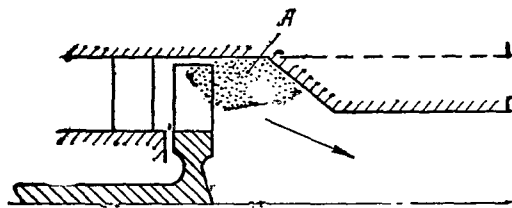


Fig. 77. Erosion of the Exit Edges of the Blades in a Turbine with an Improperly Constructed Exit Section. (The Dotted Line Indicates the Changed Exit Section).

edges of working blades was observed on the periphery. The turbine operated on a double-phase flow with a very small content of liquid particles on a regime $u/c_{ad} = 0.3$. Such erosion may be explained by the improper construction of the exit section of the turbine. Actually, due to significant whirling of the flow upon exit from the turbine, a large quantity of the liquid phase rapidly accumulated in cavity A. Only very small particles could overcome the influence of centrifugal forces and fly out with the gas flow into the exhaust pipe. The liquid phase, rotating in cavity A under the action of the whirling of the flow in a direction opposite the rotation of the working blade,

led to erosion of the exit edges and also to significant losses in turbine power. After a change in construction of the exit section (it was made purely axial without a bend, erosion ceased completely.)

An analogous phenomenon was observed by V. T. Mitrochin and A. I. Loskariv [33] in centripetal turbines. The radial clearance between the nozzle and working blades in such turbines is converted into a unique trap for particles, where they rapidly accumulate in a large number. Only the very smallest particles, for which the aerodynamic influence of the gas flow in the case defined by Stokes' law is greater than the centrifugal force acting upon them, are carried by the flow from the region of radial clearance into the working wheel and further into the exhaust pipe.

A suspended phase capable of being attracted by the gas (or vapor) is rotated in the radial clearance and, according to the observations of A. I. Loskariv, may cause erosional wear of both the nozzle and the working blades. The working blades overtake the particle and scatter it to the nozzle blades. With a small angle α_1 , a particle which has struck a nozzle blade remains in the radial clearance; in this case, mainly the nozzle blades are eroded; their exit edges may even be bent in the direction of rotation (Fig. 78a). With large angles α_1 , particles rebounding from the nozzle blades at a high relative velocity w_K impact against the working blades; here even the working blades are intensively eroded and their exit edges may be bent against the rotation (Fig. 78b). /137

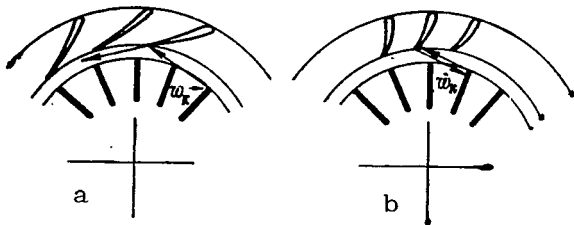


Fig. 78. Schematic Drawing of Particle Motion in a Centripetal Stage: (a) with Small Angles α_1 ; (b) with Large Angles α_1 .

In a centripetal turbine intensive erosion takes place even in the case of liquid particles. A liquid film having formed in the clearance impacts the exit edges of the nozzle blades and causes their erosion. Therefore, operating centripetal turbine on double-phase flows is inexpedient.

According to reference [40], erosional wear of the surface takes place primarily under the action of two factors: mechanical scratching activity of the sharp faces of a particle at the moment of impact, and thermochemical influence of the surrounding medium and of the particle itself on the metallic surface in the contact zone. Actually, due to contact stresses arising upon impact of a particle against a surface at a high velocity, heating and plastic deformation of the surface layer of the material and the particle may take place. Moreover, the temperature of the metal in the contact zone may exceed its melting point, so that liquid particles of the metal spin off the surface and burn in the hot gas flow, usually containing a large amount of oxygen.

This is confirmed by the surface glow, observed in reference [40], on a model subjected to a stream of high velocity ash particles. A bright yellow glow started at the moment the ash particles began to

be supplied and became more intense with an increase in flow velocity. After the appearance of erosional depressions on the model, the glow increased. Temperature measurement of the surface layer of metal by a microthermocouple, riveted flush to the surface of the model having a temperature around 480°C , confirmed the possibility of surface heating by particle impact. At the moment when the ash supply began the temperature increased abruptly by several tens of degrees ($\Delta t < 87^{\circ}\text{C}$). Certainly, a certain average temperature of the surface was measured here, since the contact zone between the particles and the surface was significantly smaller than the dimensions of the thermocouple.

In the same paper it was shown that the rate of erosional wear, to a significant degree, depends upon the angle of particle impact. As indicated in the graphs (Fig. 79) obtained in reference [40], maximum surface wear takes place when it is blown upon by particles under an angle of $i = 30-35^{\circ}$; here the amount of wear was measured in grams of metal per kg of ash (curves in the figure represent rounded off experimental points). At angles less than 15° and greater than 60° , the rate of erosional wear decreases more than twice. In the experimental process the temperature of the gas and of the steel model containing 5% nickel equalled 530, 590 and 650°C .

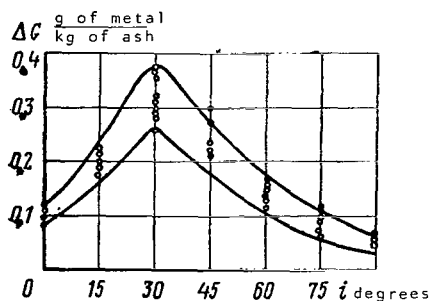


Fig. 79. Model Wear as a Function of the Angle of Impact by Ash Particles on its Surface.

A decrease in wear with angles $i < 20$ is explained by the decrease in the component force of impact normal to the surface of the model; this is the force pressing a cutting face of the particle to the surface, thus decreasing the depth of cutting and the thickness of the removed chip. Moreover, with small angles the number of particles striking a surface unit decreases significantly. On the other hand, with angles $i > 45^{\circ}$ particles cut deep into the surface of the metal so that slippage and, consequently, even removing a chip

become impossible. Under the action of particle impact the surface is distorted only by plastic deformation and the thermochemical influence of the surrounding medium. Also, particle break-up at the moment of impact evidently leads to a decrease in wear. Only at angles close to 30° do both the indicated factors (cutting [scratching] by sharp facets of particles; thermochemical influence of the medium and of the particles; and, consequently, even the velocity of erosional wear) attain maximum values.

In the same study a dependence of the rate of erosional wear on particle size (Fig. 80) was discovered. Maximum wear of a surface struck by ash particles under an angle $i = 30^{\circ}$ with velocities near the speed of sound (in gas phase) were observed with a particle size

of 35-40 μm . Decrease in wear with a decrease in particle size can be explained by the fact that their trajectories in the boundary layer deviate from straight lines, and the particles impact against the surface of the model under significantly smaller angles. With limited sizes, the small particles ($d < 5 \mu\text{m}$) do not at all reach the surface of the model. /139

Very large particles are not accelerated by the gas and impact against the surface at relatively low velocities. Moreover, as a rule large particles have a more friable structure and are several times less hard than monolith particles of average and small dimensions. Therefore, upon impact against a surface large particles are easily destroyed and their erosional influence decreases.

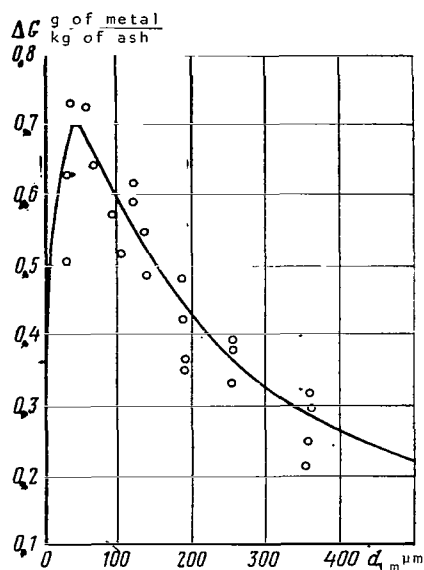


Fig. 80. Wear of a Model as a Function of Ash Particle Size.

The dust-gas mixture with particles of average dimensions formed after the destruction of large particles may have greater erosional characteristics than the original mixture. Actually, with secondary utilization of particles collected in a cyclone after being blown against the model, erosional wear of the surface increased substantially. Therefore, while in the original mixture large particles are maintained, maximum erosion may be observed in the intermediate stages of multistage turbines. Due to repeated particle break-up in the first stages, erosion of the latter stages may be substantially decreased.

Data presented in Figure 80 depends upon the experimental conditions and only qualitatively characterize the phenomenon under consideration. Under natural conditions, erosion of the flow portion elements of a turbine will, to a significant degree, be determined by the specific characteristics of the kinematics of the mixture flow in the spatial immobile and rotating blade apparatus, i.e., by the influence of particle separation in the blade apparatus under the effect of centrifugal forces; particle separation in a radial direction under the effect of the whirling of the flow between the blade rims; the shape, dimensions, structure and characteristics of particles; boundary layers on the internal and external surfaces of the flow section; secondary flows at points where flow interruption is possible in the zone of vapor vortices and in the zone of contractions between stages; finally, by the influence of the conditions of particle formation in the combustion chamber, of conduction of the double-phase /140

mixture to the turbine, etc.

In addition to the hardening of materials (which may not always provide a positive effect), in order to decrease the erosional wear of the flow section elements of an axial turbine by solid particles it is especially important to remove factors which lead to an increase in local particle concentration. For a multi-stage turbine

it is very expedient to effect preliminary particle separation in the expanded axial clearance of the first stage (Fig. 81). A mixture with an elevated concentration of particles formed in the peripheral sections, after cleaning in a separator, may be let into the subsequent stage or into the exhaust pipe from the turbine.

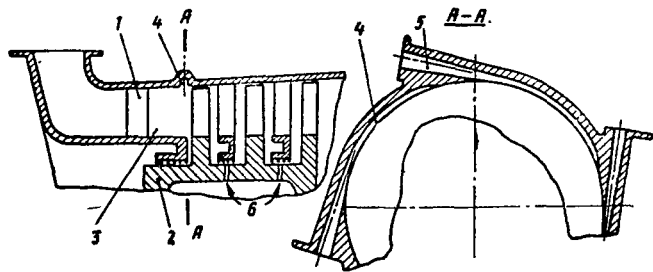


Fig. 81. Schematic Drawing of a Multi-Step Turbine with a Separating Space: (1) Nozzle Apparatus of the First Stage; (2) Rotor; (3) Separating Space; (4) Spiral Conveyor for Removing the Separated Phase; (5) Exit Nozzle; (6) Air Conductor to the Seals Between Stages.

It may prove expedient to select some of the working fluid from the zones with elevated particle concentration; for example, from the peripheral sections of a spiral conveyor in the case when a snail conveyor is used to conduct gas to the turbine.

4. Turbine Operation on Powdered Coal Fuel

The creation of powerful gas turbine installations using solid coal dust fuel has an important national economic significance. Such gas turbine installations may be used in combined operations with steam turbine installations, as independent power installations in mountain power plants, as well as for power plants in dry regions, and for driving locomotives.

Considering that the necessary resource of stationary gas turbine installations must reach 50-100 thousand hours and more, the decisive problem is the struggle with erosional injury to flow section elements of the turbine by ash particles. Let us consider the basic results of experimental use of such turbines presented in reference [38].

/141

A four-stage locomotive turbine was operated on combustion products of powdered coal fuel for 26,000 hours. After this period, intensive erosion of the working blades of the second and subsequent stages were noted near the crankshaft and the region of the exit edges (approximately 25-30% of the cross section of the blade). The flow section of the turbine and a schematic drawing of the erosional wear are given in Figure 82a. Such wear of the working blades was caused by ash particles in the gas blowing through the seals between

the stages. Actually, the velocity of the flowing gas and, consequently, the particles contained in it substantially differ from the velocity of the basic gas flow upon entrance into the working blades. Therefore, near the crankshaft the particles fall on the working blades at a large angle of attack and cause erosion of their surface. Erosion of the middle part of the nozzle and working blades was insignificant, since the particles of ash were small and easily attracted by the gas flow.

Particles present in the boundary layers on the internal and external surfaces of the flow section may also cause erosion of the nozzle and working blades. This is explained that by the fact that due to losses caused by friction of the gas on walls and the breaking action of particles during their mechanical interaction with the wall, the particle velocity in the layers near the walls may substantially differ from the velocity of the basic gas flow both in size and direction.

/142

In 1963, experiments were performed on an analogous 5-stage turbine, modernized with the aim of decreasing its erosional wear. A schematic drawing of this turbine is presented in Figure 82b.

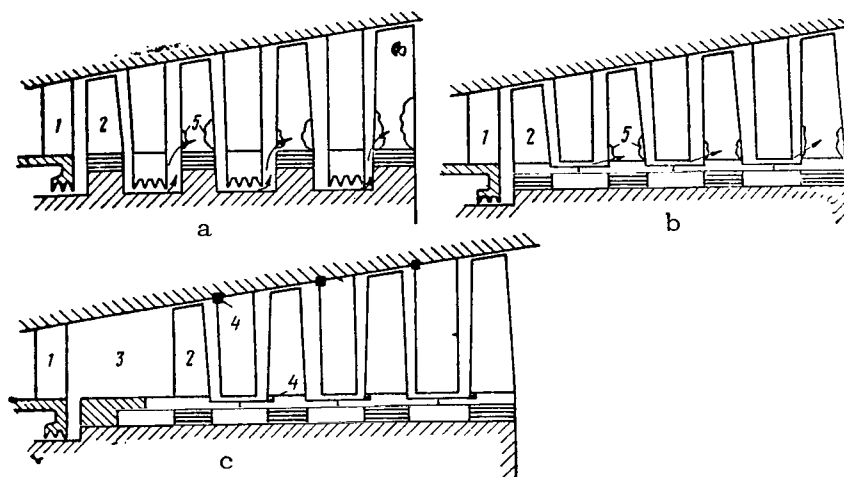


Fig. 82. Schematic Drawing of the Flow Section of a Gas Turbine Installation Operating on Powdered Coal Fuel: (a) Original Variant; (b) Improved Variant; (c) Final Variant: (1) Nozzle Blades; (2) Working Blades; (3) Separating Space; (4) Inserts of Titanium Carbide; (5) Zones of Erosional Wear.

In contrast to the preceding construction, the diameter of the seal of the nozzle apparatus at the intermediate stages was chosen to be maximally large. However, after 1100 hours of operation, erosion to a depth of 2-3 mm was discovered on the exit edges of the working blades near the crankshaft. As before, erosion was caused by particles contained in the gas flowing through the seal.

In an additional development, the axial clearance between the nozzle and working blades of the first stage increased approximately to the height of the working blades (Fig. 82c). This was done in order to separate the particles in the peripheral zones of the flow section, since wear on the peripheral sections of the nozzle and working blades is less dangerous than wear on the crankshaft sections. Moreover, by the crankshaft of the working blades and on the tails of the nozzle blades protective inserts of titanium carbide were made; they were approximately 9 times more wear-resistant than the chromium cobalt alloy X40 from which nozzle and working blades were made.

The indicated construction changes allowed a substantial decrease in erosional wear; however, as before it was inadmissible. During turbine operation the concentration of ash in the flow did not exceed 0.28 g/m^3 . The composition of the ash was the following: 19.2% Fe_2O_3 ; 21.5% Al_2O_3 ; 38.4% SiO_2 ; 7.3% CaO ; 1.6% MgO ; the rest was Na_2O , K_2O , TiO_2 and SO_3 . The softening point of the ash was 1225°C , the melting point 1244°C . Such high melting and softening temperatures are explained by the high content of refractory oxides in the ash. Particle distribution based on sizes is given in Table 7.

TABLE 7

Measuring Points	Total Weight in % of Particles Greater Than $1 \mu\text{m}$ in Size						
	20	15	10	7	5	3	2
On Entrance to the Turbine	3.16	7.33	20.6	36.6	54.6	81.2	100
After the 5th Stage	0.99	2.51	6.2	13.3	27	65	100

The turbine had the following parameters: gas temperature at intake $t_{\text{r}} = 645\text{--}675^\circ\text{C}$; gas temperature at exit $t_{\text{T}} = 400^\circ\text{C}$; gas pressure at intake $0.4 \cdot 10^6 \text{ n/m}^2$; number of revolutions $n = 5200$ /143 rpm; power developed $N_{\text{T}} = 9350 \text{ kW}$ (usable power, transmitted to the generator equal approximately 1500 kW).

From the table it is apparent that particles were significantly pulverized in the flow section of the turbine. Thus, while upon entering the turbine the size of around 80% of the particles was $d < 10 \mu\text{m}$, after the final stage there was already around 94% of such particles.

Despite the high average softening temperature of the ash, its easily melted components were progressively deposited on the nozzle blades of the first stage. In several cases, the deposit covered the flow section so extensively that in an attempt to clear the gas turbine installation, the compressor began to stall. Deposits on the nozzle blades of the final stages were insignificant and were

located basically on the spines and between the blade shafts. On the working blades there were no deposits.

As must be expected, due to particle separation and the increased axial clearance of the first stage erosion was observed primarily in the peripheral sections of the nozzle blades (except for the first stage); as before, erosion was insignificant at the base of the working blade. In order to decrease nozzle blade erosion in the future, it was proposed that some of the gas with an elevated particle content be allowed to flow from the peripheral region of the separating space behind the turbines.

In order to decrease erosion of the base section of the working blade, evidently it is very expedient to provide cooling air into the fields between the stages, as was shown above in Figure 81. This eliminates overflow of the double-phase mixture between the stages and creates a boundary layer on the walls with a decreased particle content. Moreover, the temperature conditions are improved for disk operation and for working blades in base sections subject to the greatest stress.

CHAPTER 4

THE OPERATION OF AXISYMMETRICAL NOZZLES AND TURBINES ON MOIST VAPOR

The flow of moist vapors in the flow section of a jet engine or a turbine engine is usually accompanied by both equilibrium and nonequilibrium phase shifts. This makes the problem of investigation still more complicated in comparison with the flow of double-phase mixtures with a constant phase concentration considered above. Until recently, calculation of the flow of moist vapors were generally based on thermodynamic theories. However, in the majority of cases the results of calculations were not confirmed by experimental studies, which indicated that a purely thermodynamic method was not suited to studying the flow of a moist vapor. /144

Actually, thermodynamic equations have no variable such as time. In other words, all processes in thermodynamics are considered as infinitely slow and equilibrium. It is natural that processes, characterized by very rapid changes in parameters according to time, may proceed according to other laws, whereupon it is impossible to establish these laws within the framework of thermodynamic theories.

As an example we shall mention that the supersonic flows of moist water and mercury vapors, in the majority of cases, are accompanied by supercooling and discontinuities in condensation; intensive precipitation of the condensate takes place and the vapor attains a state close to equilibrium. The possibility for the appearance of supercooling and the nature of the supercooling and discontinuities in condensation (the dependences of the partial vapor pressure upon the curvature of the liquid surface) are established from the thermodynamic dependences for moist vapor. However, development of the supercooling process and the discontinuities themselves are determined by diffusion of vapor molecules to the surface of an embryonic drop, by elimination of condensation heat escaping on its surface and by relative motion of drops and vapor; i.e., by processes which to a significant degree depend upon time.

Since the expansion of moist vapor in a supersonic nozzle continues for several milliseconds, the influence of these processes may be decisive. It is natural that, in order to describe these processes, it is necessary to introduce the methods of molecular physics, gas kinetics, hydrodynamics, etc. /145

However, it is apparent from the given example that thermodynamic methods continue to play an important role in the study of such flow. Nevertheless, several characteristics of the flow (for example, available work of the moist vapor and the parameters of its state after a discontinuity in condensation) are determined

with the aid of thermodynamic methods.

It is also necessary to bear in mind that, as a rule, all experimental studies were carried out on moist water vapor at low temperatures not exceeding 150-200°C, at which the coefficient of diffusion is relatively small; the coefficient of surface tension of the liquid, on the other hand, has elevated values. This does not exclude the possibility that in nozzles of powerful jet engines using Al + O₂, Mg + O₂, B + O₂, Li + Ft and other components as a fuel, due to the very high temperature of the working fluid and lowered gradients of the flow velocity along the nozzle as well as to the possible intensive contamination of the vapors by various particles, the condensation process is approximately equilibrium.

§1. Several Thermodynamic Relationships With Moist Vapor

As is known [9], for a saturable vapor above the flat surface of a liquid there is a dependence between its pressure and temperature definable by the Clausius-Calpeyron formula:

$$\frac{dp}{dT} = \frac{r}{T(v_n - v_k)}. \quad (173)$$

In a region removed from the critical point it is possible to ignore the specific volume of condensate v_k , which is small in comparison with the specific volume of the vapor phase v_n ; moreover, the state of a dry saturable vapor may be expressed by the equation

$$pv_n = R_n T. \quad (174)$$

In this case equation (173) will be written as:

$$\frac{dp}{p} = \frac{rdT}{R_n T^2}.$$

Assuming the heat of vapor formation to be constant ($r = \text{const}$) or a linear function of the temperature ($r = a - bT$), we obtain a clear dependence of vapor pressure upon temperature. For example, in the case of $r = \text{const}$, integration of the last equation gives

$$p \cdot \exp\left(\frac{r}{R_n T}\right) = \text{const}; \quad (175)$$

in the case where $r = a - bT$

/146

$$pT^{b/R_n} \exp\left(\frac{a}{R_n T}\right) = \text{const}. \quad (176)$$

The specific volume of the moist vapor $v = v_{\Pi}x + v_K(1 - x)$, where x is the degree of dryness of the vapor.

If we ignore the volume of the condensate, then

$$v = v_{\Pi}x. \quad (177)$$

The equation for consumption of moist vapor is

$$G = Fc_{\Pi} \text{ or } G_{\Pi} = Fc_{\Pi}. \quad (178)$$

Let an equilibrium adiabatic expansion of the vapor from the dry saturated state take place. In the expansion process some of the vapor is condensed. The equilibrium degree of dryness of the vapor is determined from the condition of the entropy constant in the expansion process

$$S = S_K(T) + c_{pK} \ln \frac{T_0}{T} + \frac{r_0}{T_0} = S_K(T) + \frac{r}{T} x = \text{const},$$

where $S_K(T)$ is the entropy of the condensate with a temperature T ; T_0 , r_0 are the temperature and heat of vapor formation in the dry saturated state at the beginning of expansion. Hence,

$$x = \frac{T}{T_0} \frac{r_0}{r} + \frac{T c_{pK}}{r} \ln \frac{T_0}{T}. \quad (179)$$

The energy equation for moist vapor is:

$$i_0 + \frac{c_0^2}{2} = i + x \frac{c_{\Pi}^2}{2} + (1-x) \frac{c_K^2}{2},$$

where $i_0 = i_K(T) + \int_T^{T_0} c_{pK} dT + r_0$ is the enthalpy of the vapor at the beginning of expansion;

$i = i_K(T) + xr$ is the enthalpy of the moist vapor;

$i_K(T)$ is the enthalpy of the condensate with temperature T ;

c_{pK} is the thermal capacity of the condensate along the left boundary curve.

Assuming $c_{pK} = c_{pK} = \text{const}$ and ignoring the particle lag behind the vapor flow (since the diameter of the particles in the condensate usually does not exceed several microns), this equation may be rewritten in the following form:

$$H = (c_p T_0 + r_0) \left(1 - \frac{T}{T_0}\right) - T c_p \ln \frac{T_0}{T} = \frac{c^2 - c_0^2}{2}, \quad (180)$$

where $H = i_0 - i$.

Let us consider the conditions necessary for the appearance of /147 condensation in the vapor flow. In the majority of cases, condensation begins on the embryonic drops. It is known that the saturated vapor pressure above a free liquid surface varies with the shape of the surface. For spherical drops, the diameter of which exceeds 10^{-9} m, the following relationship obtained from Laplace's formula is correct:

$$\frac{p}{p_\infty} = \exp \left(\frac{4\sigma}{\rho_k R_n T d} \right), \quad (181)$$

where p_∞ is the saturated vapor pressure above a flat liquid surface with a temperature T .

The ratio p/p_∞ is usually called the degree of supersaturation. From the equation is apparent that the saturated vapor pressure above a liquid droplet is greater than the saturated vapor pressure above a flat surface with the same temperature. With the given drop size, the degree of supersaturation is usually great in a region removed from the critical point. On the other hand, in the case of an approximation of the parameters of the vapor to the critical its temperature increases and the coefficient of surface tension of the liquid decreases; therefore the degree of supersaturation decreases. At the critical point $\sigma = 0$ and $p/p_\infty = 1$; however, at this point the distinction between vapor and liquid vanishes.

Thus, for vapor condensation on the surface of a liquid drop a certain supersaturation of vapor is always required. With a decrease in drop diameter the degree of supersaturation necessary rapidly increases. As an example, values of the degree of supersaturation p/p_∞ for water and mercury where $p \approx 0.1 \cdot 10^6$ m/m² depending upon drop diameter are presented in Table 8.

According to formulas (175) and (176) obtained for the flat surface of a condensate, with an increase in the saturated vapor pressure, its temperature also increases. A higher temperature T_∞

would correspond to the vapor pressure p at which its condensation begins on the surface of a given size drop above the surface of the condensate than that temperature at which condensation takes place in reality. Therefore, the actual state of the vapor

TABLE 8

Liquid	Degree of Supersaturation of Vapor P/P_∞ with Drop Diameter in m		
	10^{-7}	10^{-8}	10^{-9}
Water	1.02	1.22	7.4
Mercury	1.09	2.3	4000

at the moment of condensation on a drop may be considered as "supercooled" in relation to the equilibrium temperature T_{∞} above the flat surface of the condensate with the same pressure p . The difference between this equilibrium temperature and the actual temperature

$$\Delta T = T_{\infty} - T \quad (182)$$

is called the degree of vapor supercooling. Formula (181) was transformed by Ya. I. Frenkel to /148

$$\frac{T_{\infty}}{T} = \exp\left(\frac{4\sigma}{\rho_K r d}\right). \quad (183)$$

Then with a small degree of supercooling

$$\Delta T = \frac{4\sigma}{\rho_K r d}. \quad (184)$$

The values of the degree of supercooling ΔT for water and mercury with $p \approx 0.1 \cdot 10^6$ n/m² are presented in Table 9.

A supersaturated or supercooled vapor state is unstable and may exist for only a limited time. Condensation developing on individual very large drops as well as on the vessel walls in time returns the vapor to the equilibrium state.

Between a supercooled and dry saturated (and even superheated) vapor there are no fundamental qualitative differences, since the

TABLE 9

Liquids	Degree of Supercooling of the Vapor ΔT in °K with Drop Diameter in m		
	10 ⁻⁷	10 ⁻⁸	10 ⁻⁹
Water	0	5	39
Mercury	4	30	350

characteristics of these vapor states do not appear with internal molecular or hydrodynamic processes in the vapor, but only with their interaction with the external medium in relation to the vapor phase (for example, with the vessel surface or a particle of condensate). Actually, the same vapor may be simultaneously considered supercooled in

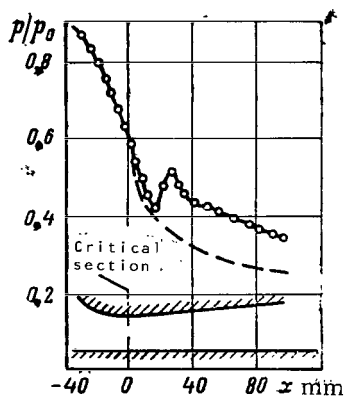
relation to the flat surface of the condensate, saturated in relation to a particle whose size satisfies equation (181), and superheated in relation to a particle of smaller size. Certainly, with an increase in supercooling in relation to the flat surface of a condensate the rate of embryonic drops formation increases; however, in view of their very small total mass the influence of this factor on the characteristics of the vapor phase evidently is insignificant.

The size of a liquid drop satisfying equation (181) is called critical. If with a given degree of supersaturation the diameter of a liquid drop is less than critical, i.e., the vapor pressure above the surface of the drop is less than the pressure of the saturated vapor above the surface, then the drop evaporates. Condensation is possible only on drops whose diameter exceeds the critical diameter (when the vapor pressure is equal to or greater than the pressure of the saturated vapor above the surface of the drop).

Embryonic drops forming with expansion of the saturated vapor have an arbitrary diameter. Conservation and further growth are possible only for the largest drops, the diameter of which exceeds the critical diameter. Smaller drops prove to be unstable in relation to the vapor and rapidly evaporate.

/149

Thus, the formation of embryonic drops larger than the critical size is a necessary condition for the beginning of condensation.



This same condition may be formulated somewhat differently: with a given average dimension of embryonic drop formation condensation is possible only with a degree of supersaturation which exceeds the values determined by formula (181). As the dimension of embryonic drops does not usually exceed 10^{-9} m, the degree of supersaturation of the vapor necessary for the beginning of condensation may be very high. Conditions for the development and the course of condensation and also discontinuities in condensation are considered below.

§2. The Exhaust of a Moist Vapor from a Supersonic Nozzle

As was already noted, almost all experimental studies of moist vapor exhaust are related to water vapor. According to the data in [16, 61], water vapor exhaust takes place with a great degree of supercooling and

Fig. 83. Static Pressure Distribution Along a Nozzle During Exhaust of a Saturated Water Vapor: $M_{calc} = 1.6$; $P_0 = 0.1 \cdot 10^6$ n/m²; $t_0 = 102^\circ\text{C}$; ----- Change in the Relative Pressure where $k = 1.3$.

with discontinuities in condensation in the supersonic part of the nozzle. A discontinuity in condensation is accompanied by a discontinuity in compression; therefore it would be more accurate to call it discontinuity in condensation compressions. The form and distribution of both discontinuities are uniform. In the majority of cases, indirect discontinuities are possible. The intensity of a discontinuity in compression accompanying a discontinuity in condensation is usually small since, after discontinuity, the velocity of the vapor remains supersonic. Figure 83 represents pressure distribution along a supersonic nozzle during saturated water vapor

exhaust with a discontinuity in condensation obtained in reference [49]. The dotted line on the graph corresponds to the calculated pressure distribution with the assumption that the vapor is expanded with complete supercooling and that the adiabatic index of supercooled vapor is $k_{\Pi} = 1.3$.

Let us consider the characteristics of vapor condensation in a flow and the conditions required for the appearance of discontinuities in condensation.

1. *Condensation in the Process of Adiabatic Exhaust of Moist Vapor from a Nozzle*

/150

In the majority of cases, industrial steam has a high frequency and is almost free of impurities and ionized dust particles, which may serve as condensation centers. Therefore, with expansion of vapor from a superheated state, condensation is possible only on embryonic droplets.

During the expansion process the vapor temperature drops and reaches the supercooled state corresponding, at least, to the beginning of condensation on present and newly-forming embryonic drops. It is necessary to note that condensation on the nozzle walls is impossible since the vapor temperature in the boundary layer is approximately equal to the temperature of a stagnant flow.

For an intensive development of condensation it is necessary, in the first place, that the number of embryonic drops be sufficiently large and, in the second place, that the rate of condensation not be significantly less than the rate of change in vapor parameters during its expansion process. Let us consider these conditions.

The rate of formation of embryonic drops with critical diameters in a moist vapor flow was studied for example, by Ya. I. Frenkel [53]. The formula obtained on the basis of the kinetic theory of liquids which Frenkel developed has the form

$$J = \frac{pN_A}{R_u T \mu_{(mo)} n_3} \left[\exp \left(- \frac{\pi \sigma d_{cr}^2}{3 k_B T} \right) \right] \frac{p d_{cr}^2}{2 k_B T} \sqrt{\frac{k_B T \ln p/p_{\infty}}{3 m_{mol}}} n_3, \quad (185)$$

where J is the number of drops forming per unit time in a unit volume of vapor;

N_A is the Avogadro number;
 μ_{md} is the molecular weight of the vapor;
 n_{emb} is the number of molecules in an embryonic drop;
 m_{mol} is the molecular mass;
 k_B is Boltzman's constant;
 d_{cr} is the critical diameter of an embryonic drop.

The formation of embryonic drops takes place as a result of

fluctuations with the chaotic heat motion of molecules. However, in a superheated vapor accumulations of molecules which are formed disperse rapidly; with a decrease in temperature and approximation of the vapor state to the saturation line, embryonic drops become more stable.

As a result of fluctuations, particles of various sizes are formed. However, with a small degree of supercooling only the largest drops, the size of which exceeds the critical, are "activated" (i.e., are transformed to a stable state in relation to the surrounding vapor so that vapor condensation may take place on their surface). The total number of such large drops in a vapor is small. According to equation (181) with an increase in the degree of supercooling the critical diameter of a drop decreases; therefore, a still greater number of embryonic drops is activated. /151

According to (185) the number of such activated embryonic drops very strongly depends upon the degree of vapor supercooling. If for saturated water vapor $J \approx 0$, with a degree of supercooling $\Delta T = 50^\circ\text{C}$ and a pressure $p \sim 0.1 \cdot 10^6 \text{ mm}^2$, then $J \sim 10^{27} \text{ sec}^{-1} \text{ m}^{-3}$. Certainly, the size of the majority of activated particles is very small and does not exceed 10^{-9} m . Therefore, the total amount of matter contained in the embryonic drops is small and composes a fraction of a percent of the "diagrammatic" moisture; i.e., that amount of condensate which would correspond to an equilibrium process.

According to equation (181), condensation on an activated embryonic drop must be developed in avalanche fashion, since with an increase in drop diameter the vapor pressure begins to substantially exceed saturated vapor pressure above its surface. However, with moist vapor expansion in a supersonic nozzle, this is not observed since the condensation rate is limited by the processes of diffusion of vapor molecules to the particle surface and elimination of the precipitating condensation heat.

Due to the small size of embryonic drops it is possible to ignore their lag behind the vapor, even with great supersonic flow rates, and to assume that condensation takes place on a drop which is immobile in relation to the vapor.

As is well known, the transfer processes depend upon the rarefaction of the gas (vapor) characterized by Knudsen's number:

$$\text{Kn} = \bar{l}/d, \quad (186)$$

where \bar{l} is the free path length of a molecule;

$$\bar{l} = \frac{\mu_n}{p} \sqrt{\frac{9\pi R_n T}{8}}. \quad (187)$$

Where $Kn < 0.001$ it is possible to consider the vapor as a solid medium to which the usual thermodynamic and hydrodynamic equations are applicable. Where $Kn > 10$ the vapor must be considered as a free molecular flow, and for calculations of condensation and heat exchange in it, it is necessary to use the equations for the kinetic theory of gases. The basic difference between exchange processes in extremely rarified media ($Kn > 10$) and processes in solvent media is the fact that there is discontinuity in temperatures and velocities on the surface being washed by such a medium.

A discontinuity in the surface temperature of a body is explained in the following way. Upon collision with a surface a molecule is either deflected or adheres to it for a certain time (is adsorbed). At this moment an energy exchange occurs between the surface and the molecules. A complete exchange is characterized by the accommodation /152 coefficient:

$$\gamma = \frac{T_0 - T_1}{T_0 - T_{sur}}, \quad (188)$$

where T_0 is the mean molecular temperature before precipitation on a surface;

T_1 is the mean molecular temperature after contact with the surface;

T_{sur} is the surface temperature.

For instantaneous mirror reflection of a molecule $\gamma = 0$; for a sufficiently prolonged duration of a molecule on the surface, significantly exceeding the period of molecular oscillations, $\gamma \rightarrow 1$. In the majority of cases $0 < \gamma < 1$.

Since it is possible to ignore molecular collisions near a surface, then even with a high value of the accommodation coefficient due to temperature differences between approaching and reflected molecules their mean temperature may substantially differ from the surface temperature. Even a discontinuity in the velocity (slipping) on the surface of a body in a rarified gas is explained in an analogous way.

As is apparent from equation (187) the free path length \bar{l} is essentially a function of pressure. For a water vapor with moderate temperatures and a pressure $p = (0.01 - 1) \cdot 10^6$ n/m², $\bar{l} = 10^{-6} - 10^{-8}$ m. Since the size of embryonic drops is $d = 10^{-8} - 10^{-9}$, then even with normal pressure $Kn = 1 - 1000$, since in relation to the embryonic drops the vapor may be considered to be intensively rarified.

The growth of drops in water vapor was considered, for example, in references [24] and [70]. Having equated the increase in mass of a drop to the mass of vapor molecules condensed on its surface,

it is possible to obtain the following differential equation for drop growth where $d \ll \bar{l}$:

$$\frac{d(\bar{d})}{d\tau} = \alpha_K \frac{Nm_{\text{mol}}}{\rho_K}, \quad (189)$$

where $N = \frac{p}{\sqrt{2\pi m_n k_B T}}$ is the number of molecules precipitating on a unit surface in a unit time;
 \bar{d} is the diameter of a drop (variable);
 α_K is the coefficient of condensation equal to the ratio of the number of molecules remaining in a drop to the number of molecules striking its surface.

The coefficient of condensation α_K is a function of the characteristics of the working fluid and the conditions of condensation, and it is possible to assume values from zero to one. For example, for water, according to the data of V.V. Shuleykin, $\alpha_K = 0.00067$ where $t = 0^\circ\text{C}$ and $\alpha_K = 0.31$ where $t = 200^\circ\text{C}$. If the release of heat, liberated upon condensation, is very small and the liquid begins to be heated, then the number of vaporising molecules increases. This leads to a retardation in drop growth. With a complete absence of heat release an active equilibrium is established in which the number of captured drops of molecules is equal to the number of evaporating molecules, and drop growth ceases. /153

Reference [70] introduces the following formula for drop growth rate, obtained from the conditions of heat exchange in rarified gases:

$$\frac{d\bar{d}}{d\tau} = \frac{3p}{8\rho_K} \sqrt{3 \frac{R_n}{T_n} (T_K - T_n)}. \quad (190)$$

The actual drop growth rate will be equal to the least of those definable according to formulas (189) and (190). Any calculations based on these formulas may have only a qualitative nature, since the conditions of condensation and the majority of physical constants (coefficients α_K , γ , σ , etc.) with the indicated sizes of embryonic drops are known with a very small degree of certainty. The slowest process, which consequently determines the rate of embryonic drop growth, is evidently the process of the release of condensation heat from the surface of the drop.

For large drops, for which $Kn < 10^{-3} (d \gg \bar{l})$, from the conditions of equality of condensation heat and heat transmitted into the surrounding medium by means of the heat conductivity of the vapor phase it is possible to obtain the following equation for the drop growth rate:

$$\frac{d\tilde{d}^3}{d\tau} = \frac{8\lambda_n}{\rho_{kr}} (T_k - T_n). \quad (191)$$

The surface temperatures of the drop T_K and of the vapor T_{II} may be evaluated in the following way. If during the process of adiabatic expansion of moist vapor pressure and temperature have attained such values which activate an embryonic drop and condensation has begun on its surface, then at the initial moment the temperature of drops may be assumed to be equal to the vapor temperature. With additional vapor expansion, the temperature continues to decrease approximately following adiabatic law:

$$\frac{p}{p_{cr}} = \left(\frac{T_n}{T_{cr}} \right)^{\frac{k}{k-1}}, \quad (192)$$

where p_{cr} and T_{cr} are the parameters of the vapor at the moment of embryonic drop activation.

Vapor expansion is accompanied by activated drop growth due to vapor condensation on its surface. The maximally possible temperature of a drop T_K will here correspond to the saturation temperature above the drop under variable conditions. From equation (181), written for an arbitrary moment of time and for the moment of activation, we obtain

/154

$$\frac{p}{p_{cr}} = \frac{p_{\infty}(T_k)}{p_{\infty}(T_{cr})} \exp \left[\frac{4\sigma}{\rho_k R_n} \left(\frac{1}{T_k d} - \frac{1}{T_{cr} d_{cr}} \right) \right]. \quad (193)$$

Equating the right-hand side of equations (192) and (193) and substituting the dependence of pressure above a flattened surface upon the temperature according to equation (176), we obtain the following relationship between the vapor temperature T_{II} and the maximally possible surface temperature of a particle T_K :

$$\left(\frac{T_{II}}{T_{cr}} \right)^{\frac{k}{k-1}} = \left(\frac{T_{cr}}{T_k} \right)^{b/R_n} \exp \left[\frac{a}{R_n T_{cr}} \left(1 - \frac{T_{cr}}{T_k} \right) + \frac{4\sigma}{\rho_k R_n} \left(\frac{1}{T_k d} - \frac{1}{T_{cr} d_{cr}} \right) \right]. \quad (194)$$

The temperature of the drop T_K and its size d enter the obtained equation. Therefore, in order to calculate the growth of drops and the condensation rate it is necessary to solve (190) and (191) together with (194).

Very approximate calculations of the condensation process of saturated water and mercury vapor with their exhaust from a supersonic nozzle show that the condensation rate is significantly less than the rate of change in temperature and pressure of the flow.

Actually, according to equation (183), supercooling of water

vapor even with $d = 10^{-9}$ m is approximately equal to 35-40°K. However, actual supercooling of vapor, observed in experiments, may exceed the indicated value of 1.5-2 times. According to the data of Osvatich [70], discontinuity in condensation with the exhaust of saturated water vapor from a Laval nozzle takes place with supercooling of $\Delta T = 60-65^\circ\text{K}$. According to the data of Stodola a discontinuity in condensation takes place with $\Delta T = 50^\circ\text{K}$. This indicates the fact that after supercooling sufficient to activate a majority of embryonic drops, condensation develops so slowly that supercooling of the vapor upon its expansion continues to rapidly increase.

It is necessary to note that a discontinuity in condensation in the Laval nozzle may arise even with supercooling of $\Delta T = 30-35^\circ\text{K}$. This refers to long nozzles. Evidently the structure and characteristics of the flow, such as its contamination by ionized particles, influence the amount of supercooling.

2. Appearance and Development of a Discontinuity in Condensation

/155

The conditions for the appearance of a discontinuity in condensation and the dependence of the moment it appears upon the flow parameters have been insufficiently studied at the present time. From numerous experiments on moist water vapor the following characteristics of discontinuity in condensation are known.

(1) Discontinuity in condensation arises only in the supersonic section of the nozzle and is accompanied by slight changes in compression, so that the velocity after a discontinuity in condensation usually remains supersonic.

(2) With an increase in the initial superheating and velocity gradient along the nozzle a discontinuity in condensation is displaced downward along the flow, i.e., towards greater M numbers of the flow.

(3) Discontinuities in condensation appear even when at the nozzle intake the vapor is moist, i.e., contains a large number of condensation centers in the form of droplets of the primary condensate. According to reference [16], in the case of small drops a discontinuity is displaced in comparison with the exhaust of saturated vapor down along the flow, and with large drops it is shifted upstream.

(4) In a discontinuity in condensation the vapor is almost transferred to an equilibrium state; however, its further expansion may take place with supercooling.

The rate of vapor condensation onto embryonic drops (insufficient, as was indicated, for an equilibrium condensation) may be noticeably increased in the case of particle lag behind the vapor

[34]. Such a disagreement in velocities arises with the passage of the mixture through a discontinuity in compression. With passage through discontinuity the number of condensation centers also may be substantially increased due to break-up of the largest embryonic drops by aerodynamic forces.

The appearance and development of discontinuity in compression in supersaturated vapor may be explained in the following way. In the exhaust process vapor condensation takes place on embryonic drops, due to which they increase in volume and begin to lag behind the vapor. In the supersonic section of the nozzle, vapor supersaturation becomes very significant, its density decreases, lag increases and the particles appear to "comb" the vapor. In addition, the condensation rate and, consequently, the amount of liberated heat increase. The heat supply with a supersonic gas flow leads to retardation of the flow; at the same time, the flow becomes less stable. Thus the thermodynamic nonuniformity of the flow is aggravated by its hydrodynamic instability due to liberation of the condensation heat. A subsequent process is of an avalanche nature. An ever-increasing perturbation becomes a slight change in condensation in which the velocity of the vapor phase is changed to its final value. Drops due to their inertia comb the front of the discontinuity; the number of condensation centers due to the break-up of large drops increases; nearly total precipitation of condensate takes place, and the vapor is almost transformed to an equilibrium state. /156

Thus, for the appearance and development of intensive condensation in a supersonic flow of supercooled vapor it is necessary for embryonic drops velocity relative to the vapor to be present; in a supersonic flow, this condition is satisfied only in the case of a discontinuity in compression, and therefore discontinuity in condensation and a discontinuity in compression are inseparably interconnected.

A discontinuity in condensation compression suggests a discontinuity in heat and usually has a low density. Nonetheless, the lack of agreement between particles and vapor velocities arising in a discontinuity and also an increase in the number of particles due to their break-up are completely sufficient for the development of intensive vapor condensation. The condensation heat serves as the basic cause for the appearance of a discontinuity in compression. The mutual accelerating influence of condensation heat liberation and the disagreement between phase velocities in a discontinuity in compression imparts an avalanche-like nature to the process.

Since in a subsonic flow of a supercooled vapor there are no discontinuities in compression, then discontinuities in condensation in a subsonic flow are improbable as well. This is confirmed even by the fact that to date not one investigator has succeeded in obtaining a discontinuity in condensation in the subsonic section of the nozzle.

The last comment does not apply to a flow of supercooled vapor in the subsonic blade grids of steam turbines. Actually, even with subsonic exhaust velocities with $\lambda \sim 0.85-0.9$ in the conduits the areas between the blades always have zones of local perisonic or supersonic vapor flows. It is only in these zones that discontinuities in condensation arise, caused by the same factors which were considered above. However, due to the great heterogeneity of the vapor flow in the turbine grids, the influence of intensively developed boundary layers, turbulence in the flow and other factors, a discontinuity of condensation may take place in the blade grids with significantly lower flow velocities than in supersonic axisymmetrical nozzles.

A discontinuity in condensation which has arisen in a supersonic flow zone is propagated even through the subsonic zones of the conduits between the blades; hence the particles (drops) of condensate which have arisen in the discontinuity penetrate into the subsonic flow zones with velocities different from the vapor velocity. Thus, even here, "combing" the vapor by condensate particles is observed. However, in subsonic flow the heat liberated upon condensation does not lead to the appearance of a discontinuity in compression. Therefore, condensation does not have such a clearly expressed avalanche nature, as in supersonic nozzles. On the other hand, the condensation zone in subsonic grids is very indefinite and, in the majority of cases, has a grid cross section and an axial clearance between the blade rims.

/157

According to a number of experimental studies [61], the condensation zone behind the nozzle apparatus of a turbine does not have a clear posterior border. The anterior border in which, as a rule, condensation arises near the convex surface of the blades, i.e., in the zone of local supersonic flow velocities (Fig. 84) is rather easily seen.

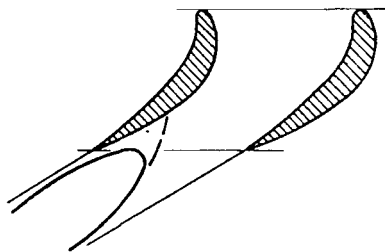


Fig. 84. A Discontinuity in Condensation Behind the Nozzle Apparatus in a Steam Turbine

It is necessary to note that gradual spontaneous condensation is possible in subsonic flows especially at low flow velocities or in vapor with suspended dust particles.

3. Moist Vapor Expansion After a Discontinuity in Condensation. The Influence of the Original Moisture on the Change in Condensation

As was indicated in [50], a system of sequential changes in condensation may be observed in supersonic nozzles with a very high degree of expansion: after the first discontinuity a second arises, etc. This indicates that the flow is nonequilibrium after the first change and is accompanied by supercooling, just as before the first discontinuity in condensation.

Such a process of moist vapor expansion may be explained in the following way. After the first discontinuity in condensation, the state of the moist vapor will be almost equilibrium. Particles of condensate, formed from embryonic drops during the discontinuity and on the order of 10^{-7} - 10^{-8} m in size, rapidly attain velocities near the vapor velocity after the discontinuity. With subsequent vapor expansion the condensation velocity is again limited by processes of molecular diffusion to a particle and by the release of condensation heat. Therefore, the vapor is transformed into the supersaturated state.

After the degree of supersaturation again attains the maximum value, a second discontinuity in condensation-compression arises, etc. In addition, condensation takes place on both particles of condensate formed in the preheating discontinuity and on new embryonic drops, formed with greater expansion in the interval between the first and second discontinuities.

The appearance of discontinuities in condensation with the expansion of moist vapor containing particles of condensate [16, 50, 61] in a nozzle may be explained analogously. In fact, if the particles of original condensate are very small (on the order of 10^{-6} - 10^{-8} m), then their lag behind the vapor is very small, and the supercooling processes and the appearance of a discontinuity in condensation proceed in a way similar to the case just examined /158 of vapor expansion between the first and second discontinuities in condensation compression. Hence partial vapor condensation takes place on the surface of primary drops in the expansion process; the degree of supercooling of the vapor drops somewhat. Therefore, the maximum degree of supercooling with which a discontinuity in condensation compression arises is reached with a greater geometrical degree of expansion; i.e., the discontinuity is displaced downward along the flow.

With large particles of primary condensate their number in the flow at the same degree of original moisture as in the preceding phase decreases in proportion to d^3 , and the total diffused flow to all particles of primary condensate decreases approximately in proportion to d^2 . Therefore, despite significant particle lag behind the flow, the vapor condensation rate remains low, and in the expansion process the vapor is transformed to a supercooled state.

It is also necessary to consider that condensation on the surface of a large drop is significantly impeded by the constant elevation of temperature of the drop above the vapor temperature in the expansion process; vapor temperature in the boundary layer around the particle also exceeds the temperature of the surrounding medium. Therefore, instead of condensation a partial evaporation of large particles may take place.

In a flow with a greatly dispersed initial moisture the appearance of a discontinuity in condensation-compression is evidently

facilitated by the heterogeneity of the flow and the presence of intensive small-scale turbulent pulsations arising with the gas flow around the particles. Therefore the maximum degree of expansion with which a discontinuity arises for large particles will prove to be less than for saturated vapor (i.e., a discontinuity is shifted upward along the flow).

§3. The Speed of Sound and Adiabatic Index for Moist Vapor

It is known that in a single-phase medium the adiabatic index k characterizes not only the dependence between thermodynamic parameters and an isentropic change of the state, but also several thermal and molecular characteristics of processes, and also the process of sound wave propagation. Therefore, it is possible to experimentally determine the adiabatic index by various methods; for example, by means of measuring the speed of sound or the heat capacity of the working fluid. Regardless of the method of determining the value of k , it is found to be single-valued for a single-phase flow.

For a double-phase flow, the cited universality of k does not develop, and this is valid even with constant compression of the phases. Actually, as follows from Chapter 1 the adiabatic index for the expansion process of the double-phase mixture, obtained experimentally, and the factor n in the subradical expression (33) may not agree with one another. /159

In a double-phase flow, experimental values of k also depend (apart from the method of determination and thermodynamic parameters of the working fluid) upon the rate of mixture expansion, dispersion and physical characteristics of particles. These dependences are still more complex for a moist vapor in which phase transitions, i.e., condensation and evaporation are possible. Therefore the different processes in a moist vapor may be characterized by different values of the adiabatic index.

1. The Speed of Sound in Moist Vapor

The propagation of sound in moist vapor is an exceptionally complex phenomenon since it is accompanied by a large number of mutually influencing complex physical processes: thermodynamic and hydrodynamic, molecular, acoustic, etc. The speed of sound in moist vapor has been studied in greatest detail with the aid of thermodynamic dependences. In references [26] and [54], other aspects of the problem under consideration were touched upon, in particular the influence on the speed of sound particle dispersion, scattering and absorption of sound by particles.

In the dissertation of Ye.V. Stekol'shchikov [46], among the most fundamental studies on this subject, an attempt was made to carry out a complex examination of the influence of the most impor-

tant factors on sound propagation in double-phase media; in particular, in moist vapor. In this study, wave equations for double-phase media with an arbitrary concentration of phases were obtained in the most general form. For a one-dimensional problem, Stekol'-shchikov introduced formulas characterizing the influence of the parameters of state, the structural-temporal parameters and others on the phase speed of sound, on the damping constant of sound and on other acoustic characteristics of double-phase mixtures.

In the same study, characteristics of experimental investigations of sound phenomena in double-phase mixtures were examined; it was shown that for similarity of wave processes in moist vapor it is necessary to have equations for 21 similarity criteria. This characterizes the exceptional complexity of the phenomenon and, in particular, indicates the practical impossibility of a more or less complete simulation of these processes. Moreover, agreement between even the basic similarity criteria and experimental studies conducted by different authors is improbable. Therefore, even the results of /160 investigations may differ substantially.

Moist vapor is a mixture of dry saturated vapor and particles of condensate with arbitrary diameters suspended in it. Therefore sound wave propagation in moist vapor will be largely analogous to sound propagation in a double-phase mixture with constant compression of phases examined in Chapter 1. However, beside the anomalies peculiar to such mixtures, in moist vapor the isentropic expansion-contraction process of the medium in a sound wave may be accompanied by phase transitions: precipitation and evaporation of the condensate.

Thus, the speed of sound in moist vapor is a function of the moisture, dispersion and thermophysical characteristics of the vapor and the condensate, as well as of the nature of the change in state of the dry saturated vapor in a sound wave.

The speed of sound in moist vapor may most simply be determined only in several limiting cases; for example, with a thermodynamic equilibrium process of sound propagation, with a totally nonequilibrium process or with a partial nonequilibrium process.

In the majority of cases, the degree of nonequilibrium of a sound wave propagation process is not precisely known. However, it is possible to assume that conditions approximating it to a thermodynamic equilibrium process do not correspond to equilibrium conditions of a unilaterally-directed intensive expansion process in a nozzle. Evidently, in certain cases the periodicity of the sound wave propagation process may substantially decrease thermodynamic nonequilibrium.

Let us consider thermodynamic equilibrium sound propagation in moist vapor [39, 52]. Taking into account that in a region sufficiently removed from the critical point it is possible to assume $\rho =$

$\frac{p}{R_p T x}$, we obtain

$$dp = \frac{R_n T x dp - R_n T p dx - R_n p x dT}{(R_n T x)^2}. \quad (195)$$

Since with isentropic expansion of moist vapor its degree of dryness is determined by formula (179), then

$$dx = \left(\frac{x}{T} - \frac{c_{p\kappa}}{r} - \frac{x}{r} \frac{dr}{dT} \right) dT. \quad (196)$$

Using expressions for dp and dx along with the retransformed equation (173) for dp it is possible to determine the equilibrium speed of sound in moist vapor

$$a_p = \sqrt{\frac{dp}{d\rho}} = \sqrt{\frac{x R_n T}{1 - \frac{R_n T}{r} \left[2 - \frac{T}{r} \left(\frac{c_{p\kappa}}{x} + \frac{dr}{dT} \right) \right]}}. \quad (197)$$

This expression with regard to the equation for an elementary /161 isentropic process $dp/d\rho = k(p/\rho)$ may be transformed to

$$a_{eq} = \sqrt{k_{eq} \frac{p}{\rho}} = \sqrt{k_{eq} x R_n T}, \quad (198)$$

where k_{eq} is the adiabatic index of a thermodynamic equilibrium adiabatic expansion of moist vapor

$$k_{eq} = \frac{1}{1 - \frac{R_n T}{r} \left[2 - \frac{T}{r} \left(\frac{c_{p\kappa}}{x} + \frac{dr}{dT} \right) \right]}. \quad (199)$$

Having set $x = 1$, we obtain the following formulas for an equilibrium speed of sound and adiabatic index in saturated vapor at low temperatures:

$$a_{eq} = \sqrt{k_{eq} R_n T}, \quad (200)$$

$$k_{eq} = \frac{1}{1 - \frac{R_n T}{r} \left[2 - \frac{T}{r} \left(c_{p\kappa} + \frac{dr}{dT} \right) \right]}. \quad (201)$$

From (198) it is apparent that with an invariable temperature of the moist vapor, the equilibrium speed of sound decreases with a decrease in the degree of dryness of the vapor x . As in Chapter

1, this may be explained by the increase in the oscillating mass with the preservation of the elastic characteristics of the medium, determined by the characteristics of the dry saturated vapor.

If the size of condensate particles is so large that the particles do not participate in sound oscillations and the heat exchange between the phases in a sound wave may be ignored, then, regardless of the original degree of vapor moisture, the speed of sound propagation in it will be equal to the speed of sound in a dry saturated vapor.

In the study of V.V. Sychev [52], a more precise formula for determining the adiabatic index of an equilibrium expansion in the region of moist vapor is presented:

$$k_{eq} = - \frac{v}{p} \left(\frac{\partial p}{\partial v} \right)_s = - \frac{v_{\Pi} x + v_{\kappa} (1-x)}{p \left[\left(\frac{\partial v}{\partial p} \right)_s^{\Pi} x + \left(\frac{\partial v}{\partial p} \right)_s^{\kappa} (1-x) \right]} \quad (202)$$

where v_{Π} , v_{κ} are specific volumes of dry saturated vapor and condensate at a given temperature;

$\left(\frac{\partial v}{\partial p} \right)_s^{\Pi}$, $\left(\frac{\partial v}{\partial p} \right)_s^{\kappa}$ are values of the partial derivatives of specific

volume according to pressure in the process $S = \text{const}$, taken for a working fluid near the right and left branches of a boundary curve in a double-phase region. This formula is valid even for temperatures near the critical. The values entering it are equal:

/162

$$\left(\frac{\partial v}{\partial p} \right)_s^{\Pi} = - \frac{c_v^{\Pi}}{T} \left(\frac{dT}{dp} \right)^2; \quad \left(\frac{\partial v}{\partial p} \right)_s^{\kappa} = \frac{c_v^{\kappa}}{T} \left(\frac{dT}{dp} \right)^2.$$

Figure 85 represents the nomogram given in reference [52] for determining the adiabatic index of an equilibrium expansion in the region of moist water vapor. The values of k_{eq} calculated according to formula (202) using the precise values of heat capacities c_v^{Π} and c_v^{κ} which obtain for water. At low temperatures the values of k_{eq} correspond with those calculated according to formula (199). The values of k_{Π} and k_{eq} for water vapor near the saturation line taken from the side of superheated and moist vapor are presented in Table 10. According to the data of this table it is possible to determine a discontinuity in the adiabatic index of an equilibrium expansion with a transition from the region of superheated vapor to the region of moist vapor. This discontinuity is caused by the appearance of phase transitions in the moist vapor.

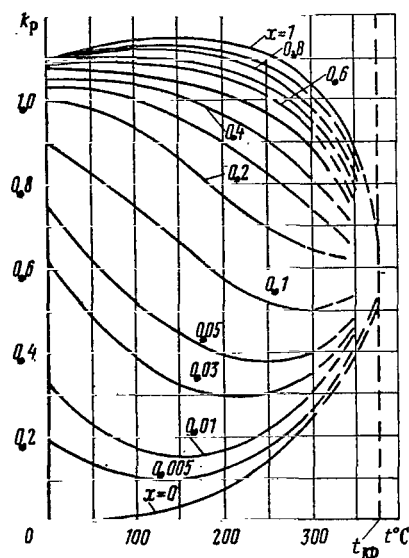


Fig. 85. The Adiabatic Index of an Equilibrium Expansion of Moist Water Vapor as a Function of Temperature (According to Data Given in [52]).

It is necessary to note that in actuality [46] a change in the adiabatic index k , the heat capacity c_v , the speed of sound and other parameters at the time of transition through the boundary curves takes place not by discontinuity but gradually, i.e., on a certain terminal portion of a change in any of the thermodynamic parameters of vapor (T , P , x etc.).

TABLE 10

t in °C	0	20	40	60	80	100	120	140	160
k_n	1.331	1.33	1.323	1.32	1.317	1.311	1.306	1.3	1.294
k_p	1.105	1.108	1.116	1.124	1.13	1.136	1.141	1.142	1.141

t in °C	120	200	220	240	260	280	300	320	340
k_n	1.288	1.284	1.279	1.27	1.262	1.253	1.243	1.22	—
k_p	1.14	1.135	1.126	1.114	1.096	1.072	1.04	0.9955	0.94

Let us now consider sound propagation in moist vapor in the case when the expansion-contraction process in a wave takes place with a complete supercooling of the vapor, i.e., without phase transitions in the sound waves. Considering the above-noted slight difference between supercooled vapor and saturated and superheated vapor at moderate temperatures, its equation of state may be considered in the form $p v_{II} = R_{II} T$, and the adiabatic index k may be assumed to be equal to the adiabatic index of superheated vapor k_{II} near the saturation line. Evidently the case under consideration will be analogous to the case of sound propagation in a double-phase mixture with constant compression of phases.

/163

If there is a large number of very small particles of condensate, (i.e., $c_K \equiv c_{II}$ and $T_K \equiv T_{II}$) in the vapor, then the speed of sound is

$$a = \sqrt{n x R_{II} T}. \quad (203)$$

Here

$$n = \frac{1 + \vartheta_n}{\frac{1}{k_n} + \vartheta_n}, \quad (204)$$

where $\vartheta_n = \frac{c_{p\kappa}(1-x)}{c_{p n^v}}$;

k_{Π} is the adiabatic index of superheated vapors near the saturation curve;

$c_{p\Pi}$ is the heat capacity of a superheated vapor at constant pressure near the saturation line.

In the case when a moist vapor contains only large particles, it is possible to assume that they do not participate in sound oscillations and that heat exchange between the phases in the sound waves is negligibly small, and the speed of sound in moist vapor will be equal to the speed of sound in superheated vapor:

$$a = \sqrt{k_{\Pi} R_{\Pi} T}. \quad (205)$$

An evaluation of the influence exerted by the size of primary condensate particles contained in the vapor on the degree of their increase by vapor, on heat exchange between particles and vapor in sound waves and, consequently, even on the value of the speed of sound in moist vapor, may be carried out according to the formulas in (37)-(41).

Let us consider several results of experimental determination of the speed of sound by several investigators. According to the careful studies of V.I. Avdonin and I.I. Novikov [1], conducted with a sound wave frequency $\nu = 500 - 1000$ Hz in a range of temperature variation from 50 to 250°C, the speed of sound in dry saturated vapor and the adiabatic index are equal to those presented in Table 11. /164

The values of k calculated according to the formula $k = a^2 / p v_{\Pi}$ are shown in Figure 86. The calculated values of k for water vapor near the saturation line, taken from superheated vapor and from a double-phase region according to data given in Table 10, are also plotted there. As is apparent from the graph, experimental values of k at low temperatures are approximately intermediate between the values of k_{Π} and k_{eq} . This indicates the existence of phase transition in the sound wave. With increase in the vapor temperature, experimental values approximate the values of k_{Π} for superheated vapor.

Investigations conducted in [62] on a dust mixture of air and saturated water, acetone and benzene vapors indicated that sound wave propagation at frequencies up to 200 Hz is accompanied by an intensive condensation and evaporation of drops so that all processes in a sound wave approximate an equilibrium process. It was noted in this study that phase transitions with a periodic expansion-contraction process proceed much more rapidly than with a single unilateral weak expansion or contraction of the mixture.

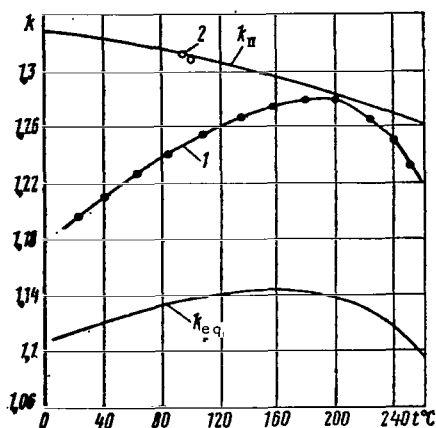


Fig. 86. The Adiabatic Index of Vapor as a Function of Temperature: k_{π} and k_{eq} are the Adiabatic Indices of an Equilibrium Expansion Near the Saturation Line, Taken from Superheated and Moist Vapor; (1) According to the Data from Measuring the Speed of Sound in [1]; (2) According to the Data from Measuring the Speed of Sound in [46].

with total supercooling and with phase transitions, approximating this process to a thermodynamic equilibrium process.

2. The Adiabatic Index of Moist Vapor Expansion in a Supersonic Nozzle

The value of the adiabatic index is determined by the flow structure and by physical phenomena taking place in the vapor. For the exhaust of a weakly superheated or a dry saturated vapor from a nozzle, it is necessary to distinguish at least two ranges of variation in value of k :

(1) Expansions from a superheated (dry saturated) state before the moment of activation of most embryonic drops. Since on this section supercooled vapor is not distinct from superheated vapor in physiological characteristics, the value of k may be accepted, as for superheated vapor, to be near a saturation curve; i.e., $k = k_{\pi}$ (cf. Table 10).

(2) Expansion from the moment of activation of most embryonic drops before discontinuity in condensation. On this section, due to the fact that vapor condensation has begun on embryonic drops, the adiabatic index k will differ from the value of k_{π} for super-

The speed of sound in saturated and moist vapor was also determined in reference [46]. With saturated vapor at 100°C, based on the data of this study the speed of sound proved to be equal to 471 m/sec.

TABLE 11

$t, ^\circ\text{C}$	a m/sec	k
50	425	1.22
100	460	1.23
150	488	1.27
200	505	1.28
250	495	1.23

The value of k corresponding to this /165 value of the speed of sound lay on the curve for superheated vapor (cf. Fig. 86); i.e., evidently in this case phase transitions were absent. An analogous result was obtained in reference [64].

The divergence of experimental data indicates that sound wave propagation in saturated and moist water vapor evidently may take both

heated vapor. The higher the rate of condensation the greater the difference will be. In this section, k for a supercooled vapor becomes less than k_{II} ; however, its value remains greater than the adiabatic index of a thermodynamic equilibrium expansion process k_{eq} ; in the opposite case, a discontinuity in condensation would not arise.

These hypotheses are confirmed by experimental data. For example, from Figure 83 it is apparent that pressure distribution along a nozzle, measured at a certain distance in front of the discontinuity, proves to be higher than the calculated distribution, given that $k = k_{II} = 1.3$. This signifies that the actual value of k on this section is less than 1.3.

In this case of moist vapor exhaust which has small particles of condensate at the beginning of expansion or in the case of vapor expansion between the first and second discontinuities in condensation, the adiabatic index will have the value $k_{eq} < k < k_{II}$. Experimental studies [16] confirm this fact. Actually, in the case of moist vapor exhaust the curve of pressure distribution along the nozzle is significantly higher than an analogous curve for superheated or dry saturated vapor.

Factors influencing the value of k may change substantially in /166 moist vapors and vapor-gas mixtures, the physical and thermodynamic parameters of which greatly differ from the parameters of water vapor. In particular, with an increase in temperature, chemical activity and contamination of vapor by impurities along with a decrease in the coefficient of surface tension and longitudinal velocity gradient in a nozzle, the possibility for significant supercooling of the vapor decreases.

§4. Coefficient of Moist Vapor Consumption

In determining moist vapor consumption one is usually confronted with a number of difficulties caused by the much more complex nature of its flow in comparison with the flow of the superheated vapor or an ideal gas. The decisive influences on moist vapor consumption, in addition to its thermodynamic and hydrodynamic parameters characterizing the flow as a whole, are the size of particles of primary condensate, the flow velocity gradient, the shape of the nozzle, etc.

Let us consider moist vapor consumption through a supersonic nozzle with the following assumptions, which have been experimentally confirmed for water vapor:

(1) The flow in the subsonic part of the nozzle takes place with supercooling, irrespective of the presence of primary condensate particles; a discontinuity in condensation occurs in the supersonic part of the nozzle.

(2) The characteristics of supercooled vapor (in particular, the adiabatic index k) with its expansion on the subsonic section of the nozzle are similar to those of superheated vapor near the saturation line. We shall ignore the influence of vapor condensation onto particles of primary condensate on the value k .

(3) During exhaust, the parameters of the vapor are far from critical, so that supercooled and dry saturated vapor satisfy the equation of state for ideal gases.

In this case, the following basic factors influence moist vapor consumption: supercooling of the vapor phase in the expansion process; mechanical and thermal interaction between vapor and particles of primary condensate; a possible change in losses in the boundary layer due to the influence of a liquid undulating film covering the nozzle walls; and clogging of the flow section of a conduit by liquid film.

The influence of the first two factors may be evaluated most simply only in the limiting cases of moist vapor exhaust with small particles when $c_K \equiv c_{II}$ and $T_K \equiv T_{II}$, or with large particles when $c_K \approx \text{const}$ and $T_K \approx \text{const}$.

In these cases and also with a thermodynamic equilibrium expansion vapor, consumption is determined by its parameters in a critical section corresponding to the throat of the nozzle.

By definition, the coefficient of consumption is

/167

$$\mu = \frac{G}{G_T}, \quad (206)$$

where G and G_T are the actual and theoretical mass consumption of vapor.

The theoretical consumption of an equilibrium expanding vapor in the critical section of a nozzle is

$$G_T = F_{cr} \frac{a_{cr}}{u_{cr}} = F_{cr} \sqrt{\frac{k_{eq} p_{cr}}{u_{cr}}}, \quad (207)$$

where $a_{cr} = \sqrt{k_{eq} p_{cr} v_{cr}}$ is the thermodynamically equilibrium speed of sound in moist vapor in the critical section; k_{eq} is the adiabatic index of a thermodynamic equilibrium expansion of moist vapor [cf. (199) or (202)].

Moist vapor consumption at the time of exhaust with supercooling of the vapor phase is determined:

in the case where $c_K \equiv c_{II}$ and $T_K \equiv T_{II}$ according to equation (59);

$$G = F_{cr} m_{cr}(n) \sqrt{\frac{p^*}{x_0 v_n^*}};$$

In the case where $c_K = \text{const}$ and $T_K = \text{const}$

$$G = F_{cr} \frac{m_{cr}(k_n)}{x_0} \sqrt{\frac{p^*}{v_n^*}},$$

where n is the polytropic index of supercooled vapor expansion given its temperature equilibrium with particles of primary condensate determined by (204);

p^* , v_n^* are total pressure and specific volume of the vapor phase according to damping parameters. For the limiting cases of flow under consideration p^* and v_n^* are univalently determined as a function of flow velocity.

The change in the coefficient of consumption $\mu_{dbl} = G/G_T$ for both cases of moist water vapor flow considered is shown in Figure 87. The basic parameters in the critical section in vapor consumption with a thermodynamic equilibrium flow are determined by means of a diagram of states from the adiabatic equation

$$H_{cr} = i_0 \rightarrow i_{cr} = \frac{a_{cr}^2}{2} = \frac{k_{eq} p_{cr} v_{cr}}{2},$$

where $i_0 = i_{0K} + x_0 r_0$ is the heat content of moist vapor at the nozzle inlet;

$i_{cr} = i_{crK} + x_{cr} r_{cr}$ is the heat content of vapor in the critical section;

/168

x_0 , x_{cr} indicate vapor moisture in initial and critical sections;

r_0 , r_{cr} represent heat vapor formation at the initial temperature and at the temperature in the critical section.

In Figure 87, the curve $x_0 = 1$ corresponds to the case of dry saturated vapor exhaust with supercooling. Values of the points on this curve exceed unity due to the increase in consumption of dry saturated vapor through a supersonic nozzle due only to supercooling. The increase in consumption of supercooled vapor in comparison with a uniformly expanding vapor is explained by the fact that the adiabatic index of supercooled vapor is greater than that of a thermodynamic equilibrium vapor.

As is apparent from the figure, with an increase in initial moisture with respect to small particles the value μ_{dbl} decreases. At the limit with a very large initial moisture when the influence

of heat exchange between the phases exceeds the influence of the difference between adiabatic indices of equilibrium expansion and expansion with complete supercooling, the coefficient of consumption $\mu_{dbl} \rightarrow 1$. Consequently, with a very great initial moisture

and small particles, vapor consumption will be approximately equal, regardless of whether expansion is accomplished uniformly or with supercooling.

/169

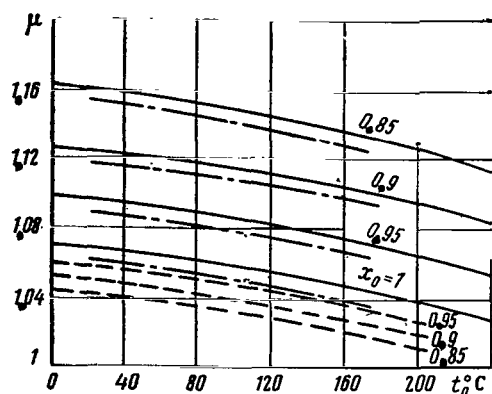


Fig. 87. Coefficient of Moist Water Vapor Consumption Through a Nozzle on Expansion of the Vapor Phase with Supercoolant; — $c = \text{const}$ and $T_K = \text{const}$ (Large Particles of Primary Condensate): - - - - $c_K \equiv c_{II}$ and $T_K \equiv T_{II}$ (Small Particles of Primary Condensate): - - - - - Exhaust with a Subsonic Ratio of Pressures $\pi = 0.6$ and the Absence of Interaction to the Phases.

approximate a thermodynamic equilibrium process since the above-given assumption of complete supercooling of the vapor phase on the subsonic section will not be satisfied.

It is also apparent from Figure 87 that due to the total influence of supercooling of the vapor phase and the mechanical and thermal interaction between the phases, moist water vapor consumption through a nozzle, calculated assuming complete flow equilibrium, will be significantly increased (from 3 - 15% where $x_0 \geq 0.85$).

The coefficient of moist vapor consumption for vapor phase expansion with supercooling and partial thermal and mechanical interaction between the vapor and particles of primary condensate may be calculated using the dependences introduced in Chapter 1.

Losses due to friction of the flow against the walls on the subsonic section of the nozzle decrease vapor consumption. According to experimental data presented in Chapter 2, a velocity coef-

On the other hand, in the case of large particles of primary condensate, with an increase in the initial degree of moisture the value of μ_{dbl} increases substantially. This is explained by the fact that due to the absence of interaction between the phases the vapor velocity in the critical section, and indeed, even the consumption of the vapor phase, will be maximum. Therefore, total moist vapor consumption will also be maximum (with a sufficiently high initial particle velocity, it is possible to ignore clogging of the critical section by particles).

It is necessary to bear in mind that with an elevated initial degree of moisture due to vapor condensation on particles, the vapor phase expansion process may

efficient in a subsonic nozzle for walls covered with a water film vary up to 2% in value where $(1 - x_0) \leq 0.2$. With moist vapor exhaust it is possible to assume the velocity coefficient on a subsonic section to be

$$\varphi_{film} = \varphi_n - k_c(0.05 - 0.15)(1 - x_0), \quad (208)$$

where $\phi_{II} = 0.96 - 0.98$ the velocity coefficient for the flow of a superheated vapor on the subsonic section of a nozzle; k_c - the coefficient of separation of primary condensate particles onto the walls of the nozzle. For large particles $k_c \approx 1 - F_{cr}/F_0$. In equation (208) the value 0.05 refers to short nozzles and liquids of low viscosity, and the value of 0.15 to long nozzles and viscous liquids.

The gas consumption given an exhaust with losses due to friction on the wall of the nozzle may be evaluated according to formula

$$G = m_{cr} F q(\varphi \lambda_{ad}) \frac{p^*}{\sqrt{RT^*}}.$$

Taking into account the influence of losses in the boundary layer the coefficient of consumption is /170

$$\mu_{fr} = \frac{G}{G_r} = \varphi \frac{1 - \frac{k-1}{k+1} \lambda_{ad}^2}{1 - \frac{k-1}{k+1} \lambda_{ad}^2 \varphi^2} \quad (209)$$

or for the critical section ($\lambda_{ad} = 1$)

$$\mu_{fr} = \varphi \frac{1 - \frac{k-1}{k+1}}{1 - \frac{k-1}{k+1} \varphi^2} \quad (210)$$

Substituting the values $\phi = \phi_{film}$ from (208) into this equation, it is possible to determine the coefficient μ_{fr} , considering the change in vapor consumption due to the influence of losses due to friction on the subsonic section of the nozzle.

According to experimental data the film thickness of low viscosity liquid in the nozzle throat is very insignificant, even with an elevated consumption of liquid in a film corresponding to the initial moisture $(1 - x_0) < 0.3$ and total separation of moisture onto the nozzle walls. This is explained by the high density of the liquid due to which, even with a film velocity equal to 10-15% of the gas velocity, its total cross sectional area is relatively small. Approximate calculations indicate that with a moderate vapor pressure, clogging of the nozzle by a film of low viscosity (for example,

water) does not exceed 0.5%, and in the majority of cases it may be ignored. Certainly, in the case of very viscous liquid or high vapor pressure, when the difference between densities of vapor and condensate are significantly decreased, the influence of flow section clogging in a conduit proves to be great.

Thus the coefficient of moist vapor consumption with comparatively low pressure and a liquid of low viscosity may be evaluated according to formula

$$\mu = \mu_{ab} \mu_{fr}. \quad (211)$$

Usually the values of the coefficient of consumption for water vapor are greater than unity.

A contracting nozzle operating with subsonic drops and pressure with complete vapor supercooling, due to the influence of analogous factors appears to be over-designed as compared to a nozzle calculated according to formulas for equilibrium vapor expansion within the same range of pressure variation. As a result, supercooled vapor consumption in the nozzle will be greater than uniformly condensing vapor.

TABLE 12

/171

Initial Pressure p_0^* in n/m ²	0.491 10	0.0784 10	0.0098 10
Final Pressure p in n/m ²	0.294 10	0.047 10	0.0058 10
Exhaust Velocity:			
Equilibrium c_{eq} in m/sec	431	408	379.4
Supercooled Vapor c in m/sec	424	400	375
Specific Volume:			
Equilibrium v_{eq} in m ³ /kg	0.597	3.36	23.63
Supercooled Vapor v in m ³ /kg	0.566	3.138	22
Ratio c_{eq}/c	1.015	1.021	1.011
Ratio v_{eq}/v	1.055	1.071	1.074
Coefficient of Consumption			
$\mu = \frac{G}{G_T} = \frac{cv_0}{c_p v}$	1.04	1.05	1.063

Results of a comparative calculation [26] for the exhaust of uniformly condensing and supercooled water vapor from a nozzle with a subsonic pressure ratio $\pi = p/p_0^* = 0.6$ are presented in Table 12. In the calculations it was assumed that in the initial section the vapor is dry saturated; the adiabatic index of supercooled vapor was assumed to be equal to the adiabatic index of superheated vapor near the saturation line (in particular, where $p_0^* = 0.491 \cdot 10^6$ n/m² and $k_H = 1.297$); losses due to friction of vapor on the walls were ignored.

The values of the coefficient of consumption μ given for the same conditions but a different initial moisture are also shown in Figure 87. It was assumed that the mechanical and thermal interaction between the phases is absent in the case of nonequilibrium expansion.

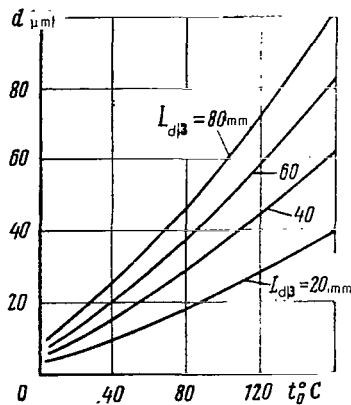


Fig. 88. Maximum Water Particle Diameter with Which It is Possible to Ignore Interaction Between Phases on a Subsonic Section of a Nozzle: L_{sub} is the Length of the Subsonic Section.

The approximate maximum values of water particle diameter in saturated water vapor with which it is possible to ignore the interaction between phases on a subsonic section of a nozzle are given in Figure 88. Calculations were performed according to the equation for particle motion (111) under the condition that the increase in particle velocity on this section not exceed 20% of the increase in vapor velocity and that the mixture velocity at the nozzle inlet be 15-25% of the speed of sound. In performing calculations it was assumed that vapor expansion takes place with complete supercooling; the value of k was selected as for a superheated vapor near the saturation curve.

/172

It is apparent from the figure that the maximum particle diameter increases with an increase in vapor temperature and the length of the subsonic section of the nozzle. This is connected, respectively, with the increase in vapor density and the decrease in the velocity gradient along the nozzle.

With exhaust from a subsonic nozzle given great supersonic pressure drops the coefficient of consumption may increase due to the following phenomenon, experimentally discovered and investigated by M.Ye. Deych and G.V. Tsiklauri [18]. In the usual cases of operation with subsonic pressure drops, the actual area of the minimum (exit) section of the nozzle due to the influence of the displacement thickness of the boundary layer is less than the geometric area of this section.⁸

During operation on great supersonic pressure drops, the subsonic boundary layer near the nozzle throat is "blown out" under the action of the pressure drop inside the nozzle and behind its section. As a result, the actual area of the throat and, consequently, the vapor consumption increase. In the subsonic nozzles studied in reference [18] with a vapor pressure at the intake $\sim 0.2 \cdot 10^6$ n/m²

⁸ With the exhaust of gas or superheated vapor this difference between areas is considered by the coefficient of consumption (author's note).

and a ratio $p/p_0^* < 0.1$, almost complete expulsion of the boundary layers in the nozzle took place, and the vapor consumption approximated the theoretical consumption calculated without taking displacement thickness into account.

§5. Equilibrium Exhaust of an Ideal Gas-Condensing Vapor Mixture from a Nozzle

In several cases jet engine nozzles as well as turbines may operate on a mixture of gas and saturated vapor of some substance. Depending upon the expansion rate and the degree of contamination of the flow by mechanical additives, as well as upon the composition and physical characteristics of the components in the mixture, the exhaust of such a mixture may have both a nonequilibrium (with discontinuities in condensation), and an equilibrium nature. For example, in a multistage turbine expansion of a mixture composed of blast furnace gas and water vapor approximates equilibrium expansion [45].

Let us consider equilibrium expansion of an ideal gas and condensing vapor mixture in a nozzle. Calculations carried out by the author of this book indicated that particles of condensate forming during the expansion process of the moist vapor in a nozzle lag behind the vapor flow very slightly. Therefore, in order to simplify the study we shall ignore condensate particle lag and losses due to friction between the phases and to incomplete heat exchange, and consider the flow of the mixture to be equilibrium. /173

Moreover, let us assume that the flow is stable, linear and without heat exchange with the surrounding medium; the expansion process is equilibrium and the mixture is homogeneous; the vapor and gas states in the expansion process are sufficiently removed from the critical so that both the gas and the dry saturated vapor may be viewed as ideal gases; the heat capacity of the gas is constant; at the beginning of mixture expansion the vapor is in a dry saturated state.

As is known from the theory of ideal gas mixture the density of components in the mixture is determined by their partial pressures and temperatures. In addition to the assumption of mixture homogeneity, the temperature and velocity of all components are considered to be equal, and for each component in the mixture it is possible to write a separate equation of consumption. For the mixture of gas and dry saturated vapor under consideration the equations for consumption have the form:

$$G_r = G_{r0} = F \rho_1 c; \quad G_n = G_{n0} x = F \rho_n c.$$

Relating the first equation to 1 kg of gas, we obtain

$$1 = f \frac{p_r}{p_{r0}} \frac{\bar{c}}{t}. \quad (212)$$

Having divided the second equation by the first, we obtain the following relationship between mass concentrations of gas and vapor:

$$\frac{g_n}{g_r} = \frac{g_{n0}x}{g_{r0}} = \frac{p_n}{p_r}, \quad (213)$$

where $g_n = \frac{G_n}{G_n + G_r}$ and $g_r = \frac{G_r}{G_n + G_r}$ are the mass concentrations of the vapor and gas phases.

Assuming equality of velocities of the gas vapor and particles of condensate, the equation for motion of a mixture may be written in the following fashion:

$$-\frac{dp_{mix}}{\rho_{mix}} = -g_r \frac{dp_r}{\rho_r} - g_n \frac{dp_n}{\rho_n} = \left(1 + g_n \frac{1-x}{x}\right) cdc,$$

where $p_{mix} = p_r + p_n$ is the pressure of the mixture;
 $\rho_{mix} = \rho_r + \rho_n$ is the density of the mixture of gas and dry saturated vapor;
 p_r, ρ_r, p_n, ρ_n are the partial pressure and density of the gas and vapor phases, respectively.

The second component in brackets on the right-hand side of the equation is caused by the presence of $g_n(1-x)/x$ kg of particles of condensate in kg of gaseous components of the mixture.

This equation, relative to 1 kg of the working fluid, i.e., to /174 a gas-dry saturated vapor-condensate particle mixture may be re-written in integral form

$$-g_{r0} \int \frac{dp_r}{\rho_r} - g_{n0} \int x \frac{dp_n}{\rho_n} = \frac{c^2 - c_0^2}{2}. \quad (214)$$

The left-hand side of this equation is the sum of partial expansion operations; for g_{r0} kg of gas and g_{n0} kg of moist vapor, respectively.

Having established the form of the functions ρ_r, ρ_n and x it is possible to calculate the values of integrals entering the expressions for partial operations of gas and moist vapor. We shall indicate, however, that to determine the total work of mixture expansion, other simpler methods are also possible. In order to do this, let us consider the processes of gas and vapor phase expansion in greater detail.

In the expansion process of the mixture the vapor condenses. Some of the condensation heat liberated here is conducted to the gas and somewhat increases its efficiency in comparison to the case of adiabatic expansion. Therefore the work of expansion of 1 kg of gas is

$$H_r = - \int \frac{dp_r}{p_r} = H_{r, ad} + \Delta A_Q,$$

where $H_{r, ad} = c_{p,r} T_0 \left[1 - \left(\frac{p_r}{p_{r0}} \right)^{\frac{k-1}{k}} \right]$ is the work of adiabatic expansion of 1 kg of gas; ΔA_Q is the increase in efficiency of 1 kg of gas due to heat conduction in the expansion process.

With the cooling of a mixture in the expansion process $(g_{\Pi 0}/g_{\Gamma 0})dx$ of gas condenses on dT and $r(g_{\Pi 0}/g_{\Gamma 0})dx$ of heat is liberated; moreover, $(g_{\Gamma 0}/g_{\Pi 0})(1-x)c_{p,K}dT$ of heat is liberated upon cooling $(g_{\Pi 0}/g_{\Gamma 0})(1-x)$ condensate on dT . The total amount of liberated heat is

$$dQ = -r \frac{g_{\Pi 0}}{g_{\Gamma 0}} dx - \frac{g_{\Pi 0}}{g_{\Gamma 0}} (1-x) c_{p,K} dT.$$

Some of the liberated heat goes to heat the vapor phase, remaining in a dry saturated state in the expansion process. As is known [9], the heat capacity of a vapor with a change in its state along the right branch of the boundary curve is

$$c_u = c_{p,K} + \frac{dr}{dT} - \frac{r}{T}.$$

Therefore in heating $(g_{\Pi 0}/g_{\Gamma 0})x$ of vapor the following amount of heat is expended

$$dQ_n = \frac{g_{\Pi 0}}{g_{\Gamma 0}} x c_n dT = \frac{g_{\Pi 0}}{g_{\Gamma 0}} x dr + \frac{g_{\Pi 0}}{g_{\Gamma 0}} \left(c_{p,K} - \frac{r}{T} \right) x dT.$$

Thus, to 1 kg of gas the following amount of heat is conducted: /175

$$dQ_r = dQ - dQ_n = - \frac{g_{\Pi 0}}{g_{\Gamma 0}} \left[d(rx) + c_{p,K} dT - \frac{r}{T} x dT \right] \quad (215)$$

This amount of heat increases the efficiency of the gas in comparison to the gas expanding adiabatically on

$$dA_Q = \left(1 - \frac{T_1}{T} \right) dQ.$$

where T_1 is the temperature of the lower heat source.

The total increase in gas efficiency due to conduction of the condensation heat is

$$\Delta A_Q = \int_{T_0}^T dQ_r - T \int_{T_0}^T \frac{dQ_r}{T}.$$

Having substituted here the expression for dQ_r , after integration we obtain

$$\Delta A_Q = \frac{g_{n0}}{g_{r0}} \left[\left(1 - \frac{T}{T_0} \right) (r_0 + c_{p\kappa} T_0) + c_{p\kappa} T \ln \frac{T}{T_0} + \int_{T_0}^T \frac{rx}{T} dT \right].$$

Let us transform the expression for the work of vapor expansion entering the left-hand side of equation (214). From the Clausius-Clapeyron equation

$$\frac{dp_n}{dT} = \frac{r}{T(v_n - v_k)},$$

ignoring the specific volume of condensate v_k , small in comparison with the specific volume of dry saturated vapor, we find

$$\frac{dp_n}{p_n} = \frac{r}{T} dT. \quad (216)$$

Thus, the work of expansion for 1 kg of moist vapor is

$$H_n = - \int x \frac{dp_n}{p_n} = - \int \frac{rx}{T} dT.$$

Using the obtained relationship for work of the gas and vapor phases, the left-hand side of equation (214) may be reduced to the following form:

$$H_{cv} = g_{r0} c_{p\kappa} T_0 \left[1 - \left(\frac{p_r}{p_{r0}} \right)^{\frac{k-1}{k}} \right] + g_{n0} \left[\left(1 - \frac{T}{T_0} \right) (r_0 + c_{p\kappa} T_0) + c_{p\kappa} T \ln \frac{T}{T_0} \right]. \quad (217)$$

The second component in the right-hand side of this equation is the work of adiabatic expansion g_{n0} kg for moist vapor. /176

Thus, the total work of expansion of 1 kg of the mixture is equal to the sum of the available work of g_{r0} kg of gas with its

adiabatic expansion from the initial to the final partial pressure and the available work of $g_{\Pi 0}$ kg of moist vapor with its adiabatic expansion from the initial to the final partial vapor pressure.

With regard to the latter relationship, assuming r to be a linear function of temperature ($r = \alpha - bT$) the equation for motion of the mixture (214) may be reduced to the following dimensionless form

$$1 - \left(\frac{p_r}{p_{r0}} \right)^{\frac{k-1}{k}} + \bar{g}_n \frac{b}{c_{p\kappa}} (m-1) \frac{c_{p\kappa}}{c_{p\tau}} \left[(1-t) \left(1 + \frac{c_{p\kappa}}{b} \frac{1}{m-1} \right) + \frac{c_{p\kappa}}{b} \frac{t \ln t}{m-1} \right] = \frac{\delta_r (\bar{c}^2 - 1)}{g_{r0}}, \quad (218)$$

where $\bar{g}_n = \frac{g_{n0}}{g_{r0}}$; $m = \frac{\alpha}{bT_0}$; $\delta_r = \frac{c_0^2}{2c_{p\tau}T_0}$.

We shall now introduce an equation for expansion of the gas phase. With the conduction of a certain amount of heat to the gas in the expansion process its entropy S increases. Simultaneously, the temperature T_1 and the heat content i_{r1} of the gas with its final pressure p_1 increases. Upon conduction of a heat dQ_r to the gas, its heat content increases to

$$di_{r1} = c_{p\tau} dT_1 = T_1 dS = T_1 \frac{dQ_r}{T}.$$

Hence, $\frac{dT_1}{T_1} = \frac{dQ_r}{T_1 c_{p\tau}}$; dQ_r is determined according to formula (215).

Integrating this equation and considering that where $T = T_0$ the values $T_1 = T_{ad}$, $x = 1$, $r = r_0$, and at the end of expansion $T = T_1$

and that $\frac{T_0}{T_{ad}} = \left(\frac{p_{r0}}{p_{r1}} \right)^{\frac{k-1}{k}}$, where T_{ad} is the final temperature with an

adiabatic expansion of gas, we finally obtain the following dependence between partial pressure of a gas and its temperature with expansion of the mixture:

$$\frac{p_r}{p_{r0}} = t^{\frac{k}{k-1} \left(\bar{g}_n \frac{c_{p\kappa}}{c_{p\tau}} + 1 \right)} \exp \left[\frac{k}{k-1} \bar{g}_n \frac{c_{p\kappa}}{c_{p\tau}} \frac{b}{c_{p\kappa}} (m-1) \left(\frac{m-t}{m-1} \frac{x}{t} - 1 \right) \right]. \quad (219)$$

The pressure as a function of temperature of the vapor phase in /177
(176) may be rewritten as:

$$\frac{p_n}{p_{n0}} = t^{-\frac{b}{R_n}} \exp \left[m \frac{b}{R_n} \left(1 - \frac{1}{t} \right) \right]. \quad (220)$$

Having divided (220) by (219) and taking (213) into account, we obtain the following expression (in implicit form) for determining the degree of vapor dryness x as a function of the dimensionless temperature of the mixture:

$$x = \frac{\left(\frac{1}{t}\right)^{\frac{b}{R_n} + \frac{k}{k-1} \left(\frac{c_{p\kappa}}{\bar{g}_n c_{p\gamma}} + 1\right)}}{\exp \left[m \frac{b}{R_n} \left(\frac{1}{t} - 1\right) + \frac{k}{k-1} \bar{g}_n \frac{c_{p\kappa}}{c_{p\gamma}} \frac{b}{c_{p\kappa}} (m-1) \left(\frac{m-t}{m-1} \frac{x}{t} - 1\right) \right]}. \quad (221)$$

Six determining parameters enter this equation:

$$k, \frac{b}{R_n}, \frac{c_{p\kappa}}{c_{p\gamma}}, \frac{b}{c_{p\kappa}}, \bar{g}_n, m.$$

Of these, the first four depend only upon the physical constants of the gas or vapor; therefore, the exhaust of a mixture with given components is completely defined by the remaining two parameters:

$$\bar{g}_n = \frac{g_{n0}}{g_{r0}} \text{ and } m = \frac{a}{bT_0}.$$

From equation (221) it is possible to determine the degree of vapor dryness with a very small and a very large content of it in the mixture. Actually let $\bar{g}_n \rightarrow 0$; i.e., let the gas flow with an insignificant vapor admixture. In this case

$$x_0 = \lim_{\bar{g}_n \rightarrow 0} x = \frac{\left(\frac{1}{t}\right)^{\frac{b}{R_n} + \frac{k}{k-1}}}{\exp \left[m \frac{b}{R_n} \left(\frac{1}{t} - 1\right) \right]}.$$

If $\bar{g}_n \rightarrow \infty$ (condensing vapor with an insignificant admixture of gas), then (221) will have the form

$$x = x_0 \exp \left\{ \frac{k}{k-1} \frac{c_{p\kappa}}{c_{p\gamma}} \bar{g}_n \left[\ln \frac{1}{t} - (m-1) \frac{b}{c_{p\kappa}} \left(\frac{m-t}{m-1} \frac{x}{t} - 1 \right) \right] \right\}.$$

Since the degree of vapor dryness is $0 \leq x \leq 1$, i.e., the limit value, then where $\bar{g}_n \rightarrow \infty$ it is necessary that

$$\ln \frac{1}{t} - (m-1) \frac{b}{c_{p\kappa}} \left(\frac{m-t}{m-1} \frac{x}{t} - 1 \right) \rightarrow 0.$$

From this equation we find the limiting value of x where $\bar{g}_{II} \rightarrow \infty$: /178

$$x_{\infty} = \lim_{\bar{g}_{II} \rightarrow \infty} x = \frac{m-1}{m-t} t - \frac{c_{p\kappa}}{b} \frac{t \ln t}{m-t}.$$

The obtained expression corresponds to the usual equation for the degree of dryness with its equilibrium adiabatic expansion from a dry saturated state.

§6. Characteristics of Moist Vapor Flow in the Flow Section of the Turbine

With moist vapor flow in a turbine the degree of moisture due to condensation increases. It is necessary to distinguish the initial (primary) vapor moisture, i.e., in front of the nozzle apparatus, and the final moisture, i.e., behind the working wheel.

As experimental studies indicate, water vapor flow in a turbine is always accompanied by supercooling. This is explained by the flow velocity gradients in turbine grids and also by the high purity of vapor usually used in steam turbine installations.

Schematizing the process of moist vapor flow in a multistage turbine it is possible to consider that in the nozzle apparatus and in a reaction working wheel vapor is expanded with total supercooling. In the cross sectional area where the flow velocity approaches the speed of sound and local supersonic zones appear, discontinuities in condensation arise, producing an equilibrium state in the vapor.⁹

Thus, with a sufficient degree of certainty it is possible to assume a moist vapor flow in the conduits between the blades; in particular, in the nozzle apparatus of the turbine moist vapor flow may be assumed to be identical to a double-phase flow with constant compression of the liquid phase equal to the initial moisture of the vapor $1 - x_0$.

However, the possibility for such a schematization for moist vapors of alkaline metals, freon, etc. requires experimental confirmation.

1. Losses in a Turbine Caused by Vapor Moisture

Drops of condensate forming in a condensation discontinuity in the axial space are usually finely dispersed ($\bar{d} < 1 \mu\text{m}$), and their

⁹ As was indicated in [24], in the axial clearance of the turbine stage complete, gradual vapor condensation into embryonic drops formed with gas expansion with supercooling in the nozzle apparatus may also take place (author's note).

velocity is near the vapor velocity. Therefore, drops impact against the working blades under calculated angles of intake and cannot cause losses due to impact. On the other hand, particles of primary condensate contained in the vapor flow before the stage are usually /179 significantly larger ($\bar{d} > 15 \mu\text{m}$), which is caused by particle coagulation in the preceding stages. As indicated above, such particles are separated on the concave surface of nozzle blades and form a film flowing onto the working blades under a large negative angle of attack, which leads to losses due to friction and to erosional wear of working blades.

With a small axial clearance, losses due to friction may be evaluated according to the following formula similar to expression (157):

$$\Delta\eta_{\text{imp}, \text{max}} = 2k_c(1-x_0)\left(\frac{u}{c_{ad}}\right)^2\left(1 + \frac{h_b}{D_{im}}\right)^2. \quad (222)$$

In this formula the value x_0 , analogous to g_r in (157), is absent in the denominator since in a steam turbine losses are based on 1 kg of moist vapor and not on 1 kg of the gas phase, as with the conclusion of (157).

As was indicated in Chapter III, formula (222) is valid even in the case when the basic mass of condensate is concentrated in the peripheral zone of the flow section, which is often observed in the intermediate stage of a multistage steam turbine.

The maximum losses due to impact, assuming $k_c = 1$, can be determined according to the following formula reduced to the initial degree of moisture:

$$\Delta\eta_{\text{imp}, \text{max}} = \frac{\Delta\eta_{\text{imp}, \text{max}}}{1-x_0} = 2\left(\frac{u}{c_{ad}}\right)^2\left(1 + \frac{h_b}{D_{im}}\right)^2.$$

The value of $\Delta\eta_{\text{imp}, \text{max}}$ as a function of the ratio u/c_{ad} is shown in Figure 47b.

From the figure it is apparent that with the value $u/c_{ad} = 0.5 - 0.6$, common for a turbine stage and various relative blade lengths h_b/D_m , the impact of liquid on the working blades caused the efficiency of the stage decrease from 0.6 - 1.4% for each percent of initial vapor moisture. From the same figure it follows that losses due to impact decrease rapidly with a decrease in u/c_{ad} .

Usually in the final stages of condensation in turbines the axial clearance between the nozzle and working blades reaches a significant size. Due to particle acceleration by the vapor flow in the axial clearance, losses due to friction of condensate on working blades decrease; it is possible to evaluate their magnitude

according to formula (163). However, losses in the axial clearance due to interaction between phases are increased.

Besides losses due to impact, in a steam turbine losses due to thermodynamic nonequilibrium of vapor flow (supercooling) appear. As was noted, with low initial moisture of water vapor it is possible to assume that the adiabatic index of vapor expansion in a nozzle apparatus is near the adiabatic index of superheated vapor near the precipitation line k_{Π} .

Since the adiabatic index of expansion for a supercooled vapor k_{Π} is greater than the adiabatic index for a thermodynamic equilibrium expansion of moist vapor k_{eq} , then with the same pressure drop the velocity and kinetic energy of a supercooled vapor will be less than an equally expanding vapor. The difference between kinetic energies amounts to the losses from supercooling.

/180

Assuming that in a turbine stage $x_0 = 1$ and that it is possible to ignore kinetic energy of the vapor at the intake to the stage as small in comparison to the work of expansion in the stage, it is possible to assume with a sufficient degree of accuracy

$$\Delta\eta_{ineq} = \frac{\Delta H_{ineq}}{H_{eq, st}} = \frac{H_{eq}^{noz} - H_{ineq}^{noz} + x(H_{eq}^{wh} - H_{ineq}^{wh})}{H_{eq, st}}$$

or

$$\Delta\eta_{ineq} = (1 - \rho) \left(1 - \frac{H_{ineq}^{noz}}{H_{eq}^{noz}} \right) + x\rho \left(1 - \frac{H_{ineq}^{wh}}{H_{eq}^{wh}} \right), \quad (223)$$

where $H_{eq} = i_0 - i$ is the work of equilibrium expansion of a vapor;

$$H_{ineq} = \frac{k_{\Pi}}{k_{\Pi} - 1} RT_0 \left[1 - \left(\frac{p}{p_0} \right)^{\frac{k_{\Pi} - 1}{k_{\Pi}}} \right] \text{ work of expansion of a supercooled vapor}$$

(indices noz, wh, and st designate, respectively, nozzle apparatus, working wheel and stage as a whole); x is the degree of vapor dryness in front of the working wheel; ρ is the degree of reactivity.

The value $1 - (H_{ineq}/H_{eq})$ for water vapor as a function of the ratio p/p_0 is presented in Figure 89. This value is equal to the decrease in efficiency in an active turbine ($\rho = 0$) due to thermodynamic in nonequilibrium. Thus, in a subsonic active turbine stage the decrease in efficiency due to supercooling of the vapor may total 2-4%. In a supersonic active stage, losses due to supercooling increase.

In a reaction stage losses due to supercooling are significantly decreased. For example, where $\rho = 0.5$, $t_0 = 150^\circ\text{C}$ and the ratio $p/p_0 = 0.4$ the decrease in efficiency is $\Delta\eta_{ineq} = 2\%$, since in an active stage with the same pressure ratio $\Delta\eta_{ineq} = 4.5\%$. This may

be explained by the fact that the expansion process in a jet turbine is accompanied by less supercooling than in an active turbine. Actually, due to the discontinuity in condensation in the axial clearance, vapor expansion in the working blades also begins from a state close to equilibrium. Moreover, the surface temperature of the working blades T_w^* is much lower than the temperature of the nozzle blades T_0^* ; therefore, partial vapor condensation may take place on the working blades which also decreases supercooling of the vapor in the working wheel.

Discontinuities in condensation arising in the region of the spaces between the rings are accompanied by weak compression waves leading to losses. In the usual multistage turbines with subsonic flow velocities in the blade apparatus, these losses will be negligibly small. In a supersonic turbine stage (with a supersonic relative velocity upon entrance to the working blades) losses in a condensation discontinuity may increase; however, at the same time the intensity of a discontinuity ahead of a working grid decreases so that the total wave losses in the space between the rings may vary insignificantly.

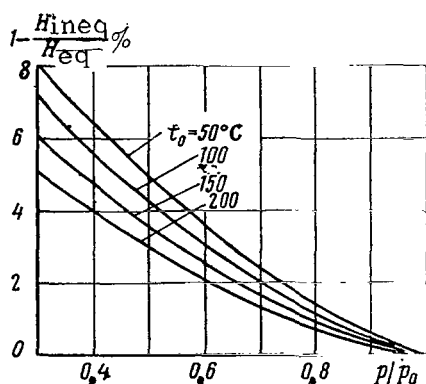


Fig. 89. Losses During Supercooling in a Blade Apparatus as a Function of the Degree of Decrease in Water Vapor Pressure.

With an increase in initial moisture due to partial vapor condensation on drops of primary condensate, losses from supercooling decrease somewhat. However, here the other types of losses from the double-phase nature of the flow rapidly increase.

Let us evaluate the total decrease in efficiency of a turbine stage operating on moist vapor. Summing the fundamental types of supplementary (in comparison with operation on a superheated vapor) losses and dividing them by the available work of vapor in a stage we obtain

$$\Delta\eta_{\text{moist}} = x_0 \Delta\eta_{\text{ineq}} + \Delta\eta_{\text{rough}} + k_c (\Delta\eta_{\text{sep}} + \Delta\eta_{\text{imp}}) + (1 - k_c) \left(\frac{A_{fr}^* + E_{\kappa}^*}{H_{\text{eq.st}}} + \Delta\eta_{\text{imp}}^* \right) \quad (224)$$

In this formula $\Delta\eta_{\text{rough}}$ (the decrease in efficiency of a stage as a result of an increase in losses due to friction on the rough film) may be determined from Figure 45. For water $\Delta\eta_{\text{rough}} = 1 - 1.5\%$.

The value $\Delta\eta_{\text{sep}} + \Delta\eta_{\text{imp}}$ considers losses due to acceleration in the axial clearance and due to impact on the working blades of

that portion of primary condensate which was separated out upon the nozzle blades. The value of $\Delta\eta_{sep}$ may be evaluated according to a formula analogous to (168):

$$\Delta\eta_{sep} = (1.3 - 1.5)(1-x_0)(1-\rho)(\Phi + E). \quad (225)$$

As was already noted, for a liquid of low viscosity (water) with $u/c_{ad} = 0.5 - 0.55$, losses due to particle acceleration in the axial clearance are largely compensated for by the decrease in losses due to impact, so that $\Delta\eta_{sep} + \Delta\eta_{imp}$ max the coefficient $\Delta\eta_{imp}$ is evaluated according to formula (163), and $\Delta\eta_{imp}$ max accord- /182

ing to formula (222). The expression $\frac{A_{fr}^* + E_K^*}{H_{eq.st}} + \Delta\eta_{imp}^*$ characterizes

the decrease in efficiency caused by that portion of primary condensate which was not separated out in the nozzle apparatus. These losses accumulate from losses due to friction of vapor on particles, kinetic energies of particles (obtained from a gas and almost completely lost with their precipitation onto elements of the flow section) and losses from the impact of these particles on the working blades.

It is necessary to note that only small particles pass through the nozzle apparatus without separating. Their velocity here may attain 70-80% of the vapor velocity. In a cross section and in the axial clearance their acceleration by the vapor continues; therefore, the velocity of these particles in front of the working wheel may be assumed to be approximately equal to the vapor velocity. Ignoring losses due to friction of vapor on small particles as small in comparison with their kinetic energy (cf. Ch. II), we obtain

$$\frac{A_{fr}^* + E_K^*}{H_{eq.st}} \approx \frac{(1-x_0) \frac{c_1^2}{2}}{\frac{c_{ad}^2}{2}} \approx (1-x_0)(1-\rho). \quad (226)$$

Let us assume that complete separation of these particles takes place in the working blades. This is completely possible since the angle of flow revolution in the working blades is usually significantly greater than in the nozzle blades. Then the value of $\Delta\eta_{imp}$ may be evaluated according to the following formula which is obtained from equation (163) where $c_{uK} = c_{u\Gamma} = c_{1u}$ and, if the blades are not very long:

$$\Delta\eta_{imp}^* = 2(1-x_0) \left(\frac{u}{c_{ad}} \right)^2 \left(1 - \frac{c_{1u}}{u} \right). \quad (227)$$

Since usually $c_{1u} > u$, then $\Delta\eta_{imp}^* < 0$, i.e., particles precipitating on working blades perform useful work.

With very fine particles ($d \leq 1 \mu\text{m}$) for which it is possible to ignore separation even in the working wheel, the value of $\Delta\eta_{\text{imp}}^*$ attains a maximum negative value, equal (with axial exit) to

$$\Delta\eta_{\text{imp}}^* = -2(1-x_0) \frac{c_{1u}u}{c_{ad}^2} = -2(1-x_0)(1-\rho) \frac{u}{c_1} \cos \alpha_1. \quad (228)$$

In this case the latter component in expression (224) vanishes; i. e., the work of vapor, expendable on acceleration of very fine particles in nozzle and working blades, is completely transformed into useful work on the turbine shaft.

/183

Thus, the decrease in efficiency in a turbine with fairly short blades, operating on moist water vapor with $u/c_{ad} = 0.5 - 0.55$, may be evaluated according to

$$\Delta\eta_{\text{moist}} = x_0\Delta\eta_{\text{ineq}} + \Delta\eta_{\text{rough}} + k_c\Delta\eta_{\text{imp, max}} + (1-k_c) \left[(1-x_0)(1-\rho) + \Delta\eta_{\text{imp}}^* \right] \quad (229)$$

In the last stages of condensation turbines where the vapor density is small, and also in small steam turbines, supplementary losses due to reduced values of Re numbers for the flow in turbine blades may appear. As is known, these losses are caused by an increase in the relative thickness of the boundary layers and lead, along with a decrease in efficiency, to a decrease in the coefficient of vapor consumption to the turbine. With numbers $\text{Re} > 6 \cdot 10^5$ the flow may be considered self-simulating; i. e., independent of Re.

2. The Influence of Vapor Moisture on the Reactivity of a Stage

As indicated above, with equal losses due to friction on the nozzle walls the consumption of supercooled vapor through a subsonic nozzle is greater than that of an equally condensing vapor. The maximum ratio of these consumptions (coefficient of consumption μ) for water vapor with complete supercooling and expansion from the dry saturated state is expressed by the curve $x_0 = 1$ in Figure 87.

In the majority of cases, the degree of reactivity of turbine stages is $\rho < 0.5$; the peripheral sections of long blades are an exception. Due to the greater drop operating in nozzle apparatus, the degree of supercooling and, consequently, even the increase in the coefficient of consumption in nozzle apparatus prove to be greater than in the working blades. Moreover, supercooling in working blades decreases somewhat due to partial condensation on the blade surface. This is equivalent to more "over-designing" of nozzle apparatus than of working apparatus. As a result, the actual degree of reactivity of a stage must be greater than the calculated one, assuming thermodynamic equilibrium of moist vapor expansion. As the experimental data from a number of authors indicate [15, 25, 41, 61], with an increase in the initial degree of water vapor moisture, the reactivity level may increase. For example, according

to the data of V.V. Pryakhin [41], with an increase in initial moisture from 0 - 5% the mean degree of reactivity ($D_m = 0.4$ m; $h_b = 50$ mm, $u/c_0 = 0.5$) increases from 0 to 6%.

An increase in reactivity with an increase in initial moisture is explained by damping of the flow by particles of the primary condensate. Due to the low viscosity of water, the influence of nozzle apparatus clogging by its film is insignificant.

With fine particles ($d < 5 \mu\text{m}$) the interaction between phases and, consequently, even the decrease in velocity of the mixture behind the nozzle apparatus will be maximal. Therefore, the increase in reactivity of the stage with an increase in initial moisture, in this case, will also be very small. With large particles ($d > 50 \mu\text{m}$) their interaction with the vapor and, consequently, even the increase in reactivity may be ignored. For example, according to experimental data [25], for a two-stage turbine operating on moist vapor with large particles of primary condensate where $1 - x_0 \leq 0.12$, the change in the degree of reactivity of the stages was insignificant. Due to the intensive separation of large particles in the nozzle apparatus (especially with initial moisture $1 - x_0 > 0.1$) the thickness of the water film on the nozzle blades attains a maximum value, due to which the reactivity of the stage may even decrease somewhat. /184

§7. Birotative Turbine Operation on Moist Vapor

As indicated in Chapter III, the efficiency of a birotative turbine operating on a double-phase flow may be much greater than that of the usual turbine. This is explained by the fact that in a birotative turbine the two basic types of supplementary losses caused by the double-phase nature of the flow are absent: losses due to impact of the liquid phase on the working blades and those due to friction on the undulating film covering the blades.

Let us consider multistage birotative turbine operation on moist vapor (Fig. 90). The drum-type turbine stator (2) rotates at low circumferential velocities $u = 30-50$ m/sec; the turbine rotor (1) rotates at usual speeds on the order of 250-350 m/sec; the power of the stator contributes 8 - 12% of the power of the rotor. Rotation of the stator and rotor may coincide, for example, with the aid of pinion device (4).

Due to the rotation of the stator, under the action of centrifugal forces the film forming on the nozzle blades is scattered to the periphery so that the working blades operate on a dried vapor. From the internal surface of the rotating stator the film flows out through special openings into the immobile corpus of the turbine. Thus, it is possible to consider that in a multistage construction the condensate is continuously removed from the flow section and the turbine operates on dry saturated vapor.

Evidently such a construction ensures high efficiency and

reliability of operation even with a very great diagrammatic vapor moisture; for example, with a profound vapor expansion from the dry saturated state near the critical region.

Certainly, even this construction has characteristic losses /185 connected with supercooling of the vapor; however, as indicated, in a jet turbine these losses are small.

Together with the condensate from the flow section of the turbine a certain amount of heat is eliminated, somewhat decreasing the efficiency of this operation. Let us evaluate the amount of losses due to elimination of heat with the condensate. In order to

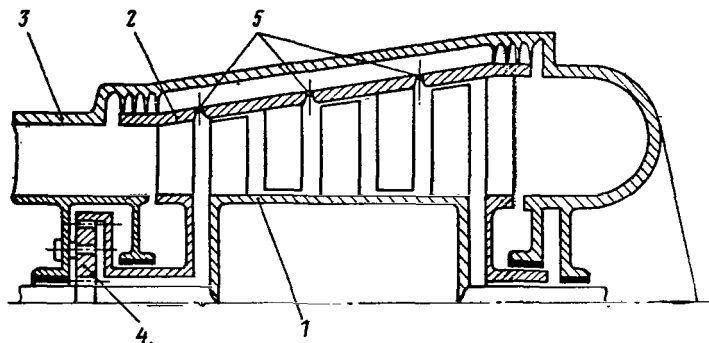


Fig. 90. Schematic Drawing of a Birotative Turbine for Operation on Moist and Supermoist Vapor: (1) Rotor; (2) Rotating Stator; (3) External Corpus; (4) Synchronizing Transmitter; (5) Openings for Moisture Removal.

simplify the analysis we shall assume that vapor is not supercooled and the condensate is continuously removed from the flow in proportion to its formation. Moreover, let us assume that the vapor is expanded from the dry saturated state.

With the cooling of the vapor to dT a certain amount of it, dx , condenses. In addition, $-r dx$ of heat is liberated. According to the first law of thermodynamics this heat will undergo a change in enthalpy x kg of vapor and in the work of its forcing in a variable pressure field, i.e.,

$$-r dx = x di_{II} - x v_{II} dp. \quad (230)$$

Using the Clapeyron-Clausius equation (173) written for the case where $v_K \ll v_{II}$ in the form $v_{II} dp = (r/T) dT$ along with the expression for the increase in enthalpy of a dry saturated vapor $di_{II} = c_{pK} dT + dr$, equation (230) may be transformed:

$$d \ln \frac{rx}{T} + \frac{c_{pK}}{r} dT = 0. \quad (231)$$

If we assume $r = a - bT$, then this equation may be integrated. After transformations we obtain the degree of vapor dryness

$$x = t \left(\frac{m-t}{m-1} \right)^{\frac{c_{pK}}{b}} - 1, \quad (232)$$

where $m = \frac{a}{bT_0}$; $t = \frac{T}{T_0}$; T_0 is the temperature of the dry saturated vapor at the beginning of expansion. /186

Let us compare the degree of dryness of the vapor, expanding with continuous removal of condensate, to the degree of dryness of a given equilibrium adiabatic moist vapor expansion. In the latter case expression (179) where $r = a - bT$ will acquire the form:

$$x_p = t \left(\frac{m-1}{m-t} \right) \left(1 - \frac{c_{pK}}{b} \frac{\ln t}{m-1} \right). \quad (233)$$

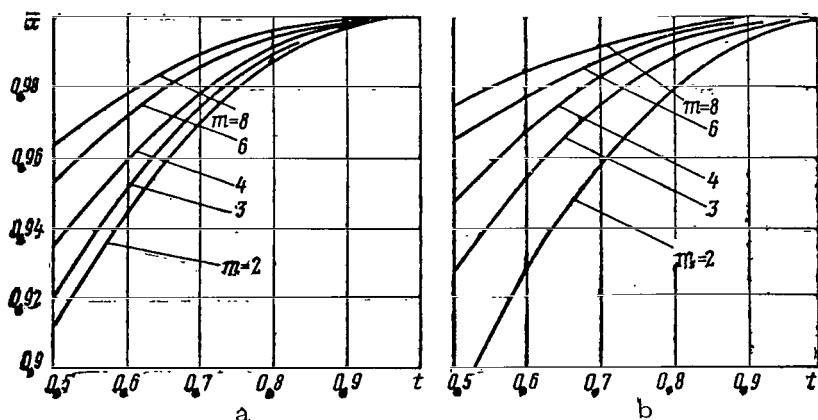


Fig. 91. Relative Dryness of Moist Vapor with Continuous Removal of Condensate as a Function of t : (a) $c_{pK}/b = 1.67$; (b) $c_{pK}/b = 1$.

The ratio of the indicated degrees of dryness is

$$\bar{x} = \frac{x}{x_p} = \frac{\left(\frac{m-t}{m-1} \right)^{\frac{c_{pK}}{b}}}{1 - \frac{c_{pK}}{b} \frac{\ln t}{m-1}}. \quad (234)$$

Values of \bar{x} as a function of the dimensionless equilibrium vapor temperature t calculated according to this formula are presented in Figure 91. The values of \bar{x} proved to be less than unity, i.e., with condensate removal the degree of vapor dryness is less than that of an equally condensing vapor. Consequently, condensation of vapor in the case of constant condensate removal takes place

more intensively than an equilibrium condensation of vapor; this is explained by the fact that for condensation of heat eliminated together with condensate a certain portion of the vapor is condensed supplementarily. /187

Let us calculate the work of expansion of a vapor phase $H = -\int x v_{II} dp$ with constant condensate removal. Substituting expression (232) for x , after integration we obtain

$$H = \frac{r_0(m-1)}{\left(\frac{c_{pK}}{b} + 1\right)} \left[\left(\frac{m-t}{m-1}\right)^{\frac{c_{pK}}{b} + 1} - 1 \right]. \quad (235)$$

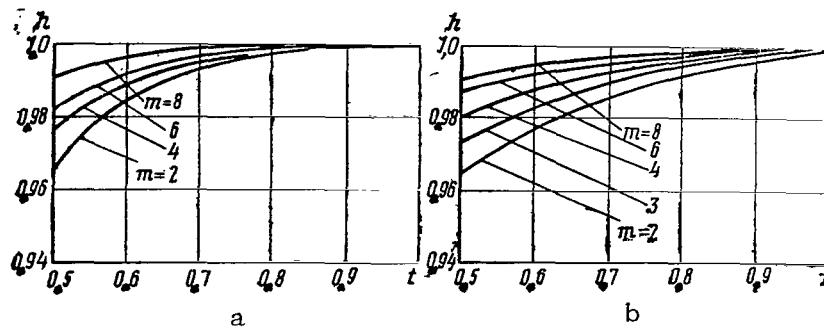


Fig. 92. Relative Work of Moist Vapor Expansion with Constant Condensate Removal as a Function of t : (a) $c_{pK}/b = 1.67$; (b) $c_{pK}/b = 1$.

Let us relate the work obtained to the work of an equilibrium expansion of condensing vapor H_{eq} , determined according to formula (180). After transformation we find

$$h = \frac{H}{H_p} = \frac{(m-1)^2}{\frac{c_{pK}}{b} + 1} \frac{\left(\frac{m-t}{m-1}\right)^{\frac{c_{pK}}{b} + 1} - 1}{(1-t) \left(\frac{c_{pK}}{b} + m - 1\right) + \frac{c_{pK}}{b} t \ln}. \quad (236)$$

The values of the relative work of moist vapor expansion calculated according to this formula as a function of the dimensionless vapor temperature t are presented in Figure 92. The decrease in efficiency of the vapor with constant condensate removal in comparison with an equilibrium expansion of moist vapor does not exceed 2-3%, even with a significant pressure drop ($t < 0.5$). A decrease in efficiency is explained by the decrease in the amount of vapor phase in comparison with the case of an equilibrium expansion.

§8. Erosion of Elements of a Turbine Operating on Moist Water Vapor

/188

With turbine operation on moist vapor the most intensive erosion

is usually observed on the working blades, so that primarily the intake edges of the blades on the periphery are worn out. In steam turbine operation there are cases when the peripheral areas of the working blades were worn out on 30-50% of the length of the cord. Cases when the upper part of the eroded blades broke off were also observed. Sometimes the wire bands attached to decrease blade vibrations and also the disks of the working wheels and the scarves of the working blades intensively erode. Nozzle blades do not erode.

After erosion a surface is rough with deep depressions and sharp prominences. Sometimes it is shaped like a sponge with large cavities.

As already noted, erosion of working blades and other elements of the rotor are caused by the liquid film flowing from the nozzle blades and breaking off into large drops in the axial clearance. With a small clearance, due to the influence of viscosity retarding the dispersion of the film, particles of the liquid have maximum size and minimum velocity. The shape of such particles may be non-spherical. In this case, erosion of the intake edges of working blades will be most intensive. With an increase in the axial clearance large drops are broken up into finer drops by the flow and particle velocity is increased; therefore, the relative velocity of their precipitation on the working blades is decreased. In addition, erosion is also significantly decreased.

Drops which have not precipitated on the nozzle blades have a velocity near the vapor velocity, and therefore they cannot cause erosion of the working blades.

1. The Kinetics of Erosional Destruction of Material

It has been established by many investigators that upon the precipitation of liquid particles with great relative velocity onto a hard surface, cavitation and fatigue phenomena arise. In studies of the I.I. Polzunov Central Scientific Research, Planning and Design Boiler and Turbine Institute, as well as in article [71] it was noted that with the precipitation of drops onto a hard surface, the increase in pressure at the impact center reaches $(0.6-3)10^9$ n/m². Such high pressures may be obtained only with the joining of vapor cavities inside a liquid; i.e., with cavitation. High pressures cause high local temperatures, significantly accelerating the process of chemical reactions; in particular, oxidation of metal.

However, experimental studies indicate that the rate of erosional wear of a surface exceeds the rate of cavitational wear 2-3 times. This may be explained in the following way. Due to anisotropy of metal grains different sections of the blade surface have different resistance, to the effect of liquid particle impact. In the first place, crystals with a great degree of plasticity are deformed in the direction of the impact. Crystals in which the axis of greatest elasticity is directed along the impact are not

/189

deformed and form cantilever projections subsequently behaving like girders with a seal. Under the action of particle impacts and cavitation elevations in pressure, the projecting portions oscillate; fatigue microcracks appear at their bases. These cracks are especially easily propagated on the borders between metal grains and lead to breaking off of metal bases and the formation of caverns.

For most materials erosional wear proceeds nonuniformly in time. In the beginning there is usually a period when there is almost no erosion. For different materials this period may extend from several minutes to several days. Then erosion becomes noticeable. The rate of erosion gradually increases. Basic destruction of the material of the blades is observed precisely in this period. The eroded surface acquires the appearance of a sponge with projections and caverns. Furthermore, a third period begins when the rate of erosion slows and may decrease to zero.

In steam turbines construction there are cases in which the working blades of the final stages, having been 20-30% destroyed along the length of the cord by erosion over the course of the first several months of use, continued to operate for several years without a noticeable increase in erosional wear.

Such a process of erosional wear may be explained in the following way. In the initial period when the blade surface is smooth, only cavitation wear is possible. Also the drops exert a mechanical influence on the surface which leads to a change in its shape. In the second period, cavitation wear is prolonged; however, fatigue chipping of whole grains of metal begins. This strongly accelerates the process of blade destruction. In the final stage, cavitation destruction evidently slows down. The liquid phase filling the caverns on the blade surface is not successfully thrown off by centrifugal forces and seems to form a protective pillow, softening the impacts of new drops. Also, fatigue wear slows down since the liquid filling the caverns damps the oscillations of projecting parts.

In the process of erosional wear there is a certain increase in the axial space between the nozzle and working blades. This also leads to a deceleration of destruction of the subsequent layers of metal of the blades.

2. Basic Factors Influencing Erosional Wear

/190

Numerous observations after turbine operation on moist water vapor indicated that erosion proceeds especially intensively when the axial clearance is small or the circumferential velocity is great (where $u < 150$ m/sec erosion was usually observed); when factors appear which increase the local concentration of particles or their dimensions, for example: separation of moisture onto the periphery in the preceding stages, the presence of bands and recesses in the preceding stages: in the case of decreased vapor pressure

when the particles are poorly attracted by the vapor flow. (With a pressure in the stage $p > 0.6 \cdot 10^6$ n/m² erosion is usually not observed).

According to the data of several investigators only one degree of vapor moisture in a stage does not determine its erosional wear. In the practice of steam turbine construction, cases are known in which a turbine operating on vapor with 5% moisture showed greater wear than a turbine operating on a vapor with 8-10% moisture. This again emphasizes that rational construction of the flow section of the turbine and proper selection of materials for the blades is of great importance in providing for high erosional resistance of the turbine.

According to statistical data introduced in [71], the rate of erosion is almost independent of whether a given stage was active or had a high degree of reaction.

It is necessary to note the close connection between the rate of erosion and the amount of losses due to particle impact on the working blade. Evidently erosion and losses due to impact represent two aspects of the same phenomena: impact of the drops on working blades. Therefore, erosion indicates the existence of a stage of great losses due to impact.

3. Basic Methods for Decreasing Blade Erosion

One of the most simple and widely used methods for increasing the erosional resistance of a blade is mechanical hardening of its surface. For example, at the S.M. Kirov Kharkov turbine plant, the special technology of electric spark application to the blade surface of a thin protective layer of very hard material (stellite, alloy Tl5K6, et al.) was developed. At the Leningrad metal plant, welding stellite layers onto the inlet edges of the working blades high-temperature silver solder is used. The resource of such hardened blades is significantly increased in comparison to that of unhardened blades. However, it is necessary to bear in mind that blades of condensed vapor turbines operate under comparatively easy conditions: the vapor temperature in the final stages is $t \leq 40^\circ\text{C}$, and the condensate, i.e., water, is not a corrosive medium.

In order to increase erosional resistance, working blades must /191 be carefully polished and the blade material must have a homogeneous fine crystalline structure lacking nonmetallic inclusions. The surface layer of the metal must be hard and viscous. As a number of experimental studies indicated, tungsten steels of the austenite class resist erosion especially well.

Moreover, in order to lower erosional wear of the working blade it is expedient:

-to use a nozzle apparatus with minimum grid thickness, which leads to a decrease in the separation of primary condensate particles on the nozzle blades;

- to use slower speeds of rotation, allowing a decrease in the force of particle impact against the blades;

- to use nozzle blades with minimum exit edge thickness, which leads to a decrease in the diameter of secondary drops formed from film destruction in the axial clearance;

- to provide a possibly greater axial clearance between the nozzle and working blades, which leads to a decrease in the diameter of secondary drops, an increase in their velocity and the partial separation of condensate in front of the working blades;

- to make the flow part smooth, without recesses and narrow fissures;

- to eliminate some of the liquid phase from the flow section through a moisture conducting apparatus;

- to use a birotative turbine.

References

1. Astaf'yev, A. I.: Nekotoryiye svoistva vlagoulavlivayushchikh ustroystv parovykh turbin (Some Characteristics of the Moisture Collecting Apparatus of Steam Turbines). Energo- /192 mashinostroyeniye, No. 2, 1960.
2. Abdonin, V. I. and I. I. Novikov: Skorost'zvuka na krivoy fazogo ravnovesiya par-zhidkost' (The Speed of Sound on a Curve of Vapor-Liquid Phase Equilibrium). Prikladnaya mekhanika i technicheskaya fizika, No. 1, 1960.
3. Bailey, Nielson, Serra and Zupnik: Tsecheniye zapylennoy gaza v osesimmetrichnom soople (The Flow of a Dust-Laden Gas in an Axisymmetric Nozzle). Raketnaya Tekhnika, No. 6, 1961 (trans. from Eng.).
4. Baranov, V. A., V. V. Pryakhin and O. P. Kustov: Vliyaniye vysoty lopatki i nekotorykh rezhimnykh parametrov na ekonomichnost' turbinoy stupini pri rabote na vlazhnom pare (The Influence of Blade Height and Some Regime Parameters on the Economy of a Turbine Stage Operating on Moist Vapor). Teplo-energetika, No. 2, 1965.
5. Bayvel', L. P. and T. M. Zil'berebal: Nekotoryye rezul'taty izmereniya stepini vlazhnosti para na experimental'noy parovoy turbine nizkogo davleniya (Some Results of Measuring the Degree of Vapor Moisture on an Experimental Low Pressure Steam Turbine). Energomashinostroyeniye, No. 8, 1964.
6. Bernasconi, S.: Uber die Kondensation Verschiedener Dämpfe bei adiabatischer Expansion. (The Condensation of Different Vapors under Adiabatic Expansion). Zeitschrift für angewandte mathematik, Vol. 10, Fasc. 5, 1959.

7. Brauer, H.: Stromung and Warmeubergang bei Rieselfilm (Flow and Heat Transition in the Case of a Trickle Film). VDJ, H. Nr. 457, 1956.
8. Carlson: Eksperimental'noye opredeleniye teplovogo zapazdyvaniya pri techenii gaza s tverdymi chastitsami v sopele (An Experimental Determination of the Heat Lag During the Flow of a Gas with Solid Particles in a Nozzle). Raketnaya Tekhnika, No. 7, 1962 (trans. from Eng.).
9. Carlson: Eksperimental'noye opredeleniye otstavaniya chastits pri techenii smesi gaza i chastits v sopele (An Experimental Determination of Particle Lag During the Flow of a Mixture of a Gas and Particles in a Nozzle). Raketnaya tekhnika i kosmonavtika, No. 2, 1965 (trans. from Eng.).
10. Carlson and Hoaglund: Soprotivleniye i teplootdacha chastits v soplakh raketnykh dvigateley (The Resistance and Heat Emission of Particles in Rocket Engine Nozzles). Raketnaya tekhnika i kosmonavtika, No. 11, 1964 (trans. from Eng.).
11. Chen: Koeffitsiyent soprotivleniya chastits v gazovykh potokakh (The Coefficient of Resistance of Particles in Gas Flows). Raketnaya tekhnika i kosmonavtika, No. 4, 1965 (trans. from Eng.).
12. Collingham, R. E. and J. L. Firey: Process Design and Development, Vol. 2, No. 3, 1963.
13. Dekhtyarev, L. I.: Ob erozii turbinnykh lopatok (Concerning Erosion of Turbine Blades). Teplosilovoye khozyaystvo, No. 9, 1939.
14. Deych, M. Ye., G. A. Filippov et al.: Vliyaniye vlazhnosti na effektivnost' obandazhennoy i neobandazhennoy turbinnykh stupeney (The Influence of Moisture on the Efficiency of Bandaged and Nonbandaged Turbine Stages). Energomashinostroyeniye, No. 8, 1964.
15. Deych, M. Ye., G. A. Filippov et al.: Issledovaniye struktury potoka vlazhnogo para v soplakh za turbinnoy stupen'yu (A Study of the Flow Structure of Moist Vapor in Nozzles Behind a Turbine Stage). Teploenergetika, No. 8, 1966.
16. Deych, M. Ye., G. A. Filippov et al.: Poteri energii, voznikayushchiye pri techenii vlazhnogo para v turbinnoy stupeni (Energy Losses Arising During the Flow of Moist Vapor in a Turbine Stage). Teploenergetika, No. 12, 1966.
17. Deych, M. Ye., V. F. Stepanchuk et al.: Eksperimental'noye issledovaniye skachkov kondensatsii (An Experimental Study of Condensation Discontinuities). Teplofizika vysokikh temperatur, Vol. 2, No. 5, 1961.
18. Deych, M. Ye. and G. V. Tsiklauri: Raskhodnyye kharakteristiki suzhivayushchikhsya osesimmetrichnykh sopel na peregretoy i vlazhnom pare (Consumption Characteristics of Tapering Axisymmetric Nozzles on Superheated and Moist Vapor). Acad. of Sci., USSR Press, Energetika i transport, No. 3, 1964.
19. Frenkel', Ya. I.: Kineticheskaya teoriya zhidkosti (The Kinetic Theory of Liquid). Acad. of Sci. USSR Press, 1945.
20. Fuks, N. A.: Mekhanika aerorozley (The Mechanics of Aerosols). Acad. of Sci. USSR Press, 1955.

21. Fulmer, Wirtz.: Izmereniye skorostry ot del'nykh chastits pri modelirovani protsessu istekniya iz reaktivnogo sopla (Measuring the Velocities of Individual Particles by Simulation of the exhaust process from a Jet Nozzle). Raketnaya tekhnika i kosmonautika, No. 8, 1965 (trans. from Eng.). /193
22. Gilbert, Alport and Dunlop: Dinamika dvukhfaznykh techeniy v raketnykh soplakh (The Dynamics of Double-Phase Flows in Rocket Nozzles). Raketnaya tekhnika, No. 12, 1962 (trans. from Eng.).
23. Gilbert, M., L. Davis and D. Altman: Velocity Lag of Particles in Linearly Accelerated Combustion Gases. Jet Propulsion, Vol. 95, No. 1, 1955.
24. Glauz: Smeshannoye dozvukovoye i sverkhvukovoye tekhnicheskoye gaza s tverdymi chastitsami (A Mixed Subsonic and Supersonic Flow of a Gas with Solid Particles). Raketnaya tekhnika, No. 5, 1962 (trans. from Eng.).
25. Gorbis, Z. R.: Teploobmen dispersnykh skvoznykh potokov (Heat Exchange of Dispersion Through Flows). Energiya Press, 1964.
26. Hoaglund: Posledniye dostizheniya v issledovanii tekhnicheskoy gaza s tverdymi chastitsami v sople (Recent Achievements in the Study of a Gas Flow with Solid Particles in a Nozzle). Raketnaya Tekhnika, No. 5, 1962 (trans. from Eng.).
27. Hoffman and Lorentz: Parametricheskoye issledovaniye tekhnicheskoy gaza s tverdymi chastitsami v konicheskikh soplakh (A Parametric Investigation of a Gas Flow with Solid Particles in Conic Nozzles). Raketnaya tekhnika i kosmonautika, No. 1, 1965 (trans. from Eng.).
28. Katsnel'son, B. D. and F. A. Timofayava: Issledovaniye koefitsiyenta teplootdachi chastits v potoke v nestatsionarnykh usloviyakh (A Study of the Coefficient of Heat Emission of Particles in a Flow under Nonstationary Conditions). Kotloturbostroyeniye, No. 5, 1948.
29. Kinney, G. R.: Internal Liquid Film Cooling Experiments with Airstream Temperatures to 2000°F in 2- and 4-inch Diameter Horizontal Tubes. NASA Report 1087, 1952.
30. Kirillov, I. I., A. I. Nosovitskiy and I. P. Fadeyev: Vliyaniye vlazhnosti na k.p.d. turbinnykh stupeney (The Influence of Moisture on the Efficiency of Turbine Stages). Teploenergetika, No. 7, 1965.
31. Kirillov, I. I. and R. B. Yablonik: Kinetika protsessu kondensatsii para v turbinnoy stupeni (The Kinetics of the Vapor Condensation Process in a Turbine Stage). Energomashinostroyeniye, No. 4, 1963.
32. Kirillov, I. I. and R. M. Yablonik: Vliyaniye pereokhlazhdeniya i struktury vlazhnogo para na yego raskhod soplami (The Influence of Supercooling and the Structure of a Moist Vapor on Its Consumption by Nozzles). Energomashinostroyeniye, No. 10, 1962.
33. Kirillov, I. I., R. M. Yablonik et al.: Aerodinamika protochnoy chasti parovykh i gazovykh turbin (The Aerodynamics of the Flow Section of Steam and Gas Turbines). Mashgiz, 1958.

34. Kirillov, I. I. and R. M. Yablonik: Problema usovershenstvovaniya turbinnykh stupeney, rabotayushchikh na vlazhnom pare (The Problem of Improving Turbine Stages Operating on Moist Vapor). Teploenergetika, No. 10, 1962.
35. Kliegel: Tekheniye smesi gaza s chastitsami v sople (The Flow of a Gas-Particle Mixture in a Nozzle). Voprosy raketnoy tekhnika, No. 10, 1965 (trans. from Eng.).
36. Komov, G. A.: Issledovaniye techeniya zapylennoy gaza v sople Lavalya (A Study of the Flow of a Dust-Laden Gas in a Laval Nozzle). Inzhenerno-Fizicheskiy Zhurnal, No. 3, 1966.
37. Krayko, A. N. and L. Ye. Sternin: K teorii techeniy dvukhskorostnoy spolshnoy sredy s tverdymi ili zhidkimi chastitsami (Toward a Theory of the Flows of a Two-Speed Continuous Medium with Solid or Liquid Particles). Prikladnaya Matematika i Mekhanika, Vol. 29, 1965.
38. Kutateladze, S. S. and M. A. Styrikovich: Gidravlika gazozhidkostnykh sistem (The Hydraulics of Gas-Liquid Systems). Gosenergoizdat, 1958.
39. Levich, V. G.: Fiziko-khimicheskaya gidrodinamika (Physical-Chemical Hydrodynamics). Fizmatgiz, 1959.
40. Lorentz and Hoffman: Sopostavleniye kharakteristik konicheskogo i profilirovannogo sopel, rabotayushchikh na smesi gaza s tverdymi chastitsami (A Comparison of the Characteristics of Conic and Profiled Nozzles Operating on a Mixture of Gas and Solid Particles). Raketnaya tekhnika i kosmonautika, No. 1, 1966 (trans. from Eng.).
41. Loshkavev, A. I.: K teorii erozionnogo iznosa lopatochnogo apparata tsentrostremitel'nykh turbin (Toward a Theory of the Erosional Wear of the Blade Apparatus in Centripetal Turbines). Acad. of Sci. USSR Press, Energetika i transport, No. 2, 1965.
42. Lyakhovskiy, D. N.: Konvektivnyy teploobmen mezhdue gazom i vzveshennymi chastitsami (Convective Heat Exchange Between Gas and Suspended Particles). Zhurnal tekhnicheskoy fiziki, Vol. 10, 1940.
43. Mahrenholtz, O.: Förderung eines Flüssigkeitsfilmes an einer senkrechten Wand durch einen Gasstrom (Advance of a Liquid Film on a Perpendicular Wall Through a Gas Flow). Kältetechnik, Vol. 10, No. 5, 1958.
44. Marble, F. E.: Dynamics of a Gas Containing Small Solid Particles. Combustion Propulsion Fifth AGARD Colloquium, Braunschweig, pp. 9-13, April 1962.
45. Marchik, E. A.: Dvizheniye kondensirovannoy fazy v mezhlopatochnykh kanalakh stupeni osevoy gazovoy turbiny (The Motion of the Condensed Phase in the Interblade Conduits of a Stage in an Axial Gas Turbine). Teploenergetika, No. 10, 1965.
46. Maxwell, W. R., W. Dickinson and E. F. Coldin: Adiabatic Expansion of a Gas Flow Containing Solid Particles. Aircraft Engineering, Vol. 10, No. 18, 1946.
47. Neighbors, Strimbeck, Cargill and Smith: Razrabotka gornorudnym upravleniyem gazoturbinnykh silovykh ustanovok na puley-gol'nom toplive (The Development of Gas Turbine Power Instal-

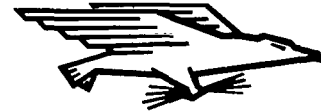
- lations on Pulverized Coal Fuel by Mining Management).
Energeticheskiye Mashiny i ustanovki, Vol. 87, No. 2, Series A, 1965 (trans. from Eng.).
48. Novikov, I. I.: Pokazatel' adiabaty nasyshchennogo i vlazhnogo para (The Adiabatic Index of Saturated and Moist Vapors). Doklady, Acad. of Sci., USSR, Vol. 59, No. 8, 1948.
 49. Olesevich, K. V.: Iznos elementov gazovykh turbin pri rabote na tverdom toplive (The Wear of Elements of Gas Turbines Operating on Solid Fuel). Mashgiz, 1959.
 50. Oswatitsch, K.: Kondensationserscheinungen in Überschalldüsen. (Condensation Phenomena in Supersonic Nozzles). "Z. angew. Math. und Mech.", No. 22, 1942.
 51. Preiskorn: Erosionschäden an Endstufen von Kondensations-Dampfmaschinen und Massnahmen zu ihrer Minderungen. (Erosion Damage at the Final Stages of Condensation-Steam Turbines and Measures for Its Alleviation). Maschinentechnik, Vol. 7, No. 11, 1958.
 52. Pryakhin, V. V.: Issledovaniye vliyaniya vlazhnosti para na kharakteristiki turbinnykh stupeney s tsilindricheskimi lopatkami (A Study of the Influence of Vapor Moisture on the Characteristics of Turbine Stages with Cylindrical Blades). Dissertation for the Degree of Candidate in Technical Sciences, Moscow Power Engineering Inst., 1965.
 53. Rezenberg, S. Sh.: Vliyaniye termoforeza na protsess osedaniya chastits zoly na okhlazhdayemykh lopatkakh gazovykh turbin (The Influence of Thermophoresis on the Process of Ash Particle Settling on the Cooled Blades of Gas Turbines). Energomashinostroyeniye, No. 8, 1961.
 54. Salikov, A. P.: Zol'nyye otlozhdeniya v gazovykh turbinakh pri rabote na tyazhelykh mazutakh (Ash Deposits in Gas Turbines Operating on Heavy Mazuts). Teploenergetika, No. 6, 1957.
 55. Sazanov, B. V.: Osobennosti raboty turbin na nasyshchennom gaze i metodika ikh teplovogo rascheta (Characteristics of Turbine Operation on Saturated Gas and a Method for Thermal Calculation of Them.) Energetika, College Press, No. 3, 1963.
 56. Saltanov, G. A.: Issledovaniye volnovoy struktury potoka vlazhnogo para (A Study of the Wave Structure of a Moist Vapor Flow). Dissertation, Moscow Power Engineering Inst., 1965.
 57. Shcheglyayev, A. V.: Parovyye turbiny (Steam Turbines). Gosenergoizdat, 1955.
 58. Sommerfield, M.: Issledovaniya raketnykh dvigateley na tverdom toplive (A Study of Rocket Engines Operating on Solid Fuel). Foreign Literature Press, 1963.
 59. Stekol'shchikov, Ye. V.: Issledovaniye skorosti zvuka v dvukhfaznykh sredakh (A Study of the Speed of Sound in Double-Phase Media). Dissertation, Moscow Power Engineering Inst., 1965.
 60. Steltz: Kriticheskoye i dvukhfaznoye techeniye para (Critical and Double-Phase Vapor Flow). Energeticheskoye mashinostroy-

- eniye, Vol. 83, No. 2, Series A, 1961 (trans. from Eng.).
61. Stepanchuk, V. F. and G. A. Saltanov: Eksperimental'noye issledovaniye skachkov uplotneniya vo vlazhnom pare (An Experimental Study of Shock Waves in Moist Vapor). Teploenergetika, No. 9, 1965.
 62. Stepanchuk, V. F. and G. A. Saltanov: Raschet kosykh shachkov kondensatsii (Calculation of Transverse Discontinuities in Condensation). Teplofizika vysokikh temperatur, No. 4, 1965.
 63. Stepanov, G. Yu.: Girodinamika reshetok turbomashin (Hydrodynamics of Turbine Engine Grids). Fizmatgiz, 1962.
 64. Sychev, V. V.: Novoye uravneniye dlya pokazatelya adiabaty vlazhnogo para (A New Equation for the Adiabatic Index of Moist Vapor). Teploenergetika, No. 3, 1961.
 65. Traupel, W.: Zur Theorie der Nassdampfturbine. (The Theory of the Moist Vapor Turbine). Schweizerische Bauzeitung, Vol. 77, No. 20, 1959.
 66. Venediktov, V. D.: Issledovaniye raboty birotativnoy turbiny na dvukhfaznom potoke s zhidkimi chastitsami (An Investigation of the Operation of a Birotative Turbine on a Double-Phase Flow with Liquid Particles). Teploenergetika, No. 2, 1964.
 67. Venediktov, V. D.: Ravnovesnoye istecheniye iz sopla smesi ideal'nogo gaza i kondensiruyushchegosya para (Equilibrium Exhaust from a Nozzle of a Mixture of an Ideal Gas and Condensing Vapor). Inzhenerno-Fizicheskiy Zhurnal, Vol. 10, No. 2, 1966.
 68. Venediktov, V. D.: Issledovaniye raboty turbin i sopel dvigateley na dvukhfaznykh potokakh (An Investigation of Turbine and Nozzle Operation in Engines on Double-Phase Flows). Dissertation, P. I. Baranov Central Scientific Research Inst. of Aircraft Engines, 1963.
 69. Vukalovich, M. P. and I. I. Novikov: Tekhnicheskaya termodinamika (Technical Thermodynamics). Gosenergoizdat, 1952.
 70. Vulis, L. A.: Termodinamika gazovykh potokov (The Thermodynamics of Gas Flows). Gosenergoizdat, 1950.
 71. Yablonik, R. M.: Ispytaniya modeley turbinnykh stupeney na uvlazhennom vozdukh (Experiments Using Models of Turbine Stages on Moisturized Air). Teploenergetika, No. 5, 1962.
 72. Yablonik, R. M. and V. V. Lagarev: Issledovaniye techeniya vlazhnogo para v napravlyayushchikh kanalakh parovykh turbin (A Study of a Moist Vapor Flow in the Guide Conduits of Steam Turbines). Teploenergetika, No. 11, 1963.

Translated for the National Aeronautics and Space Administration by:
 Aztec School of Languages, Inc.
 Research Translation Division (478)
 Maynard, Massachusetts and McLean, Virginia
 NASW-1692

NATIONAL AERONAUTICS AND SPACE ADMINISTRATION
WASHINGTON, D. C. 20546
OFFICIAL BUSINESS

FIRST CLASS MAIL



POSTAGE AND FEES PAID
NATIONAL AERONAUTICS AND
ADMINISTRATION

CIVIL ENGINEERING DEPT. 70151 00903
AIR FORCE WEAPONS LABORATORY 701017
KIRTLAND AFB, NEW MEXICO 87117

ATTN: E. LOU BOGART, CHIEF, TECH. LIBRARY

POSTMASTER: If Undeliverable (Section 158
Postal Manual) Do Not Return

"The aeronautical and space activities of the United States shall be conducted so as to contribute . . . to the expansion of human knowledge of phenomena in the atmosphere and space. The Administration shall provide for the widest practicable and appropriate dissemination of information concerning its activities and the results thereof."

— NATIONAL AERONAUTICS AND SPACE ACT OF 1958

NASA SCIENTIFIC AND TECHNICAL PUBLICATIONS

TECHNICAL REPORTS: Scientific and technical information considered important, complete, and a lasting contribution to existing knowledge.

TECHNICAL NOTES: Information less broad in scope but nevertheless of importance as a contribution to existing knowledge.

TECHNICAL MEMORANDUMS: Information receiving limited distribution because of preliminary data, security classification, or other reasons.

CONTRACTOR REPORTS: Scientific and technical information generated under a NASA contract or grant and considered an important contribution to existing knowledge.

TECHNICAL TRANSLATIONS: Information published in a foreign language considered to merit NASA distribution in English.

SPECIAL PUBLICATIONS: Information derived from or of value to NASA activities. Publications include conference proceedings, monographs, data compilations, handbooks, sourcebooks, and special bibliographies.

TECHNOLOGY UTILIZATION PUBLICATIONS: Information on technology used by NASA that may be of particular interest in commercial and other non-aerospace applications. Publications include Tech Briefs, Technology Utilization Reports and Technology Surveys.

Details on the availability of these publications may be obtained from:

SCIENTIFIC AND TECHNICAL INFORMATION DIVISION
NATIONAL AERONAUTICS AND SPACE ADMINISTRATION
Washington, D.C. 20546